2018

Molecular Brain Adaptations to Ethanol: Role of Glycogen Synthase Kinase-3 Beta in the Transition to Excessive Consumption

Andrew D. van der Vaart
Virginia Commonwealth University

Molecular Brain Adaptations to Ethanol: Role of Glycogen Synthase Kinase-3 Beta in the Transition to Excessive Consumption

A dissertation submitted in partial fulfillment of the requirements for the degree of Doctor of Philosophy at Virginia Commonwealth University.

by

Andrew Donald van der Vaart
Bachelor of Arts, University of Virginia, 2009

Director: Michael F. Miles, M.D., Ph.D.,
Professor, Departments of Pharmacology and Toxicology, Neurology

Virginia Commonwealth University,
Richmond, Virginia,
February 2018

Acknowledgments

I would like to sincerely thank all of the people in my life who have provided support, guidance, and contributions to this endeavor. I thank the VCU M.D.-Ph.D. program and the NIAAA for giving me the opportunity to practice research without fear of mistakes for long enough to learn something.

I must thank my mentor Dr. Michael Miles. An intrepid captain, Dr. Miles navigated me through my first grant, first first-author paper, and countless fretful nights. His reassurances and ability to calmly cut through the noise has been instrumental. I could not have imagined how much I would grow in this environment. To study under his keen scientific mind has been so gratifying.

I also owe a special thank-you to Dr. Kenneth Kendler. Dr. Kendler took a risk on a youth with his head in the clouds when he recruited me to VIPBG. Since then we have had many expansive conversations which have never failed to inspire me. Thank you for showing me that to study psychiatry is to study humanity.

And to my committee members: Dr Negus for patiently ensuring I learn the fundamentals of pharmacology, Dr Brunzell for her insight into cellular signaling and Dr. McQuiston for keeping my neuroscience knowledge anchored by the appropriate scaffolds. Thank you all.

I could not have traversed this road without the support of my friends and family. Ellen, you really were on the frontlines. Thank you for holding me up, even when the winds were cold. Thank you Mom, Dad, and Rob, all of whom have supported me since before I was self-aware. Thank you to Guy who was the greatest lab partner a

sentimental fool could ask for. And to the rest of the Miles lab- Rory, Kristin, Jessica, Jim, Jennifer—thank you for the memories, they are vivid ones!

Table of Contents

Clarification of Contributions

Without the technical and scientific contributions of those listed below, the work reported herein would not have been possible. All other work included within this dissertation, aside from cited, is exclusively my own.

Chapter 3

CIE animals were run at MUSC in the laboratory of Dr. Howard Becker under care of Marcelo Lopez. Maren Smith, Guy Harris, and myself harvested tissue. Microarray and gene list overlap analyses were performed by Maren Smith. q-RT-PCR and analyses were run by Maren Smith, Guy Harris, and myself. Correlations with ethanol drinking behavior were performed by Guy Harris. Dr. Jennifer Wolstenholme ran Ingenuity Pathway Analyses and helped write the paper and make the figures, from which the chapter is adapted (van der Vaart et al., 2017).

Chapter 4

Guy Harris and I performed the acute ethanol dose-response and harvested the tissue. Guy Harris, Phoebe Lin, and I ran the intermittent ethanol access (IEA) experiment outlined the the “chronic” section. Chris Pais helped run the IEA experiment outlined in the acute-on-chronic section. Akhil Ramaswamy performed cryostat sectioning and contributed to immunohistochemistry. Dalton Jun-da Huey contributed to running Western blots. Guy Harris and I ran the Analox analyses.

Chapter 5

Annie Meng performed all experiments described in the Viral-mediated overexpression section; I performed statistical analyses on her raw data. Akhil Ramaswamy helped greatly with cryostat sectioning of the viral-mediated deletion brains and contributed to the immunohistochemical staining of the viral-mediated and tamoxifen-mediated brains. Guy Harris acquired excellent images of the tamoxifen-mediated deletion.

Chapter 6

Chris Pais helped with running IEA, reading bottles, and changing cages during the tideglusib gavage experiment. Guy Harris, Kristin Mignogna, and Chris Pais all helped harvest tissue. Jessica Jurmain and I ran the tideglusib i.p. experiment. Justin Poklis obtained blood ethanol readings.

List of Tables

Chapter 1

There are no tables in Chapter 1.

Chapter 2

There are no tables in Chapter 1.

Chapter 3

Chapter 4

Chapter 5

Chapter 6

Supplemental Tables

Available upon email request from Dr. Michael Miles at michael.miles@vcuhealth.org

List of Figures

Chapter 1

There are no figures in Chapter 1.

Chapter 2

Chapter 3

Chapter 4

Chapter 5

Chapter 6

Chapter 7

Supplemental Figures are given in the Appendix.

List of Abbreviations (excluding rarely mentioned genes)

AAV-CMV	Adeno-associated-virus with a cytomegalovirus promoter
Akt	also known as protein kinase B
AUD	alcohol use disorder
B6	Short for C57BL/6J mice
BDNF	brain derived neurotrophic factor
Camk2a	Calcium calmodulin dependent kinase. The *Camk2a* gene encodes the CAMKII protein
CIE	chronic intermittent ethanol (vapor)
D2	Short for DBA/2J mice
DA	dopamine
DNA	deoxyribonucleic acid
Dnm3	Dynamin 3 gene, encodes dynamin III protein
eQTL	expression quantitative trait locus
GSK3A	glycogen synthase kinase 3-alpha
Gsk3b	glycogen synthase kinase 3-beta. The *Gsk3b* gene in mice encodes the GSK3B protein. In humans the gene would be called *GSK3B*. In cases where we refer to the function of the overall entity (as gene and protein) we default to GSK3B
HTT	huntingtin gene
IEA	intermittent ethanol access
IHC	immunohistochemistry
IL	infralimbic (cortex)
LD (Box)	light-dark (box)
LRS	likelihood ratio statistic
Mbp	myelin basic protein
Mobp	myelin associated oligodendrocyte basic protein
mPFC	medial prefrontal cortex
NAC	nucleus accumbens
NeuN	Neuronal Nuclei (marker)

Nr2c2	Nuclear receptor subfamily 2 group c (gene)
PCR	polymerase chain reaction
PFC	prefrontal cortex
PSD95	post-synaptic density protein 95
q-RT-PCR	quantitative real time polymerase chain reaction
QTL	quantitative trait locus
TBS-T	Tris-Buffered-Saline containing Tween (0.2%)
WGCNA	weighted gene co-expression network analysis

Abstract

Alcoholism is a complex neuropsychiatric disease that is characterized by compulsive alcohol use and intensifying cravings and withdrawals, often culminating in physiologic dependency. Fundamental alterations in brain chemistry underlie the transition from initial ethanol exposure to repetitive excessive use. Key mediators of this adaptation include changes in gene expression and signal transduction. Here we investigated gene expression pathways in prefrontal cortex and nucleus accumbens following acute or chronic ethanol treatment, to identify genes with potentially conserved involvement in the long-term response of the corticolimbic system to repeated ethanol exposure. We investigated *Gsk3b*, which encodes glycogen synthase kinase 3-beta, as a highly ethanol responsive gene associated with risk for long-term maladaptive responses to ethanol. On the level of the protein, we found that GSK3B and to a lesser extent the GSK3A isoform showed robust increases in inhibitory phosphorylation following acute ethanol. This inhibition may underlie aspects of the behavioral response to acute ethanol, as pre-treatment with a GSK3B inhibitor (tideglusib) augmented ethanol's locomotor effects. Following long term ethanol exposure, we re-tested GSK3B phosphorylation and found that its ethanol response is blunted, consistent with molecular tolerance as a corollary to increased consumption. As the prefrontal cortex (PFC) plays a vital role in the reward pathway via its glutamatergic projections to the nucleus accumbens, we investigated the role of the *Gsk3b* gene specifically in PFC and in glutamatergic neurons. Overexpression of *Gsk3b* in the PFC robustly increased ethanol consumption, while deletion in Camk2a-positive neurons significantly attenuated ethanol consumption. Pharmacologic antagonism of GSK3B also decreased drinking in

a model of binge-like consumption. Collectively this data implicates GSK3B as a mediator of excessive ethanol intake via its kinase activity, wherein inhibition of the kinase via phosphorylation exerts a protective effect in the context of acute ethanol, but desensitizes with repeated exposure.

Chapter 1

Introduction

Alcohol Use Disorder (AUD) is a chronic relapsing disease characterized by compulsive use of alcohol, negative consequences due to alcohol use, and a negative emotional state when not using. The DSM-5 (2013) classifies AUD as a spectrum disorder with severity ranging from mild, i.e. problem drinking, to severe, i.e. alcohol dependence, based on clinical criteria. Alcohol dependence is marked by physiological symptoms upon its withdrawal, including hallucinations, tremors, and seizures. In some cases this alcohol withdrawal syndrome can be fatal (Finn and Crabbe, 1997). The level of central nervous system (CNS) dysfunction associated with the mere removal of ethanol at this point in AUD pathophysiology demonstrates the extent of fundamental adaptation that has occurred with chronic exposure.

While alcohol dependence represents a primary disease endpoint in itself, adverse outcomes occur all along the pathophysiological process. In 2014, alcohol contributed to more than 200 diseases, according to the World Health Organization. Nearly 6% of all global deaths were attributable to alcohol, with the largest share of these (29.6%) coming from unintentional injuries (such as motor

vehicle accidents), followed by cancers (21.6%), and liver cirrhosis (16.6%) (Organization, 2014). In the United States, alcohol is the third leading preventable cause of death, after tobacco and poor diet (Mokdad *et al*, 2004). AUD has an extremely high co-morbidity with other addictions (Hakkarainen and Metso, 2009), as well as psychiatric disorders more generally (Tomasson and Vaglum, 1998). Alcohol may exacerbate or even cause certain symptoms of bipolar disorder (BD) and post-traumatic stress disorder (PTSD) (Jaffee *et al*, 2009; Nickerson *et al*, 2014), and greatly increases the risk of overdose deaths from respiratory depressant effects when combined with opioids and/or other sedatives (Health and Human, 2015).

According to the 2015 NSDUH, 6% of adults in the U.S. meet the clinical criteria AUD (SAMHSA, 2015). Moreover, 26.9% of adults reported binge drinking in the past month, which may represent a temporary loss of control over ethanol consumption, and a potential precursor for AUD (SAMHSA, 2015). Given that the large majority of adults (>85%) have at least tried alcohol at some point in their lifetimes while only 10% of these develop AUD, a critical priority for intervention regards the mechanisms mediating transition from casual social drinking to compulsive injurious consumption. Genetic predisposition has been found to play a substantial role (Kendler *et al*, 2012), explaining 49% of the variance according to twin and adoption studies (Verhulst *et al*, 2015). However, identifying specific genetic variants which contribute meaningfully to the neuropsychiatric—as opposed to metabolic—phenotype has proven arduous (Tawa *et al*, 2016). Similarly ill illuminated are specific neurobiological

mechanisms which underlie the risk of relapse, which can occur even years after last use (Vaillant, 2003). While current pharmacologic or psychodynamic interventions can contribute (in relatively equivocal measure) toward decreasing problematic alcohol use (Weisner *et al*, 2003), less than 20% of alcoholic patients remain abstinent even with treatment (Thompson *et al*, 2017). Given such poor responses, there is a great need for development of more targeted AUD treatments. Identifying novel treatments based on defined neurobiological targets is one arm of the pharmacogenetic endeavor. The other is a more precision-based approach in the application of treatments, i.e. predicting successes based on an as-yet-undefined genetic panel (Ragia and Manolopoulos, 2017). Together these arms converge on the goal of defining how ethanol interacts with genetic risk alleles to manifest molecular mechanisms promoting its use, and targeting these accordingly.

Aspects of ethanol's acute molecular sites of action have been characterized, but repeated ethanol exposure leading to AUD evokes mechanisms still only poorly defined (Starkman *et al*, 2012). The primary action of acute ethanol is CNS depression, which occurs through the combinatorial effect of ethanol on ion channel proteins, including (1) positive allosteric modulation of the $GABA_A$ receptor and (2) negative allosteric modulation of the NMDA receptor (Weight *et al*, 1992). Consequences of these primary actions vary spatiotemporally, but include increased dopamine release along the mesolimbic and mesocortical pathways (Soderpalm and Ericson, 2013). The former of these dopaminergic pathways projects from the Ventral Tegmental

Area (VTA) to the Nucleus Accumbens (NAC) and seems to assign reward/salience to stimuli (Saddoris *et al*, 2015), and the latter projects from the VTA to the prefrontal cortex (PFC), the region largely responsible for executive function, and thereby informs decision-making according to reward/salience (Jenni *et al*, 2017). These pathway-specific increases in dopaminergic signaling are pathognomonic for drugs of abuse (Koob and Le Moal, 1997). With repeated ethanol exposures there emerge homeostatic responses, such as tolerance to the dopaminergic effect (Diana *et al*, 1993) and neuronal hyperexcitability upon each withdrawal from the depressant action (Grant *et al*, 1990). On a behavioral level, more ethanol must be consumed to achieve the same intoxicating effect. What accounts for this attempt at homeostasis? There are opportunities for adaptation at perhaps every known level of a biological system. Neuronal excitability may be altered by an immediate change in the level of activity of a particular receptor (Bespalov *et al*, 2016), or a change in receptor density or subunit composition at the synapse over time (Casarett and Doull, 1975; Harms *et al*, 2005). A given receptor subunit may be regulated as a functional protein, post-translationally, translationally, transcriptionally, or epigenetically (Lempradl *et al*, 2015; Zong *et al*, 2017). It seems likely that these different layers of regulation can operate cooperatively on different time-scales. More permanent adaptations might be expected following persistent regulation on a more transient level—for example, lowered transcriptional activity of a gene might follow a period of low functional activity of its protein. Elucidating the means of such

cross-talk is a continuing directive of systems biologists and molecular geneticists.

In the case of alcoholism, we hypothesize that there are fundamental shifts in responsiveness of the CNS which occur from initial ethanol exposure to chronic, repeated ethanol exposures. Further we hypothesize that this transition underlies altered behavioral responses to ethanol, including promotion of maladaptive excessive ethanol intake. To test this hypothesis we have developed the following specific aims: (1) To characterize acute and chronic responses to ethanol in the corticolimbic reward pathway at the level of gene expression. (2) To determine whether acute and chronic ethanol show differential effects on the protein activity of a previously identified genetic hub of ethanol response in PFC, *Gsk3b*. (3) To determine whether genetic or pharmacologic modulation of *Gsk3b* alter ethanol-related behaviors, particularly ethanol consumption.

Thus, this dissertation begins by comparing genome-wide expression analyses of the effect of a single acute dose of ethanol vs. chronic intermittent ethanol (CIE) on gene expression changes in PFC and NAC across a recombinant inbred panel of mice (Crabbe *et al*, 1994). The effect of genetic variation across the mice strains on ethanol-induced expression changes is assessed via the identification of expression quantitative trait loci (eQTLs) (Doss *et al*, 2005) which may represent critical regulatory hot-spots of pharmacogenomic effect.

Gene expression networks are a means of understanding large scale genomic responses as the perturbations of many genes in tandem. Network hubs

represent points of highest interconnectivity, that is genes whose changes in expression correlate to those of many other network members at once. One such hub that emerged from prior network analyses of ethanol-responsive genes (Wolen *et al*, 2012) was *glycogen synthase kinase 3-beta* (*Gsk3b*). *Gsk3b* encodes one of two isoforms of glycogen synthase kinase 3 (GSK-3), an enzyme uniquely suited to integrate cellular signals and direct subsequent cellular response (Grimes and Jope, 2001). To assess its response to ethanol-induced changes in neuronal activity specifically, we characterize the phosphorylation state of its major regulatory site, serine-9 (S9), following acute ethanol treatment, withdrawal from long-term ethanol, and acute ethanol challenge after long-term ethanol. Based on prior studies we hypothesize that acute ethanol increases phosphorylation at S9 (Neznanova *et al*, 2009), but that chronic ethanol alters the response at this phospho-site.

GSK3B has been found to play a role in mechanisms of learning and memory generally (Kimura *et al*, 2008; Nelson *et al*, 2013), as well as behavioral conditioning in the context of drugs of abuse (Dobashi *et al*, 2010; Miller *et al*, 2014). Given the hub-like nature of the *Gsk3b* gene in the context of acute ethanol in the prefrontal cortex, we expect that each successive ethanol exposure may have continual downstream effects, with consequences on ethanol-related behavioral adaptations. The hypothesis that genetic modulation of *Gsk3b* in mouse medial prefrontal cortex (mPFC) alters ethanol self-administration is thoroughly investigated, using a viral over-expression vector and two methods of gene deletion. Finally, pharmacologic agents targeting

GSK3B protein are explored pre-clinically, with emphasis on the FDA Phase II approved small molecule inhibitor tideglusib (Lovestone *et al*, 2015).

Chapter 2

Background and Significance

2.1 Primary Binding Sites of Ethanol

Historically, the observation that alcohols and other general anesthetics exhibited a linear relationship of potency to lipid solubility led to the hypothesis that these agents acted by non-specific disruption of membranes (Janoff *et al*, 1981). Membrane-bound ion channels would then be altered secondary to disruption of the phospholipid bilayer. However significant weaknesses in this theory would eventually become evident, including differences in the anesthetic potency between stereoisomers with equal lipid solubilities, and the sudden loss of anesthetic effect with increasing chain lengths of alcohols or alkanes (Liu *et al*, 1993). Moreover, alcohols were found capable of modifying the activity of luciferase, a soluble enzyme, and this effect too showed distinct cut-off lengths (Moss *et al*, 1991). This latter finding is consistent with the “cut-off effect” reflecting size constraints of hydrophobic pockets wherein alcohols bind and modulate protein activity, rather than a loss of membrane solubility above a certain carbon chain length. Subsequent experiments have provided mounting

evidence that ethanol exerts its psychoactive effects by specific binding to proteins and consequent functional changes (Harris *et al*, 2008).

However, while ethanol binds specifically, it also binds promiscuously. Many proteins have been confirmed, and many more theorized, to contain ethanol binding sites (Howard *et al*, 2011). Furthermore, the molecule's small size and polarity make it freely diffusible and only transiently bound in a given hydrophobic pocket. Thus ethanol's global action can be seen as the spatial and temporal sum of many transient displacements of disordered water molecules from protein pockets (Klemm, 1998). Each of these displacements allows for allosteric effects on protein functioning, with ethanol varying in its potency and efficacy between its varied targets.

At pharmacologically relevant concentrations, ethanol is an efficacious positive allosteric modulator of the γ-aminobutyric acid type A ($GABA_A$) receptor, and negative allosteric modulator of the N-methy-D-aspartate (NMDA) glutamate receptor. Ethanol's GABAergic agonism accounts for its anxiolysis (Weight *et al*, 1992) and at higher doses, sedative effects (Lu and Greco, 2006); while NMDA antagonism likely accounts for the dissociative anesthetic effects (Krystal *et al*, 1998), and some degree of motor and memory impairment (Khanna *et al*, 1993). While these are not the only membrane-bound receptors bound by ethanol, they are each thought to contribute significantly to its reinforcing effects (Koob *et al*, 1998).

2.1.1 $GABA_A$ Receptors

$GABA_A$ receptors are pentameric ligand-gated ion channels which allow for the selective influx of chloride (Cl^-) ions into the neuron upon GABA binding. The resulting hyperpolarization increases the threshold for firing an action potential, thereby accounting for GABA's famed status as the major *inhibitory* neurotransmitter of the nervous system. Allosteric to the ligand-binding site there exists a well-characterized benzodiazepine-binding site, between the α- and γ-subunits of α- and γ-subunit containing $GABA_A$ receptors (Sigel, 2002). Benzodiazepine binding induces a conformational change which results in a greater affinity of GABA for the $GABA_A$ receptor, and thus a greater frequency of channel opening and subsequent neuronal hypoexcitability (Sigel, 2002). This GABA potentiation accounts for the anxiolytic and sedative effects of benzodiazepines—effects which show cross-tolerance with ethanol (Khanna *et al*, 1998). Some degree of mechanistic conservation in the CNS adaptations to benzodiazepines and ethanol is suggested by this cross-tolerance.

Evidence for the primary site of ethanol action comes from studies of site specific mutagenesis and chimeric receptors. Mihic et al. (1997) used the observation that alcohols and anesthetics increase $GABA_A$ activity but decrease the activity of $GABA_A$ receptors composed totally of rho1 subunits, to create a series of chimeric constructs. Differential modulation of these allowed for the identification of a region necessary and sufficient for alcohols' enhancement of $GABA_A$ receptor function. The region contained transmembrane domains (TM) 2 and 3—homologous between $GABA_A$ and glycine receptors—and particular

amino acid residues on these domains were found to be critical for alcohol and anesthetic enhancement of $GABA_A$ and glycine receptor function (Mihic *et al*, 1997). Subsequent studies have confirmed the role of TMs 2 and 3 while also providing some evidence of the involvement of TMs 1 and 4 (Lobo *et al*, 2008; Lobo *et al*, 2004; Lobo *et al*, 2006; Wick *et al*, 1998).

Significant differences in ethanol responsiveness have been observed between $GABA_A$ receptors based on their subunit composition, which dictate differences in spatial effects of ethanol, both on the microscopic (i.e. synaptic vs. extrasynaptic) and macroscopic (i.e. brain region) scales. The most common isoforms of GABA receptors are pentamers of 2α, 2β, and one γ or δ subunit. It has been found that γ subunit containing receptors are relatively insensitive to ethanol (Wallner *et al*, 2006), while δ-containing receptors are ethanol-responsive even at low doses, consistent with levels achieved in moderate social consumption (Santhakumar *et al*, 2007). $GABA_A$ receptors containing δ subunits are restricted to extrasynaptic sites, which exert tonic inhibitory effects on the neuron, as opposed to γ-containing receptors, which cluster within postsynaptic densities and mediate phasic bursts of inhibition (Nusser *et al*, 1998; Wei *et al*, 2004). As might be expected, low doses of ethanol preferentially enhance tonic inhibition over phasic inhibition, and the effect is most robust in neuronal cell types enriched for δ subunits, including cortical interneurons (Glykys *et al*, 2007), as well as granule cells of the dentate gyrus and cerebellum (Wallner *et al*, 2006; Zhang *et al*, 2007).

2.1.2 NMDA Receptors

Glutamate, the major excitatory neurotransmitter of the CNS, binds three receptor subtypes: NMDA receptors (NMDAR), α-amino-3-hydroxy-5-methyl-4-isoxazolepropionic acid (AMPA) receptors, and metabotropic receptors. Of the two former, ionotropic subtypes, AMPA receptors mediate an immediate response while NMDA ion channels open after an initial (AMPA-mediated) depolarization (Blanke and VanDongen, 2009). NMDA receptors are further distinguished by their Mg^{2+}-gating, permeability to Ca^{2+}, and sensitivity to ethanol antagonism (Lovinger *et al*, 1989; Moykkynen and Korpi, 2012)

The inhibitory actions of ethanol on NMDA-activated ion currents have been demonstrated throughout the brain (Hoffman *et al*, 1990), although the precise nature of ethanol-receptor binding is less well understood. The very rapid reduction in channel activity in response to ethanol suggests direct interaction of ethanol on NMDAR subunits (Ron and Wang, 2009). The NMDAR is a heteromeric complex made up of three subunits: NR1, NR2, and NR3. In turn each subunit has multiple subtypes, determined either by genetic variants or by alternative splicing from a single gene (Blahos and Wenthold, 1996). NR1/NR2B transmembrane segments contain the binding pockets for uncompetitive NMDAR antagonists such as ketamine and memantine (Johnson and Kotermanski, 2006). It may be speculated that ethanol exerts its effects through similar action (Bonnet and Scherbaum, 2015) but the ethanol binding site remains undefined.

What is well-characterized is the dynamic response of NMDARs to repeated ethanol exposures. Given the critical role of NMDARs in memory and

neuroplasticity (Blanke *et al*, 2009), it makes sense that these receptors would underlie aspects of ethanol tolerance and long-term facilitation, an activity-dependent increase in synaptic strength (Ron *et al*, 2009). Still, it makes them attractive targets for addiction medicine, insofar as addiction may be conceived as maladaptive learning (Lewis, 2017). Acutely, NMDARs can develop resistance in 1-2 hours to the depressive effects of ethanol on long-term-potentiation (LTP) (Tokuda *et al*, 2007). Upregulation of NMDAR function in a period following ethanol exposure may actually serve to better encode the reinforcing aspects of the behavior (Everitt and Robbins, 2005). Chronically, NMDARs show hyperactivity upon ethanol withdrawal, to the point of seizures and NMDA-mediated excitotoxicity (Gillman and Lichtigfeld, 1997); this aspect of NMDAR response could contribute to neuronal loss observed in late-stage alcohol patients (Moselhy *et al*, 2001).

One mechanism underlying NMDA receptor tolerance to ethanol may be via NR2 phosphorylation by Src family protein tyrosine kinases, particularly Fyn (Ron *et al*, 2009). Acute tolerance to ethanol inhibition of NMDAR channel activity is not observed in Fyn deletion ($Fyn^{-/-}$) mice, while it is intact in Fyn heterozygotes ($Fyn^{+/-}$); correspondingly, NR2B phosphorylation is increased in $Fyn^{+/-}$ mice but this increase is not observed in the $Fyn^{-/-}$ mice (Miyakawa *et al*, 1997). Thus as ethanol negatively modulates NMDAR function, a compensatory increase in activity, mediated by Fyn kinase phosphorylation of the NR2B subunit, is the intact response. This mechanism was further elucidated when it was revealed that, in the hippocampus, the scaffolding protein RACK1 localizes

Fyn kinase to the NR2B subunit (Yaka *et al*, 2002). Under basal conditions RACK1 prevents Fyn phosphorylation of NR2B; however activation of the cAMP/PKA pathway (such as by ethanol) leads to the dissociation of the molecular complex, allowing the kinase action of Fyn and subsequent upregulation of NMDAR channel activity (Yaka *et al*, 2003a). On a behavioral level, the regulation of ethanol sensitivity by the actions of Fyn kinase is evidenced by the longer ethanol-induced sleep time in $Fyn^{-/-}$ mice than heterozygous $Fyn^{+/-}$; and the increase in sleep time in $Fyn^{+/+}$ mice to the same level of the Fyn-deletion mice upon systemic administration of the NR2B inhibitor ifenprodil (Miyakawa *et al*, 1997; Yaka *et al*, 2003b). Farris and Miles (2013) showed that $Fyn^{-/-}$ mice might additionally show longer ethanol-induced sleep time due to severe disruptions in myelin-related gene expression.

While Fyn kinase deletion produces increased sensitivity to the sedative-hypnotic effects of ethanol, it does not alter rewarding properties of ethanol, as measured by the acquisition of conditioned place preference (CPP) (Yaka *et al*, 2003b). NR2A deletion or heterozygosity, however, does ablate ethanol induced CPP compared to wild-type $NR2A^{+/+}$ mice (Boyce-Rustay and Holmes, 2006). Taken together it would appear that NR2A subunit activity is necessary for the rewarding aspects of ethanol, whereas NR2B subunit activity is necessary for ethanol sensitivity but not necessarily ethanol reward. Similarly to the scaffolding protein RACK1 localizing Fyn to the NR2B subunit, PSD-95 appears to anchor Fyn and other protein tyrosine kinases (PTK) to NR2A (Tezuka *et al*, 1999). Unlike RACK1, this interaction does not appear to be inhibitory but rather

facilitates phosphorylation (Zhao *et al*, 2015). Given the homeostatic response of Fyn kinase phosphorylation of NR2B to regulate ethanol sensitivity, it may be postulated that compensatory changes in NR2A activity, possibly through PSD-95/PTK, would underlie tolerance to the rewarding effects of ethanol. What is unclear is the level of NR2A activity that is necessary for ethanol induced reward—ethanol itself is a negative modulator of NMDAR activity, but full *deletion* of the NR2A subunits ablates ethanol induced CPP. If it is rebound activity of NR2A-containing NMDARs that encodes ethanol reward-related learning, then presumably increased PSD-95/PTK activity would serve to increase the rewarding effects of ethanol, i.e. sensitization.

2.1.3 Intracellular Signaling Enzymes

It should be noted that there is also evidence that ethanol directly binds certain intracellular targets. There are numerous enzymes that may contain ethanol binding sites, although not necessarily with a direct impact on the CNS. For example, alcohol dehydrogenase (ADH) has a well delineated binding site (Hammes-Schiffer and Benkovic, 2006) but outside of its obvious relevance of ethanol metabolism generally, it seems unlikely that ethanol binding ADH *per se* produces changes in neurotransmitter signaling (Inoue *et al*, 1981).

Adenylate cyclase (AC) plays a regulatory role in essentially all cells via production of 3',5'-cyclic AMP (cAMP) from ATP. Among the various isozymes of AC, ethanol has been observed to exert varying degrees of effect on function, as measured by intracellular cAMP levels (Yoshimura and Tabakoff, 1995). On the

extremes, AC3 shows no ethanol response, while AC7 shows a several-fold increase in activity. Chimeric studies on utilizing these isoforms would go on to reveal two ethanol binding domains in adenylate cyclase (Yoshimura *et al*, 2006). While the degree of allosteric modulation varies between isoforms, those showing ethanol response (AC2, AC5, AC6, and AC7) are activated. The downstream effects that would be predicted by AC activation—most immediately, an increase in intracellular cAMP and thereby activation of cAMP-dependent protein kinase (protein kinase A)—are consistent with empirical observations of ethanol's acute effects in neurons (Newton and Messing, 2006). In $GABA_A$ receptor expressing neurons in the VTA, a potentiation of inhibitory post-synaptic currents was observed for days after a single ethanol exposure in mice, and this effect could be further enhanced with the adenylate cyclase activator forskolin or decreased with a PKA inhibitor (Melis *et al*, 2002). While it cannot be said the extent to which direct ethanol action on AC contributed to the observed potentiation, it is plausible that ethanol-induced AC activation would have at least enhanced the normal response to upstream G-protein signaling: in essence, turning up the "gain" on extracellular signals. Such interactions may account for plasticity changes beyond those mediated by receptors alone.

An enzyme which has received significant attention in the alcohol literature is protein kinase C (PKC). In particular, two isoforms of PKC have been shown to mediate robust and opposite effects in rodent gene knockout studies. Mice lacking PKCδ show decreased sensitivity to ethanol's GABA potentiation and increased ethanol self-administration (Harris *et al*, 1995). Conversely, PKCε

knockout exhibit increased sensitivity to ethanol's sedative effects, and double the GABA-induced Cl- influx compared with ethanol-treated wild-type mice (Hodge *et al*, 1999; Proctor *et al*, 2003). PKCε activity is inhibited by pharmacologically relevant concentrations of ethanol, and experiments employing photoactive alcohols and mass spectroscopy have identified an alcohol-binding site in a cysteine-rich regulatory region of PKCε (C1B), which is also its activator-binding domain (Das *et al*, 2009). These findings provide strong support that ethanol inhibits PKCε activity via direct binding. Again, to what extent a direct ethanol-enzyme interaction modulates the ethanol's effect on the GABAergic system is unclear. There is evidence that active PKCε phosphorylates the γ2 subunit of $GABA_A$ receptors, and that this mediates a suppression of allosteric activation (Qi *et al*, 2007). Thereby ethanol's inhibition of PKCε would serve to sensitize its own response. Increases in the active, phosphorylated form of PKCε have been shown to modulate acute functional tolerance (Wallace *et al*, 2007), perhaps representing a homeostatic cellular response to ethanol's inhibition of the enzyme.

PKCε also plays a crucial role in the surface expression of $GABA_A$ receptors. The adaptor protein 2 (AP2) interaction site on β1-3 $GABA_A$ subunits is phosphorylated by PKC, which regulates cell surface stability and endocytosis (Smith *et al*, 2012). Furthermore specific phosphorylation by PKCε activates the vesicular ATPase and trafficking factor, N-ethylmaleimide-sensitive factor (NSF) (Chou *et al*, 2010), which then translocates to the plasma membrane and to synapses, where it reduces the expression of $GABA_A$ receptors. Receptors of

different subunit composition show differential sensitivity to PKC-induced internalization (Connolly *et al*, 1999). Ethanol has been shown to alter $GABA_A$ receptor expression and subunit composition via PKC-γ and PKA-dependent mechanisms (Carlson *et al*, 2013; Kumar *et al*, 2010). Specific ethanol induced alterations in $GABA_A$ subunit composition potentially mediated by the ε isoform of PKC have not, to our knowledge, been reported—despite its role in mediating ethanol sensitivity. Regardless, these intracellular kinases collectively represent a potential means of neuronal adaptation to repeated ethanol exposures, including through cellular feedback to the synapse via receptor regulation.

2.2 Glycogen Synthase Kinase 3

In some cases ethanol has been shown to modulate protein kinase activity in the absence of an identified binding site. For example, at this point there is no evidence of ethanol directly targeting the serine-threonine kinase glycogen synthase kinase-3, however there is mounting evidence of ethanol-induced changes in GSK3 activity and downstream effects (French and Heberlein, 2009; Luo, 2010; Neznanova *et al*, 2009; Velazquez-Marrero *et al*, 2016).

2.2.1 GSK3B and Plasticity

An integrator of cellular signaling, glycogen synthase kinase-3 is also increasingly recognized as a major mediator of synaptic plasticity (Bradley *et al*, 2012; Peineau *et al*, 2008). There are two isoforms of GSK3, alpha and beta, encoded by different genes: *GSK3A* and *GSK3B* respectively (Woodgett, 1990).

These protein isoforms show a high degree of homology in their kinase domains but differ in other regions (Peineau *et al*, 2008). Each is analogously regulated by inhibitory phosphorylation of an N-terminal serine: Ser-21 in the case of GSK3A, Ser-9 for GSK3B (Sutherland and Cohen, 1994; Sutherland *et al*, 1993). Depending on the stimulatory context, this upstream phosphorylation can be carried out by Akt, protein kinase A, or protein kinase C (Fang *et al*, 2000; Tsujio *et al*, 2000). Dephosphorylation, resulting in activation of GSK3, is carried out by protein phosphatases 1 (PP1) and 2A (PP2A) (Salcedo-Tello *et al*, 2011). There is a secondary phosphorylation site on GSK3, Tyr216 and Tyr279, with a reported activating effect on the kinase activity (Frame *et al*, 2001). There is evidence that this tyrosine represents an autophosphorylation site and may be secondary to GSK3 activity (Cole *et al*, 2004).

Deletion of each GSK3 isoform produces distinct substrate phosphorylation profiles in mammalian cortical tissue, providing evidence for substrate specificity (Soutar *et al*, 2010). It should be said that nearly 100 proteins are at least proposed to be substrates for GSK3 (Sutherland, 2011), and so a full accounting of isoform-specific effects would require a costly phosphorylation panel. Regardless, Soutar et. al found that phosphorylation of tau and CRMP seemed to depend specifically on the beta isoform of GSK3, while c-Myc and β-catenin were regulated by both isoforms to an equivalent degree (Soutar *et al*, 2010). Both GSK3A and GSK3B are highly expressed in brain, particularly cortex and hippocampus (Salcedo-Tello *et al*, 2011). In adult rodents, GSK3B is the more abundant isoform in hippocampus (Lee *et al*, 2006), and is

more often investigated for its roles in long-term potentiation (LTP) and long-term depression (LTD) than the alpha isoform (Peineau *et al*, 2008). LTP and LTD constitute the two major of forms synaptic plasticity understood to underlie information storage in the CNS, accounting for synaptic strengthening or weakening based on recent patterns of activity. Most mechanisms of LTP and LTD have been studied (via electrophysiology) in the hippocampus, but appear to be utilized widely in the brain (Bliss *et al*, 2007).

The great majority of LTP- and LTD-exhibiting synapses are glutamatergic (Peineau *et al*, 2008). Synapses show NMDAR-dependent bidirectionality in synaptic response, with differing NMDA activity patterns inducing either LTP or LTD (Malenka and Bear, 2004). Using patch electrodes with a modifiable input and an output read-out of excitatory post-synaptic potential (EPSP), low frequency stimulation (LFS) can reliably induce LTD, an effect which is blocked by NMDA antagonism (Oliet *et al*, 1997). Peineau et al. (2007) have found that GSK3B activity is also necessary for this LFS induced LTD. The GSK3B inhibitor SB41528 showed no effect on baseline synaptic activity in rat hippocampal slices as measured by field EPSP, but 60 minutes after LFS, control slices showed synaptic activity of 65% (±5%) of baseline, while SB41528-treated slices maintained 103% (± 2%) of their baseline field EPSP (Peineau *et al*, 2007). The experimenters validated these findings using the GSK3B inhibitor kenpaullone which also abolished the LTD, and multiple doses of the less specific GSK3B inhibitor lithium, which showed dose dependent effects on LTD (Peineau *et al*, 2007). Using Western blots for the phospho-Ser9 form of GSK3B, Peineau et al.

found a decrease in inhibitory phosphorylation, indicating heightened GSK3B activity, in the CA1 area of the hippocampus during LTD. This effect lasted at least 20 minutes following the delivery of LFS, indicating heightened GSK3B activity may play a role in the maintenance of LTD (Peineau *et al*, 2007).

Perhaps the best characterized form of LTD depends on NMDAR activity as the stimulus and AMPA receptor regulation as the response. Phosphorylation and the subsequent removal of AMPA receptors from the synapse is the primary mechanism of the decrease in post-synaptic excitability observed in LTD (Kessels and Malinow, 2009). PSD-95, an abundant scaffolding protein in the post-synaptic density, mediates interactions of NMDA and AMPA receptors with the structure of the synapse (Scannevin and Huganir, 2000). Nelson et al. (2013) have provided evidence that the effect of GSK3B on LTD described above depends at least in part on the phosphorylation of PSD-95 on its threonine-19 (T19) residue. In rat hippocampal neurons, phospho-PSD-95-T19 was increased with LTD, while this effect was attenuated by pharmacologic suppression of GSK3B (Nelson *et al*, 2013). A non-phosphorylatable PSD-95 mutant (T19A) was found to resist internalization from dendritic spines, and overexpression of PSD-95-T19A led to impaired AMPA receptor internalization and impaired induction of LTD (Nelson *et al*, 2013). In combination with the Peineau et al. findings, it seems that low-frequency NMDAR stimulation increases GSK3B activity, which in turn phosphorylates the AMPA receptor anchor PSD-95, and phospho-PSD-95-T19 subsequently internalizes its associated AMPA receptors, thereby decreasing the synaptic strength.

A very similar mechanism has been described at GABAergic synapses, wherein GSK3B targets a unique phosphorylation site, Ser270, on the $GABA_A$ receptor scaffolding protein gephyrin (Rui *et al*, 2013; Tyagarajan *et al*, 2011). Tyagarajan et al. (2011) introduced point mutations to a then-uncharacterized phospho-site on gephyrin: S270A, a non-phosphorylatable mutant, and S270E, a phosphomimetic mutant. Neurons expressing these gephyrin mutants were assessed for dendritic gephyrin clustering and GABAergic activity. The non-phosphorylatable S270A mutant was associated with significantly higher degrees of gephyrin surface expression and corresponding GABAergic activity as measured by miniature inhibitory postsynaptic currents (mIPSCs) (Tyagarajan *et al*, 2011). Multiple protein kinase inhibitors were tested for their effect on gephyrin clustering in the gephyrin-270A transfected cells, and the GSK3B inhibitor GSK3-IX was found to reverse the aberrant phenotype (Tyagarajan *et al*, 2011). Rui et al. (2013) built upon these findings by transfecting a constitutively active GSK3B non-phosphorylatable mutant (GSK3B-S9A) into hippocampal neurons, and finding a decrease in $GABA_A$ receptor surface expression, which was rescued by the GSK3B inhibitory peptide GID5-6. Moreover, this decrease in $GABA_A$ surface expression corresponded with overall dendritic shrinkage in the GSK3B-S9A neurons—also rescued by GID5-6 (Rui *et al*, 2013). The authors contend that neurotrophin signaling normally acts to inhibit GSK3B via Ser9 phosphorylation and promote dendritic growth. Bath application of brain-derived neurotrophic factor (BDNF) to hippocampal neurons elevated phospho-GSK3B-S9 in the somatodendritic compartment, indicating BDNF inhibits GSK3B activity

(Rui *et al*, 2013). This increase in inhibitory phosphorylation was blocked with an inhibitor (K252a) of Trk, the BDNF receptor (Rui *et al*, 2013). (Rui *et al*, 2013).

Another BDNF-GSK3B interaction has been reported in the context of synaptic plasticity. The endocytosis enzyme dynamin 1 mediates activity dependent bulk endocytosis (ADBE), a method of large-scale synaptic vesicle (SV) retrieval via invagination of the presynaptic membrane (Clayton and Cousin, 2009). This is the dominant form of SV retrieval during high-intensity firing, presumably because it more efficiently recycles neurotransmitters from the synapse to maintain a stock supply in the highly active, neurotransmitter-releasing neuron (Clayton *et al*, 2010). To trigger ADBE, dynamin 1 must be de-phosphorylated by the calcium-dependent phosphatase calcineurin (Clayton *et al*, 2009). When the firing is complete, dynamin I is re-phosphorylated by cyclin dependent kinase 5 (cdk5) and GSK3B (Clayton *et al*, 2010; Evans and Cousin, 2007). This re-phosphorylation is what “loads” dynamin I to be ready to initiate ADBE upon the next instance of high-intensity firing (Smillie *et al*, 2013). Smillie et al. (2010) found that extracellular BDNF prevents this re-phosphorylation event by inhibition of GSK3B. Thus BDNF prevents the “run-down” of post-synaptic activity by arresting the usual recycling of neurotransmitters from the synapse back into the pre-synaptic membrane (Smillie *et al*, 2013). This indicates that when BDNF is released during high-frequency firing, neurotransmission is strengthened, albeit at the risk of neurotransmitter depletion in the pre-synaptic neuron.

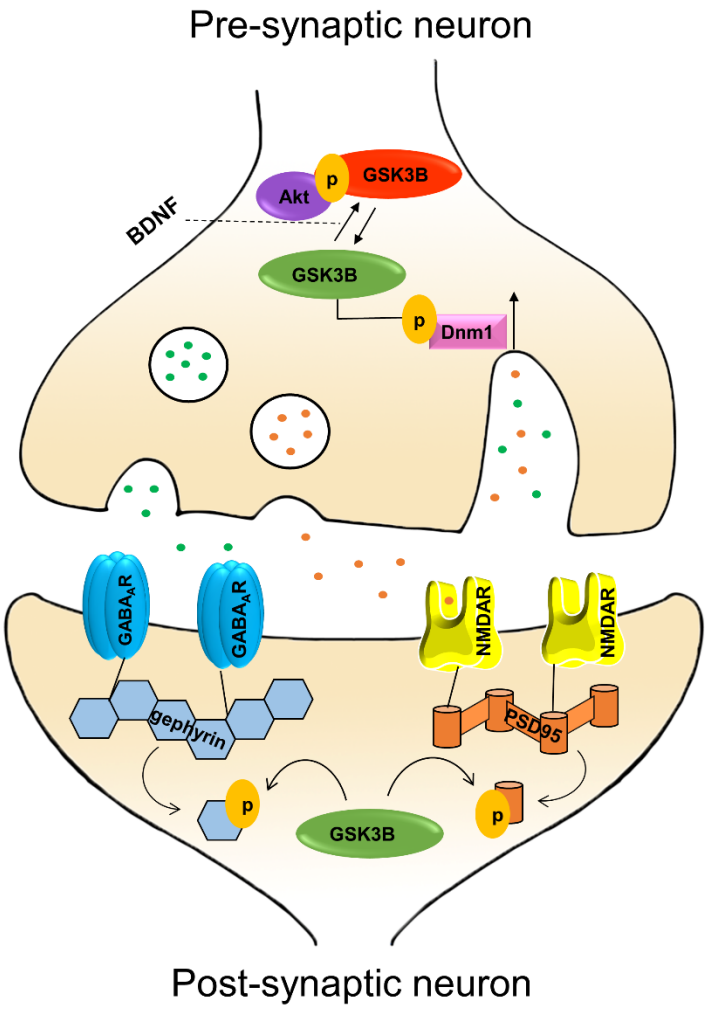

Figure 2.1. Regulation of pre- and post-synaptic dynamics by GSK3B. GSK3B phosphorylation of Dnm1 regulates activity dependent bulk endocytosis subject to regulation by BDNF. GSK3B phosphorylation of gephyrin and PSD95 is necessary for turnover of these scaffolding proteins.

In light of the above findings, a picture emerges of GSK3B as a consistent regulator of synaptic plasticity **(Figure 2.1)**. At both the post-synaptic and pre-synaptic membranes, GSK3B can regulate fundamental dynamics of membrane turnover in response to neuronal signaling. If there is a consistent directionality, it would be that GSK3B inhibition seems to correspond to a more stable synapse, while high GSK3B activity seems to correspond to a more dynamic synapse, characterized by receptor turnover. Oversimplification, however, must be cautioned against. It is unlikely that the role of GSK3B at the synapse is unidirectional. Regardless, GSK3B can function both pre- and post-synaptically to modify neurotransmission. The actual predominant action would be dependent on the type of synapse, state of activity, and coincident modulators (e.g. BDNF). These mechanisms discussed above should be kept in mind when considering the emerging evidence of GSK3B's role in addictive disorders.

2.2.2 GSK3B in Addiction and Neuropsychiatric Disorders

Miller et al. have demonstrated that cocaine activates GSK3B in the caudate putamen and nucleus accumbens (NAC) core, and that GSK3B activation is necessary for cocaine conditioned place preference (Miller *et al*, 2014). Inhibitory phosphorylation of GSK3B and the activating phosphorylation of the upstream kinase Akt were both decreased 30 minutes after an acute cocaine injection, while phospho-GSK3A-S21 was not significantly altered (Miller *et al*, 2014). The Akt de-phosphorylation, which would correspond to its disinhibition of GSK3B, was blocked by a D2 receptor antagonist specifically, while the GSK3B de-

phosphorylation was blocked by antagonists at D1, D2, or glutamatergic NMDA receptors (Miller *et al*, 2014). These results suggest that cocaine's activation of GSK3B occurs through convergent pathways, one of which is a D2-mediated inhibition of Akt. Moreover, Miller et al. found that administration of the GSK3B inhibitor SB216763 prevented the development of cocaine induced place preference, while showing no effect on acquisition of a contextual fear conditioning response. Thus cocaine's activation of GSK3B is not an incidental effect but rather a critical step in reward-based learning. As an extension of this work, Shi et al. studied the Akt/GSK3 pathway in the context of cocaine cue-induced memory reconsolidation, following conditional place preference (Shi *et al*, 2014). In mice that we re-exposed to an environment previously paired with cocaine, levels of phospho-Akt-T308, phospho-GSK3A-S21 and phospho-GSK3B-S9 were decreased in the NAC and hippocampus (Shi *et al*, 2014), indicating that re-exposure inhibited Akt and thus activated GSK3. Mice would typically re-exhibit a conditioned place preference for the previously cocaine-paired chamber, however treatment with SB216763 abrogated this response (Shi *et al*, 2014). Together with the above, these results suggest that GSK3B activation plays a key role in both the consolidation and re-consolidation of cocaine-associated memory.

The effects of GSK3B activity on reward-based learning serve as an additional layer atop previously established evidence for its role in the hyperlocomotor effects of cocaine and other stimulant drugs. Pharmacologic inhibition of GSK3B has been shown to attenuate hyperactivity produced by

acute injection of cocaine or amphetamine (Enman and Unterwald, 2012; Miller *et al*, 2009); and injection of a peptide decreasing S9 phosphorylation of GSK3B into the NAC enhances cocaine-induced hyper-locomotor activity while leaving basal locomotor activity unchanged (Kim *et al*, 2013). Urs et al. found that selective *Gsk3b* gene deletion from D2 receptor-expressing neurons attenuated amphetamine induced hyperlocomotion, while deletion from D1 receptor positive neurons had no effect on this phenotype (Urs *et al*, 2012). Thus it would seem that the D2-Akt-GSK3B pathway found to be activated by cocaine (Miller *et al*, 2014) might also underlie amphetamine induced hyperlocomotion.

In addition to stimulants, GSK3B has been studied in the context of morphine. Tolerance to the antinociceptive effects of a 10 mg/kg morphine dose for 8 days develops by 8 days of repeated administration, in Wistar rats assessed by tail-flick assay (Parkitna *et al*, 2006). This tolerance effect was prevented when morphine injections were preceded by an intrathecal administration of either the GSK3 inhibitor 216763 or the cdk5 inhibitor roscovitine (Parkitna *et al*, 2006). Moreover, a single administration of either inhibitor restored the antinociceptive effect of morphine in a dose-dependent manner, in rats previously tolerant to the morphine (Parkitna *et al*, 2006). These experiments seem to indicate that GSK3B activity underlies the development and maintenance of morphine tolerance. A subsequent study confirmed that chronic morphine treatment activates GSK3B in midbrain (Dobashi *et al*, 2010). Dobashi et al. also demonstrated that valproate, an anticonvulsant with GSK3B inhibition as one of many effects, can serve to attenuate morphine tolerance.

Psychomotor stimulants and morphine have all been found to activate GSK3B in brain, with this activation underlying some aspect of neuroadaptation. However, GSK3B activation does not appear to be a defining feature of drugs of abuse, as all reports of ethanol in adult brain find inhibition of GSK3B. Neznanova et al. found that an acute intraperitoneal (i.p.) injection of ethanol significantly increased phospho-GSK3B-S9 in rat medial PFC (Neznanova *et al*, 2009). The effect was observed in both alcohol accepting (AA) and alcohol non accepting (ANA) selectively bred rat lines, but the effect was more marked in the AA rat line—possible due to higher baseline GSK3B activity (Neznanova *et al*, 2009). Neasta et al. studied mouse NAC and similar found a significant increase in p-GSK3B-S9 as well as p-GSK3A-S21, after an acute i.p. injection of ethanol and to a lesser extent after long-term ethanol drinking (Neasta *et al*, 2011). Cheng et al. (2016) investigated distinct D1 and D2 receptor-dependent pathways in the dorsomedial striatum (DMS) following repeated cycles of binge-like ethanol consumption, and found that chronic ethanol increased GSK3B phosphorylation. This decrease in GSK3B activity occurred in conjunction with an enhancement of GABAergic signaling in this D2 receptor expressing neurons of the DMS, presumably through increased $GABA_A$ receptor surface expression (Cheng *et al*, 2016). Further, the authors delineated the D1 receptor dependent pathway as promoting ethanol consumption (“Go”) whereas the D2 receptor dependent pathway suppressed ethanol consumption (“No-Go”) (Cheng *et al*, 2016). The D2 agonist quinpirole applied to the DMS was found to decrease ethanol drinking as well as decrease GABAergic IPSPs, indicating disinhibition of

the No-Go pathway. Concurrent administration of the GSK3B inhibitor SB216763 attenuated both of these effects, indicating that D2-mediated activation of GSK3B normally serves to decrease $GABA_A$ receptor surface expression and activate the No-Go pathway (Cheng *et al*, 2016). When this pathway is disrupted via repeated ethanol binges, GSK3B is inhibited and in turn, the entire No-Go pathway is inhibited, via $GABA_A$ receptor build-up in D2 receptor positive neurons of the DMS (Cheng *et al*, 2016). It is interesting to consider that cocaine's activation of D2 receptor mediated activation of GSK3B underlies its rewarding effects, whereas ethanol's inhibition of GSK3B in D2-receptor neurons promotes ethanol consumption. How these seemingly disparate behavioral effects might relate to one another remains to be elucidated.

In developing neurons, there is evidence that high GSK3B activity sensitizes neurons to ethanol induced neurotoxicity. Ethanol induces excitotoxic cell death in Drosophila olfactory neurons, however genetic deletion or pharmacologic inhibition of GSK3B protects against this neurotoxic effect (French *et al*, 2009). Similarly, lithium is protective against ethanol induced neuroapoptosis in an animal model of fetal alcohol spectrum disorder (FASD) (Luo, 2010). It remains to be determined whether or to what extent ethanol induced excitotoxicity in sensitive neurons might actually serve to re-enforce ethanol self-administration.

Aside from ethanol-specific contexts, the role of GSK3B in neurodegeneration has been of significant clinical interest (Salcedo-Tello *et al*, 2011). The GSK3B mediated effects on tau phosphorylation are particularly

relevant to Alzheimer's Disease, the pathology of which is partially defined by hyperphosphorylated tau. Following pre-clinical studies of the novel GSK3B inhibitor tideglusib (Sereno *et al*, 2009), the FDA approved this drug for Phase II trials of Alzheimer's Disease and subsequently Progressive Supranuclear Palsy (Lovestone *et al*, 2015; Tolosa *et al*, 2014). Unfortunately, tideglusib did not achieve clinical efficacy through any of its primary endpoints, although it was determined to be well-tolerated, with the only adverse outcome a transient elevation of liver enzymes (Lovestone *et al*, 2015; Tolosa *et al*, 2014). There is evidence that oral tideglusib reduced the progression of brain atrophy in patients with progressive supranuclear palsy, as assessed by MRI, although this was as part of a secondary exploratory analysis (Hoglinger *et al*, 2014). At the time of this writing, tideglusib is in clinical trials for Autism Spectrum Disorders (ASD) (Anagnostou, 2018).

Preclinical studies have certainly pointed to GSK3B as a potential therapeutic target for psychiatric disorders (Jope and Roh, 2006). In 1996, it was discovered that lithium acts to potently inhibit GSK3B, while not inhibiting protein kinases generally (Klein and Melton, 1996). This would prove to be a precipitating finding for a line of investigation of the role of GSK3B in bipolar disorder, which has been largely born out (Luykx *et al*, 2010). Cortical GSK3B has consistently been shown to play a key role in mood-related phenotypes (Latapy *et al*, 2012; Urs *et al*, 2012). GSK3 is hyperactive in the hippocampus and cerebral cortex of Fmr1 knockout mice, and these mice show anxiety-like behavior during social interaction, which is ameliorated with chronic lithium

treatment (Mines *et al*, 2010). GSK3B inhibition, either pharmacologic or genetic, also rescued aberrant mood-related behaviors in *Tph2* knockin mice, which are serotonin-deficient in striatum, frontal cortex, and hippocampus (Beaulieu *et al*, 2008). Latapy et al. (2012) generated a CamKIIcre-floxGSK3B mouse to delete the *Gsk3b* gene postnatally in forebrain. These mice were shown to exhibit a marked reduction in basal anxiety via the open field test and light-dark emergence test (Latapy *et al*, 2012). A number of other studies have found that GSK3B inhibitors mimic the actions of antidepressants in the tail suspension test and forced swim test (Beaulieu *et al*, 2008; Can *et al*, 2011; Du *et al*, 2010; Gould *et al*, 2004; Kaidanovich-Beilin *et al*, 2004).

It should be noted that patients with psychiatric disorders are also at a much greater risk of developing substance use disorders and AUD, although extricating causality is complex. Overall, individuals with any mental disorder are 2.7 times more likely to have some addictive disorder (Regier *et al*, 1990). Among patients with alcohol dependence, the odds ratios of having a mood disorder is 3.6, bipolar disorder is 6.3, and generalized anxiety disorder is 4.6 (Kessler *et al*, 1996). Given the above findings in preclinical models, GSK3B activity in response to ethanol may correspond to a particularly relevant signaling pathway underlying addiction in patients with co-morbid psychiatric disorders.

2.3 Modeling Alcohol Use Disorder

Studies on ethanol exposure in animal models and AUD in humans have found a strong predictive relationship between responses to acute ethanol and

risk for long-term excessive consumption or abusive intake (Schuckit, 1994). Thus studies on initial sensitivity to ethanol in animals can provide insight into potential risk conferring pathways in humans. For example, low basal myelin expression confers ethanol sensitivity to mice (Farris *et al*, 2013; Kerns *et al*, 2005a), and so genotypes associated with altered myelin genes in humans might be predicted to confer risk for AUD.

Repeated cycles of ethanol exposure in mice, such as through the chronic intermittent ethanol (CIE) vapor model are associated with changes in gene expression (Smith *et al*, 2016), synaptic plasticity (Holmes *et al*, 2012), and gross changes in anatomic structure of cortical neurons (Beaudet *et al*, 2016). Together these neuroadaptations are believed to underlie the escalation in drinking (Griffin *et al*, 2009), tolerance to aversive symptoms of intoxication (Lopez *et al*, 2012) and withdrawal-like symptoms (Werner *et al*, 2009) observed in mice having undergone this model. However, it is a limitation of the model that it relies on involuntary exposures to ethanol vapor rather than allowing AUD-type pathogenesis to develop purely in the context of self-administration.

In mice strains with a predisposition to drink ethanol freely, such as C57BL/6J mice, a number of paradigms to intensify this phenotype have been explored (Crabbe, 2014). Generally these are modifications of two-bottle choice procedures, wherein mice have access to one water bottle and one bottle containing an ethanol solution. Drinking-in-the-dark (DID) paradigms utilize the 2 or 4-hour period of high activity early in the dark cycle, to give limited access of either a single ethanol bottle or a two-bottle choice period (Barkley-Levenson and

Crabbe, 2014). Intermittent ethanol access (IEA) allows for a full 24 hour period of ethanol access, using 2-bottle-choice, which leads to a substantial escalation in ethanol preference over water in C57BL/6J mice as well as C3H/HeJ mice (Barkley-Levenson *et al*, 2014). In either case the intermittent schedule encourages binge-like consumption that is not observed under constant ethanol access, 2-bottle-choice (Hwa *et al*, 2011).

Using these paradigms to model AUD-related behaviors, genetic techniques can be used to explore the role AUD candidate risk genes. Genetic deletion, or knockout (KO) mice allow for the study of a complete genetic loss of function, as in the case of μ-opiate receptor KO and CB1 receptor KO mice, both which have shown reduced ethanol consumption and preference (Hall *et al*, 2001; Thanos *et al*, 2005). Given innumerable potential compensatory mechanisms during development in the brains of constitutive KO mice, gene manipulation techniques which provide spatiotemporal specificity are preferred. Cre-loxP manipulation is widely used as a means to selectively delete (or express, by deletion of a stop cassette) genes of interest at a given time and in a cell-specific manner (Pina and Cunningham, 2017; Sauer, 1993). Cre recombinase is a bacteriophage-derived enzyme which performs site specific recombination at DNA recognition sites known as loxP sites. DNA located between these loxP sites is referred to as “floxed” and will be excised from the chromosome following Cre-mediated recombination (Nagy, 2000). To achieve deletion, animals with loxP sites selectively added, in order to flox a gene of interest, must be exposed to Cre. Cre can be delivered as a gene insert in a viral

vector: injection of the vector into tissue will result in transduction of the viral genome and subsequent Cre expression. In this case regional specificity is provided by the location of injection itself. Cellular specificity can be conferred by the viral serotype of the vector (Howard *et al*, 2008) and by the promoter driving the Cre transgene (Liu *et al*, 2008). However, size constraints can limit the effective use of many eukaryotic promoters (Shinohara *et al*, 2016).

An alternative Cre delivery is by chemically mediated induction. The most common of these are the tetracycline-inducible Cre-LoxP system and the tamoxifen-inducible Cre-loxP system (Feil *et al*, 2009); we will focus on the latter. The tamoxifen-inducible system uses a modified estrogen receptor (ER) with a strong affinity for tamoxifen, fused to Cre. In the absence of treatment the ER is sequestered in the cytosol by heat shock protein 90 (Hsp90) (Gunschmann *et al*, 2014). Upon tamoxifen treatment, tamoxifen binds the ER, releasing Hsp90, and the Cre-ER fusion protein translocates to the nucleus. In the nucleus Cre recombines the floxed gene, resulting in a knockout (Gunschmann *et al*, 2014). Under this system a high degree of cellular specificity is possible because the inducible Cre-ER gene can be inserted into the region of any promoter of interest (Feil *et al*, 2009). Selective breeding is then required to cross mice bred to carry floxed alleles with those bred to carry the Cre-ER gene under the promoter of interest. The convergence of a Cre-mediated knockout with specific cellular promoters allows the experimenter to investigate the role of a candidate gene as it functions only in a particular cell type. Furthermore when this method is complimented with viral-vector mediated studies, the combination of regional and

cellular specific readouts can serve to delineate a prospective pathway. In this dissertation we follow these lines of evidence in the context of GSK3B function in glutamatergic projection neurons and the promotion of excessive ethanol intake.

Chapter 3

Effects of Acute and Chronic Ethanol on the Genome

3.1 Introduction

Alcohol-use disorder is the complex result of a multitude of central nervous system (CNS) adaptations following long-term, repeated episodes of heavy ethanol consumption and withdrawal. Although AUD is a uniquely human trait possibly requiring decades to develop, key facets of ethanol-induced behaviors and cognate molecular adaptations following acute ethanol exposure can be studied across a spectrum of animal models including monkeys, mice, rats, flies, and worms (Becker and Hale, 1993; Bettinger *et al*, 2012; Bhandari *et al*, 2009). Each of these organisms demonstrates some type of tolerance to ethanol's effects, indicating a conserved tendency of the CNS to restore homeostasis. Changes in stress reactivity, gene expression, and neuronal signaling all accompany acute ethanol exposure and have been postulated to lead to chronic adaptation—essentially an allostatic imprint on the CNS (Costin *et al*, 2013; McBride *et al*, 2005).

In comparing biological pathways potentially mediating acute-to-chronic adaptation, it may be postulated that there exist several distinct response profiles:

(1) pathways which are acutely perturbed, but under tight homeostatic pressure to return to a baseline.

(2) pathways showing acute alterations which, upon repeated exposures, continue to show alterations, i.e. adapt to a new baseline.

(3) pathways which do not show any acute response, but are only induced upon chronic exposure.

The habituation of the hypothalamic-pituitary-adrenal (HPA) axis to stress is a quintessential example of the first type of response, with an induction of immediate early genes (i.e. c-fos) observed following an acute stressor, but a diminished or even absent response following repeated stressors (Melia, Ryabinin, Schroeder, Bloom, & Wilson, 1994). In the context of ethanol, its corticosterone-increasing effect has also been found to show such habituation (Seeley, Hawkins, Ramsay, Wilkinson, & Woods, 1996) as has the ethanol induced activation of serum glucocorticoid kinase 1 (Sgk1) (Costin et al 2013). Brain-derived Neurotrophic Factor (BDNF) has garnered considerable interest in mediating addictive aspects of ethanol, and its expression is acutely induced in the striatum, with a long-term blunting of this response following repeated ethanol exposure (Logrip, Janak, & Ron, 2009).

BDNF in the frontal cortex is an example of the second type of response. Its expression shows ethanol-induced reductions during intoxication, but unlike in striatum, these cortical perturbations can persist through chronic exposure and

withdrawal (Logrip *et al*, 2009; Smith *et al*, 2016). Wolstenholme et al. (2017) have found long-term changes in myelin-related gene expression in the PFC of mice repeatedly exposed to ethanol during adolescence. *Mag*, *Cnp*, *Pten*, and *Mpp* showed expression changes immediately following repeated adolescent exposure, which persisted into adulthood even without subsequent exposures (Wolstenholme *et al*, 2017).

The third type of response profile—changes observed only upon chronic exposure—is well evidenced by changes in the expression and localization GABA and NDMA receptors following chronic ethanol (Carpenter-Hyland *et al*, 2004; Papadeas and Grobin, 2001). While acute ethanol directly targets these receptors, it is only after long-term repeated exposures that changes in expression level and localization are observed.

The focus of this chapter will be on gene expression changes fitting response profiles (2) and (3). Genome-wide expression changes following an acute ethanol exposure will be compared to changes observed following chronic ethanol exposure, in the corticostriatal pathway. They will be assessed for overlap to identify transcriptional changes which are conserved from acute to chronic ethanol exposure, as well as those unique to the chronic treatment condition. The acute condition consisted of a single i.p. injection of ethanol (1.8 g/kg) or saline, while the chronic condition used the chronic intermittent ethanol (CIE) vapor model.

The chronic intermittent ethanol vapor model (CIE) has been widely used in rodent studies (Lopez and Becker, 2005; Lopez *et al*, 2012; O'Dell *et al*, 2004;

Roberts *et al*, 2000) as a tool to approximate the repeated cycles of heavy consumption and withdrawal that are seen in humans during development of AUD. CIE-exposed rats or mice will show alterations in the amount and pattern of ethanol consumption, generally increasing their ethanol consumption following CIE vapor exposure (Becker, 2013; Griffin *et al*, 2009; Lopez *et al*, 2005; O'Dell *et al*, 2004). Genomic studies have correlated patterns of gene expression following CIE with coincident changes in ethanol consumption (Osterndorff-Kahanek *et al*, 2013).

The CIE model provides a powerful tool for discovery and hypothesis testing of processes and mechanisms underlying progressive ethanol consumption. Its application to the recombinant inbred (RI) panel of BXD mice allows for additional insights to be made into genetic variation underlying changes in gene expression. The BXD panel, generated from crosses between C57BL/6J and DBA/2J, is currently the largest and best-characterized RI line, allowing for genomic mapping of quantitative traits to loci of allelic variation (Andreux *et al*, 2012). In this experiment we have used ethanol-induced expression change as the quantitative phenotype, thus generating expression quantitative trait loci (eQTLs) in both acutely and chronically treated animals.

Because variation in initial sensitivity to ethanol has itself been shown to confer risk in human alcoholism (Schuckit, 1994), identification of acutely ethanol-responsive genes might in itself be helpful in identifying human susceptibility loci. Assessing acutely responsive genes for overlap with chronic ethanol responsive genes might further identify those initial sensitivity genes with

continuing roles in CNS adaptation. Finally, analysis of ethanol-responsive genes within human genetic data provides a direct application of candidate gene discoveries to a patient population. This chapter concludes with this type of application, based on a gene network centered on *Gsk3b*.

3.2 Materials and Methods

Animals. Male and female C57BL/6J and DBA/2J mice for CIE experiments were purchased from Jackson Laboratory at 10 weeks old (Bar Harbor, ME). After 1-week acclimation to the animal facility, mice were singly housed for 72 h prior to the drinking experiments. Male and female BXD RI strains for CIE (n = 43 strains) at 12–16 weeks old were supplied by the University of Tennessee Health Sciences Center (Memphis, TN). BXD mice were single-housed immediately, and began the drinking experiments after 72-h acclimation to single housing. All mice were housed individually in an AALAC-accredited facility under 12-h light/dark cycles with free access to food and water. All animal housing and care was conducted in accordance with the NIH Guide for the Care and Use of Laboratory Animals (Council, 2011).

Chronic Intermittent Ethanol. Chronic intermittent ethanol procedures were performed at Medical University of South Carolina with approval by the Institutional Animal Care and Use Committee, according to well-established procedures shown to cause increased ethanol consumption (Lopez *et al*, 2005). Since the CIE model is a complex and time-consuming behavioral analysis, as an initial genetic analysis of CIE-evoked behaviors and gene expression

alterations, we utilized a design where single animals per strain/treatment were used for most strains to maximize the number of strains for genetic and genomic analysis. After 6 weeks of limited access (2 h/day) baseline drinking with 2-bottle choice 15% v/v ethanol and water, mice (n = 119) representing 43 BXD RI strains and progenitors were divided into two groups: CIE and control. CIE mice received ethanol vapor in Plexiglas® inhalation chambers (60 × 36 × 60 cm) for 16 h/day for 4 days. Control mice were also placed in the inhalation chambers for 16 h/day for 4 days, but did not receive ethanol vapor. After 4 days in the inhalation chamber, mice underwent 72 h of complete ethanol abstinence, followed by 5 days limited-access drinking (2-bottle choice 15% v/v ethanol and water, 2 h/day) (Lopez *et al*, 2005). This cycle was repeated such that BXD mice underwent four sessions of inter-cycle ethanol consumption and five sessions of inhalation chamber exposure. Ethanol levels in the inhalation chambers were set to produce blood ethanol concentrations of 200–300 mg/dL. Prior to each vapor chamber session, mice were injected intraperitoneally (i.p.) with 1 mmol/kg pyrazole, an alcohol dehydrogenase inhibitor used to stabilize blood ethanol concentration. Blood was collected from mice after the 3rd day in the inhalation chamber during each inhalation chamber cycle. Mice were sacrificed 72 h after the 5th inhalation chamber session. A schematic of the CIE protocol employed here is given in **Fig. 3.1**.

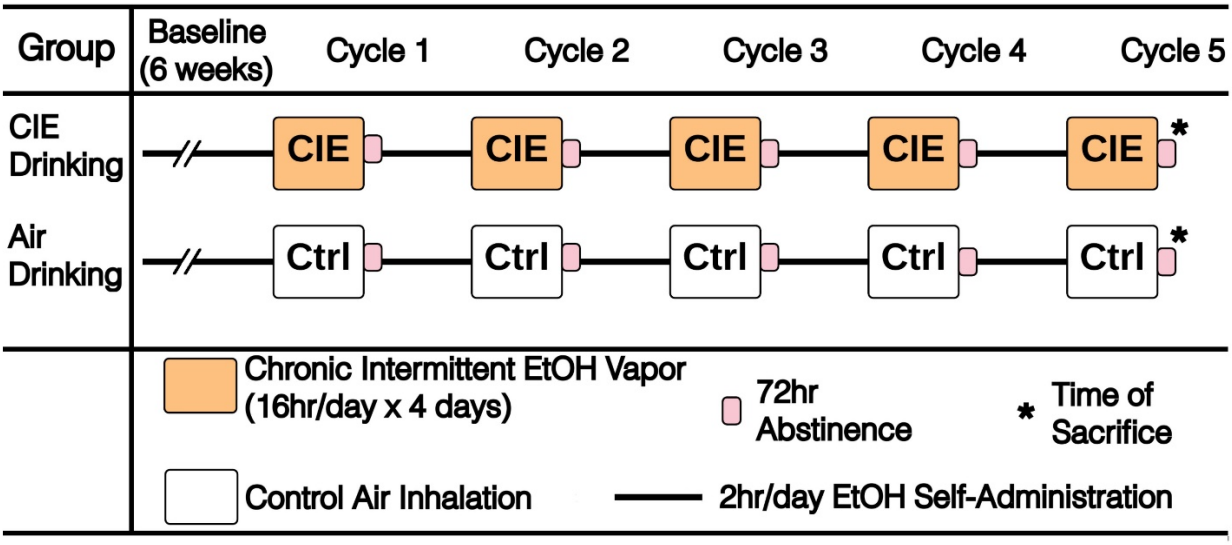

Fig. 3.1. Schematic of Chronic Intermittent Ethanol (CIE) model. Following 6 weeks baseline drinking, male and female BXD mice and their progenitors (n = 48) underwent 4 cycles of CIE by Plexiglas® vapor chamber 16 h/day × 4 days, 72 h ethanol abstinence, then 2-bottle choice drinking 2 h/day × 5 days. After the final cycle of CIE, mice were sacrificed 72 h after a 5th vapor-chamber session (van der Vaart *et al*, 2017).

Tissue Harvesting and RNA Isolation. Surviving mice (n = 72) were sacrificed 72 h after CIE procedures by cervical dislocation and decapitation. Brains were immediately removed, and specific regions dissected using a brain punch micro-dissection and snap freezing in liquid nitrogen. Tissue samples were shipped on dry ice to Virginia Commonwealth University, and stored at −80 °C until RNA isolation. Total RNA was isolated from prefrontal cortex (PFC) and nucleus accumbens (NAC), as described (Kerns *et al*, 2005b; Wolen *et al*, 2012). Briefly, brain tissue from individual mice (n = 72) was ground with a glass homogenizer, and RNA extracted using Stat 60 (AMS Biotechnology, Abingdon, UK). RNA quality was assessed by capillary gel electrophoresis with the Experion™ Automated Electrophoresis System (BioRad Laboratories, Hercules, CA). Samples showing poor RNA quality (i.e., RIN < 8, n = 2 for NAC, n = 3 for PFC) were eliminated from analysis.

For qPCR validation of *Dmn3*, NAC brain tissue from separate cohorts of C57BL/6J and DBA2/J mice having undergone the same CIE with drinking procedure described were used. Brain regions were harvested using brain punch micro-dissection as previously described (Kerns *et al*, 2005b). Brain tissues were immediately snap frozen in liquid nitrogen, and stored long-term at −80 °C. NAC tissue was lysed using Stat 60, and RNA was extracted with the Qiagen miRNeasy Mini Kit. RNA quality was assessed with the Experion™ System and RNA yield was determined using a NanoDrop 2000 UV spectrophotometer (Thermo Fisher Scientific, Waltham, MA).

CIE gene expression microarray analysis. Gene expression was quantified with Affymetrix GeneChip® Mouse Genome 430 2.0 arrays (Affymetrix, Santa Clara, CA). Arrays were run on PFC and NAC from 70 mice comprised of 19 BXD RI strains, C57BL/6J and DBA/2J progenitors, and C57BL/6J + DBA/2J F1 (n = 1–2 per strain per treatment group for BXDs, B6D2F1, C57BL/6UT, and DBA/2J; n = 6 CIE C57BL/6J; n = 8 CTL C57BL/6J; Supplemental Table 3.1). RNA samples from PFC and NAC were processed separately using standard protocols outlined by Affymetrix. RNA samples were randomized for cRNA preparation, and re-randomized before hybridization and scanning to minimize batch effects.

Mouse Genome 430 2.0 arrays were initially analyzed using Affymetrix Expression Console software. Array quality was assessed based on average background, scaling factor, present probesets, and 3′/5′ ratios of *Actin* and *Gapdh*. Robust multichip analysis (RMA) with quantile normalization was performed within the R statistical package for generation of normalized expression values from control and CIE-treated animals (Irizarry *et al*, 2003). CIE-responsive genes were identified within each brain region by using the Significance-score (S-score) algorithm (GeneNetwork Accession: GN:299 for PFC and GN:407 for NAC) (Kennedy *et al*, 2006; Kerns *et al*, 2003; Zhang *et al*, 2002). The S-score is a method developed to measure change in expression between compared oligonucleotide microarrays using probe-level data, and so is particularly suited to comparisons of smaller numbers of chips. The algorithm uses relative changes in probe-pair intensities to essentially create z scores

centered around zero for individual probesets, with values reflecting significance of expression change in the positive or negative direction. Thus, while not technically a measure of magnitude of expression change, S-scores generally correlate to fold change. S-scores were generated using the S-score R package from each BXD RI strain, C57BL/6J, DBA/2J, and C57BL/6J + DBA/2J F1 mice separately. Because only one CIE and one control sample was available for most BXD RI strains, significance of gene expression response across the BXD cohort was determined using Fisher's Combined Probability Test with S-scores as previously described (Wolen *et al*, 2012). Ethanol-"responsive" genes were identified as probesets with a q value < 0.05.

Comparison of CIE and acute ethanol genomic responses in BXD mice. CIE responsive genes identified by Fisher's Combined S-scores in the PFC and NAC were compared to probesets previously identified as responsive to acute ethanol exposure (4 h, 1.8 g/kg i.p., 6–8/strain) across 29 or 36 strains of the BXD RI cohort in PFC and NAC, respectively (GEO: GSE28515, GeneNetwork Accession: GN:137 for PFC and GN:154 for NAC) (Wolen *et al*, 2012). Overlap analyses were performed using GeneWeaver (Baker *et al*, 2012) and visualized with Venny (Oliveros, 2007). Overlaps of interest were Acute PFC vs. CIE PFC, Acute NAC vs. CIE NAC, and overlap between all four groups (two brain regions each with two treatment paradigms). Probesets exclusively regulated in the PFC with CIE, and exclusively regulated in the NAC with CIE, were also examined. Significance of overlap between pairwise combinations was determined using Fisher's test for count data (Fisher, 1922).

Pathway enrichment and gene ontology analyses of ethanol-responsive gene sets. ToppGene (http://toppgene.cchmc.org/), an open-source gene ontology analysis tool, was used for gene-set enrichment analysis for Gene Ontology (GO) terms among the Biological Process, Molecular Function, and Cellular Component categories. GO analyses were performed in June 2016. Results were filtered for FDR < 0.05 for all the comparisons to increase stringency of the analysis. Results were further filtered to remove terms containing fewer than two genes or greater than 1000 genes, and terms with similar definitions and gene lists were trimmed for clarity. Gene Ontology results were then summarized using REVIGO (http://revigo.irb.hr/). REVIGO reduces and summarizes GO results by clustering redundant terms into overarching categories representing biological functions (Supek *et al*, 2011). Ingenuity Pathways Analysis (Ingenuity Systems Inc., Redwood City, CA) was used to identify gene networks coordinately regulated exclusively by CIE in the PFC and NAC, or by acute ethanol and CIE within the PFC or NAC. Ingenuity Pathway Analysis (IPA) was also used to identify over-represented potential upstream regulators such as transcription factors that may be responsible for regulating expression of genes in the set. Networks were limited to 35 molecules, and scored by IPA based on the hypergeometric distribution, calculated using the right-tailed Fisher's exact test. Results were reported as the negative log of this value, such that a score of 20 indicates that there is a 1 in 10^{20} chance of producing a network containing at least the same number of genes of interest from 35 randomly chosen genes.

eQTL analyses of ethanol-responsive gene sets. Gene expression data in the form of S-score values for significant ethanol-responsive probesets (acute and CIE) were used as the quantitative trait values to be analyzed across the BXD cohort, and are accessible in GeneNetwork (GN299 for PFC and GN407 for NAC, www.genenetwork.org). GeneNetwork web-based tool sets were used for genetic mapping, and correlation of quantitative traits such as gene expression data and behavioral parameters (Wang *et al*, 2003). GeneNetwork employs genotype data from 3809 markers, selected based on their being informative (i.e., different between progenitor strains). GeneNetwork outputs peak "likelihood ratio statistic" (LRS) locations for each trait, which can be directly converted to log odds ratios (LOD) by dividing by 4.61. In our analysis, we defined "suggestive" eQTLs as markers with an LRS > 10 (LOD > 2.17) (Williams, 2012). This lenient threshold allowed for a high number of associations between genomic loci and ethanol-responsive transcripts, useful for an exploratory genetical genomics analysis. Within the subsets of suggestive eQTLs for a given brain region and treatment paradigm, significance of individual eQTLs was determined using permutation testing, wherein 5000 random reassignments of genotypes and trait values are compared to the actual observation. Genes were considered significant in the permuted data analysis at $p < 0.05$ (Williams and Broman, 2010). Cis-eQTLs were defined as loci within 5 Mb of the gene showing associated ethanol-responsive expression. To identify genomic regions regulating large numbers of ethanol-responsive genes, the genome was split into 10-Mb bins and the numbers of significant or suggestive eQTLs were counted

within each bin. In the absence of cis-eQTLs, QTLminer (Alberts and Schughart, 2010), which integrates gene annotations, expression, and single nucleotide polymorphisms (SNPs), was used within GeneNetwork to identify candidate regulatory genes. Within QTLminer, our *interval* was set as 1 Mb on either side of the peak LRS of interest; the strains for *nsSNP*s were set as DBA/2J and C57BL6/J. Input datasets were expression data from treatment of interest (acute or CIE). Dataset 1 used S-score, while Datasets 2 and 3 used RMA values of ethanol-treated and control animals, respectively. (http://www.genenetwork.org/webqtl/main.py?FormID=qtlminer)

Correlation of gene expression with ethanol-drinking behavior. To assess the relationship between ethanol-responsive gene expression and ethanol-drinking behavior across the BXD cohort, we correlated the average ethanol intake over the 5-day period of 2-bottle choice following the 3rd and 4th cycles of ethanol or air vapor exposure to gene expression (RMA values) in ethanol vapor-exposed (CIE, PFC GN:791, NAC GN:795) or air-exposed (control, PFC GN:789, NAC GN:793) mice. RMA values were generated using an SNP mask to remove probes and probesets that target regions of known SNPs between the D2 and B6 strains. Additionally, the RMA files were corrected for possible batch effects using the ComBat function (Johnson, 2007). These RMA files allowed us to identify probesets whose expression correlated with ethanol-drinking behavior in the ethanol-exposed animals, but not in controls. In each comparison, Spearman correlations were used, with *p* values for each probeset's correlation coefficient calculated using a two-tailed *t* test. The probesets were then ranked in ascending

order from the smallest *p* value. Spearman correlations with a *p* value < 0.05 were considered significant. GO analysis was performed using the ToppGene Suite (as described above) on the lists of significantly correlated genes in the air-exposed or the CIE-exposed mice in both the PFC and the NAC.

We also queried GeneNetwork for other BXD phenotypes related to ethanol consumption after the 3rd cycle of ethanol vapor treatment (GN:12967). The top 500 Spearman correlations were filtered for the term “ethanol” and *p* values < 0.05 were considered significant.

Quantitative real-time reverse transcription – qPCR. Total RNA (1 µg) from 18 DBA/2J and 20 C57BL/6J mice (n = 4–5/group) was reverse transcribed into cDNA using an iScript cDNA synthesis kit (Bio-Rad). Quantitative real-time PCR was performed using iQ SYBR Green Supermix and the CFX system (Bio-Rad), according to manufacturer’s instructions. Three technical replicates were performed for each cDNA, and relative abundance of target transcripts were normalized to *Ppp2a* and *Ublcp1* as reference genes using GeneNorm in the CFX software. Primers were designed to minimize secondary structure formation and cross intron-exon boundaries to reduce genomic DNA amplification. Primers were validated to produce a single PCR product via DNA gel electrophoresis (not shown).

Gsk3b Network Derivation. Microarray data for derivation of the acute ethanol *Gsk3b* correlation network have been previously reported (Putman *et al*, 2016; Wolen *et al*, 2012). Briefly, prefrontal cortex tissue samples were derived from a total of 468 animals across the BXD panel of inbred mice. An average of 8 mice

per strain were treated with either saline or 1.8g/kg ethanol. Four hours following treatment, animals were rapidly sacrificed by cervical dislocation, brains removed, chilled, microdissected and processed for RNA isolation (Kerns *et al*, 2005a). Affymetrix M430 type 2.0 microarrays were used for hybridization utilizing standard procedures. Expression response to ethanol was derived using the S-score method to compare ethanol vs. saline expression from pairs of arrays for each strain (Farris and Mayfield, 2014; Kerns *et al*, 2003; Zhang *et al*, 2002). The S-score is a method developed for Affymetrix oligonucleotide arrays that is particularly suited to comparing expression on a small number of chips. The S-score output for each probe set measures the change in expression between compared arrays is essentially a z-score centered around zero, with positive or negative S-scores reflecting ethanol-induced increases and decreases in gene expression, respectively. Genes correlating with Gsk3b at defined Pearson correlation cutoffs and random networks of genes of the same size were determined using weighted gene correlation network analysis (WGCNA) as described previously (Smith *et al*, 2016). The hub-like nature of *Gsk3b* (Wolen *et al*, 2012) in an ethanol responsive gene network was assessed and illustrated by selecting genes with an S-Score correlation greater than 0.9 and calculating edge weights between these genes using WGCNA (Langfelder and Horvath, 2008). Randomly selected groups of genes of the same number were also assessed with WGCNA. A minimum edge weight threshold of 0 was used so that all edge weights among 10000 random permutations of gene groups could be

counted and compared (after normalization) to the *Gsk3b* gene group. Graphics were created in the R statistical framework using ggplot2 (Wickham, 2009).

***Set-based Human Association Analysis*.** The Collaborative Study on the Genetics of Alcoholism (COGA) is a family-based study of alcohol dependence (Bierut *et al*, 2002). Full acknowledgement of COGA investigators is included below. COGA provided genotype information for this study but no new human subjects were recruited nor individual identifier information disclosed. Alcohol-dependent probands were identified through inpatient or outpatient alcohol treatment programs at seven sites around the United States (Reich, 1996). All individuals aged 18 or older were interviewed using the Semi-Structured Assessment for the Genetics of Alcoholism (SSAGA) (Bucholz *et al*, 1994; Hesselbrock *et al*, 1999). From this sample, an independent case-control sample was selected for a genome-wide association study (GWAS), with genotyping conducted by the Center for Inherited Disease Research using the Illumina 1 million SNPchip platform. Genome wide data was generated on 2000 individuals, 1905 (1022 males 883 females) of which remained after all data cleaning (Bierut *et al*, 2010). All 1205 cases met criteria for DSM-IV Alcohol Dependence, as assessed by the SSAGA, and all 700 controls were screened against Alcohol Dependence and related substance use disorders. The program Plink (Purcell *et al*, 2007) was used to conduct all association tests. Logistic regression association analyses were conducted using an additive genetic model. Sex and two principal components to adjust for race were used as covariates in analyses.

Human homologs of genes correlating with *Gsk3b* in ethanol-induced microarray expression change in mouse mPFC were selected for association analysis. Groups of genes correlating ≥ .80, ≥ .85, ≥ .90, and ≥ .95 with S-scores of *Gsk3b* responses to ethanol were assessed for risk-conferring SNPs, with a p-value<0.05 defined as significant in these gene group-based analyses. SNPs located within the genes, as well as SNPs 2Kb up and downstream from the genes were included. For analyses on individual genes, a slightly stricter p-value of <0.01 defined as risk-conferring. P-values of SNP sets were determined empirically by random resampling (10000 permutations).

3.3 Results

Identification of significant ethanol-responsive gene expression following CIE. Chronic intermittent ethanol by vapor chamber significantly affected gene expression across the BXD cohort in both the PFC and NAC. In all, the expression of 759 genes in the PFC and 867 genes in NAC were ethanol-responsive by CIE at a significance level of $q < 0.05$ (Supplemental Table 3.2). We previously found that an acute dose of ethanol significantly altered 1479 genes in PFC and 1373 genes in NAC (Wolen *et al*, 2012), using a similar genomic and statistical approach. In this study, we compared the probesets altered by acute ethanol to our CIE findings (**Fig. 3.2**, Supplemental Table 3.3) to gain potential insights into conserved vs. unique mechanisms of CIE-induced expression changes. The degree of overlap between ethanol-responsive probesets was significant ($p < 0.05$) by Fisher's exact test, when comparing treatment paradigms (Acute PFC vs. CIE PFC, Acute NAC vs. CIE NAC). In the

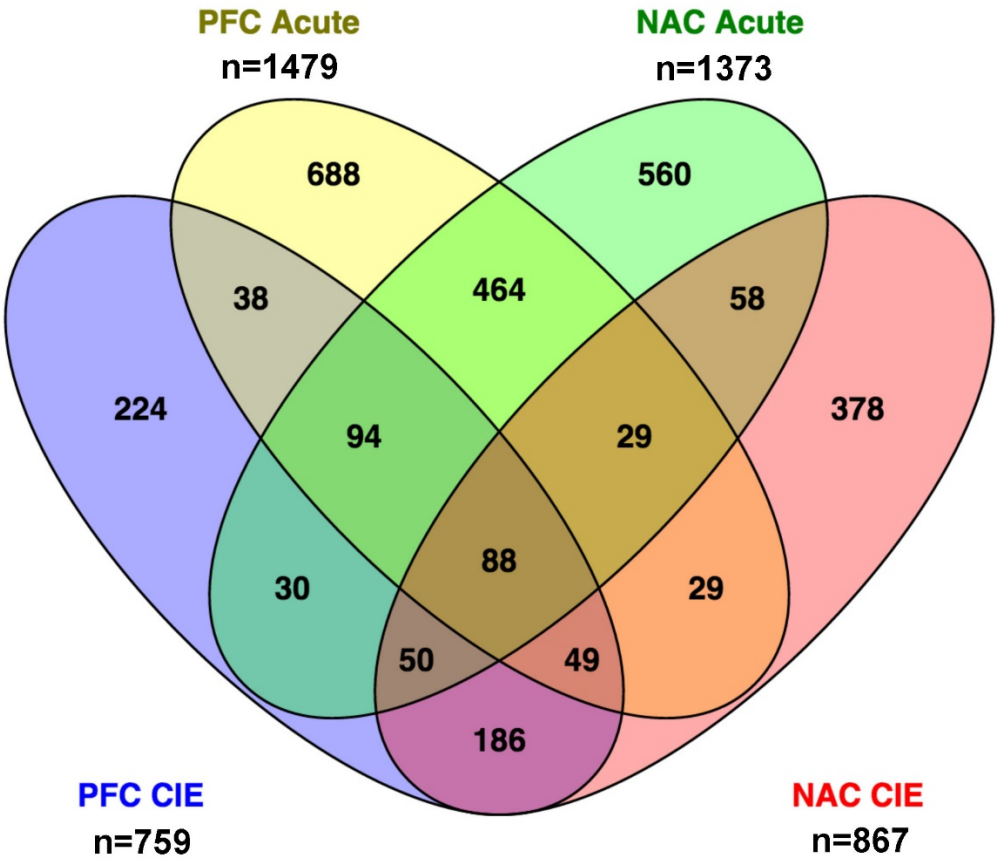

Geneset	# probesets
CIE PFC exclusive	224
CIE NAC exclusive	378
CIE PFC ∩ Acute PFC	269
CIE NAC ∩ Acute NAC	225
CIE PFC ∩ Acute PFC ∩ CIE NAC ∩ Acute NAC	88

Fig. 3.2. CIE-responsive genes overlap with acute ethanol responsive genes. Gene expression response to CIE or acute ethanol was measured by Fisher's combined S-scores in the PFC and NAC. Ethanol-responsive genes were defined as those with *p* values ≤ 0.05. CIE-responsive genes identified were compared to probesets previously identified as responsive to acute ethanol exposure across the BXD RI cohort in PFC and NAC. Both pairwise and hierarchal overlap was examined. Significance of overlap between each pairwise combination was determined using Fisher's test for count data (Fisher, 1992).

PFC, ~35% of CIE-responsive probesets were also significantly responsive to acute ethanol (n = 269 probesets), while in NAC ~26% of CIE-responsive probesets were also responsive to acute ethanol (n = 225 probesets). We found 224 probesets unique to the CIE PFC, and 378 unique to CIE NAC, representing effects specific to brain region and to chronic ethanol.

Bioinformatic analyses of gene sets in the PFC and NAC following CIE or acute ethanol. Bioinformatic analysis using ToppGene or Ingenuity Pathway Analysis was performed to identify significantly over-represented biological themes within gene sets (see Supplemental Tables 3.4–3.8). Five gene sets developed from our overlap analyses were queried: **(1)** genes unique to CIE PFC, **(2)** genes unique to CIE NAC, **(3)** overlapping genes between acute PFC and CIE PFC, **(4)** overlapping genes between acute NAC and CIE NAC, and **(5)** overlapping genes between both treatment conditions in PFC and NAC.

(1) Genes exclusively regulated by chronic ethanol in the PFC

224 probesets were modulated by only CIE and exclusively in the PFC (Supplemental Fig. 3.1 and Supplemental Table 3.4). Five molecular functions were significantly over-represented: protein complex binding, cytoskeletal protein binding, MHC II receptor activity, cell adhesion molecule binding, and calmodulin binding. Of the 51 Biological Process categories identified, the major themes are involved in action potentials and synaptic transmission, antigen processing and presentation, dopamine receptor signaling, and brain developmental processes, including locomotor behavior and learning.

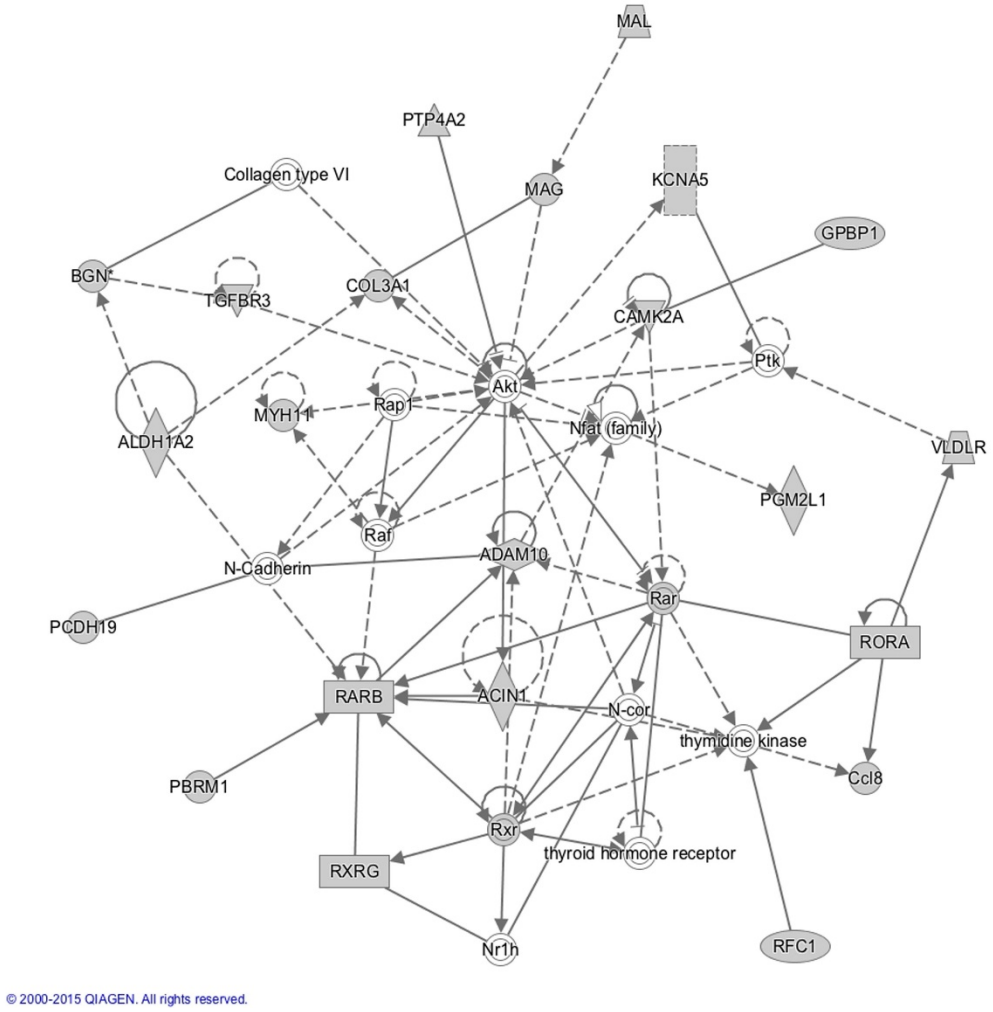

Fig. 3.3. Network of genes exclusively regulated by CIE in the PFC. Gene network was generated by Ingenuity Pathways Analysis (www.ingenuity.com). Solid arrowheads reflect “acts on” interactions while lines without arrows indicate binding interactions only. Solid and dotted lines indicate, respectively, direct vs. indirect interactions.

Ingenuity Pathway Analysis (IPA) generated several novel networks, one of which (**Fig. 3.3**) contained CaM kinase II and two myelin-associated genes (*Mag* and *Mal*), with Akt as the major integration point. Two types of collagen and N-Cadherin were also in this pathway. The top upstream regulators of this gene set were Huntingtin (HTT), which regulates 32 of the 193 genes analyzed ($p = 1.22 \times 10^{-15}$), and β-estradiol, which may regulate 39 out of 193 genes in the set ($p = 4.06 \times 10^{-10}$).

(2) Genes exclusively regulated by chronic ethanol in the NAC

378 probesets were exclusively altered by ethanol in the NAC only following CIE (Supplemental Fig. 3.2 and Supplemental Table 3.5). Only three Molecular Function categories were significantly over-represented: neuropeptide hormone activity, phorbol ester receptor activity, and protein heterodimerization activity. Substantially more Biological Processes were identified (55 categories) and can be described by the main themes of synaptic transmission, negative regulation of cell death, neuron projection development, behavior, including behavioral fear response, learning or memory, and regulation of nervous system development. The 10 significant Cellular Component categories reflect many parts of the neuron or synapse including the synapse, axon, dendrite, and synaptic vesicles. An additional category from ToppFun is the Mouse Phenotype. For genes altered by ethanol in NAC of CIE BXD mice, significant results in the Mouse Phenotype category highlight potential problems in neurological function: abnormal fear/anxiety-related behavior, synaptic transmission, increased susceptibility to induction of seizure, abnormal learning/memory/conditioning, and

locomotor activation. These phenotypic categories are consistent with the gene ontology findings discussed above.

IPA analysis identified gene networks that involved genes within the synapse, BDNF, and GABA receptor subunits. CREB1 was identified as the top upstream regulator with 34 genes potentially regulated out of 304 in the analysis ($p = 1 \times 10^{-14}$).

(3) Genes regulated by both acute and chronic ethanol in PFC

In the PFC, 269 probesets were in common after overlapping gene sets from the CIE protocol and acute ethanol (Supplemental Fig. 3.3 and Supplemental Table 3.6). Thirty-eight identified Molecular Functions included some rather diverse categories, including mRNA binding, syntaxin binding, GABA-A receptor activity, calcium-dependent protein binding activity, voltage-gated potassium channel activity, toll-like receptor 4 binding, and structural constituent of the myelin sheath. Over-represented Biological Processes (109 categories) were complementary to the Molecular Function categories and included synaptic transmission, mRNA processing, learning or memory and cognition, neurotransmitter secretion, and axon development. Similarly, the 43 categories from the Cellular Component analysis identified many specific parts of the neuron (somatodendritic compartment, synapse, dendrite, neuronal body, dendritic spine, and post-synaptic membrane). These also included ion channel complexes, voltage-gated potassium channel, SWI/SNF family complex, GABA-A receptor, nuclear chromatin and myelin sheath, and axonal region. Mouse

Phenotypes identified abnormalities in synaptic transmission, specifically miniature EPSCs, learning, memory and cognition, and abnormal gait.

(4) Genes regulated by both acute and chronic ethanol in the NAC

In the NAC, 225 probesets were similarly regulated by ethanol following acute ethanol and the CIE protocol (Supplemental Fig. 3.4 and Supplemental Table 3.7). Surprisingly, no Molecular Functions were significantly over-represented in the ToppFun analysis. However, 91 categories in the Biological Processes were significantly over-represented. These categories included such processes as synaptic transmission, neurotransmitter secretion, behavior, CNS development, and glutamate receptor signaling. Again, categories identified in the Cellular Component analysis (29 categories) identified many parts of the neuron including neuron projection, synapse, clathrin-coated vesicles, GABA and glutamate transport vesicles, dendritic spine, and neuronal cell body. Similar to the PFC, Mouse Phenotypes identified were primarily abnormalities in learning and memory, synaptic transmission, miniature EPSCs, and synaptic depression.

The novel networks identified by IPA were again similar in theme and generated networks containing calcium-channel and glutamate-receptor subunits along with synapse structural components (**Fig. 3.4**). Upstream regulators of these genes were similar to the regulators of PFC genes regulated by CIE and acute ethanol: HTT (28 genes/191 analyzed, $p = 2.6 \times 10^{-12}$), BDNF (18 genes/191 analyzed, $p = 5.8 \times 10^{-11}$) and HDAC4 (11 genes/191 analyzed, $p = 1.12 \times 10^{-9}$).

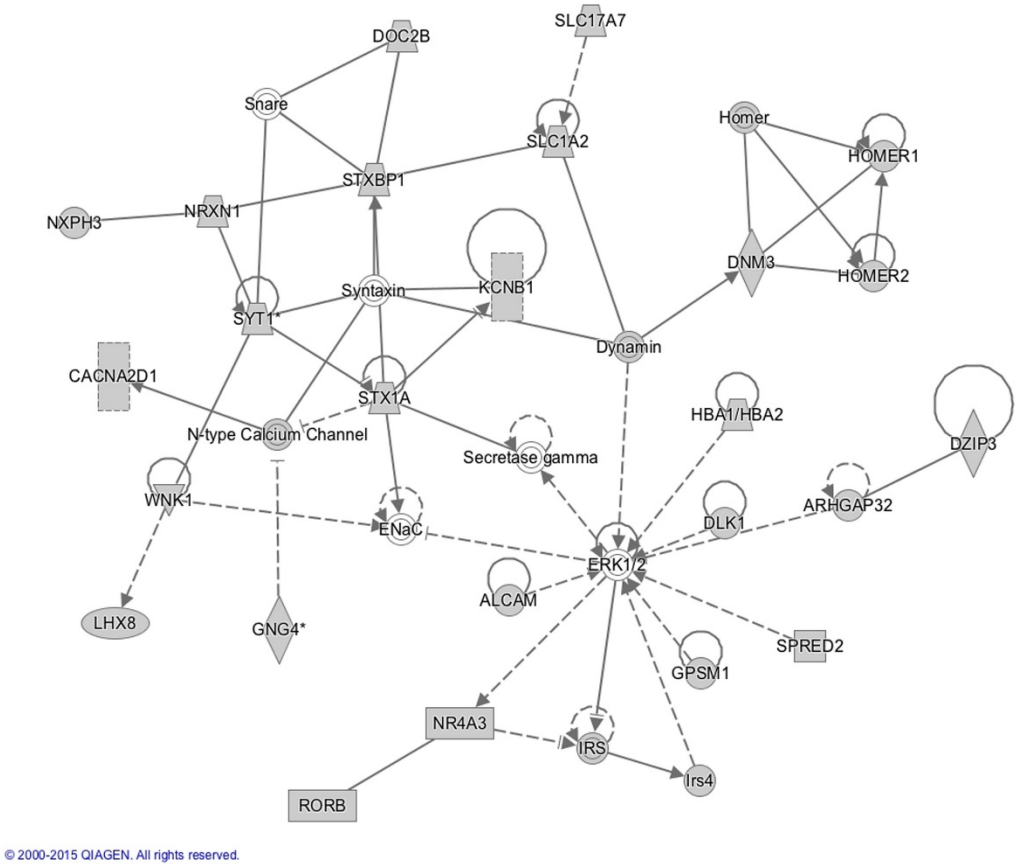

Fig. 3.4. Top-ranked network in the NAC, regulated by both acute and chronic ethanol. Gene network enriched in genes involved in synapse structural components and calcium channels was generated by Ingenuity Pathways Analysis (www.ingenuity.com). Solid arrowheads reflect “acts on” interactions while lines without arrows indicate binding interactions only. Solid and dotted lines indicate, respectively, direct vs. indirect interactions.

(5) Genes regulated by acute and chronic ethanol in both PFC and NAC

We were also interested in examining the genes which were in common between both PFC and NAC in regulation by acute ethanol and CIE (Supplemental Fig. 3.5 and Supplemental Table 3.8). We reasoned that this group might reflect genes with a particular sensitivity to ethanol pharmacology, based on their regulation across region and paradigm. Eighty-eight probesets were similarly regulated by both ethanol protocols in both brain regions (**Fig. 3.2**). GO analysis identified 16 Biological Process categories (enzyme regulator activity, protein-domain specific binding, SMAD binding, voltage-gated cation channel activity, calmodulin binding, and GTPase regulator activity). The 56 Molecular Function categories were similar in theme to the previous gene set comparisons and included synaptic transmission, neurotransmitter transport, signal release, regulation of calcium ion transport, and regulation of hormone levels, as well as learning and memory. However, there were unique categories that included receptor clustering and DNA methylation. Mouse Phenotypes found abnormalities in synaptic transmission, miniature EPSCs, and learning and memory.

Each of the top novel networks generated by IPA contained either CREBBP, FOS and NEDD4, or voltage-gated potassium channel subunits and structural components of the synapse. Importantly, the genes regulated by CIE and acute ethanol in the PFC and NAC shared several upstream regulators with the PFC or NAC alone and included HTT (15 genes/78 analyzed, $p = 9.5 \times 10^{-9}$),

BDNF (10 genes/78 analyzed, $p = 7.35 \times 10^{-8}$), and HDAC4 (6 genes/78 analyzed, $p = 1.64 \times 10^{-6}$).

eQTL analyses of ethanol-responsive genes. In addition to assessing overlap of the mRNA transcripts with ethanol-induced expression changes, we sought to define genetic intervals associated with genome-wide expression changes, following acute or chronic ethanol in either the PFC or NAC. Cis eQTLs are chromosomal regions associated with altered expression of genes located within the same region (<10 megabases), while trans eQTLs are chromosomal regions associated with gene expression changes across the genome (distal to the genetic variant).

PFC

We used S-scores as a measure of ethanol-induced expression change. When S-scores were analyzed as a quantitative genetic trait, we found that 633 probesets with significant ethanol responses in the CIE PFC showed at least a suggestive (LRS ≥ 10) eQTL, with 15 of these reaching empirical significance ($p < 0.05$, Supplemental Table 9). S-scores avoid the potential false-positive cis-eQTLs that can result from genetic polymorphisms affecting probeset hybridization performance (Wolen *et al*, 2012). In PFC, none of the observed eQTLs were cis-regulated. Top trans eQTLs in PFC from CIE or acute ethanol (Wolen *et al*, 2012) treatment are shown in **Table 3.1**, ranked by LRS. There was no overlap between the two lists of top-ranked eQTLs.

Table 3.1: PFC—ten highest ranked eQTLs (by LRS), CIE and acute. All significant eQTLs identified in the PFC were trans.

CIE				
Probeset	*Gene*	*Location (Chr: Mb)*	*Max LRS*	*Max LRS Location (Chr: Mb)*
1438012_at	*Ppm1l*	Chr3: 69.358475	23.3	Chr16: 97.799871
1422546_at	*Ilf3*	Chr9: 21.198197	23.3	Chr16: 11.886515
1432269_a_at	*Sh3kbp1*	ChrX: 156.266314	23.1	Chr16: 97.617114
1423506_a_at	*Nnat*	Chr2: 157.387623	22.8	Chr7: 67.179978
1436098_at	*Bche*	Chr3: 73.439883	22.6	Chr7: 57.048459
1426543_x_at	*Endod1*	Chr9: 14.160201	22.6	Chr16: 97.799871
1448380_at	*Lgals3bp*	Chr11: 118.254260	22.2	ChrX: 48.285597
1458263_at	*Cugbp2*	Chr2: 6.494081	21.9	Chr1: 194.086272
1460218_at	*Cd52*	Chr4: 133.649510	21.7	ChrX: 56.488673
1418580_at	*Rtp4*	Chr16: 23.613274	21.6	ChrX: 48.285597
Acute				
1442026_at	*Zbtb16*	Chr9: 48.460145	26.4	Chr7: 35.483869
1418508_a_at	*Grb2*	Chr11: 115.505490	26.4	Chr13: 54.980446
1431028_a_at	*Pank1*	Chr19: 34.886667	23.7	Chr11: 58.057819
1427345_a_at	*Sult1a1*	Chr7: 133.816669	22.1	Chr2: 162.978274
1448534_at	*Ptpns1*	Chr2: 129.456079	22	ChrX: 70.273782
1450056_at	*Apc*	Chr18: 34.477683	21.9	Chr16: 67.888886
1417409_at	*Jun*	Chr4: 94.716397	21.7	Chr1: 20.623897
1451403_at	*Ppp1r37*	Chr7: 20.116409	21.7	Chr13: 52.866221
1434661_at	*Syngr1*	Chr15: 79.949377	21	Chr13: 54.980446
1452958_at	*Asphd2*	Chr5: 112.814574	20.4	Chr7: 25.722934

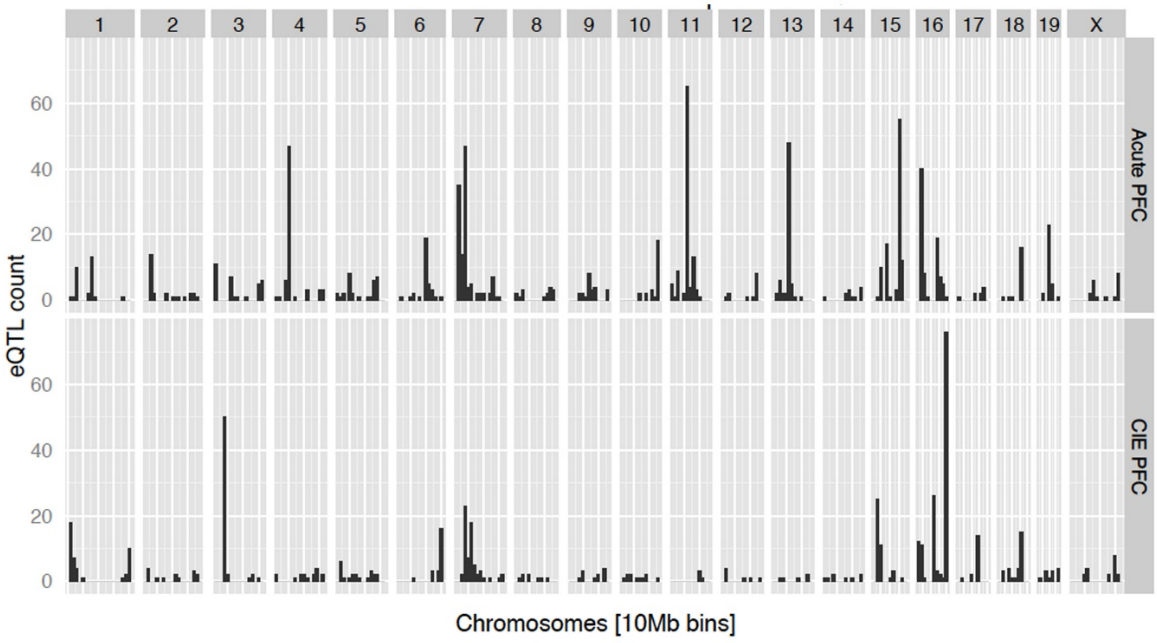

Fig. 3.5. PFC—eQTLS regulated by acute and CIE. Histograms of significant or suggestive eQTLs (LRS > 10) across the genome, divided into 10-Mb bins. In the eQTL analyses, transcripts were filtered by significant ethanol response ($p < 0.05$) in PFC following acute or chronic ethanol. Ethanol vs. control S-score was used as the trait of interest.

Histograms of the number of ethanol-responsive genes with suggestive or significant eQTLs in 10-Mb chromosomal bins are shown in **Fig. 3.5**. In the CIE PFC experiment, large peaks representing “trans-bands” were seen on Chr3 (peak LRS: 39.9 Mb) and Chr16 (peak LRS: 97.8 Mb). Highly suggestive (LRS > 18) trans-regulated genes at the Chr3 locus were *Ube2b, Cplx2*, and *Smarca4*. Significant trans-regulated genes at the Chr16 locus were *Ppm1l, Ilf3, Shk3kbp1, Endod1,* and *Syn2*. Analysis by QTLminer within GeneNetwork suggested that the highest-ranked candidate regulatory gene within 1 Mb of the Chr3 peak was the cell adhesion molecule, FAT tumor suppressor homolog 4 (*Fat4*). The highest-ranked candidate gene for the Chr16 peak was Down syndrome cell adhesion molecule (*Dscam*). There was minimal overlap between the acute PFC eQTL bands and the CIE PFC bands, which may indicate distinct sites of genomic regulation of ethanol-responsive transcripts in acute vs. chronic ethanol in the PFC. All ethanol-responsive eQTLs in PFC with LRS ≥ 10 following acute or CIE ethanol treatment are given in Supplemental Tables 3.9–3.10.

NAC

In CIE NAC, 699 probesets with significant ethanol response showed at least a suggestive eQTL with 69 of these reaching empirical significance ($p < 0.05$, Supplemental Table 11). There was one significant cis-eQTL, Nuclear Receptor Subfamily 2, Group C, Member 2 (*Nr2c2*) (eQTL map shown in **Fig. 3.6**). There were four suggestive cis-eQTLs: *Pcolce, Dnm3, Gfap,* and *Fbxo39*. Top-ranked eQTLs from CIE treatment are compared to those from acute ethanol (Wolen *et al*, 2012) in **Table 3.2**.

Table 3.2: NAC—ten highest ranked eQTLs (by LRS), CIE and acute.

CIE				
Probeset	*Gene*	*Location (Chr: Mb)*	*Max LRS*	*Max LRS Location (Chr: Mb)*
1420957_at	*Apc*	Chr18: 34.472690	31.9	Chr6: 92.514677
1452360_a_at	*Jarid1a*	Chr6: 120.362354	28.6	Chr6: 94.596952
1419127_at	*Npy*	Chr6: 49.773622	28.5	ChrX: 147.758346
1456656_at	*Lin7a*	Chr10: 106.859723	27.4	Chr6: 94.596952
1422164_at	*Pou3f4*	ChrX: 108.010303	27.1	Chr4: 16.419441
1424504_at	*Rab22a*	Chr2: 173.530582	26	Chr6: 94.596952
1435635_at	*Pcmtd1*	Chr1: 7.150977	25.3	Chr6: 92.514677
1421738_at	*Gabra2*	Chr5: 71.352858	24.2	Chr6: 94.596952
1425014_at¥	*Nr2c2*¥	Chr6: 92.117447	24.2	Chr6: 92.514677
1431020_a_at	*Fgfr1op2*	Chr6: 146.546009	24.2	Chr19: 28.477768
Acute				
1440901_at	*Dgkb*	Chr12: 38.863144	26.9	Chr3: 10.327101
1447454_at	*Kif5c*	Chr2: 49.485000	26.7	Chr18: 3.516538
1425382_a_at	*Aqp4*	Chr18: 15.551957	26.2	Chr3: 10.327101
1429882_at	*Cdh11*	Chr8: 19.687909	26	Chr18: 3.516538
1438069_a_at	*Rbm5*	Chr9: 107.662114	24.9	Chr3: 10.327101
1421933_at	*Cbx5*	Chr15: 103.026753	24.8	Chr12: 28.507707
1433413_at	*Nrxn1*	Chr17: 91.488263	24.2	Chr3: 10.327101
1440439_at	*Jazf1*	Chr6: 52.961885	23.9	Chr18: 3.516538
1421905_at	*Ncoa6ip*	Chr4: 3.502142	23.8	Chr3: 10.018672
1445717_at	*Luc7l2*	Chr6: 38.548642	23.1	Chr17: 27.985169

¥ = cis eQTL

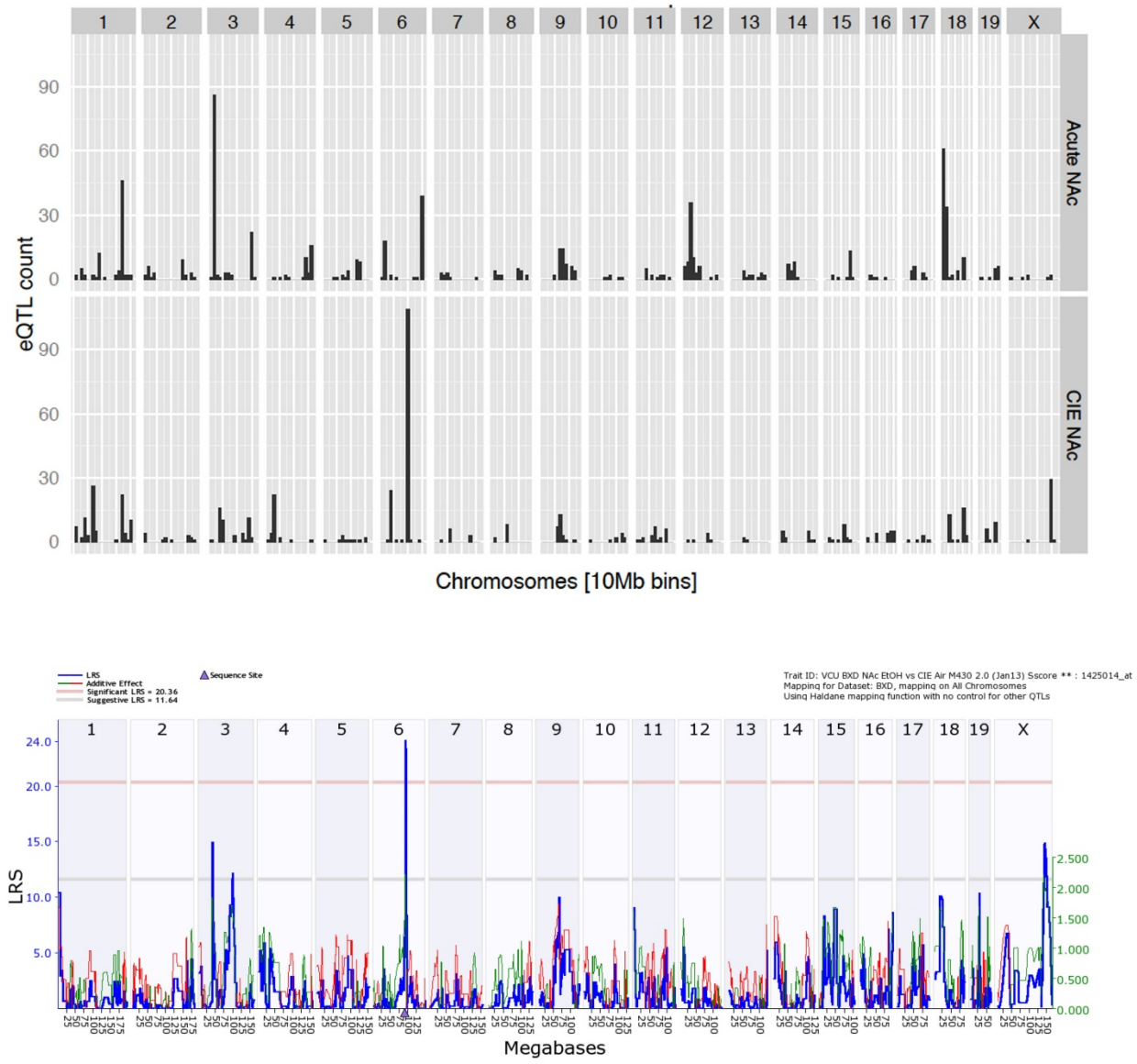

Fig. 3.6. NAC—eQTLS regulated by acute and CIE. (Top) Histograms of significant or suggestive eQTLs (LRS > 10) across the genome, divided into 10-Mb bins. In the eQTL analyses, transcripts were filtered by significant ethanol response ($p < 0.05$) in NAC following acute or chronic ethanol. Ethanol vs. control S-score was used as the trait of interest. (Bottom) Mapping of *Nr2c2* S-Score shows significant peak at its own locus (purple triangle at bottom of peak), demonstrating a cis eQTL.

Histograms of the number of ethanol-responsive genes with suggestive or significant eQTLs in 10-Mb bins are shown in **Fig. 3.6**. In CIE NAC, a large peak, corresponding to 109 ethanol-responsive transcripts, was observed on Chr6:90–100Mb. This locus was also the site of the significant *Nr2c2* cis-eQTL, indicating that this gene may play a role in regulating the ethanol-induced expression changes of a large number of genes. 34 trans-eQTLs were significantly linked to this region, including *Apc*, *Gabra2*, *Slc1a2,* and *Homer1.* All significant eQTLs at this locus are shown in **Table 3.3**.

In both the acute and chronic treatments, a trans-band was observed at Chr1:160–170Mb; however, the ethanol-responsive transcripts regulated at this site differed between the treatment conditions. The suggestive cis-eQTL *Kidins220* was located at this site following acute ethanol, whereas the suggestive cis-eQTL *Dnm3* was found at this site in the CIE NAC data. All ethanol-responsive eQTLs in NAC with LRS ≥ 10 following acute or CIE ethanol treatment are given in Supplemental Tables 3.11–3.12.

Correlation of gene expression with ethanol-drinking behavior. As an initial effort to genetically correlate gene expression to behavioral outcomes of CIE treatment, we generated Spearman correlation analyses between ethanol consumption (g/kg averaged over a 5-day drinking period) following the 3rd and 4th cycles of air or CIE treatment versus RMA expression values from the same treatment groups. Our premise was that expression correlated with ethanol consumption following CIE should reveal a different biological function "signature" than seen with air-treated controls. PFC gene lists for correlations

Table 3.3: All significant eQTLs in CIE NAC, Chr6:90-95 Mb trans-band

Probeset	*Gene*	*Location (Chr, Mb)*	*Max LRS*	*Max LRS Location (Chr: Mb)*
1420957_at	*Apc*	Chr18: 34.472690	31.9	Chr6: 92.514677
1452360_a_at	*Jarid1a*	Chr6: 120.362354	28.6	Chr6: 94.596952
1456656_at	*Lin7a*	Chr10: 106.859723	27.4	Chr6: 94.596952
1424504_at	*Rab22a*	Chr2: 173.530582	26	Chr6: 94.596952
1435635_at	*Pcmtd1*	Chr1: 7.150977	25.3	Chr6: 92.514677
1421738_at	*Gabra2*	Chr5: 71.352858	24.2	Chr6: 94.596952
1425014_at	*Nr2c2*¥	Chr6: 92.117447	24.2	Chr6: 92.514677
1439940_at	*Slc1a2*	Chr2: 102.623749	24.1	Chr6: 92.570486
1455998_at	*G630041M05Rik*	Chr1: 135.556378	23.8	Chr6: 92.514677
1417736_at	*Smc6l1*	Chr12: 11.298458	23.2	Chr6: 94.596952
1426259_at	*Pank3*	Chr11: 35.599852	23	Chr6: 92.514677
1439450_x_at	*Kiaa1033*	Chr10: 83.053882	22	Chr6: 92.514677
1457361_at	*Zfp804a*	Chr2: 82.097416	21.9	Chr6: 92.570486
1436023_at	*Bclaf1*	Chr10: 20.043434	21.7	Chr6: 92.570486
1453612_at	*Nek1*	Chr8: 63.533396	21.6	Chr6: 92.514677
1457625_s_at	*Cdkl2*	Chr5: 92.453971	21.5	Chr6: 92.514677
1419277_at	*Usp48*	Chr4: 137.172327	21.4	Chr6: 94.596952
1421768_a_at	*Homer1*	Chr13: 94.119180	21.4	Chr6: 92.514677
1449120_a_at	*Pcm1*	Chr8: 42.415987	21.2	Chr6: 94.596952
1452470_at	*4933409L06Rik*	Chr1: 157.791229	21	Chr6: 94.596952
1452708_a_at	*Luc7l*	Chr17: 26.403234	21	Chr6: 94.596952
1456088_at	*Birc4*	ChrX: 39.460010	21	Chr6: 92.570486
1429432_at	*1810043M20Rik*	Chr1: 164.640706	20.9	Chr6: 92.514677
1445081_at	*Scai*	Chr2: 38.928170	20.9	Chr6: 92.514677
1423184_at	*Itsn2*	Chr12: 4.642424	20.9	Chr6: 92.514677
1457891_at	*Cugbp2*	Chr2: 6.487216	20.3	Chr6: 94.596952
1434643_at	*Tbl1x*	ChrX: 74.900816	20.3	Chr6: 92.570486
1422842_at	*Xrn2*	Chr2: 146.853329	20.1	Chr6: 92.514677
1424658_at	*Taok1*	Chr11: 77.349717	20	Chr6: 92.514677
1450051_at	*Atrx*	ChrX: 103.072338	20	Chr6: 92.514677
1459984_at	*Mia3*	Chr1: 185.000000	19.9	Chr6: 92.514677
1453414_at	*E130113K08Rik*	Chr11: 86.752656	19.5	Chr6: 92.514677
1440437_at	*Herc1*	Chr9: 66.315187	19.1	Chr6: 92.514677
1460729_at	*Rock1*	Chr18: 10.119892	19	Chr6: 94.596952
1437502_x_at	*Cd24a*	Chr10: 43.303878	18.4	Chr6: 90.308023

¥ = cis eQTL

Table 3.4: PFC—Spearman correlations of gene expression (RMA) with ethanol consumption after the 3rd and 4th cycles of vapor chamber exposure

CIE-treated				
Probeset	*Gene*	*Pval.corr*	*Corr.Spear*	*Cycle**
1458499_at	*Pde10a*	9.47E-05	0.712173913	BOTH (4th)
1421860_at	*Clstn1*	0.00091914	0.632173913	BOTH (3rd)
1425833_a_at	*Hpca*	0.001181409	0.62173913	BOTH (3rd)
1439618_at	*Pde10a*	0.002053437	0.597391304	BOTH (3rd)
1442019_at	*Gas7*	0.003023388	0.579130435	BOTH (3rd)
1416562_at	*Gad1*	0.003799673	0.567826087	BOTH (4th)
1425810_a_at	*Csrp1*	0.003932856	0.566086957	BOTH (4th)
1430449_at	*Kidins220*	0.005147076	0.552173913	BOTH (3rd)
1425281_a_at	*Tsc22d3*	0.005676965	0.546956522	3rd
1429859_a_at	*Arl2bp*	0.005769573	0.546086957	BOTH (3rd)
1449932_at	*Csnk1d*	0.005769573	0.546086957	BOTH (3rd)
1420899_at	*Rab18*	0.00635219	0.540869565	3rd
1436713_s_at	*Meg3*	0.006874531	0.536521739	4th
1418586_at	*Adcy9*	0.007548179	0.531304348	BOTH (4th)
1449264_at	*Syt11*	0.007665626	0.530434783	BOTH (3rd)
Air-treated				
Probeset	*Gene*	*Pval.corr*	*Corr.Spear*	*Cycle**
1439196_at	*Hook3*	0.000319626	-0.696216827	BOTH (4th)
1444435_at	*1110014F16Rik*	0.001608394	-0.631846414	4th
1427150_at	*Mll3*	0.001962023	-0.622811971	4th
1427319_at	*A230046K03Rik*	0.002110577	-0.619424054	4th
1427353_at	*Clasp1*	0.002868941	-0.604743083	4th
1437020_at	*Ep400*	0.003364405	-0.596837945	4th
1417754_at	*Topors*	0.00428699	-0.584415584	4th
1416501_at	*Pdpk1*	0.004572405	-0.581027668	4th
1452187_at	*Rbm5*	0.004771353	-0.578769057	4th
1423559_at	*Kcnc1*	0.005083271	-0.575381141	4th
1430820_a_at	*Bbx*	0.005190943	-0.574251835	4th
1450401_at	*Ncoa6ip*	0.005411987	-0.571993224	4th
1426327_s_at	*Zfp91*	0.005758193	-0.568605308	4th
1453512_at	*Mbnl2*	0.006248242	-0.564088086	4th
1460417_at	*AB041803*	0.006248242	-0.564088086	4th

*Cycle column: reveals if the probeset was significantly correlated with ethanol consumption after the 3rd or 4th cycle. If the probeset was significantly correlated after both cycles, then the row is labeled BOTH and the cycle with the strongest correlation is listed and the cycle is denoted in parenthesis.

from CIE- or air-treated animals are contained in Supplemental Table 3.13. Only four genes were in common between the CIE (n = 58) and air (n = 170) gene lists. **Table 3.4** shows the top 15 correlated genes in PFC for ethanol consumption in CIE-treated and air-treated animals. Bioinformatic (GO) analysis of PFC genes significantly correlated to 3rd- and 4th-cycle drinking after CIE exposure revealed enrichment for Biological Processes related to neuron ensheathment, sodium ion channel activity, and neuron projection development (Supplemental Table 3.14). Highly correlated genes after CIE exposure included *Mobp* and *Mbp* (components of the myelin sheath), *Scn2b, Scn4b, Kcnma1, and Gad1.* In contrast, bioinformatic (GO) analysis of PFC genes significantly correlated to 3rd- and 4th-cycle drinking after air exposure revealed enrichment for Molecular Processes related to DNA and RNA polymerase binding, biological processes related to synaptic transmission and neurotransmitter secretion, cellular processes related to the synapse and neuronal projection, and mRNA splicing and processing (Supplemental Table 3.15). Highly correlated genes after air exposure included *Hook3*, *Trpm7*, *Clasp1,* and *Kcnc1*.

A similar correlation analysis was conducted for gene expression in NAC of air- or CIE-treated animals (Supplemental Table 3.16). There was an overlap of 13 genes between the CIE (n = 150) and the air (n = 160) gene lists. Interestingly, multiple genes involved in neurodevelopment (including *Smarca5, Ddx6, Qk,* and *Ndrg1*) were highly correlated to drinking in the NAC after the 3rd and 4th cycles of air exposure, but were not significantly correlated with drinking after CIE exposure. *Dnm3*, a hub gene that emerged from IPA network analysis

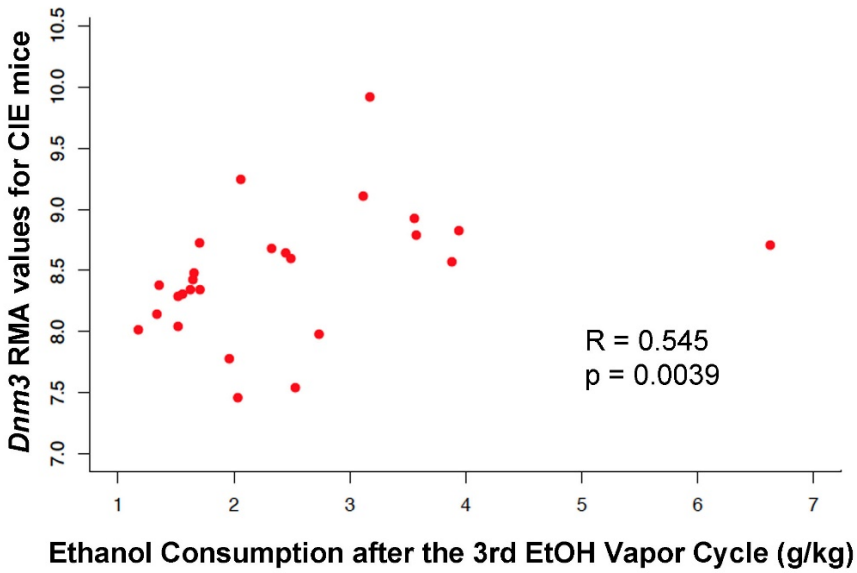

Fig. 3.7. *Dnm3* expression and ethanol drinking. Correlation of RMA expression values for *Dnm3* [1436875_at] in the NAC and total ethanol consumption after the 3rd cycle of ethanol vapor exposure (g/kg). Spearman correlation across microarray expression values for 26 strains of mice from the BXD cohort. The red dots represent the drinking and expression values for each respective strain of mouse. There was a significant (p = 0.00287) positive correlation (rho = 0.561) using the Spearman rank order test.

Table 3.5: NAC—Spearman correlations of gene expression (RMA) with ethanol consumption after the 3rd and 4th cycles of vapor chamber exposure

CIE-treated				
Probeset	*Gene*	*Pval.corr*	*Corr.Spear*	*Cycle**
1450769_s_at	*Stard5*	0.00030775	-0.651965812	4th
1417943_at	*Gng4*	0.000359169	-0.646495726	3rd
1449571_at	*Trhr*	0.000531398	-0.632136752	BOTH (4th)
1446176_at	*Mrg1*	0.001404264	0.593162393	3rd
1437403_at	*Samd5*	0.001449756	0.591794872	BOTH (3rd)
1419271_at	*Pax6*	0.002071286	-0.576068376	3rd
1441917_s_at	*Tmem40*	0.002233124	-0.572649573	3rd
1447669_s_at	*Gng4*	0.002300826	-0.571282051	3rd
1438782_at	*Axcam*	0.003169373	-0.556239316	3rd
1439633_at	*Syt7*	0.003803452	-0.547350427	3rd
1436875_at	*Dnm3*	0.003964172	0.545299145	3rd
1434779_at	*Cbln2*	0.004665976	-0.537094017	3rd
1442019_at	*Gas7*	0.00512194	0.532307692	BOTH (3rd)
1434877_at	*Nptx1*	0.005398996	-0.52957265	3rd
1453771_at	*Gulp1*	0.005470202	-0.528888889	4th
Air-treated				
1452161_at	*Tiparp*	0.000433941	0.672924901	BOTH (4th)
1458830_at	*Fgf14*	0.00095138	-0.64229249	3rd
1459288_at	*Kcnd2*	0.001176552	-0.633399209	3rd
1456257_at	*Fam126b*	0.001232344	0.631422925	3rd
1436713_s_at	*Meg3*	0.001727521	-0.616600791	BOTH (3rd)
1443237_at	*Ptprd*	0.002284704	-0.603754941	BOTH (3rd)
1420917_at	*Fnbp3*	0.002432929	0.600790514	4th
1416180_a_at	*Rdx*	0.002698052	0.595849802	BOTH (4th)
1427351_s_at	*Ighg*	0.002810732	0.593873518	3rd
1430979_a_at	*Prdx2*	0.004016181	0.576086957	3rd
1452444_at	*Napb*	0.004094228	0.575098814	BOTH (3rd)
1426432_a_at	*Slc4a4*	0.004094228	0.575098814	4th
1437864_at	*Adipor2*	0.004173545	0.574110672	BOTH (4th)
1442025_a_at	*Zbtb16*	0.004254147	0.57312253	3rd
1437869_at	*Ppp2r3a*	0.004503832	0.570158103	4th

*Cycle column: reveals if the probeset was significantly correlated with ethanol consumption after the 3rd or 4th cycle. If the probeset was significantly correlated after both cycles, then the row is labeled BOTH and the cycle with the strongest correlation is listed and the cycle is denoted in parenthesis.

(**Fig. 3.4**) and as a suggestive eQTL (Supplemental Table 3.12), was also significantly correlated to drinking **(Fig. 3.7**). **Table 3.5** shows the top 10 genes whose expression in NAC most highly correlates with ethanol consumption in CIE-treated and air-treated animals.

Of note, ethanol intake during the 3rd cycle (GN:12967) strongly correlated to ethanol consumption after the other cycles of ethanol vapor exposure from this study, giving additional validity to the robustness of the dataset and the reproducibility of drinking data across these BXD strains (Supplemental Table 3.17). Ethanol intake during the 3rd cycle also correlates inversely with drinking phenotypes performed in other labs using drinking paradigms without ethanol vapor exposure (GN:12624, R = −0.714, p = 0.0012 and GN:13578, R = −0.763, p = 0.014). These strong inverse correlations suggest that the chronic exposure to ethanol vapor has a distinctly different biological effect from simple voluntary ethanol consumption. Importantly, our phenotype of interest was positively correlated with change in ethanol consumption after a chronic mild stressor relative to control (GN:13573, R = 0.700, p = 0.033) and negatively correlated with ethanol consumption in the non-stressed control group (GN:13578, R = −0.763, p = 0.014), further supporting the notion that chronic stress dramatically alters ethanol consumption in mice. Ethanol intake during the 3rd cycle was positively correlated corticosterone levels in plasma, 3 days following the 5th and final ethanol vapor exposure (GN:13023, R = 0.497, p = 0.006), suggesting that increased levels of stress hormones following a chronic stressor may be a potential driving

mechanism leading to increased consumption. Ethanol intake during the 3rd cycle is also inversely correlated with an anxiety assay (GN:12430, R = −0.499, p = 0.0044). Finally, 3rd-cycle ethanol intake inversely correlated with the difference in acute ataxia in animals previously exposed to ethanol relative to naïve controls, which is a measure of ethanol sensitization and an inverse measure of ethanol tolerance (GN:10497, R = −0.821, p = 0.02 and GN:10498, R = −0.821, p = 0.02). This suggests that animals which are more likely to be sensitized to the acute effects of ethanol, and thus have a lower tolerance, are less likely to consume ethanol after repeated exposures to ethanol vapor. Future behavioral studies are necessary to directly test this relationship.

Validation of Dnm3 downregulation by CIE in male DBA/2J mice. Dynamin-3 (*Dnm3*) is a member of the dynamin family, which possesses mechano-chemical properties involved in actin-membrane processes, predominantly in membrane budding. In BXD RI strains, *Dnm3* is significantly ethanol-responsive in PFC and NAC, in both acute and chronic ethanol treatment paradigms (Supplemental Table 3). The direction of ethanol response with CIE showed wide variation across the BXD cohort (**Fig. 3.8A**), with the D2 progenitor strain showing strong down-regulation and B6 mice showing little response. The direction of the *Dnm3* response to ethanol across the BXD strains showed a strong relationship with the genotype at the *Dnm3* gene locus, as expected given the suggestive *Dnm3* cis-eQTL seen in NAc (**Table 3.2**). We performed qPCR on a larger cohort of DBA/2J and C57BL/6J mice following CIE. We noted a down-regulation in CIE mice that was led by D2 males (two-way ANOVA for interaction $p < 0.05$, partial

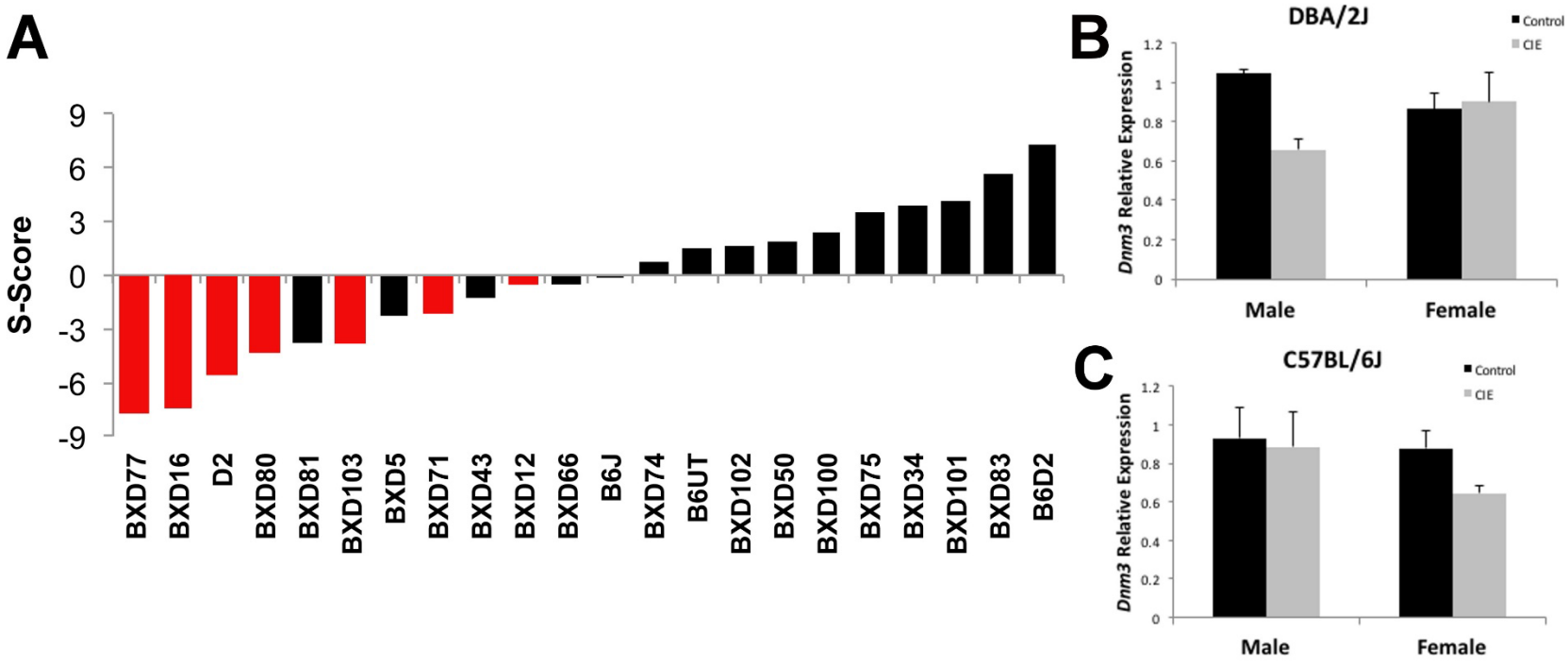

Fig. 3.8. CIE induced changes in Dnm3 expression in the NAC. (A) S-score strain distributions for the ethanol-responsive gene, *Dnm3* [1436875_at], in the NAC. A positive S-score indicates that *Dnm3* expression is up-regulated in the NAC in ethanol-vapor exposed animals relative to air-vapor exposed animals of the same strain. BXD strains with a D2 genotype at the *Dnm3* locus are colored red and strains with a B6 genotype are colored black. **(B)** Quantitative PCR results for *Dnm3* mRNA expression in the NAC of D2 mice from later cohorts (cohorts 3, 4, and 5). *Dnm3* was significantly down-regulated ($p < 0.05$, partial $\eta^2 = 0.249$) in the NAC of D2 males exposed to ethanol vapor (grey bars, n = 4-5/group) relative to those exposed to air-vapor (black bars, n = 4–5/group). **(C)** *Dnm3* expression in male and female B6 mice (n = 5/group) exposed to Air or CIE. *Dnm3* expression was not significantly altered by CIE and ethanol drinking in B6 males and females (Two-way ANOVA $p > 0.05$, partial $\eta^2 = 0.06$).

η^2 = 0.249, **Fig. 3.8B**). *Dnm3* expression appeared to be unaffected by CIE in B6 mice (two-way ANOVA $p > 0.05$, partial η^2 = 0.066, **Fig. 3.8C**), although we acknowledge the possibility that these data may be underpowered.

Gsk3b-centric Ethanol-Responsive Gene Network is Associated with Risk for Alcohol Dependence

Previous analyses using graph theoretic modeling (Wolen *et al*, 2012) identified coordinately regulated gene networks following acute ethanol treatment in PFC. One network highly enriched for significantly ethanol-responsive genes included *Gsk3b* as an interconnected hub gene. From these data and prior knowledge on the role of GSK3B in synaptic plasticity and affective disorders we hypothesized that a *Gsk3b*-centric gene expression correlation network would show genetic association with alcohol dependence in humans. We therefore further investigated the correlation structure of the *Gsk3b* ethanol-responsive network from our prior microarray data (Wolen *et al*, 2012) on acute ethanol-induced expression changes (S-Scores). Analysis of individual probeset (gene) correlations with *Gsk3b* expression following acute ethanol treatment in mPFC (n= 29 mouse strains) showed that 34 genes had correlations ≥ 90% with *Gsk3b*. There was a highly unique degree of interconnectivity in this *Gsk3b* network (**Fig 3.9A**) compared to randomly chosen similar sized networks from the rest of the genome (**Fig. 3.9*B***). This illustrates the concept that *Gsk3b* is a central member of a unique gene network in mouse mPFC that is strongly co-regulated by ethanol.

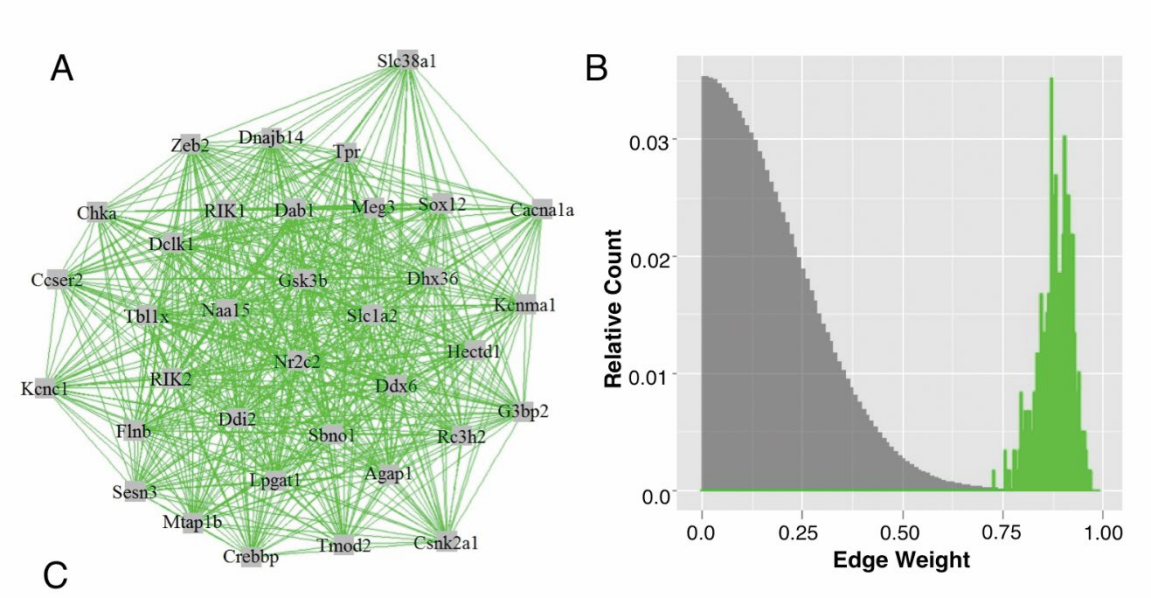

SET	NSNP	NSIG	ISIG	EMP1
95%	144	40	3	0.07029
90%	1610	122	56	0.003999
85%	5362	256	144	0.04519
80%	12901	664	392	0.2324
GSK3B alone	115	19	1	0.0288

Figure 3.9 *Gsk3b*-centered ethanol-responsive network derived from mouse PFC is enriched for AUD risk-conferring SNPs in human GWAS data. (*A*) Network of genes with S-Score, a measure of ethanol-responsiveness, correlation of $r \geq 0.9$ with *Gsk3b*, found in the PFC of BXD mice (*B*) Comparative histogram of WGCNA-calculated edge weights (gene-gene expression correlations) of the 35 genes in the *Gsk3b* network (green) and edge weight values of 10000 permutations of randomly selected groups of 35 genes (grey) from the BXD PFC microarray. (*C*) SNP-set level analyses of human GWAS (COGA dataset, n=1205 cases, 700 controls) were performed on groups of homologous genes. Results are shown for genes at multiple levels of correlation (80-95%) with *Gsk3b* in mouse PFC. The result of a SNP-set analysis within the *GSK3B* gene alone is also given. NSNP = total number of genotyped SNPs in given gene or geneset; NSIG = number of significantly risk-conferring SNPs; ISIG = number of independent (non-LD) risk-conferring SNPs; EMP1 = empiric p-value.

We next queried gene-based human association data from the Collaborative Study on the Genetics of Alcoholism (COGA) project (Bierut *et al*, 2010; Bierut *et al*, 2002) to determine if the uniquely correlated *Gsk3b* ethanol-responsive network informed genetic studies on alcohol dependence. The above mouse expression correlation analysis was used to create gene sets based on ≥ 95%, 90%, 85%, and 80% correlation with *Gsk3b* S-Score measurement of ethanol responsivity. Set-based analyses revealed significant enrichment of risk-conferring alleles in the groups of human homolog genes correlating ≥85% and ≥90% with *Gsk3b* in the mouse BXD study. The latter of these human homolog groups showed peak signal, p=0.004 (**Fig. 3.9*C***). Additionally, set-based analyses of SNPs within individual genes showed significant enrichment of *GSK3B* (p=0.029), *DNAJB14* (p=0.025), *G3BP2* (p=0.017), and *KCNMA1* (p=0.0096) (Supplemental Table 3.18). Taken together, these results indicate that a significant risk for alcohol dependence may be mediated via GSK3B and related pathway genes, particularly as these relate to initial ethanol sensitivity.

3.4 Discussion

This chapter describes an exploratory genetic and genomic analysis of transcriptome responses to chronic ethanol by intermittent vapor chamber and consumption in BXD mice, and comparison of these changes to acute ethanol transcriptome responses. Our goal was to gain potential insights into conserved vs. unique mechanisms of ethanol-induced expression changes. A striking

finding in this study was the significant number of ethanol-responsive genes regulated by both acute ethanol and CIE across the BXD cohort, indicating that the initial transcriptional response from acute ethanol significantly informs long-term effects of ethanol. Furthermore, while we found significant expression changes unique to CIE treatment, our bioinformatics analysis showed a remarkable overall conservation of functional groups among the expression responses, either unique or shared across CIE vs. acute ethanol and PFC vs. NAC. Finally, these initial studies identified provisional expression/behavioral correlations and eQTLs, which may lead to identification of novel targets for future intervention in abusive ethanol consumption.

Our use of the BXD panel across two treatment paradigms provided the opportunity to compare both acute and chronic ethanol exposure paradigms on gene regulation in a genetic panel. A major strength of this approach was that we were able to employ 43 BXD strains exposed to CIE and 29 BXD strains exposed to acute ethanol, providing a wide range of genotypes. However, our overall power was likely reduced since this initial analysis was able to utilize only 1–2 mice per strain/treatment due to the overall complexity of the animal-treatment paradigm. Using the S-score algorithm to directly compare control vs. treated samples within strains, together with a statistical comparison of S-scores across strains, allowed our analysis to identify large groups of ethanol-responsive genes, despite strain-dependent differences in the magnitude or even direction of the ethanol regulation. The number of strains employed here also provided reasonable ability to identify expression/behavioral correlations. However, a more

definitive analysis of within-strain expression levels or behavioral results will have to await an ongoing enlarged study that will provide a more powerful genetic analysis of both expression networks and behavioral responses to CIE. Despite these caveats, the studies presented here contribute multiple unique findings.

One of our major assumptions in the experimental design of these studies was that by comparing our prior BXD studies on acute ethanol to these CIE-evoked responses, we would be able to define expression changes more explicitly involved in the long-term neuroadaptive events responsive for progressive ethanol consumption with the CIE paradigm. Unexpectedly, our studies found a striking overlap between CIE and acute ethanol responses, extending even across both PFC and NAC. This occurred despite the studies occurring nearly a decade apart, employing different investigators doing the primary assays, and having very different experimental designs. The CIE treatment entailed a chronic vapor exposure and repeated oral consumption with a 72-h abstinence period prior to harvesting brain tissue. In contrast, the acute ethanol data was a single i.p. injection with brain tissue harvested 4 h later at a time when blood ethanol levels would just be reaching non-detectable levels. While we did indeed identify gene responses unique to CIE, the overlap between acute and chronic ethanol may provide valuable mechanistic clues to major mechanisms of ethanol action on the CNS. It would make intuitive sense that certain reliable ethanol actions, such as direct receptor or signaling molecule interactions (e.g., binding to $GABA_A$ receptor subunits), would produce consistent downstream responses acutely or chronically. Thus, our list of 88 genes that are

ethanol-responsive across both treatments and in both brain regions studied may represent these particularly “reliable” downstream ethanol effectors. Indeed, when this list was studied for enrichment, synaptic transmission was by far the dominant theme, with voltage-gated cation channel activity, and calcium-regulated responses as over-represented functions (see Supplemental Table 3.8). *Kcnma1* and *Gabra2* were prominent members of the functional groups over-represented in these 88 ubiquitously regulated probesets. These genes both have substantial biochemical, structural, pharmacological, and genetic prior validation as a prominent target of direct ethanol action (Tapocik *et al*, 2014; Treistman and Martin, 2009), at least partially substantiating our conclusions regarding this group of 88 genes.

Genes unique to CIE PFC showed an enrichment of myelin genes, with *Mag* and *Mal* identified in the pathway shown in **Fig. 3.3**. The PFC expression of two other major myelin sheath components, *Mobp* and *Mbp*, correlated with drinking data in CIE-treated animals. The CIE PFC geneset also showed enrichment for cytoskeletal binding and cell adhesion molecules and overall, showed the greatest functional over-representation differences from any of the other treatment group analyses (see Supplemental Tables 3.4–3.8). In the eQTL analysis of CIE PFC, top QTL candidates at the two major trans-regulated peaks, Chr3 and Chr16 (**Fig. 3.5**), were identified as the cell adhesion molecules *Fat4* and *Dscam*, respectively. Thus, it is conceivable that a distinct mechanism of chronic ethanol response in PFC operates through altered cellular adhesion and potentially an interaction with CNS myelin to drive resulting behavioral changes.

Except for the gene group uniquely regulated by CIE in PFC as noted above, the other comparison groups showed remarkable similarities in the highest ranked over-represented functional categories (Supplemental Tables 3.4–3.8). Although there were differences in the component genes, these categories all concerned synaptic transmission or neuronal structure. In the PFC, overlap between acute and chronic treatments showed over-representation of genes related to the $GABA_A$ receptor, whereas in the NAC, both treatments altered genes related to GABA and glutamate transport vesicles. It is interesting to consider that ethanol has been shown to potentiate GABA release both through altered receptor expression and altered release (Kumar *et al*, 2010; Roberto *et al*, 2003). As preliminary analyses, our data seem to indicate that these alternate mechanisms may show brain-region specific differences in effect (both acutely and chronically), though further studies would be necessary to confirm this possibility.

When comparing gene sets unique to treatment condition, brain region, or both, there remained a striking similarity in the top upstream regulators identified by IPA. This is perhaps not surprising, given the functional group over-representation overlaps noted above. In particular, HTT and BDNF were identified in nearly every set out of the five queried, despite the fact that many of these gene sets were completely distinct (by definition). This may be partially explained by these genes serving as major regulators of neuronal signaling in general, but likely indicates particular relevance of these genes in ethanol-induced signaling across multiple pathways. BDNF signaling has, in particular,

been closely linked to the mechanisms underlying progressive ethanol consumption resulting from the CIE model or similar intermittent ethanol access models (Darcq *et al*, 2015; Smith *et al*, 2016; Tapocik *et al*, 2014). This extensive genomic analysis across the BXD strains serves as strong affirmation of BDNF signaling as an important regulatory point for progressive ethanol consumption, and may implicate targets for future therapeutic intervention development.

The eQTL analyses revealed several important points. The first was that there are distinct regulatory hotspots in the BXD genome that influence groups of CIE-responsive genes, as seen previously with our genetical genomics study on acute ethanol (Wolen *et al*, 2012). However, the majority of observed eQTLs were remote to the QTL location (trans-eQTL). No significant cis-eQTLs were seen in PFC with CIE, and only several significant or suggestive cis-eQTLs were found in NAC (see below). It is possible that our experimental design with limited replication and use of the S-score algorithm could have decreased our power to detect cis-eQTLs. However, the S-score actually is advantageous in that it eliminates confounding false-positive cis-eQTL occurring due to SNPs within DNA segments corresponding to microarray probe positions (Wolen *et al*, 2012). RNA-seq analysis in future studies might be an advantageous approach for cis-eQTL identification as well as CIE-induced changes in splicing or non-coding RNA expression.

The large number of trans-eQTLs identified in this study and their grouping into regulatory hotspots, or trans-bands (see histograms in **Figs. 3.5 & 3.6**), may have implications for future identification of the major

regulators of CIE-responsive gene networks. Strikingly, we observed minimal overlap in the position of major trans-bands between CIE- and acute-ethanol treatments. This suggests that distinct genetic variation underlies ethanol-induced expression changes from acute to chronic treatment, *even if* individual gene expression or function group changes themselves are conserved.

The one significant cis-eQTL identified in the CIE NAC condition was also found on the largest trans-band, in Chr6:90–95Mb. The cis transcript is Nuclear Receptor 2, Group C, Member 2 (*Nr2c2*), located at Chr6:92091390–92173057 on the mouse genome. Its eQTL map is shown in Supplemental Fig. 3.6; its peak LRS (with S-score) is within 100 Kb of its genomic location. In a genome-wide association study (GWAS) of human alcohol and nicotine co-dependent participants, the gene region *SHE3BP5-NR2C2* was found to be enriched for risk-conferring SNPs, with the region being the only to reach genome-wide significance in the meta-analysis (Zuo *et al*, 2012). *Nr2c2*‘s expression has also been shown to be significantly altered by subchronic morphine in adult rats (Schwarz and Bilbo, 2013), providing further evidence of its potential role in addiction. In our study, *Nr2c2* expression did not correlate with drinking behavior in the CIE-treated animals; however, its expression did correlate significantly among air-treated controls during both free-drinking cycles analyzed, suggesting that its expression pattern may confer risk before ethanol use becomes chronic. With chronic treatment, its expression is significantly altered, but does not correlate with consumption. Significant trans-eQTLs in the *Nr2c2* trans-band include *Gabra1, Homer1*, and *Slc1a2,* indicating that alterations in synaptic

transmission could occur via altered *Nr2c2* regulation; however, such specific mechanisms remain to be elucidated.

Four suggestive cis-eQTLs were also found in CIE NAC: *Pcolce, Dnm3, Gfap,* and *Fbxo39*. Of these, *Dnm3*, located at Chr1:160Mb, was particularly interesting. *Dnm3* expression in the NAC was correlated with ethanol drinking in CIE-treated animals, and appeared as a hub in the top-ranked network of CIE NAC and acute-NAC overlapping genes (**Fig. 3.4**). Its gene expression levels varied considerably across BXD strains, and particular strains showed greater differences in expression between CIE and control groups than seen in progenitor strains (**Fig. 3.8A**). This finding suggests that transgressive or epistatic genetic interactions may be involved in the *Dnm3* transcriptional response to chronic ethanol. In the DBA2/J strain, *Dnm3* showed strong down-regulation with chronic ethanol, a finding validated by q-PCR (**Fig. 3.8**). Ethanol-induced expression changes of *Dnm3* (down-regulation in the case of the particularly sensitive DBA2/J strain) could represent a major mechanism of ethanol neuroadaptation. The expression of 21 other genes shows ethanol response at the Chr1:160–170Mb trans-band in which *Dnm3* is a suggestive cis-eQTL. It is thus reasonable to suggest that these expression changes could be mediated via *Dnm3.* The NAC expression for 15 of 21 of these genes also correlated significantly with drinking in CIE-treated animals. This is not overly surprising, given that all genes regulated by a common locus would be expected to correlate with each other to some degree, but does illustrate the possibility of a *Dnm3*-regulated network affecting ethanol-drinking behavior. As in the case of

Nr2c2, specific mechanisms by which this candidate gene exerts ethanol-relevant effects are unknown. Our IPA network (**Fig. 3.4**) indicates an interaction between dynamin family members, GTPases involved in endocytosis and vesicular trafficking (Urrutia *et al*, 1997), and the Homer family, involved in regulation of glutamatergic post-synaptic densities (de Bartolomeis and Iasevoli, 2003). Additional targeted studies will be necessary to explore this relationship in the context of CIE exposure.

The application of a *Gsk3b*-centric network (**Fig. 3.9**) derived from acute ethanol response microarray data in mouse PFC, to human GWAS data, reveals that these network genes are enriched for risk-conferring SNPs in alcohol-dependent patients. This is important for several reasons. For one it serves as an example cross-species data integration—using an informed subset of genes to test for genetic risk can identify susceptibility loci that may not achieve genome-wide significance independently. For another it may identify human SNPs with mechanistic roles that may eventually inform more targeted treatments. We have thus far only tested a network of genes identified in the PFC following acute ethanol exposure; other networks or gene sets identified, i.e. region-specific CIE-responsive genes, may be tested in the future.

Overall, the genetical genomics studies across BXD strains was intended as an initial analysis on genetic factors influencing ethanol-regulated behaviors and brain gene expression in the corticolimbic dopamine pathway. Our findings show remarkable functional genomics overlap between CIE and acute ethanol treatment, but also have identified brain expression changes unique to CIE. Our

genetic analysis of expression results provide initial details on a limited number of genetic loci that may have an important impact on the molecular adaptations to CIE. Future studies on expanding and validating the findings here, including our results on candidates such as *Dnm3*, may lead to identification of novel targets for therapeutic intervention in the progression from acute ethanol exposure to the compulsive consumption seen in AUD.

Chapter 4

Effects of Acute and Chronic Ethanol on GSK3B Activity, Downstream Targets, and Behaviors

4.1 Introduction

Acute ethanol (1.8 g/kg, i.p.) causes major expression changes in a network of genes centered around *Gsk3b* in the PFC (Wolen *et al*, 2012). Results from several published studies suggest that ethanol inhibition of the GSK3B protein contributes mechanistically to regulation of this Gsk3b-centric expression network. In the PFC of drug-naïve male rats, an acute dose of ethanol (1.5 g/kg) significantly increased phosphorylation of GSK3B at its inhibitory serine-9 residue (Neznanova *et al*, 2009). The increase in p-GSK3B-S9 was not observed at the 20 minute time point, but was robust at 45 minutes (Neznanova *et al*, 2009). In the NAC of male C57BL/6J mice, an acute dose of ethanol (2 g/kg) significantly increased inhibitory phosphorylation of GSK3B as well as GSK3A, 15 minutes after treatment (Neasta *et al*, 2011). Sachs et al. (2014) similarly found that a 2 g/kg dose of ethanol increased p-GSK3B-S9 phosphorylation in the NAC 20 minutes after treatment. However, while this effect was observed in wild-type animals, mice with congenital serotonin deficiency (tryptophan hydroxylase

knock-in) exhibited a significantly blunted response of ethanol induced GSK3B phosphorylation (Sachs *et al*, 2014). These serotonin deficient mice also exhibited reduced ethanol sensitivity and increased ethanol preference in two bottle choice tests, illustrating the role of serotonin in ethanol behavioral responses and perhaps a serotonin-GSK3B pathway in particular (Sachs *et al*, 2014). It should be noted that the tyrosine hydroxylase knock-in was constitutive and that many concomitant CNS changes might be expected in the context of serotonin deficiency. Regardless, it is interesting that an attenuated response of GSK3B phosphorylation to ethanol corresponded to altered behavioral effects, including increased ethanol preference. To our knowledge specific manipulation of GSK3B and subsequent observations of ethanol-related behaviors have not been reported.

There is evidence that GSK3 phosphorylation underlies certain behavioral effects of another NMDA antagonist, ketamine. A subanesthetic dose of ketamine (10 mg/kg, i.p.) robustly increased serine phosphorylation of both GSK3A and GSK3B (Beurel *et al*, 2011). This GSK3 inhibition appears to be necessary for the rapid antidepressant effect of ketamine, as evidenced by knock-in mice with constitutively active GSK3; these mice showed a completely ablated ketamine antidepressant effect as assessed by a learned helplessness paradigm (Beurel *et al*, 2011). On the other hand, treatment with high-dose lithium mimicked the effect of subanesthetic ketamine in wild-type mice (Beurel *et al*, 2011).

While ketamine has become well-known for its acute antidepressant effect (Andrade, 2017), ethanol has long been known to exhibit an acute anxiolytic effect (Ellinwood *et al*, 1983). Whether GSK3B inhibition might underlie aspects of ethanol anxiolysis is unknown. We hypothesized that GSK3B in the PFC of male and female mice would show dose-dependent increases in Serine-9 phosphorylation following i.p. ethanol treatment. As a speculative hypothesis, we predicted that this inhibition may contribute to the anxiolytic effect of ethanol, and therefore that treatment with a GSK3B inhibitor might potentiate the effect of ethanol on anxiolytic behavior.

Prior reports of the effect of chronic ethanol treatment on GSK3B activity in brain are less consistent. There are two studies which show increased inhibitory phosphorylation of GSK3B following repeated ethanol exposure: one in the NAC of rats (Neasta *et al*, 2011), and the other in the dorsomedial striatum (DMS) of mice (Cheng *et al*, 2016). Both of these experiments harvested brain tissue 24 hours after last access. Thus it is unclear to what extent this GSK3B inhibition is due to repeated, long-term ethanol exposure, or corresponds to the state of ethanol withdrawal. These studies did not compare animals currently intoxicated with ethanol (following long-term exposure) to animals 24 hours into withdrawal, and the temporal profile of ethanol's GSK3B-inhibiting effects are not known. Moreover, it has yet to be determined whether each ethanol exposure shows a greater or lesser degree of GSK3B phosphorylation in chronically exposed animals as that observed in ethanol-naïve animals given a single dose. A greater response would resemble the profile of a sensitizing effect, whereas a

diminished response might be described as tolerance to ethanol's GSK3B inhibiting actions. Based on the study described above (Sachs *et al*, 2014) of serotonin deficient mice with a blunted GSK3B phosphorylation response to ethanol showing lower ethanol sensitivity and higher drinking, we might expect the tolerance-like effect. That is, animals with a history of repeated ethanol exposure and escalating use might show blunted ethanol-induced GSK3B phosphorylation following an acute dose of ethanol, compared to naïve animals receiving the same dose.

To establish escalated ethanol consumption, we have used the intermittent ethanol access (IEA) paradigm. This model allows for behavioral correlates to chronic ethanol exposure which can be studied in themselves. Specifically, we will compare the observed escalations in ethanol drinking during an initial 2 hour binge period at the beginning of each dark cycle, with the pattern of daily (24 h) ethanol drinking week to week. We will also verify binge-like ethanol drinking at the 2 hour time point with blood alcohol content readings from a subset of animals.

In addition to the activity of GSK3B, as determined by the level of phosphorylation at the serine-9 (S9) residue, we will assess the alternate isoform GSK3A, which is regulated at an analogous inhibitory serine-21 (S21). Additionally we will assess levels of synaptic scaffolding proteins, gephyrin and PSD-95, both reported targets of GSK3B (Nelson *et al*, 2013; Tyagarajan *et al*, 2011).

4.2 Materials and Methods

Animals. Male and female C57BL/6J mice (aged 8 weeks) were obtained from Jackson laboratories (Bar Harbor, Maine). For pilot studies on anxiety-like behavior, male C57BL/6J mice were obtained from the VCU transgenic core facility at 4 weeks and housed in our vivarium until ≥8 weeks old. All mice were housed in a temperature and light controlled room (12 hr light:dark cycle) with free access to Teklad laboratory diet (Envigo, Hungtingdon, UK) and tap water. All procedures were approved by the VCU Institutional Animal Care and Use Committee and followed the NIH Guide for the Care and Use of Laboratory Animals.

Antibodies. Rabbit anti-phospho-GSK3A/B-S21/9 (#8556), phospho-GSK3B-S9 (#5558) and total GSK3A/B (#5676) are from Cell Signaling Technology (Danvers, MA). Rabbit anti-gephyrin (#720218) and total PSD-95 (#51-6900) are from Thermo Scientific (Rockford, IL). Rabbit anti phospho-PSD-95-T19 (ab17167) is from Abcam (Cambridge, MA). Mouse anti-B-actin (A5441) is from Sigma-Aldrich (St. Louis, MO). Mouse anti-NeuN (MAB377) is from Millipore (Billerica, MA). Secondary antibodies used for Western blotting were Amersham ECL donkey anti-rabbit IgG, HRP-linked antibody, and Amersham ECL sheep anti-mouse IgG, HRP-linked antibody, both from GE Healthcare (Chicago, IL). Secondary antibodies used for immunofluorescence were goat anti-rabbit AlexaFluor 488 (A11008) and goat anti-mouse AlexaFluor 594 (A11005), both from Life Technologies (Grand Island, NY).

Preparation of Solutions. For the Western blot dose-response (0.5-4.0 g/kg) study, ethanol was diluted to 18% v/v in normal (0.9%) saline. For i.p injections in behavioral studies and immunohistochemistry (IHC), ethanol was diluted to 20% v/v in normal saline. For intermittent ethanol access, ethanol was diluted to 20% v/v in tap water. The GSK3B inhibitor tideglusib (Selleck Chemicals, Houston, TX) was prepared for gavage by suspension in 26% peg-400 (Sigma), 15% Cremophor EL (Sigma), and water. 200 mg/mL tideglusib was homogenized into vehicle by vortexing and subsequent bath sonication at 40 degrees Celsius for 30-60 minutes.

(Acute) Systemic Administration of Alcohol. For all molecular studies (Western blots and IHC) mice were habituated to the i.p. administration procedure with daily injections to saline for three days immediately prior to the experimental procedure. On the day of the experiments, mice were injected with saline or ethanol (0.5 g/kg, 2.0 g/kg, 4 g/kg) and sacrificed 30 minutes later. For Western blotting experiments mice were sacrificed by cervical dislocation and decapitation; for IHC mice were sacrificed by perfusion under anesthesia (isoflurane, Butler Schein, Dublin, OH). See **Figure 4.1A** for overview of experimental design.

Western Blot Analyses. Tissue was homogenized on ice by suspension RIPA buffer containing Halt protease and phosphatase inhibitor cocktail (Thermo), and probe sonication for 2-3 short bursts. Immunoblotting was performed using an Xcell Surelock Mini-Cell kit (Thermo). Tissue homogenates were denatured with NuPage LDS Sample buffer and Sample Reducing Agent (Thermo), and heated

at 70 degrees Celcius for 10 minutes. Samples were separated via electrophoresis at 120 V on 4%-12% Bis-Tris gels at room temperature in 1X NuPage MES Running Buffer (Thermo), followed by transfer onto PVDF membrane at 12 V, at 4 degrees Celsius in 1X NuPage Transfer Buffer in 20% methanol. Membranes were blocked with bovine serum albumin (5% w/v), and incubated overnight at 4 degrees C in primary antibody. Dilutions of antibodies for phospho-proteins, gephyrin, and PSD-95 were 1:1000. Dilution of antibody to total GSK3A/B was 1:5000. Dilution of antibody to B-actin was 1:20000. Following incubation membranes were washed extensively in Tris Buffered Saline containing 0.1% Tween-20 (TBS-T) and incubated in the appropriate secondary antibody for 1 hour at room temperature. Dilution of secondary antibody was 1:15000 for phospho-protein staining and 1:30000 for total protein staining. Membranes were again washed in TBS-T 3 times for 5-10 minutes each wash. Membranes were incubated in ECL Prime (GE Healthcare) (1:1 in TBS-T) before being exposed to GeneMate Blue Ultra Autorad film (BioExpress, Kayville, UT). Blots were stripped using Restore Stripping Buffer (Thermo) before re-staining for total protein (after primary phospho-stain) or B-actin as a loading control. Films were scanned using a flatbed scanner and analyzed using densitometric analysis with ImageJ (NIH).

Immunohistochemistry. Thirty minutes after i.p. injection, mice were deeply anesthetized with isoflurane and perfused transcardially with 1X phosphate-buffered saline (PBS) followed by 4% formaldehyde in PBS. Brains were removed and post-fixed in 4% formaldehyde overnight at 4 degrees C, then

transferred to 30% sucrose in PBS. When brains had sunk to the bottom of the sucrose vial (72 hours at 4 degrees), they were snap frozen in isopentane on dry ice. Frozen brains were cut (20 micron thick coronal sections) using a Leica CM3050 cryostat (Leica Biosystems, Wetzlar, Germany). Sections were collected into 24-well plates, floating in PBS with 0.2% sodium azide. Free-floating sections containing PFC were selected and incubated in citric acid buffer (10 mM sodium citrate in distilled water and 0.05% Tween 20) at 80 degrees Celsius for 20 minutes, as an antigen retrieval step. Sections were allowed to cool before incubation with gentle shaking in 5% goat serum in PBS with 0.2% Triton, for blocking and permeabilization. Sections were then incubated in primary antibodies in 3% goat serum in PBS with 0.1% Tween-20 (PBS-T) overnight at 4 degrees Celsius with gentle agitation. Sections were washed 3 times for 5 min each in PBS-T on a shaker, before incubation in secondary antibody for 2 hours at room temperature, with gentle agitation. Sections were again washed 3 times in PBS-T with agitation and placed on slides in one drop of PBS combined with one drop of PBS-T. Liquid was wicked off and slides were allowed to air dry momentarily. Sections were mounted with VectaShield Antifade mounting medium (Vector Laboratories, Burlingame, CA) and a coverslip. Slides were assessed using a Leitz DMRD microscope and images were taken using an attached Olympus CK40 inverted scope camera.

Light/Dark Assays. The light-dark (LD) box contains two equally sized compartments (30 cm x 15 cm x 15 cm), separated by a black plastic partition with an opening in the middle to allow for light-dark transitions (Med Associates,

Fairfax, VT). The box is enclosed in a sound-attenuating box equipped with overhead lighting and fan ventilation. The system is interfaced with Med Associates software that allows for automatic measurement of activity using a set of 16 infrared beam sensors along the X-Y plane. The activity chambers contain CM1820 28V 170mA (22 lux) light bulbs.

A pilot experiment was performed to assess the utility of the LD box test for assessing ethanol-induced anxiolytic behavior using a repeated-measures paradigm. Previously the LD box was used as an anxiolytic assay in animals unexposed to the chamber (Putman *et al*, 2016). In this experiment all mice (n=6, males) were habituated to the LD box for 1 hour with no treatment on Day 1. Over the course of the next week each mouse received one of 4 pre-treatments on Days 2, 3, 4, and 5 of the experiment. Pre-treatments were i.p. saline, 0.5 g/kg ethanol, 1.0 g/kg ethanol, or 2.0 g/kg ethanol. Doses were given in varied order from mouse to mouse. Mice were placed in the light side of the chamber, facing the entrance to the dark, immediately following the injection, and their activity recorded.

Subsequently, an additional set of C57BL/6J mice (n=9, males) was tested using a similar repeated measures paradigm. All mice were habituated to the LD boxes, and subsequently tested with either pre-treatment of Tideglusib (200 mg/kg) or vehicle, via gavage, followed 30 minutes later by i.p. injection of either saline or the highest dose of ethanol previously tested (2.0 g/kg) and then immediate placement in the LD box. All mice received both i.p. injections (that is saline on Day 1 and ethanol on Day 2, or vice versa) but each mouse received

only 1 type of gavage treatment (that is Tideglusib on Day 1 and Tideglusib on Day 2, or Vehicle on Day 1 and Vehicle on Day 2).

Overall, relative time spent in the light was treated as inverse to the level of anxiety-like behavior.

(Chronic) Intermittent Ethanol Access (Two Bottle Choice Paradigm). C57BL/6J mice (n=21/group/sex) were allowed one week to habituate to our out-of-vivarium room (lights on at 0200, lights off at 1400). Mice were then given access to bottles of tap water (continuous) or 20% v/v ethanol (intermittent). Ethanol bottles were placed on cages immediately before the dark cycle on Mondays, Wednesdays, and Fridays (**Fig 4.1B**). Readings were taken at a 2 hour (binge) time point using a red lamp. Readings were taken for 5 weeks, with blood and tissue collection during week 6.

Blood Ethanol Content. At the time of the usual binge reading, blood was collected via cheek punch using Goldenrod sterile lancets (Braintree Scientific, Braintree, MA) from a subset of animals (n=5 EtOH-drinking females, 5 EtOH-drinking males, and one no-EtOH exposed control mouse of each sex). Blood was centrifuged and stored at -20 degrees Celsius until analysis. Analysis was performed using an Analox AM1 Alcohol Analyzer (North Yorkshire, UK) according to manufacturer's instructions. One male EtOH sample was excluded due to insufficient plasma.

"Acute-on-Chronic" Ethanol Paradigm. Following the studies on a single systemic administration of ethanol (acute) and intermittent ethanol access (chronic), these paradigms were combined into a mixed acute and chronic

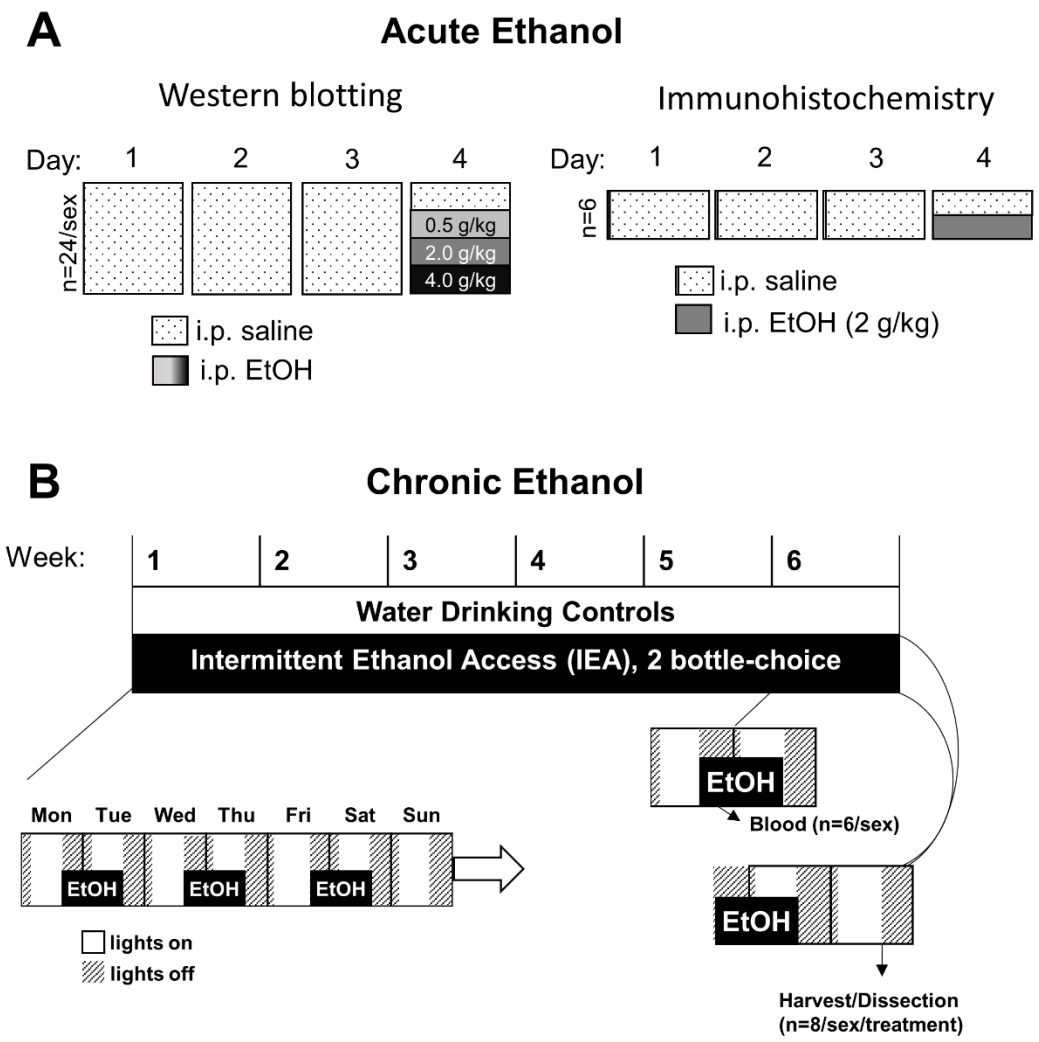

Figure 4.1 Acute and chronic ethanol paradigms for Western blot studies. **A.** "Acute Ethanol" paradigm for Western blots and IHC: 3 days of i.p. habituation to saline injections followed by either saline or ethanol. **B.** "Chronic ethanol" paradigm: Intermittent Ethanol Access (IEA) schedule. All mice had access to water and food ad libitum. Ethanol (20% v/v) was placed on cages Mondays, Wednesdays, and Fridays. The period of ethanol access began with each dark cycle (except Sunday, when ethanol was not available). Binge readings were taken 2 hours into the dark cycle using a red lamp.

Acute on Chronic Ethanol

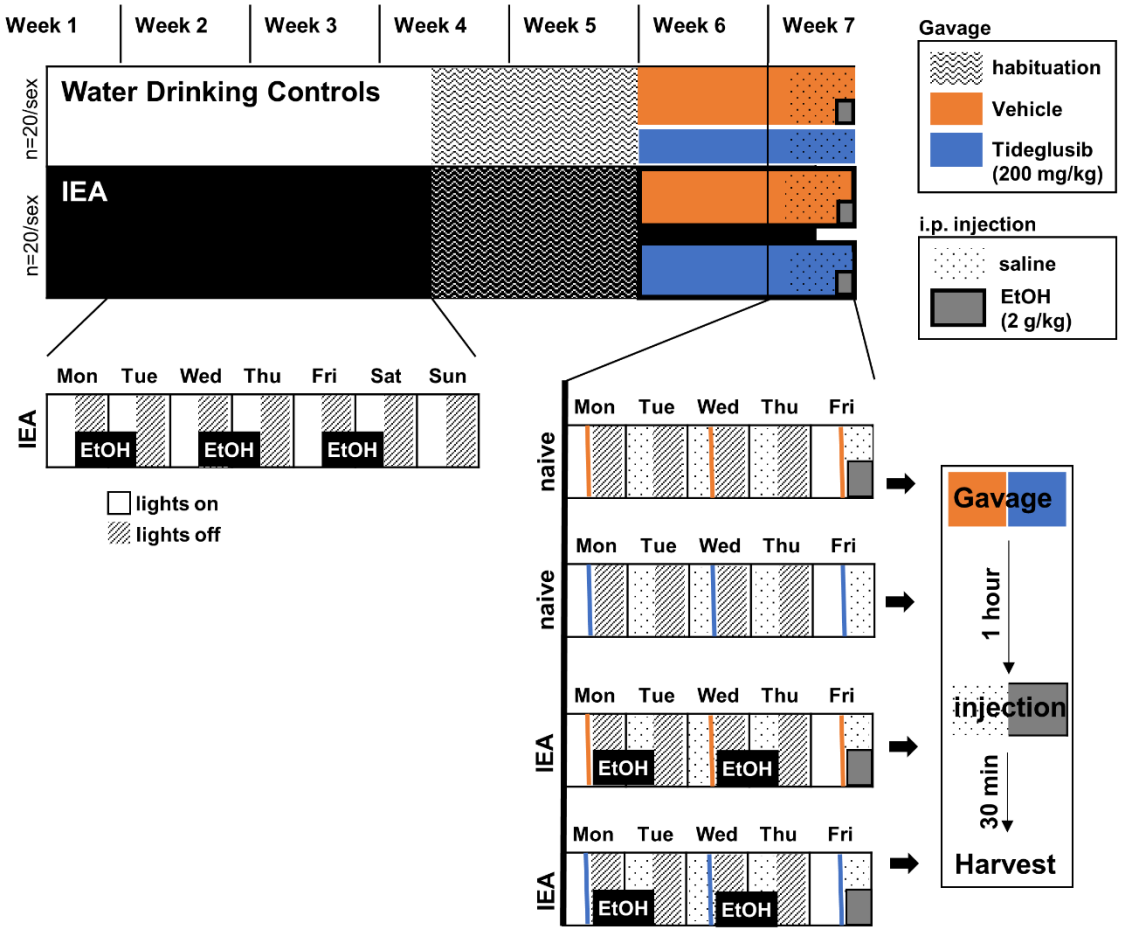

Figure 4.2 Acute-on-chronic ethanol paradigm for Western blot studies. Male and female mice underwent >6 weeks of intermittent ethanol access (IEA) or water-only drinking before i.p treatment with either i.p. saline or ethanol. All mice were gavaged for the last 2 weeks to allow for an additional treatment condition, the administration of a GSK3B inhibitor (tideglusib).

paradigm (**Fig. 4.2**). Both males and females were given access to either water only or continuous water and intermittent ethanol access (IEA) (n=20/sex/access). After 3 weeks of free drinking and readings taken at 2 and 24 hours, all animals were habituated to gavage (3 days of 0.1% saccharin, 2 days of vehicle). Gavage occurred prior to ethanol access, Mondays Wednesdays and Fridays. Animals subsequently received either gavaged vehicle or tideglusib (200 mg/kg) in the hour preceding ethanol access during Weeks 6 and 7. Animals receiving water-only were on the same gavage schedule. During Week 7 we began saline habituation in addition to gavage treatments, for the 3 days prior to the day of sacrifice. On the day of sacrifice, a Friday, 24 hours after last ethanol access, animals received gavage, an i.p. injection of either saline or ethanol (2 g/kg) an hour later, and were sacrificed 30 minutes after the injection. Western blots were run as in acute and chronic ethanol studies. Studies of the effect of tideglusib on ethanol drinking behaviors will be discussed in Chapter 6.

Statistical Analyses. Quantified Western blot data was normalized to saline controls and compared using t-tests when comparing two groups, or ANOVA to account for multiple doses or treatments. Thus acute ethanol dose response studies used a 1-way ANOVA to compare ethanol doses within each sex (as males and females were run as separate experiments). The effect of chronic ethanol (IEA) on p-GSK3B and total proteins was compared with t-tests within each sex (again, protein studies were run separately).

The effect of acute ethanol +/- IEA was analyzed via ANOVAs first within sex and then with sexes pooled, because throughout this experiment animals

and tissue samples were run concurrently. To combine samples run across 4 membranes, each of which was stained for both phospho- and total GSK3, we Z-transformed phospho/total scores according to each membrane, to create normalized scores that would not be artificially skewed by differences in staining intensity between entire membranes. Z-scores were converted to positive values by addition of a factor which would bring the Vehicle-Water-Saline sample scores to an average = 1. Within sex, a 2 way-ANOVA was run with two factors: (1) acute (ethanol vs. saline i.p. injection) and chronic (IEA vs. water-only). A 3-way ANOVA was then run which included Tideglusib treatment nested within the "chronic" factor (because here we only studied Tideglusib treatment within the IEA condition). When sexes were pooled, we first assessed for effect of sex with acute and chronic ethanol and found it non-significant as a main effect and interaction. We then carried out 2- and 3-way ANOVAs on the pooled sexes as just described for within-sex comparisons. For all Western blot analyses, 2-way ANOVAs were run in Prism and 3-way ANOVAs were run in JMP Pro 13.

Ethanol induced anxiolysis used one or two-way ANOVA, the latter when Tideglusib was included as pre-treatment. Anxiolytic behavioral assays were analyzed in Prism.

IEA Analyses: Ethanol consumption values over the 2 h and 24 h periods were calculated as ratios of grams ethanol consumed over kilograms per animal. For weekly analyses, week means were calculated for each animal giving values in g/kg/day. The first day of the experiment was excluded from the analyses of weekly means, as we have previously observed an immediate escalation on the

second day of intermittent ethanol access in C57BL/6J mice (Macleod unpublished, van der Vaart unpublished). Statistics were performed using JMP Pro 13. We used a Mixed Model repeat measures ANOVA to analyze by sex, week, and sex*week. Multiple comparisons of sex*week were performed using Tukey's post hoc test. Blood Ethanol Concentrations were analyzed using linear regression with sexes pooled.

4.3 Results

4.3.1. Acute Ethanol

Acute ethanol increases inhibitory phosphorylation of GSK3 in PFC of C57BL/6J mice. First, we aimed to determine whether an acute dose of systemically administered ethanol inhibited GSK3 in the PFC. Levels of phosphorylation of GSK3A (Serine-21) and GSK3B (Serine-9) 30 minutes after i.p. ethanol (0.5-4.0 g/kg) were assessed via Western blotting in male and female mice. As shown in **Figure 4.3,** male mice showed a significant effect of ethanol treatment on phosphorylation of both GSK3A ($F_{3,17}$=4.80, p=0.0134) and GSK3B ($F_{3,17}$=6.99, p=0.0029). As shown in **Figure 4.4**, female mice also showed a significant effect of ethanol treatment on phosphorylation of GSK3A ($F_{3,20}$=3.58, p=0.032) and GSK3B ($F_{3,20}$=3.16, p=0.047). A qualitative comparison between the male and female blots suggested a difference in the response profile, wherein male mice showed the increase in phosphorylation at the 0.5 g/kg dose and above, while female mice showed increases in phosphorylation only at the 2.0-4.0 g/kg doses. This would suggest that while acute ethanol inhibited GSK3A

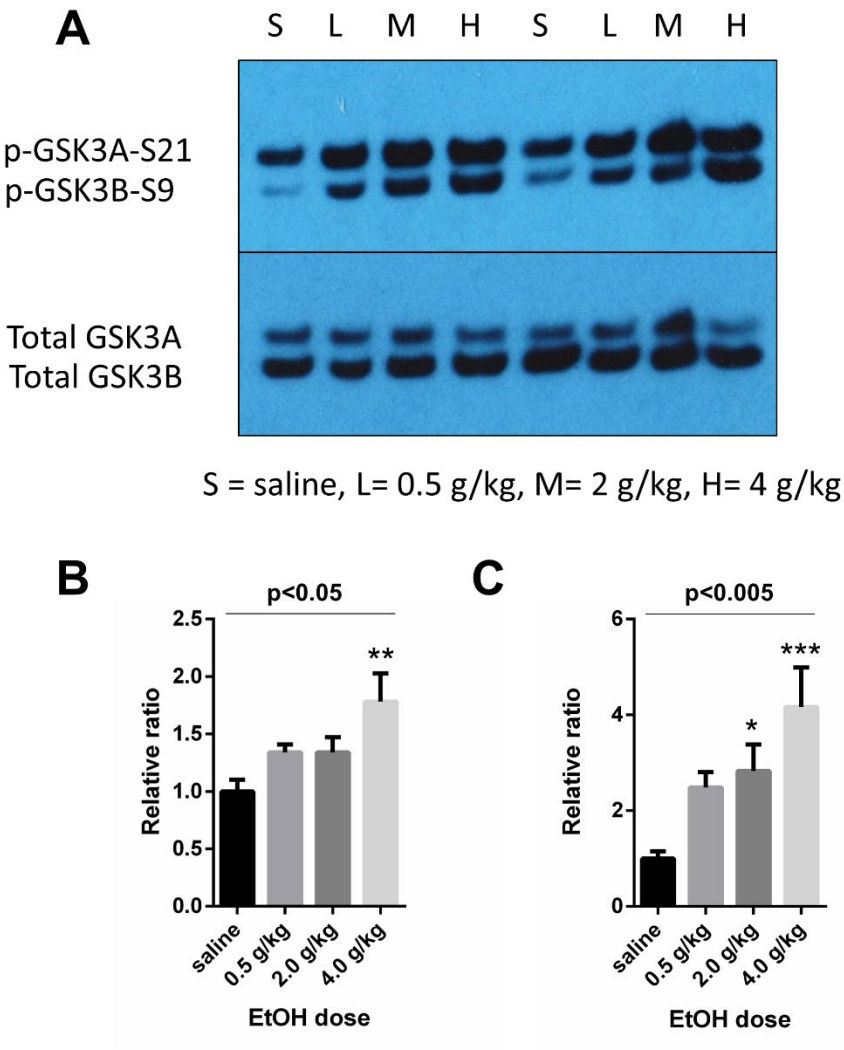

Figure 4.3 Acute ethanol increases inhibitory phosphorylation of GSK3 in PFC of male C57BL/6J mice. Male mice (n=5-6/dose) were harvested 30 min after i.p ethanol. **A.** Phospho- and total GSK3A/B were assessed via Western blot (representative film). **B.** p-GSK3A-S21 / total GSK3A shows main effect of ethanol ($p<0.05$), with the 4.0 g/kg dose ($p<0.01$) differing significantly from saline via post-hoc test. **C.** p-GSK3B-S9 / total GSK3B shows main effect of ethanol ($p<0.005$), with the 2.0 and 4.0 g/kg doses differing significantly from saline via post-hoc testing ($p<0.05$ and $p<0.005$, respectively).

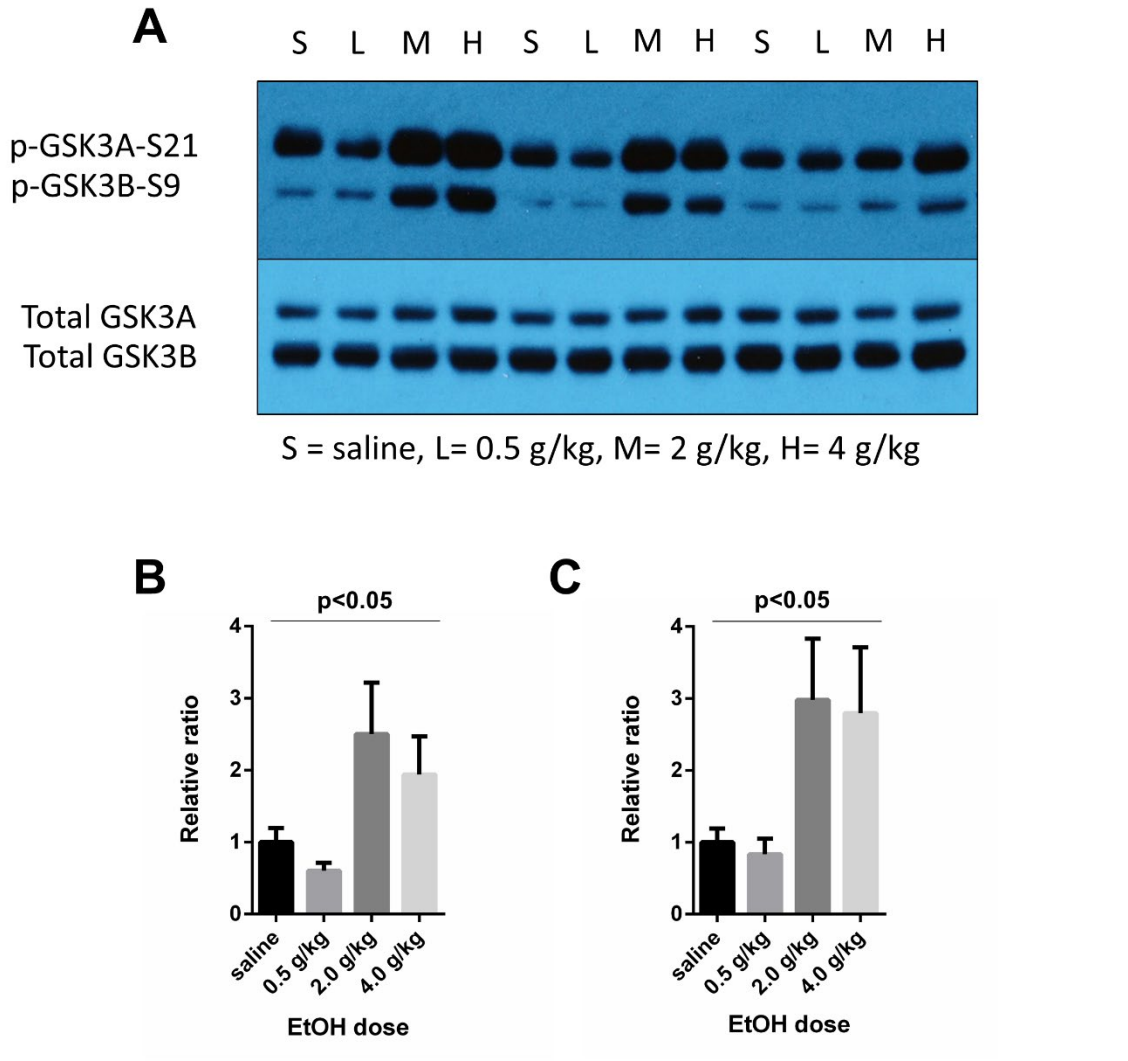

Figure 4.4 Acute ethanol increases inhibitory phosphorylation of GSK3 in PFC of female C57BL/6J mice. Female mice (n=6/dose) were harvested 30 min after i.p ethanol. **A.** Phospho- and total GSK3A/B were assessed via Western blot (representative film). **B.** p-GSK3A-S21 / total GSK3A shows main effect of ethanol ($p<0.05$). **C.** p-GSK3B-S9 / total GSK3B shows main effect of ethanol ($p<0.05$).

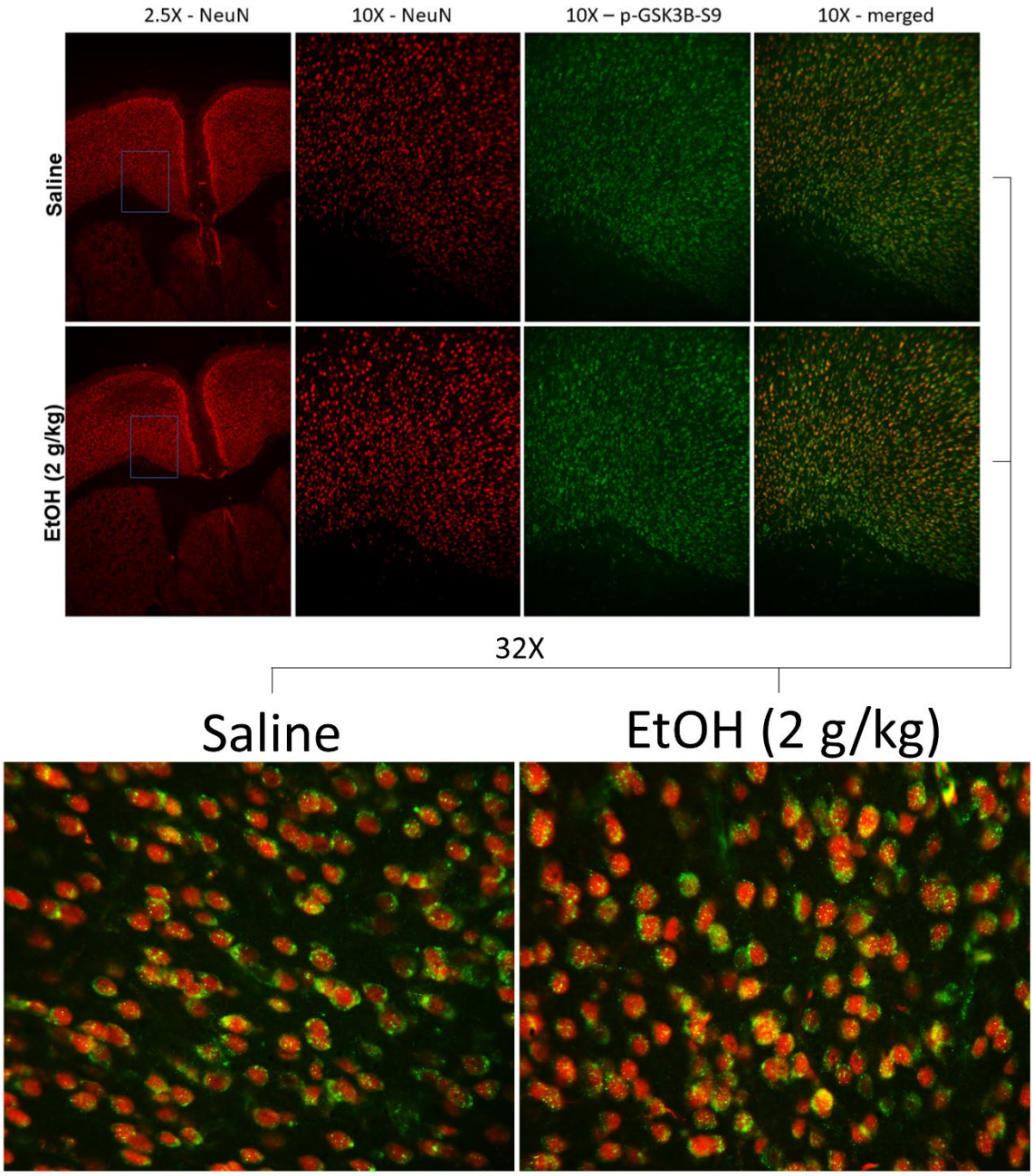

Figure 4.5 Acute EtOH-induced p-GSK3B-S9 appears to show punctate staining. Male mice were perfused 30 minutes after a single 2.0 g/kg ethanol dose and stained for p-GSK3B-S9 (green) and the neuronal nuclei marker NeuN (red). Signals appeared qualitatively similar at 2.5 and 10X; upon closer inspection of PFC at 32X, punctate staining in the p-GSK3B-S9 channel can be observed overlaying neurons and appeared qualitatively greater in the ethanol treated condition.

and GSK3B in both male and female mice, males may be more sensitive to this effect.

To further characterize ethanol-induced GSK3B phosphorylation in the PFC, we conducted pilot IHC studies of male mice (n=3/treatment) treated with saline or ethanol (2g/kg) for 30 min. and then perfused. Following staining for neuronal nuclei (NeuN) and p-GSK3B-S9, qualitative analysis revealed possible increased p-GSK3B staining in ethanol treated mice, with a punctate pattern (**Figure 4.5, 32X**) overlaying neurons. Since Western blot data had confirmed the phosphorylation results and GSK3B staining was virtually entirely neuronal, we did not pursue a more quantitative analysis of the IHC results. To test the effect of acute ethanol on a reported downstream synaptic target of GSK3B, we assessed levels of phospho-PSD95-T19 (**Figure 4.6**). Acute ethanol treatment did not show a significant effect on PSD95 phosphorylation in male ($F_{3,17}$=1.13, p=0.36) or female mice (F3,20=0.18, p=0.908). In male mice, we did observe a suggestive, non-significant linear trend (p=0.083) of phosphorylated/total PSD95, inverse to ethanol treatment. Such a trend toward decreased phosphorylation at this threonine-19 residue would be expected, given GSK3B inhibition following acute ethanol.

Acute ethanol shows significant effect on anxiety-like behavior. We conducted a pilot study on a repeated measures protocol for light-dark (LD) box assays. Our intent was to determine whether a cohort of animals could be tested on successive days for anxiety-like behavior without confounding effects of day in

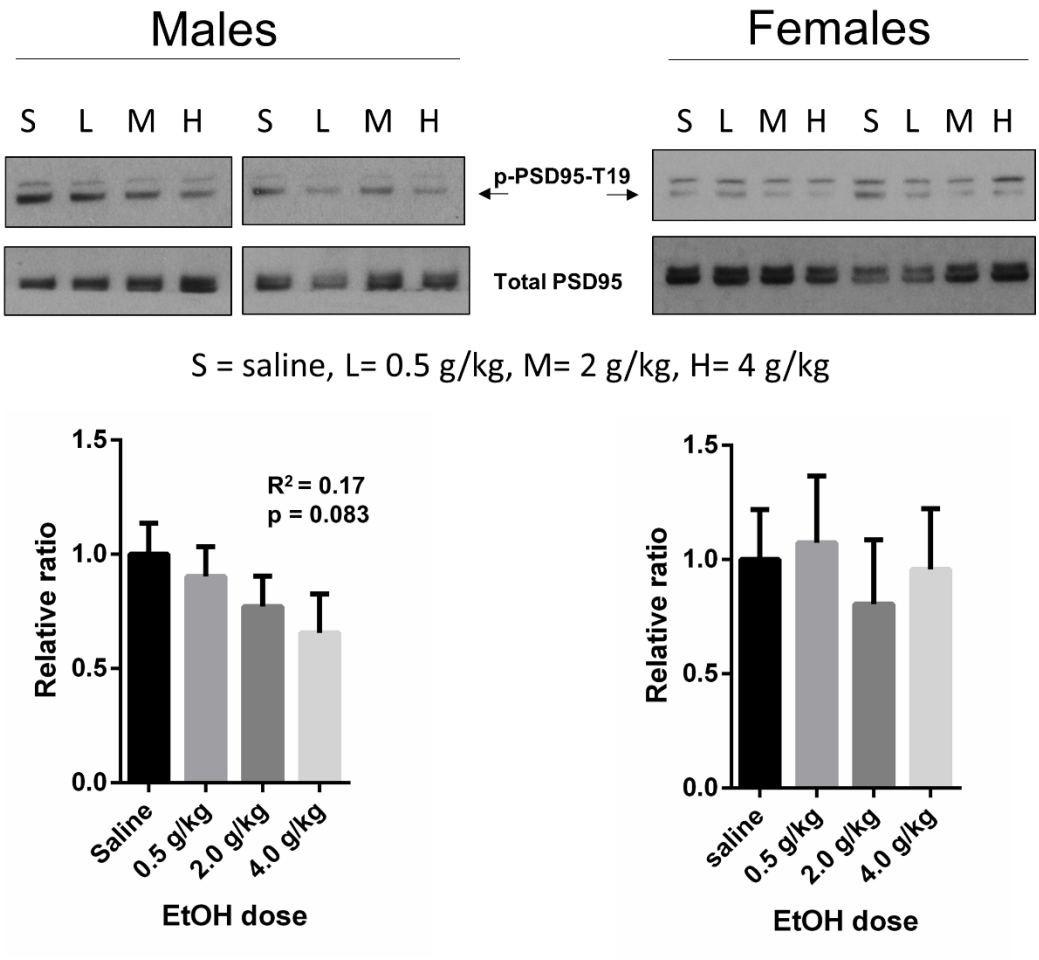

Figure 4.6 Effect of acute ethanol on p-PSD95-T19 levels in PFC. PSD95 did not show significant alterations in phosphorylation of its threonine-19 residue in either male or female mice as an effect of ethanol treatment. However, a post-hoc test for linearity showed a suggestive inverse trend with increasing dose in male mice.

the LD box. Each day, animals were given saline or a dose of ethanol (0.5-2.0g/kg) and placed in the light side of the chamber. Locomotor behavior was recorded for a full hour, but we carried out initial analyses on the first 5-minute bin. By one-way RM ANOVA, there was a significant effect of ethanol treatment ($F_{1.34,6.70}$=14.14, p=0.0058) on %Time in the light, with no observable effect of day in the box (**Figure 4.7A-B**). We assessed overall locomotor activity via total distance traveled, and found a linear trend across increasing ethanol doses (**Figure 4.7C**). Thus the pilot study determined that using repeated treatment over successive days was a viable method of assessing ethanol-induced effects on anxiety-like behavior and locomotor activity.

Pre-treatment with the GSK3B inhibitor tideglusib augments the effect of acute ethanol on locomotor activity. A separate cohort of C57BL/6J mice (n=9, males) was used in assays of the GSK3B inhibitor, tideglusib, to assess its potential effect on acute ethanol induced behavioral changes. On a given day, each animal received a gavage of either vehicle of tideglusib (200 mg/kg), and 30 minutes later, an i.p. injection of either saline or ethanol (2 g/kg). The dose of tideglusib was determined based on preclinical studies of this drug (Bharathy *et al*, 2017). The dose of ethanol was determined based on the effect of this dose observed in the pilot study. The first 10-minute bin in the LD box was assessed via 2-way RM ANOVA to test the effects of injection (saline vs. ethanol) and gavage (vehicle vs. tideglusib). Results are shown in **Figure 4.8**. Effects on anxiety-like behavior, as determined by %time in light **(A)**, were found to be

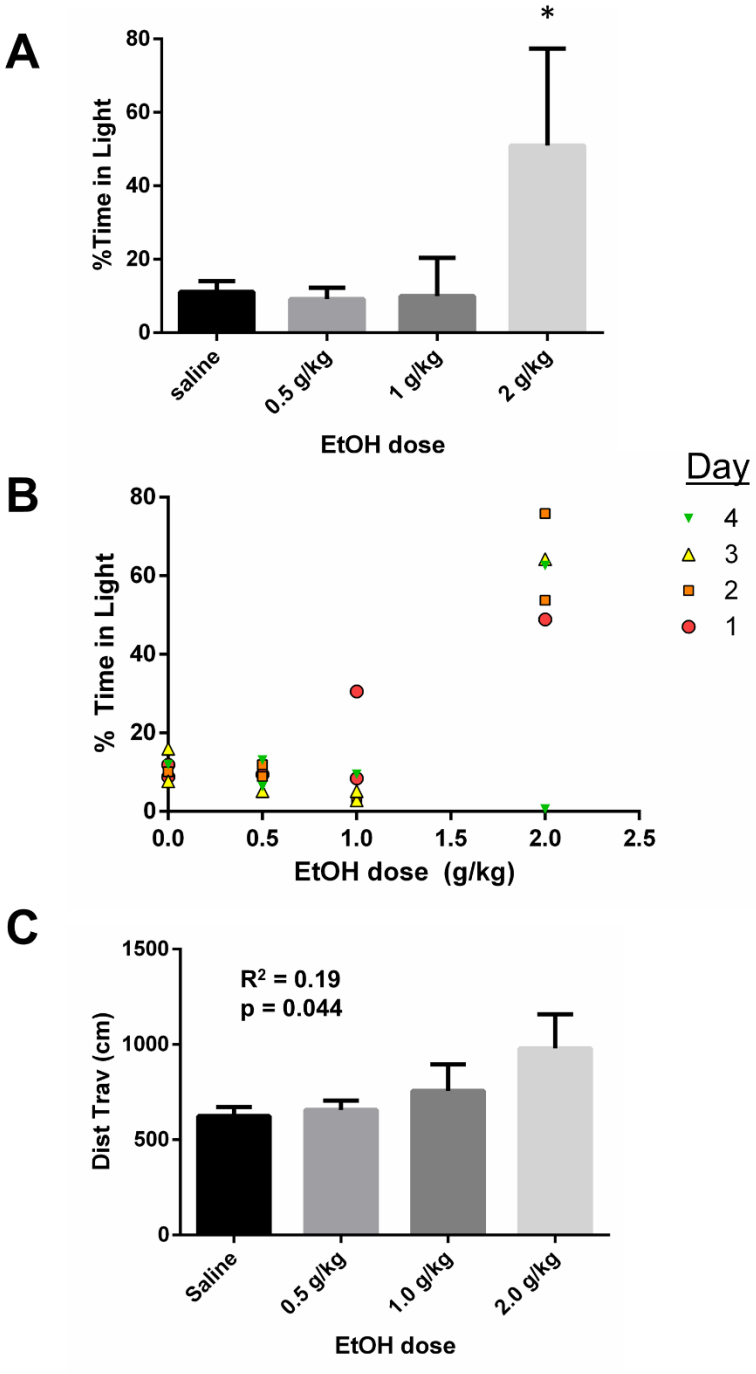

Figure 4.7 Pilot study of acute ethanol on LD box assay. N=6 male mice each received saline or each of 3 ethanol doses over the course of a week. **A. Acute ethanol (i.p.) shows anxiolytic-like effects.** One-way RM ANOVA of %Time in Light shows main effect of treatment ($p<0.01$); 2 g/kg dose differs from saline and each other dose at $p<0.05$ by Tukey's post-hoc. **B.** There is no discernible pattern of day in LD box at each dose**. C. Significant linear trend of total distance traveled with increasing ethanol dose.**

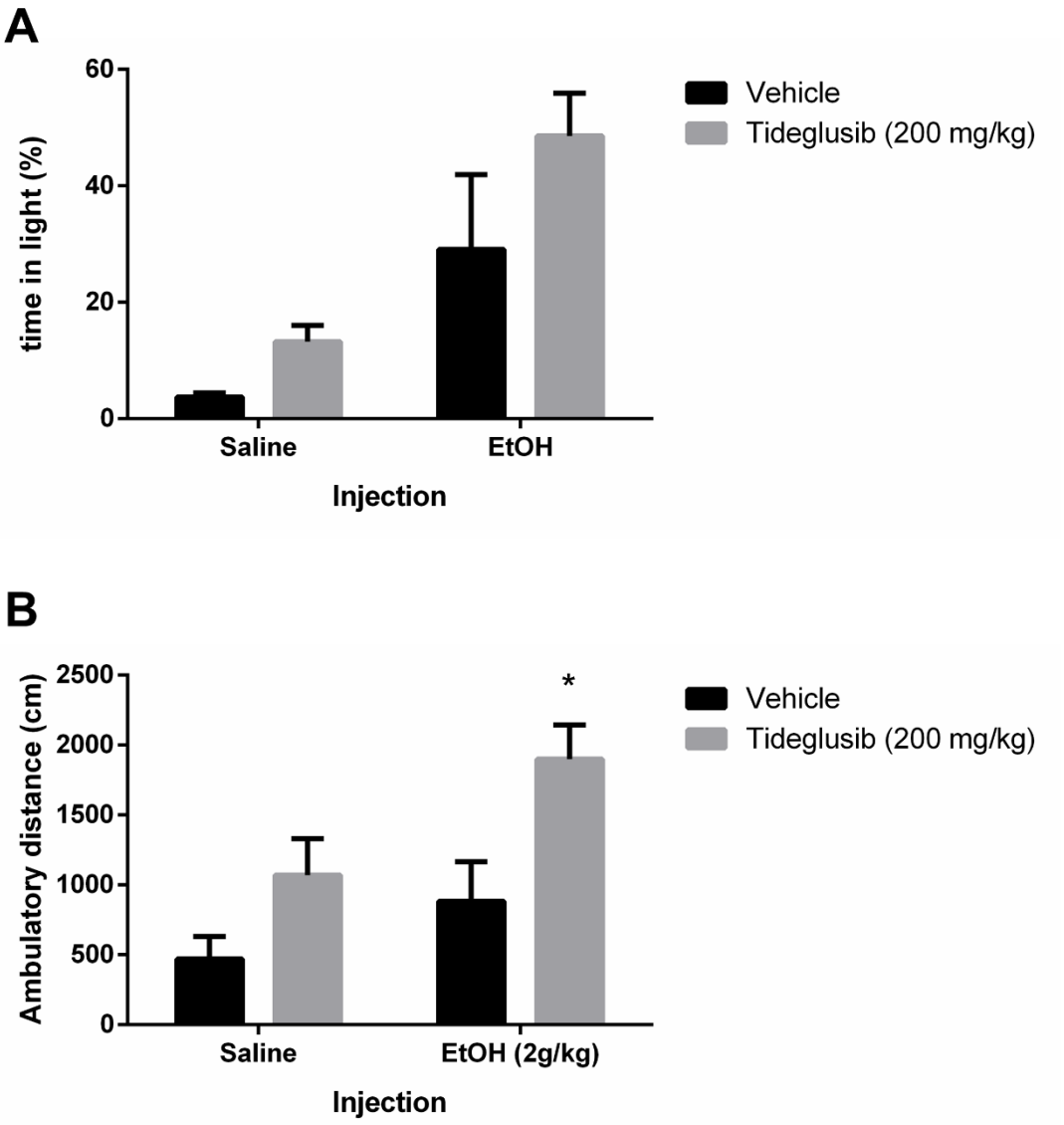

Figure 4.8 GSK3B inhibition augments acute ethanol locomotor effects. Gavage pre-treatment with tideglusib vs. vehicle was given 30 min prior to i.p. ethanol vs saline and then animals assayed in LD box for anxiety-like behavior and locomotion. First 5-minute bin data shown here. **A.** Acute ethanol (i.p.) shows anxiolytic-like effects. Two-way RM ANOVA of %Time in Light shows significant main effect of ethanol ($p<0.01$), and suggestive but non-significant effect of tideglusib ($p<0.1$). **B.** Two-way RM ANOVA of Distance Traveled shows significant main effect of ethanol and significant main effect of tideglusib ($p<0.05$ for each). Difference between tideglusib and vehicle within EtOH treatment condition was significant (*$p<0.05$) by Sidak's post-hoc test.

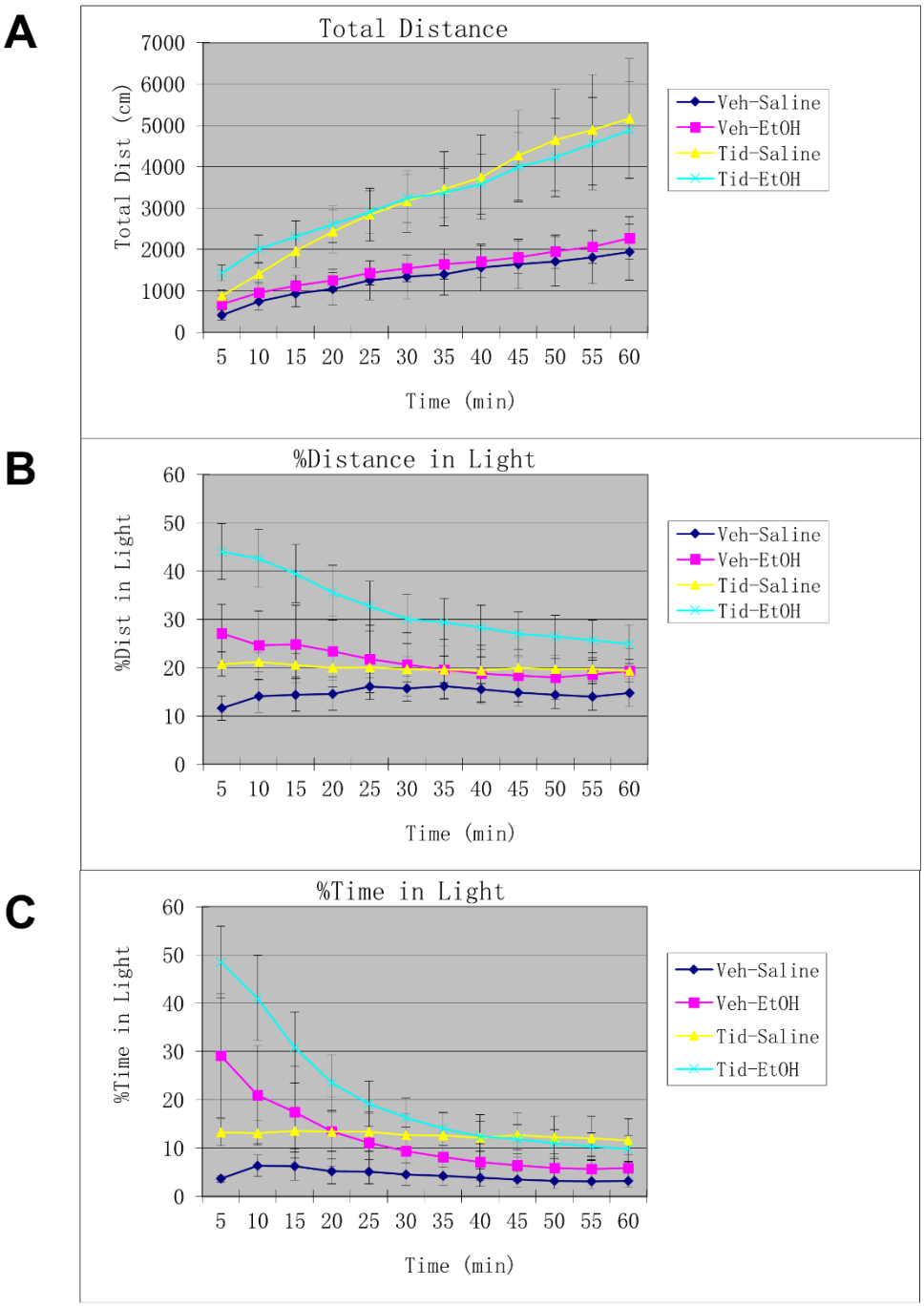

Figure 4.9 Full hour test data from LD boxes (cumulative bins). A. Total distance traveled, **B.** %distance traveled in the light, **C.** %time spent in the light. Veh/Tid refers to gavage pre-treatment, Saline/EtOH refers to acute i.p. injection. The anxiolytic-like effects of ethanol (B & C) appear to occur preferentially in the earlier bins, while effects of tideglusib on locomotor behavior appear stable over the course of the test.

significant for injection ($F_{1,7}$=15.39, p=0.0057), non-significant for gavage ($F_{1,7}$=4.75, p=0.0657), and non-significant for interaction ($F_{1,7}$=0.413, p=0.541). Effects on locomotor activity, as determined by total distance traveled **(B)**, were found to be significant for injection ($F_{1,7}$=5.77, p=0.047) and gavage ($F_{1,7}$=11.71, p=0.011), and non-significant for interaction ($F_{1,7}$=0.655, p=0.445). When the data is examined over the course of the 1 hour mice spent in the LD box (**Figure 4.9**), there appear to be differences in the time course between the effects of ethanol and tideglusib. While differences between saline and ethanol injections are more pronounced in the early time bins (particularly in **C.** %time in light), by the end of the session the differences between vehicle and tideglusib gavage are more apparent (see **A.** and **C.**). Qualitatively, there appears to be a more sustained effect of tideglusib on locomotor activation and possibly anxiolytic-like behavior than that of ethanol. Alternatively, tideglusib could be viewed as increasing the acute anxiolytic properties of ethanol.

4.3.2. Chronic Ethanol

Chronic ethanol (IEA) does not significantly alter phosphorylation or total levels of GSK3. After 6 weeks of intermittent ethanol access or water-only access, male and female mice (n=8/sex/access) were harvested 24 hours after last available ethanol and tissue was assessed via Western blot. Representative images and quantifications are shown in **Figure 4.10**. There was insufficient evidence to reject the null hypotheses that chronic ethanol does not alter levels of GSK3A/B phosphorylation or total protein. Rather than listing all statistical

Table 4.1: **Results of t-tests for Western blots of p-GSK3A/B after chronic ethanol.**

	p-GSK3A-S21	Total GSK3A	p-GSK3B-S9	Total GSK3B
Males	t=0.06504 p=0.9491	t=0.2635 p=0.7963	t=0.4053 p=0.6914	t=0.09361 p=0.9268
Females	t=1.407 p=0.1813	t=0.9145 p=0.3760	t=0.6402 p=0.5324	t=0.04710 p=0.9631

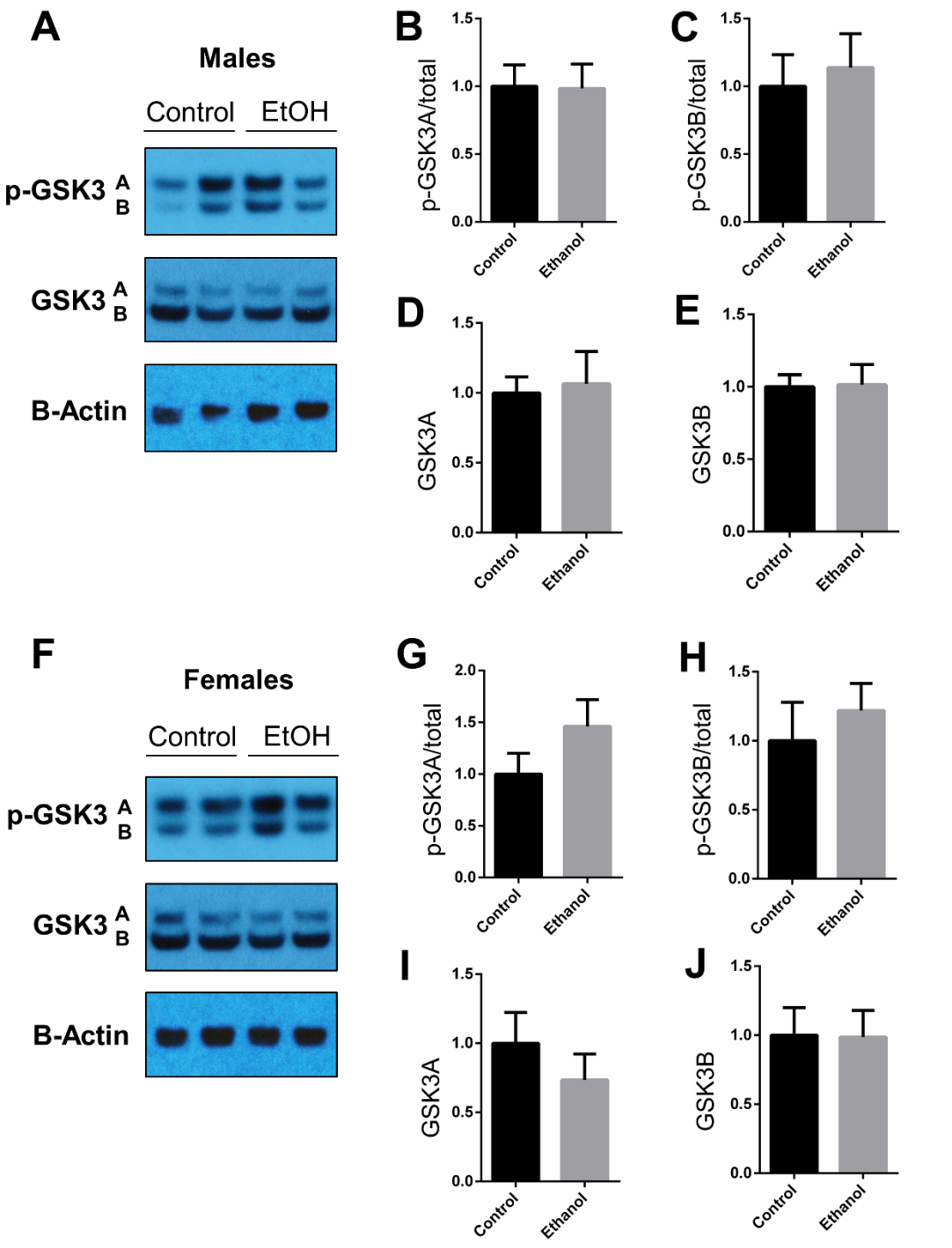

Figure 4.10 Chronic ethanol does not significantly alter GSK3 phosphorylation or total protein in mPFC. p-Proteins normalized to the total form of the same protein; total proteins normalized to B-Actin. **A.** Representative films of p-GSK3, total GSK3, and B-actin in male C57BL/6J mice. **B.-E.** Analyses of quantified Western blots. **F.** Representative films of p-GSK3, total GSK3, and B-actin in female C57BL/6J mice. **G.-J.** Analyses of quantified Western blots.

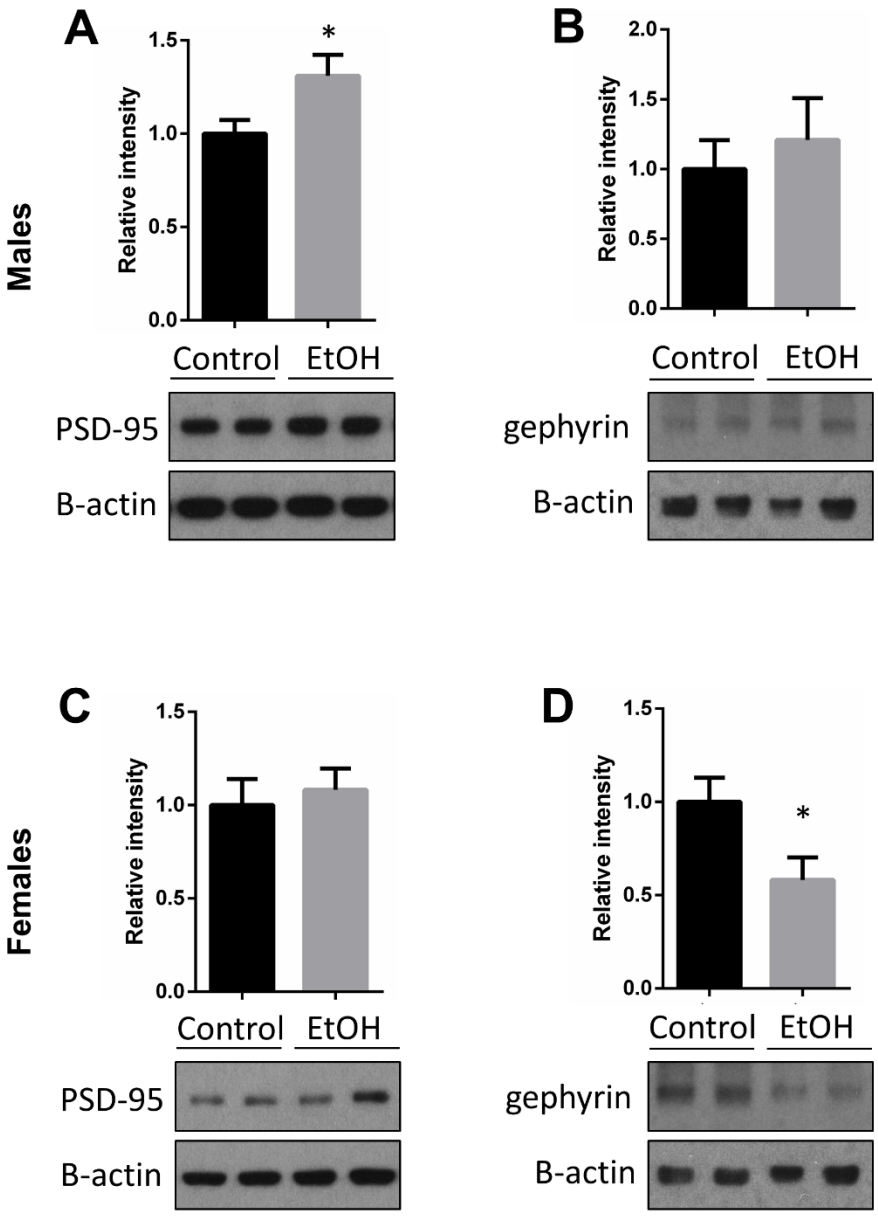

Figure 4.11 Chronic ethanol significantly alters synaptic scaffolding proteins in mPFC. Tissue was harvested after 6 weeks of intermittent ethanol access, 24 hours after last access period. **A.** PSD95 is significantly increased in male mice (*p<0.05). **B.** Gephyrin is not significantly altered in male mice. **C.** PSD95 is not significantly altered in female mice. **D.** Gephyrin is significantly decreased in female mice (*p<0.05).

outcomes in the text, results of two-tailed t-tests for all conducted are given in **Table 4.1**.

Chronic ethanol (IEA) significantly alters synaptic scaffolding proteins in PFC. We carried out subsequent Western blot analyses on the scaffold proteins, PSD95 and gephyrin, in male and female mice. Results are shown in **Figure 4.11**. In males, PSD95 was significantly increased following IEA ($t=2.32$, $p=0.036$), while gephyrin was not significantly altered ($t=0.586$, $p=0.568$). On the other hand, in female mice, PSD95 was not significantly altered ($t=0.453$, $p=0.657$) while gephyrin was significantly decreased ($t=2.37$, $p=0.033$). Thus these may represent alternative means of adaptation of the PFC to chronic ethanol exposure, through either upregulation of a glutamatergic anchor protein or downregulation of a GABAergic anchor protein, which show sex specificity.

Characterization of Ethanol-Drinking Behaviors in Male and Female C57BL/6J Mice. We set out to determine the extent to which C57BL/6J mice will undergo an immediate binge period during the first two hours of ethanol access, whether there was an escalation in this binge-like consumption, and whether male and female mice showed any differences in this behavior or the IEA model generally. Daily values of 2 hr and 24 hr consumption and preference are plotted out in **Figure 4.12**.

Given fluctuations in the data, we took 3-day averages from ethanol access days to obtain weekly means. The first day was dropped from this

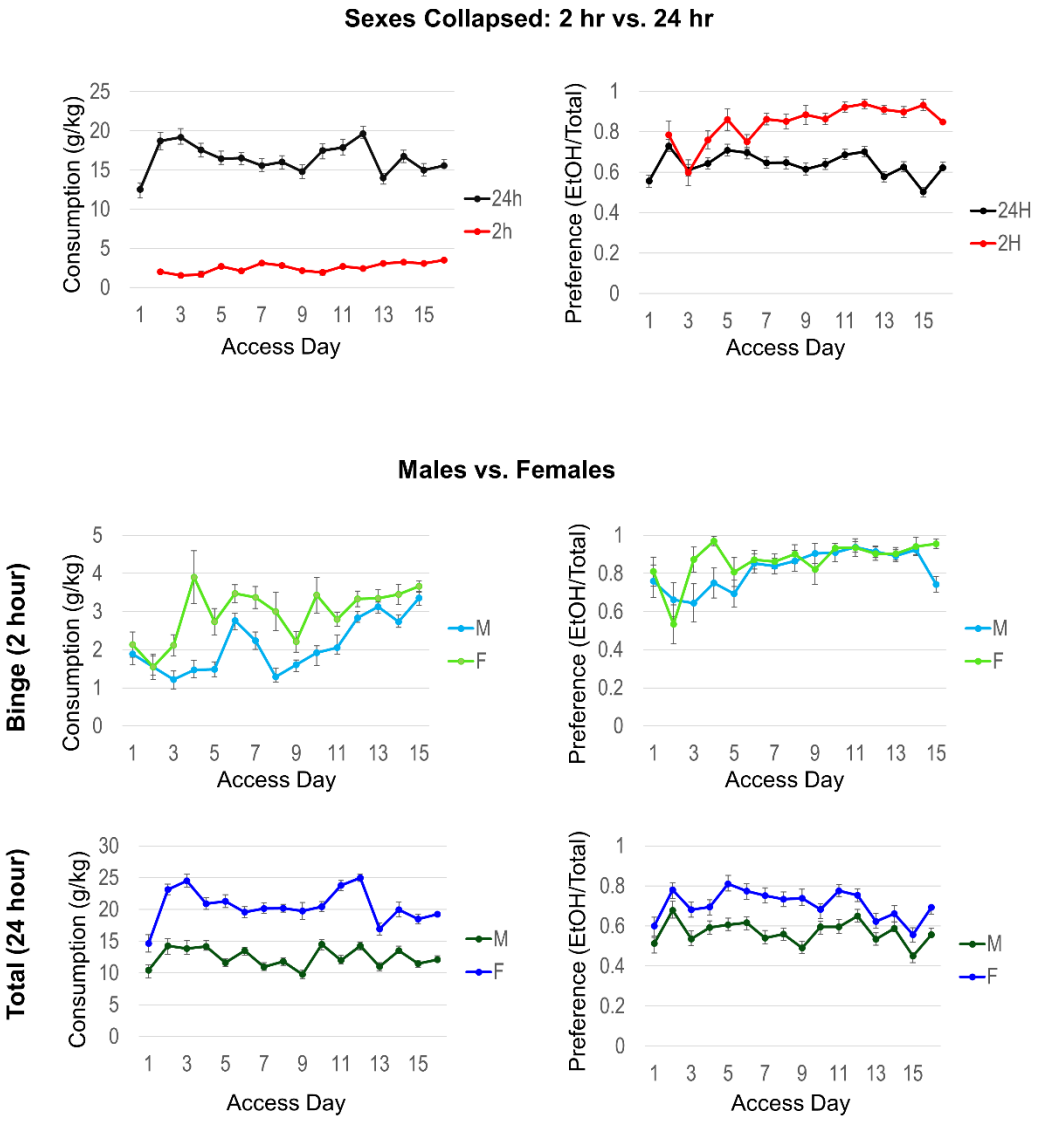

Figure 4.12 Intermittent Ethanol Access (IEA) behavioral characterization. C57BL/6J mice (n=21/sex) were given access to 20% v/v ethanol in addition to tap water at the start of their dark cycle on Mondays, Wednesdays, and Fridays over the course of five weeks. Changes in fluid volume were measured at 2 hours and 24 hours after placement of bottles on cages. Consumption is reported as g EtOH/kg body weight; preference is reported as mL EtOH / mL total fluid.

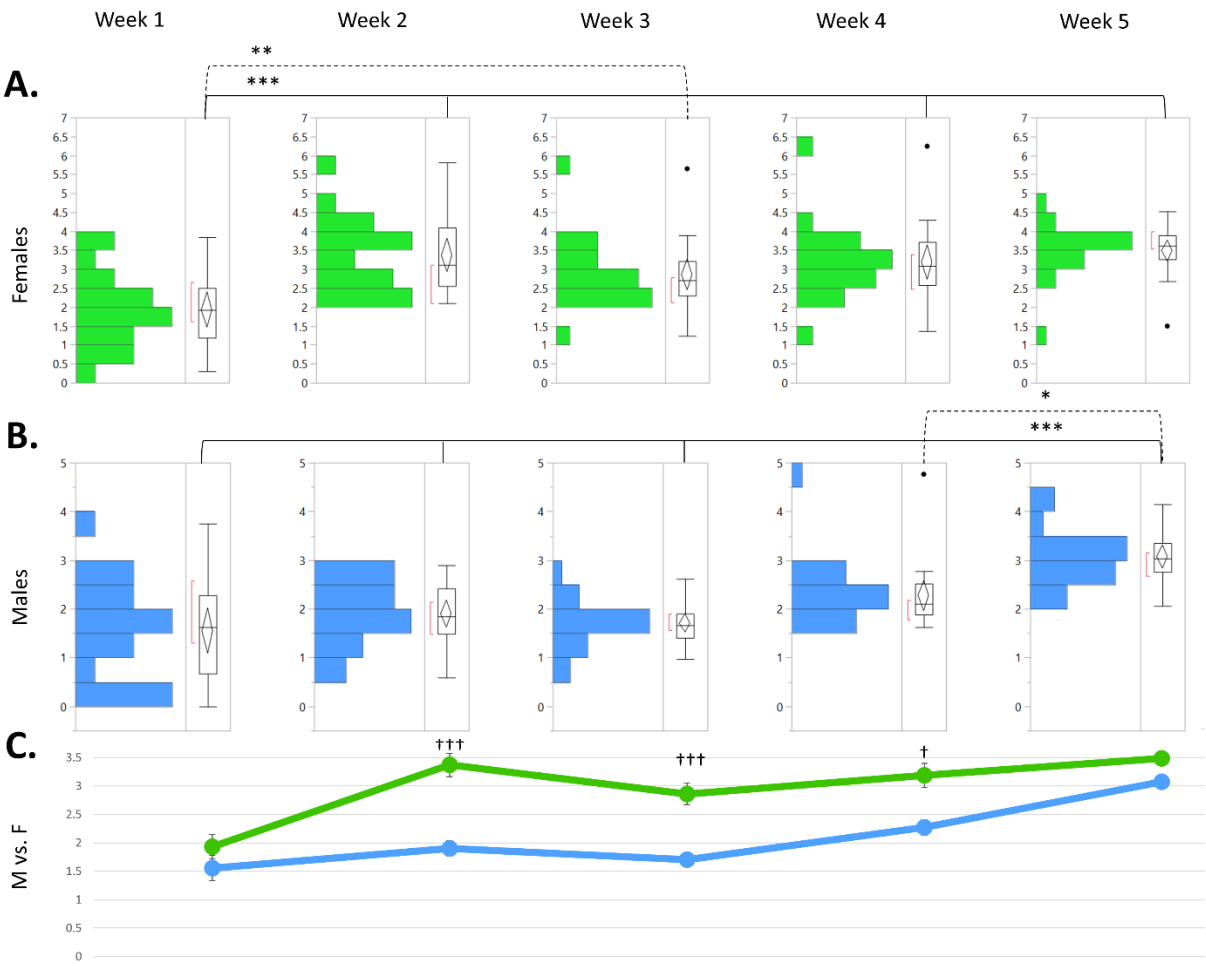

Figure 4.13 Mean ethanol binge consumption (weekly). A.-B. Within-Sex Comparisons: A. Females show significantly greater binge (2 h) ethanol consumption at Weeks 2-5 than at Week 1. **B.** Males show significantly greater ethanol consumption at Week 5 than Weeks 1-4. ***p<0.0005, **p<0.005, *p<0.05. **C. Between-Sex Comparisons:** Females show significantly greater ethanol consumption at Weeks 2-4 than males, but no significant difference at Weeks 1 or 5. †††p<0.0005, ††p<0.005, †p<0.05

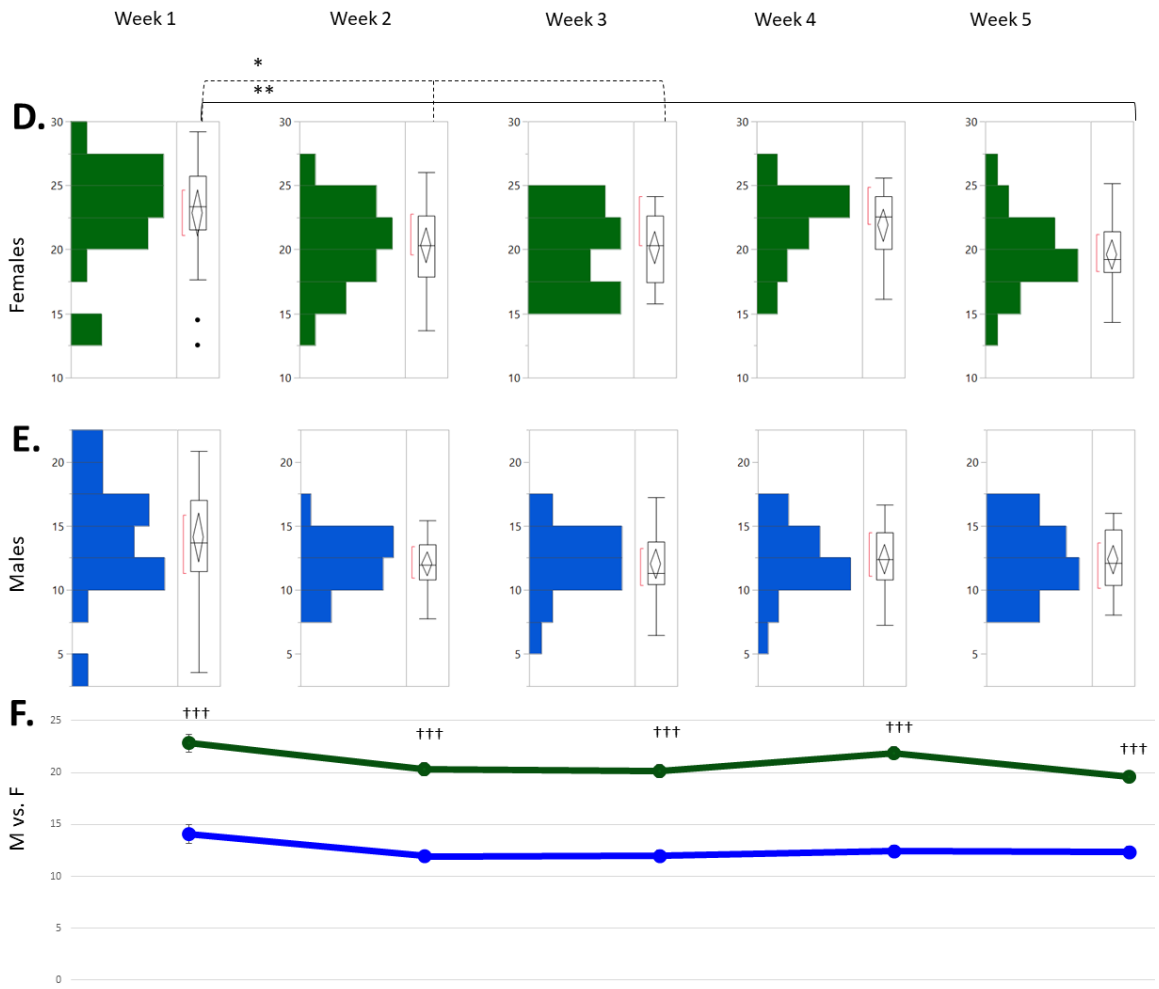

Figure 4.14 Mean ethanol 24-hour consumption (weekly). D.-E. Within-Sex Comparisons D. Females show significantly lower total (24 h) ethanol consumption at Weeks 2, 3, and 5 than Week 1. Note that the first reading (Access Day 1) was excluded from the weekly analysis, and showed the lowest mean ethanol consumption overall. **B.** Males do not show any significant differences in total ethanol consumption from week to week. **F. Between-Sex Comparisons** Females show robustly greater total ethanol consumption over the entire course of the experiment.

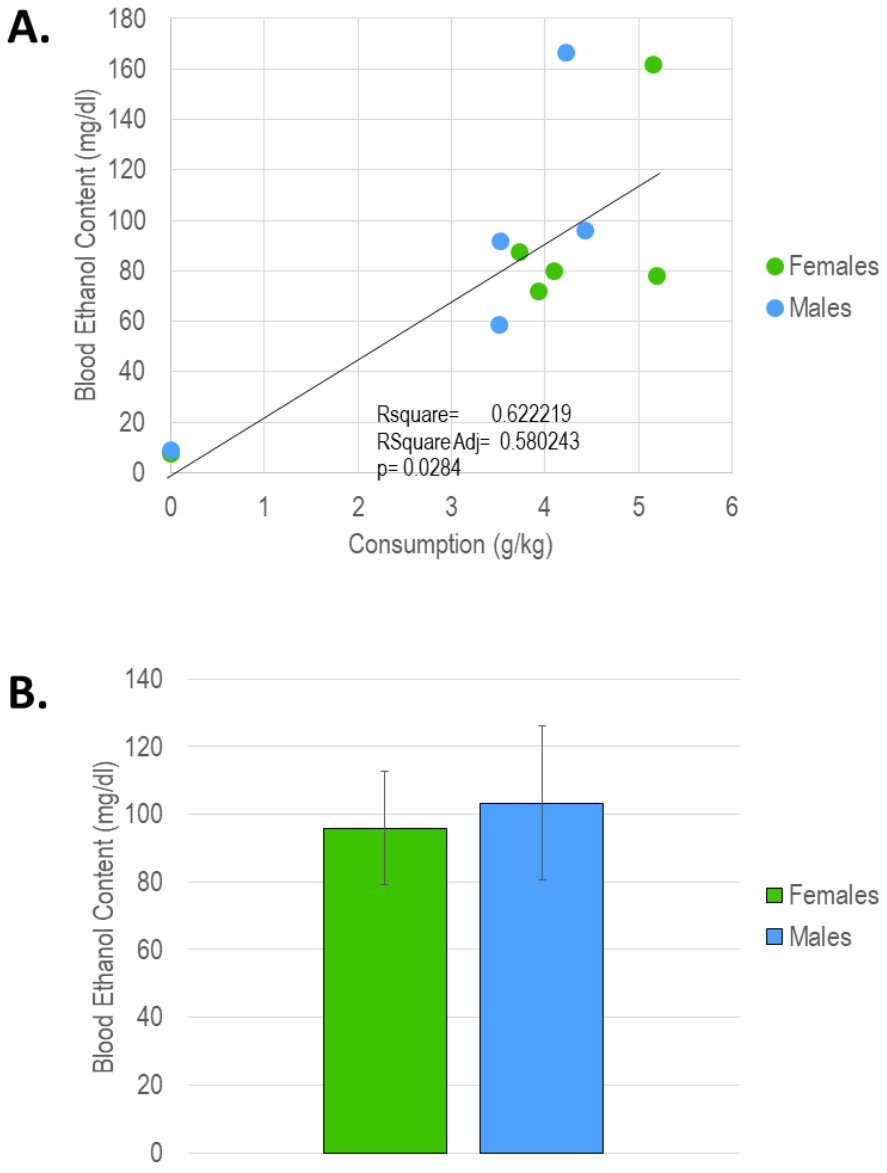

Figure 4.15 Blood Ethanol Content (BEC). A. Blood samples taken at 2 h at the end of 5 weeks of IEA from 9 EtOH drinking mice and 2 non-EtOH controls show a linear relationship with consumption. **B.** Mean blood ethanol content in ethanol drinking mice is approximately 100 mg/dl in both female and male mice, on average, after a 2 h access period.

analysis as it is an expected outlier. Drinking data from the last week (Week 6) is also not reported because of interventions such as blood draws confounding the data. We found that there was significant escalation in binge-like ethanol drinking as determined by increases in consumption in the first 2 hours after ethanol access (**Figure 4.13**). In female mice, Weeks 2-5 all showed significantly greater ethanol consumption ($p<0.005$ for Week 3, $p<0.0005$ for Weeks 2, 4, and 5) than was observed in Week 1. In male mice, Week 5 consumption was significantly higher than Weeks 1-4 ($p<0.05$ compared to Week 4, $p<0.0005$ compared to Weeks 1-3). Between male and female mice, females drank significantly more ethanol during the 2-hr binge period than males during Weeks 2-4 ($p<0.0005$ for Week 2, $p<0.05$ for Week 4). There was not a significant escalation in daily ethanol consumption based on the 24-hour readings (**Fig. 4.14**), although the first day of ethanol access had the lowest consumption over the course of the experiment (see **Fig. 4.12**). Females drank significantly more than male mice during the 24-hour access periods consistently through the experiment ($p<0.0005$ Weeks 1-5).

Blood Ethanol Concentration (BEC). After 5 weeks of IEA, blood was drawn at the usual 2 hour binge point to verify that mice were achieving binge-like consumption. Blood was collected via cheek punch from 9 ethanol-drinking mice and 2 non-drinking controls. These values show a significant linear relationship when plotted against consumption values obtained from readings at the same time point (**Fig. 4.15A**). Mean BEC values were approximately 100 mg/dl (0.10

g%) on average for both male and female mice (**Fig. 5.15B**). This confirms that after 5 weeks of ethanol access, both male and female mice are consuming an excessive amount of ethanol. Moreover, the lack of sex difference at this time point is in line with our observation that male and female mice were consuming similar amounts of ethanol during the binge period by Week 5.

4.3.3. Acute-on-Chronic Ethanol

It has been shown that a 2.0 g/kg dose of ethanol produces a BEC in C57BL/6J of about 180 mg/dl (Crabbe *et al*, 2003), which is only slightly above the highest BECs we recorded at our 2 hour binge time point. We have shown that a 2 g/kg ethanol injection in the PFC of naïve mice produces a robust phosphorylation at the GSK3B inhibitory residue. We however found no significant effect of chronic ethanol on GSK3B phosphorylation 24 hours into ethanol withdrawal. We next sought to determine whether long-term ethanol exposure might alter the reactivity of GSK3B to an acute dose of ethanol. We used the same combined antibodies to the A and B isoforms on GSK3 as previously but have focused our analyses on relative p-GSK3B-S9 specifically.

In the PFC of male C57BL/6J mice (**Fig. 4.16**) two-way ANOVA of acute and chronic ethanol (excluding Tideglusib treated animals) revealed a significant main effect of *acute* ethanol ($F_{1,15}$=7.083, p=0.0178), and non-significant effects of *chronic* (IEA) ethanol ($F_{1,15}$=0.0433, p=0.183) and *acute*chronic* interaction ($F_{1,15}$=1.19, p=0.293). By Sidak's post-hoc test, acute i.p. ethanol significantly

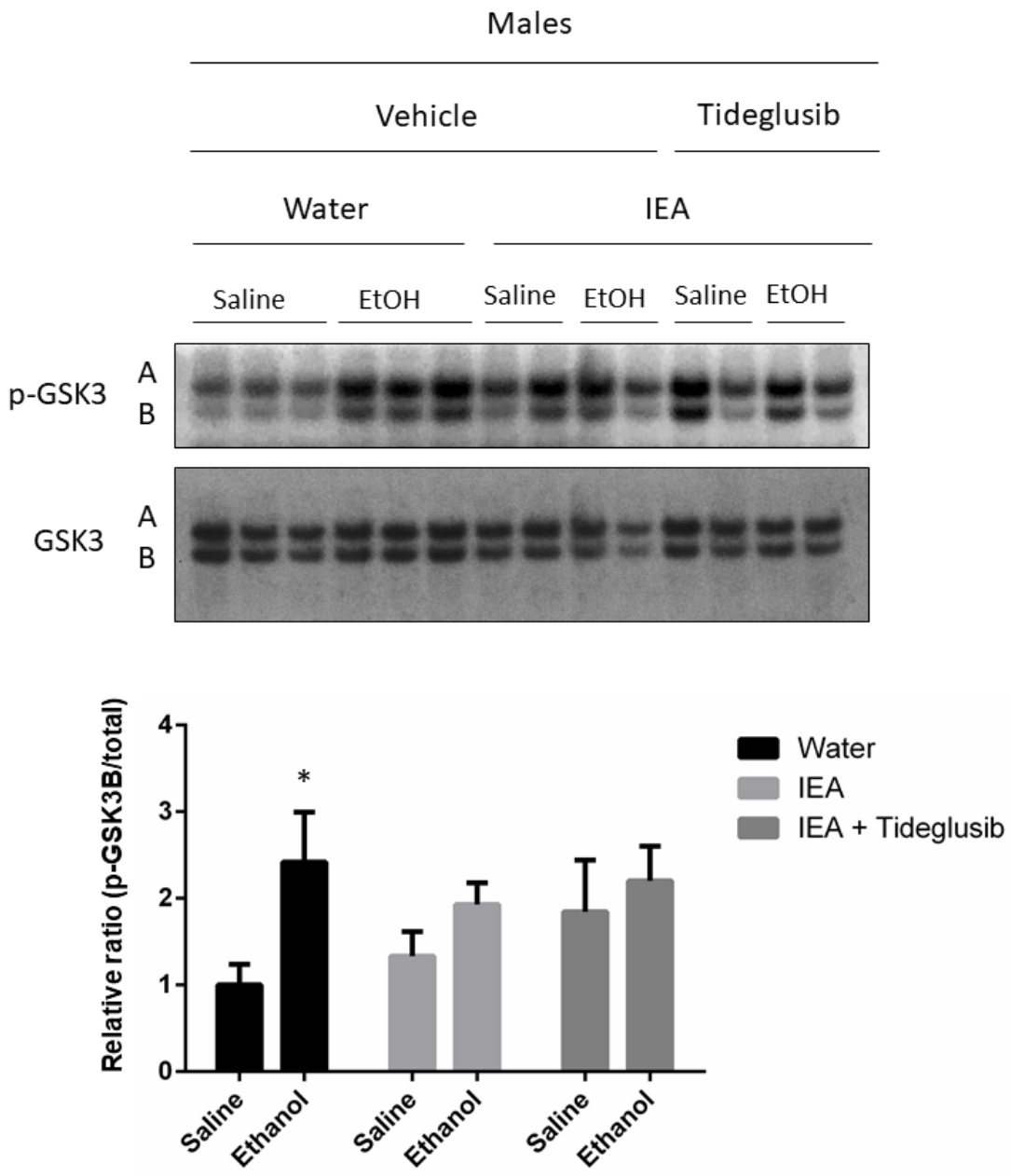

Figure 4.16 Acute-on-chronic ethanol effects on GSK3B phosphorylation in mPFC (males). (Top): Representative films of phospho- and total GSK3 Western blots. (Bottom): Quantified results of p-GSK3B. *Acute* (i.p.) ethanol vs. saline is on the X-axis. *Chronic* ethanol (IEA vs Water) is shown in legend. A 2-way ANOVA excluding Tideglusib treated animals found significant main effect of *acute* ethanol. By Sidak's post hoc, acute ethanol increased p-GSK3B within the chronic water condition (*$p<0.05$), but not within the IEA condition. Subsequent 3-way ANOVA did not find significant effects of Tideglusib.

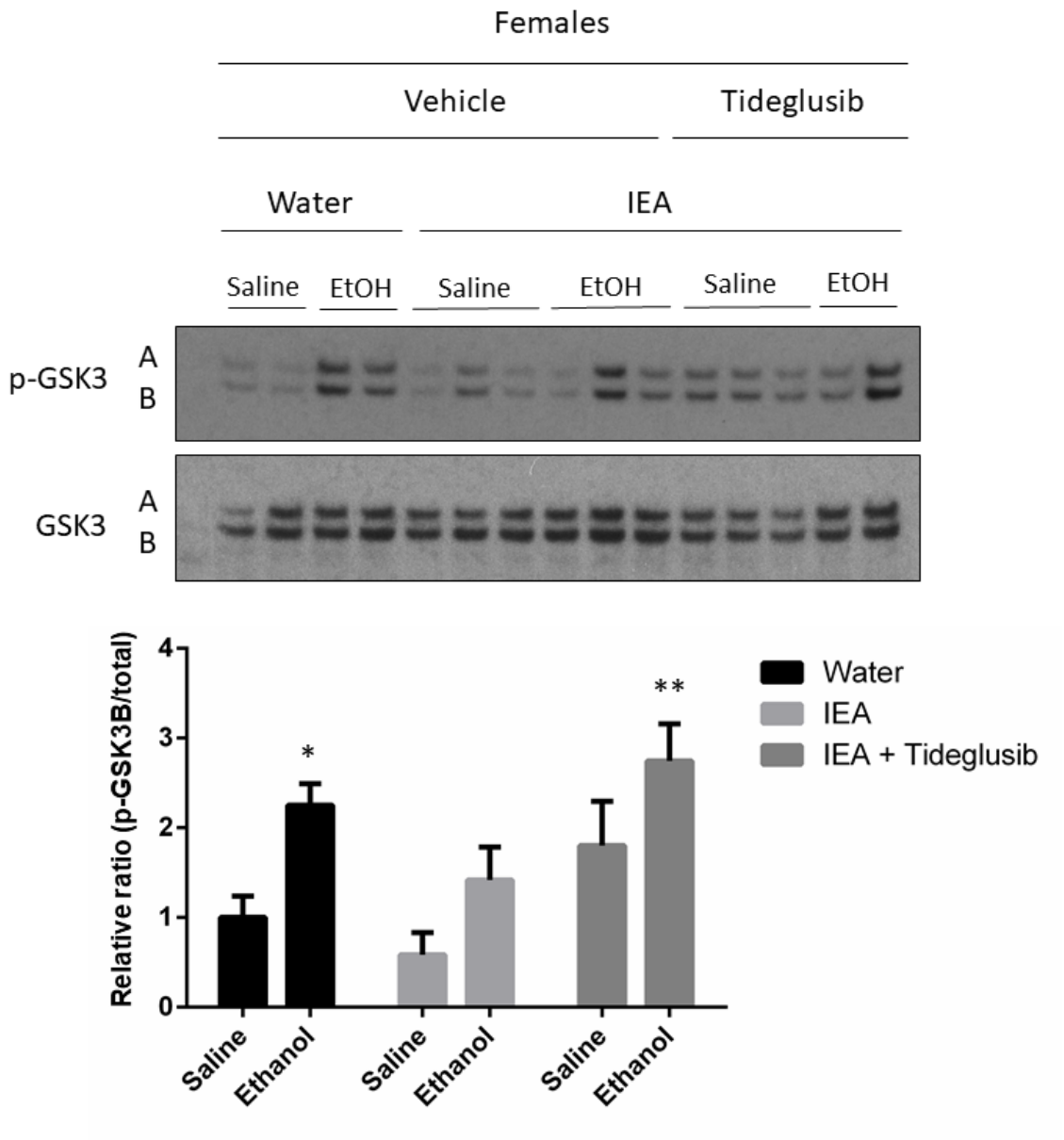

Figure 4.17 Acute-on-chronic ethanol effects on GSK3B phosphorylation in mPFC (females). (Top): Representative films of phospho- and total GSK3 Western blots. (Bottom): Quantified results of p-GSK3B. *Acute* (i.p.) ethanol vs. saline is on the X-axis. *Chronic* ethanol (IEA vs Water) is shown in legend. A 2-way ANOVA excluding Tideglusib treated animals found significant main effects of *acute* and *chronic* ethanol. By Sidak's post hoc, acute ethanol increased p-GSK3B within the chronic water condition (*$p<0.05$), but not within the IEA condition. Subsequent 3-way ANOVA found significant main effect of Tideglusib treatment, with Tideglusib-IEA-Ethanol significantly (**$p<0.01$) different from control (Vehicle-Water-Saline) by Tukey's post-hoc.

increased GSK3B phosphorylation within the water-only drinking (ethanol-naïve) mice (adj. p=0.0305, * in **Fig. 4.16**); within the chronically ethanol exposed (IEA) mice the effect of i.p. ethanol was not significant (adj. p=0.506). To include Tideglusib treatment in the analysis, we had to account for the unbalanced design of these protein assays, wherein only animals in the IEA condition received tideglusib (all water-drinking controls analyzed on these blots received vehicle). Thus tideglusib treatment was included as a factor, and nested within *chronic* in a three-way ANOVA. There was not a significant main effect from *treatment* ($F_{1,22}$=0.87, p=0.360), nor any significant interactions.

In the PFC of female C57BL/6J mice (**Fig. 4.17**) two-way ANOVA of acute and chronic ethanol (excluding Tideglusib treated animals) revealed significant main effects of *acute* ethanol ($F_{1,16}$=13.95, p=0.0018) and *chronic* ethanol ($F_{1,16}$=5.011, p=0.0398) and non significant *acute*chronic* interaction ($F_{1,16}$=0.563, p=0.464). By Sidak's post-hoc test, acute i.p. ethanol significantly increased GSK3B phosphorylation within the water-only drinking (ethanol-naïve) mice (adj. p=0.0118, * in **Fig. 4.17**); within the IEA mice the effect was not significant (adj. p=0.0993). When tideglusib treatment was included as a factor, and nested within *chronic* in a three-way ANOVA, there was a significant main effect of *treatment* ($F_{1,22}$=9.96, p=0.0046), a significant main effect of *acute* ethanol ($F_{1,22}$=10.65, p=0.0035), and non-significant effects of *chronic[treatment]* ($F_{1,22}$=3.86, p=0.0621), *acute*treatment* ($F_{1,22}$=0.0247, p=0.877) and *acute*chronic[treatment]* ($F_{1,22}$=0.434, p=0.517). Tukey's post hoc testing of the

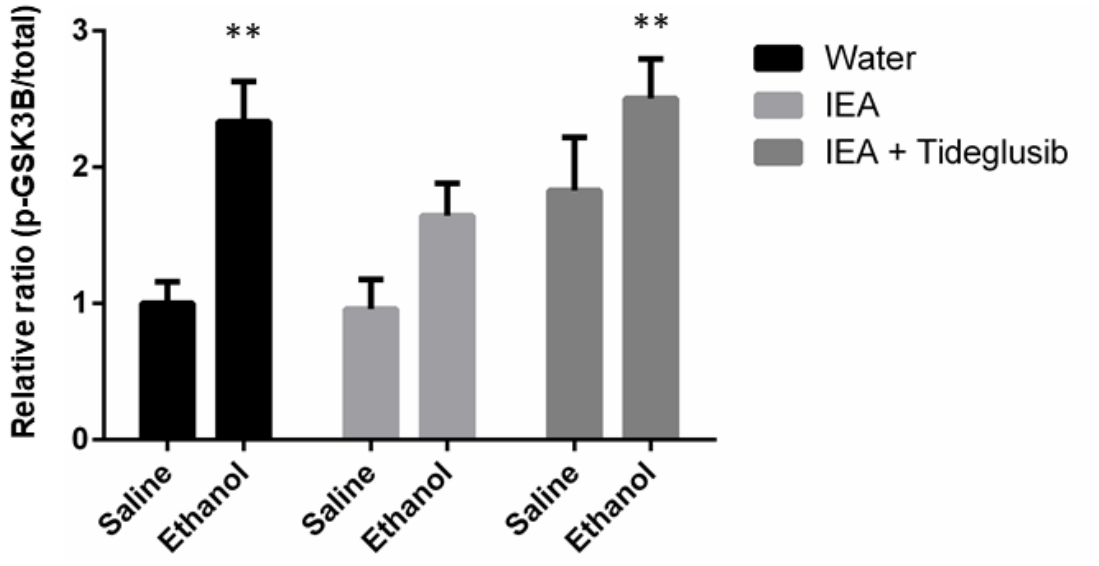

Figure 4.18 Acute-on-chronic ethanol effects on GSK3B phosphorylation in mPFC (pooled). Quantified results of p-GSK3B following the acute-on-chronic ethanol paradigm in male and female PFC tissue as shown in the figures above were pooled together to increase statistical power. Upon finding no significant effect of sex on relative p-GSK3B levels, three-way ANOVA found significant main effects of *acute* ethanol and tideglusib *treatment* ($p<0.001$, $p<0.01$, respectively). Tukey's post hoc testing revealed significant differences from control (Vehicle-Water-Saline) for the Vehicle-Water-Ethanol group and the Tideglusib-IEA-Ethanol group (**$p<0.01$).

three-way ANOVA found a significant difference between Tideglusib-IEA-Ethanol and Vehicle-Water-Saline (adj p=0.009, ** in **Fig 4.17**), as well as differences between Tideglusib-IEA-Ethanol and Vehicle-IEA-Saline (adj. p=0.001) and between Vehicle-IEA-Saline and Vehicle-Water-Ethanol (adj. p=0.0136).

Given the relatively low power of conducting within-sex analyses with 6 groups, and the fact that animals and tissue were run with sexes in parallel, we pooled all samples together to achieve an n of 8-10/group (n=56 total). Pooled results are shown in **Figure 4.18**. We first ran a two-way ANOVA with sex and the other factors combined into a single *acute-chronic-treatment* factor. This model found a robust effect of *acute-chronic-treatment* ($F_{5,44}$=5.78, p=0.0003) but no significant effect of sex ($F_{1,44}$=0.477, p=0.493) or *sex*acute-chronic-treatment* ($F_{5,44}$=0.677, p=0.643). Given the lack of sex effect this factor was dropped from subsequent analysis. In the pooled samples, a two-way ANOVA of *acute* and *chronic* ethanol (excluding tideglusib treated animals) found significant main effect of *acute* ($F_{1,35}$=13.14, p=0.0009) and no significant effect for *chronic* ($F_{1,35}$=0.880, p=0.355) nor *acute*chronic* ($F_{1,35}$=1.045, p=0.314). Sidak's post hoc testing found a significant effect of acute ethanol within the chronically water-drinking controls (adj. p=0.0041); within the IEA animals there was not a significant effect of acute ethanol on GSK3B phosphorylation (adj. p=0.150). Subsequent three-way ANOVA with Tideglusib treatment included found significant main effects of *treatment* ($F_{1,50}$=8.34, p=0.0057) and *acute* ethanol ($F_{1,50}$=12.74, p=0.0008). There were no significant effects from *chronic[treatment]* ($F_{1,50}$=1.98, p=0.166), *acute*treatment* ($F_{1,50}$=0.500, p=0.483), or

Table 4.2 Results of Tukey's pairwise comparisons after 3-way ANOVA of p-GSK3B-S9 in the acute-on-chronic ethanol model (sexes pooled). After multiple tests corrections, the Tideglusib-IEA-Ethanol group is significantly different from Vehicle-treated animals receiving saline i.p., with and without IEA. The Vehicle-Water-Ethanol group is significantly different from these same two Vehicle-saline groups (+/- IEA).

treatment	chronic	acute	-treatment	-chronic	-acute	t Ratio	Prob>|t|	Lower 95%	Upper 95%
Tideglusib	IEA	Ethanol	Tideglusib	IEA	Saline	1.72	0.5283	-0.49168	1.84414
Tideglusib	IEA	Ethanol	Vehicle	IEA	Ethanol	2.25	0.2340	-0.27260	1.99347
Tideglusib	IEA	Ethanol	Vehicle	IEA	Saline	4.15	0.0017*	0.44105	2.64975
Tideglusib	IEA	Ethanol	Vehicle	Water	Ethanol	0.46	0.9974	-0.93426	1.27444
Tideglusib	IEA	Ethanol	Vehicle	Water	Saline	4.04	0.0024*	0.40023	2.60892
Tideglusib	IEA	Saline	Vehicle	IEA	Ethanol	0.47	0.9971	-0.98371	1.35211
Tideglusib	IEA	Saline	Vehicle	IEA	Saline	2.26	0.2302	-0.27093	2.00926
Tideglusib	IEA	Saline	Vehicle	Water	Ethanol	-1.32	0.7752	-1.64624	0.63395
Tideglusib	IEA	Saline	Vehicle	Water	Saline	2.15	0.2780	-0.31175	1.96844
Vehicle	IEA	Ethanol	Vehicle	IEA	Saline	1.84	0.4517	-0.41938	1.78931
Vehicle	IEA	Ethanol	Vehicle	Water	Ethanol	-1.85	0.4429	-1.79469	0.41400
Vehicle	IEA	Ethanol	Vehicle	Water	Saline	1.73	0.5202	-0.46020	1.74849
Vehicle	IEA	Saline	Vehicle	Water	Ethanol	-3.79	0.0051*	-2.45020	-0.30042
Vehicle	IEA	Saline	Vehicle	Water	Saline	-0.11	1.0000	-1.11572	1.03407
Vehicle	Water	Ethanol	Vehicle	Water	Saline	3.68	0.0072*	0.25959	2.40938

*acute*chronic[treatment]* ($F_{1,50}$=1.56, p=0.218). The results of Tukey's post-hoc testing from the three-way ANOVA are given in **Table 4.2**. There are two groups which differ significantly from the Vehicle-treated, water-drinking, saline-injected controls: naïve animals injected with ethanol (Vehicle-Water-Ethanol), and ethanol-drinking animals pre-treated with Tideglusib and subsequently injected with ethanol (Tideglusib-IEA-Ethanol). These two groups are denoted with asterisks in **Figure 4.18**. We interpret these findings as follows: IEA blunts the response of GSK3B inhibitory phosphorylation following an acute dose of ethanol. A pharmacologic GSK3B inhibitor could restore this inhibitory phosphorylation such that the same dose of ethanol results in a comparable level of GSK3B activity as in the ethanol-naïve state. Behavioral correlates of the application of a GSK3B inhibitor following a period of IEA will be discussed in Chapter 6.

4.4 Discussion

In agreement with prior literature on acute ethanol's effects on GSK3 phosphorylation in rodent PFC (Neznanova *et al*, 2009), a single i.p. injection of ethanol significantly increased p-GSK3A and p-GSK3B in the PFC of C57BL/6J mice. This is the first report of the effect being replicated in female mice, as well as to characterize multiple doses of ethanol. Moreover, we have provided evidence that inhibitory GSK3B phosphorylation may contribute to the locomotor effects of acute ethanol, as the GSK3B inhibitor tideglusib augmented the locomotor stimulatory effects and appeared to add to the anxiolytic-like effect. As

there is evidence of GSK3B phosphorylation mediating the rapid antidepressant effects of ketamine (Beurel *et al*, 2011), GSK3B phosphorylation may account for some of ethanol's short-term effects on mood-related phenotypes.

The upstream mechanism of ethanol's GSK3B inhibition remains to be elucidated. One well-characterized kinase known to phosphorylate GSK3B is Akt (Beaulieu *et al*, 2009). Akt is activated downstream of growth factors such as BDNF and in turn phosphorylates the S9 residue of GSK3B, an action thought to underlie certain mood-stabilizing agents (Mai *et al*, 2002). If ethanol acutely increases BDNF in the PFC, this might account for its inhibition of GSK3B. Co-administration of a BDNF receptor (TrkB) antagonist with ethanol could serve as a test of this hypothesis: if the antagonist (e.g. ANA-12) blocked the ethanol induced increase in GSK3B, this would be evidence for an ethanol-BDNF-Akt pathway. It should be noted that Akt is only one potential upstream kinase and that many pathways converge on GSK3B. For example, Miller et al. (2014) found that cocaine inhibited Akt and activated GSK3B by decreasing its phosphorylation in the NAC. Blockade of D2 receptors prevented the cocaine-induced inhibition of Akt, while D1, D2, and NMDA antagonists each blocked cocaine-induced activation of GSK3B (Miller *et al*, 2014).

Given the inhibition of GSK3B as well as GSK3A following an acute ethanol dose, it might be expected that as a homeostatic response, GSK3 activity may basally increase in the PFC. Alternatively, if each ethanol dose perturbs GSK3 for much longer than ethanol stays in the bloodstream, a sustained decrease in GSK3 activity might be expected following intermittent cycles of

ethanol exposure. However we found evidence for neither of these conditions in our study of intermittent ethanol access (IEA), with PFC tissue harvested 24 hours after the last drinking session. Neither p-GSK3A-S21 nor p-GSK3B-S9 were significantly altered by IEA compared with water-drinking controls. However, it is still possible that the single 24-hour time point did not detect temporal trends in adaptation via altered GSK3 activity.

There was evidence for alterations in PFC synaptic scaffolding proteins with ethanol treatment. In male mice, the PFC showed an increase in total PSD95, while in female mice the PFC showed decreased gephyrin. PSD95 has recently been shown to increase in RNA expression in the NAC of male rats after 8 weeks of IEA compared to water-drinking controls (Liu *et al*, 2017). Prior work on chronic ethanol induced plasticity has shown increased NMDA receptor clustering and PSD-95 expression in hippocampal neurons (Carpenter-Hyland and Chandler, 2006). As a homeostatic response it is relatively unsurprising: if ethanol repeatedly antagonizes NMDA receptors, upregulation of the protein which anchors these receptors to the synapse may be a means of restoring balance. Interestingly, while we did not see this PSD-95 effect in female mice, we saw what might be seen as the parallel inverse: decreased gephyrin. As ethanol repeatedly potentiates GABA receptors, downregulation of their anchor protein would also restore balance. In male rats, chronic ethanol vapor (CIE) and withdrawal were found to increase gephyrin in the amydala (Diaz *et al*, 2011). Chronic ethanol exposure has often been shown to alter the expression of $GABA_A$ receptors in the cerebral cortex (Krystal *et al*, 2006), and to enhance

internalization of alpha-1 subunit containing $GABA_A$ receptors in particular (Kumar *et al*, 2003), but the role of gephyrin in this response has been little studied.

As both PSD-95 and gephyrin contain GSK3B target residues (Nelson *et al*, 2013; Tyagarajan *et al*, 2011), it is interesting to consider the interplay between alterations in the levels of these synaptic scaffolds and GSK3B activity. While we did not see a significant effect of acute ethanol on p-PSD95-T19, the GSK3B target site, there was a suggestive inverse trend with increasing ethanol ($p<0.1$), specifically in male mice. Phosphorylation by GSK3B normally serves to remove a scaffold protein from the membrane. If each ethanol exposure decreases GSK3B activity and corresponds to some degree of decreased PSD-95 phosphorylation, this might be expected to stabilize its expression at the synapse. This same logic could apply to gephyrin. Why then, does chronic ethanol cause PSD-95 to persist at a higher expression in males while gephyrin shows decreases in females? A crucial piece of information might be the rate of turnover of each of these scaffolding proteins in comparison with their receptors. Does an increase in total PSD-95 necessarily correspond to more stable expression, and does this in turn imply enhanced NMDA signaling? Or might the increase in total PSD-95 correspond to increased turnover, to allow for insertion of new NMDA receptors in place of non-responsive or tolerant channels? If the latter, then acute GSK3B inhibition in the context of chronic ethanol could actually counter the effects of increased PSD-95, by inhibiting turnover and preventing signal enhancement.

Another interesting male-female distinction is observed in the chronic (IEA) behavioral results. Females showed a near immediate escalation in binge consumption, as soon as Week 2, and drank significantly higher binge amounts than male mice until Week 5, when males caught up. Thus male mice escalate binge consumption much more slowly than female mice. However, by Week 5, the fact that males and females did not significantly differ in binge consumption is striking considering the robust differences in total daily consumption through the course of the experiment. This means that male mice eventually consume a much greater proportionate binge amount relative to their daily consumption. One consistent observation across both sexes is that the drinking patterns of the overall cohort seem to converge around a mean value. That is, the histograms in Week 1 show a much greater spread than those by the end of the 5 weeks under investigation. Thus it might be considered that individual differences in inbred lines may show up early in long-term IEA experiments relative to later.

Finally, we used another cohort of male and female mice to investigate the relative effects of a single acute (2 g/kg) dose of ethanol on GSK3B phosphorylation in naïve versus IEA-exposed mice. We hypothesized that repeated cycles of exposure and escalating ethanol consumption might correspond to habituation to the effect of ethanol on GSK3B phosphorylation. Two-way ANOVAs of males, females, and the pooled samples consistently found a main effect of acute ethanol, but that this effect was significant specifically in the naïve (non-IEA) condition in post-hoc testing. This supports our hypothesis of a blunted response following chronic ethanol exposure. We also included

tideglusib-treated mice in subsequent three-way ANOVAs and found a significant treatment effect in the pooled sample, and that both (1) the naïve animals injected with ethanol and (2) the IEA animals pre-treated with tideglusib and then injected with ethanol showed significant ($p<0.01$) differences from control (vehicle-water-saline). Observing Figure 4.18, it would appear that tideglusib treatment by itself raises relative p-GSK3B-S9 to similar levels as IEA animals given an injection of ethanol. Treatment of acute ethanol on top of tideglusib treatment restores levels of p-GSK3B-S9 to those seen in naïve animals treated with acute ethanol only. Implications of tideglusib treatment will be further discussed in chapter 6.

Full acute dose responses in the naïve and IEA groups would be necessary to conclude that chronic ethanol (IEA) shifts the responsiveness of GSK3B inhibitory phosphorylation downward. However we would predict based on our selected dose of 2 g/kg and the dose-responses previously performed in naïve animals only, that following chronic treatment, a greater dose of ethanol would be required to achieve an equivalent inhibitory GSK3B phosphorylation. Thus we propose the novel hypothesis that a certain level of GSK3B inhibition in the PFC normally serves to counteract the motivation to self-administer ethanol. This may correspond to a certain level of positive effects, i.e. anxiolysis, to achieve satiety, or to a certain level of dysphoria, which only sets in at higher ethanol doses. As more ethanol is required to achieve this same level of GSK3B inhibition, escalating consumption ensues.

Chapter 5

Genetic Modulation of *Gsk3b* and Ethanol Drinking

5.1 Introduction

To examine the role of a particular isoform of a ubiquitously expressed intracellular kinase, by far the most specific means of functional targeting is at the level of the gene. In humans, the *GSK3B* gene is located on the long arm of chromosome 3; in mice the *Gsk3b* gene is on chromosome 16. These mouse and human genes share 92.7% identity in DNA sequence, and the encoded proteins share 99% amino acid sequence homology (NCBI, 2017). Homozygous disruptions in *Gsk3b* lead to death around mid-gestation (Patel *et al*, 2008) or neonatally (Liu *et al*, 2007), consistent with the GSK3B protein playing a crucial role in development.

Several alternatives to pancellular or constitutive *Gsk3b* gene deletions have been developed and assayed in rodents previously. Transgenic mice overexpressing *Gsk3b* have been proposed as a model for hyperactivity and mania (Prickaerts *et al*, 2006). In this case the overexpression was mediated via targeted mutation of the GSK3B-S9 phospho-residue, causing constitutive activity of the protein. In addition to hyperlocomotion, these mice were found to

show an increased acoustic startle response, despite no differences in basal or stress-induced plasma adrenocorticotrophic hormone or corticosterone levels (Prickaerts *et al*, 2006). They also showed increases in Akt1 expression and BDNF in the hippocampus, possibly as compensatory responses to constitutively active GSK3B (Prickaerts *et al*, 2006).

Conditional genetic deletion of *Gsk3b* has been carried in neurons specifically expressing dopamine D1- vs D2- type receptors (Urs *et al*, 2012). These mice were generated by crossing D1 or D2 promoter driven Cre-lines with homozygous floxed *Gsk3b* mice (Urs *et al*, 2012). The homozygous Gsk3b-flox mice carried alleles with a LoxP site flanking the second exon, allowing for Cre-mediated excision and an inactivated GSK3B protein product (Patel *et al*, 2008). Thus Urs et al. achieved cellular selectivity as Cre-mediated deletion would only occur in cells with active promoter-driven expression (i.e. cells expressing either dopamine D1 or D2 receptors). However, there was no temporal selectivity outside of that provided by the temporal expression pattern of the D1 and D2 receptors. The authors found that deletion in neither neuronal type altered immobility in the tail suspension test or latency to cross in a dark-light emergence test; however D2 specific deletion of *Gsk3b* significantly attenuated amphetamine-induced hyperlocomotion, and deletion in either neuronal cell type prevented amphetamine-induced disruption of prepulse inhibition (Urs *et al*, 2012). Based on corresponding pharmacologic agents in these same assays, the authors concluded that dopamine receptor-dependent GSK3B activation may

underlie aspects of antipsychotic, but not antidepressant, actions (Urs *et al*, 2012).

In another study of specific *Gsk3b* deletion (Latapy *et al*, 2012), the gene was postnatally deleted in forebrain neurons expressing the alpha isoform of the calcium/calmodulin-dependent protein kinase II (CAMKIIα, encoded by *CAMK2A* in humans or *Camk2a* in mice). These mice were generated via breeding Camk2a-Cre mice to the same Gsk3b-floxed line as above. *Gsk3b* deletion in this neuronal population did seem to mimic antidepressant actions, in contrast to the D1-/D2- deletions above. The open field test and light-dark emergence test revealed a marked reduction in basal anxiety-like behavior in the *Gsk3b*-deletion mice (Latapy *et al*, 2012). These findings expound upon previous findings that *Gsk3b* haploinsufficiency or GSK3B pharmacologic inhibition rescues the anxiogenic-like phenotype observed in serotonin deficient mice expressing tryptophan hydroxylase knock-in (Beaulieu *et al*, 2008). Of note, these serotonin deficient mice have since been found to exhibit increased ethanol preference (Sachs *et al*, 2014).

Based on the convergence of neuronal signaling pathways on GSK3B and the strong effect of ethanol described in the previous chapter, we investigated the role of the GSK3B in alcohol-drinking behavior with both regional and cellular specificity, and without the potential confounds of developmental disruptions. Here we describe 3 genetic manipulation techniques:

(1) Viral-mediated over-expression of *Gsk3b* in the medial PFC (mPFC).

(2) Viral-mediated deletion of *Gsk3b* in the mPFC, specifically infralimbic cortex (IL)

(3) Conditional deletion of *Gsk3b* in Camk2a-expressing neurons using tamoxifen-inducible Cre

Based on observations in the prior chapter consistent with molecular tolerance to ethanol's inhibitory effects, we hypothesize that GSK3B activity level in frontal cortex drives ethanol-seeking behavior. This hypothesis is further supported by there being high GSK3B activity specifically in the frontal cortex of serotonin-deficient mice (Beaulieu *et al*, 2008) who show high ethanol preference (Sachs *et al*, 2014); and by higher constitutive GSK3B activity in the prefrontal cortex of alcohol-preferring vs. non-preferring rats (Neznanova *et al*, 2009). We test this hypothesis using two-bottle choice ethanol drinking paradigms for all genetically modified mice.

5.2 Materials and Methods

5.2.1 Viral-mediated overexpression

Animals. Male C57BL/6J mice (age 7-8 weeks, Jackson Laboratories, Bar Harbor, Maine) were habituated to a climate-controlled vivarium for 1 week prior to beginning experiments with ad libitum food and water access unless indicated. Animals were kept on a 12-h light cycle (lights on 0600). All injections of the overexpression vector and subsequent validation studies and behavioral tests were carried out by Annie Meng. Mice were singly housed following surgery and for the duration of ethanol-drinking studies.

Viral vector stereotactic injections. Mice were injected with an AAV2 vector containing either Gsk3b cDNA (AAV-GSK3B, n=16) or mock AAV2 (AAV-IRES,

n=14) driven by a CMV promoter. Both vectors also expressed hrGFP fluorescent reporter protein. For viral injection bilaterally into mPFC, mice were anesthetized with ketamine (120 mg/kg, i.p.) and xylazine (12 mg/kg, i.p.) and small burr holes were drilled through the skull immediately above the mPFC. Two microsyringes were slowly lowered to the following coordinates relative to bregma: anterior-posterior +0.1, medial-lateral +0.06 and -0.06, dorsal-ventral -0.21. At each site, 1 µl of the virus was injected at the speed of 0.1µl per min, the needle was left in place for an additional 10 min and then slowly raised. Efficiency of viral transduction in anesthetized mice was assessed 2-3 weeks following injections using the IVIS200 in vivo imaging system (Xenogen, Alameda, CA). Photons emitted from hrGFP-expressing cells in mPFC were quantified over a defined period of time ranging from up to 5 minutes using the software program Living Image (Xenogen) as an overlay onto the Igor program (Wavemetrics, Portland, OR).

Immunohistochemistry. Mice were heavily anesthetized with pentobarbital, perfused transcardially with 0.9% saline for 2 min, and then perfused with a solution of 4% paraformaldehyde in 0.1 M PBS, pH 7.4, for 15 min with a flow rate of 2.5 ml/min. Brains were removed, post-fixed for 12 h in 4% paraformaldehyde, and transferred to PBS containing 30% sucrose. Brains were frozen on dry ice, and sections cut at 25 µm using a Leica sliding microtome. Sections were then rinsed in PBS, incubated in blocking solution for 30 min, and incubated with a rabbit-anti-GSK3B polyclonal antibody (1:100, Abcam, Cambridge, MA, USA) and a mouse anti-NeuN monoclonal antibody (1:500,

Millipore, MA, USA), overnight, at 4°C. Sections were then washed and incubated in a goat-anti-rabbit FITC-conjugated secondary antibody (1:2000, Invitrogen, Grand Island, NY) and a donkey anti-mouse conjugated Texas red secondary antibody (1:2000 Invitrogen, Grand Island, NY). A confocal laser scanning microscope (Fluoview FV1000, Olympus, Japan) was used to obtain z-stacks. All exposure settings were kept constant for each group.

q-RT-PCR. For quantitative validation of *Gsk3b* expression, aliquots of total RNA (1 µg) from AAV-GSK3B (n=4) or pAAV-IRES (n=6) injected mice were reverse-transcribed into cDNA according to the manufacturer instructions of the first strand cDNA synthesis kit (Bio-Rad, Hercules, CA, USA). The primers used in this study were synthesized by Operon (Huntsville, AL, USA) and sequences for *Gsk3b* sense and antisense, 5`-tccgattgcggtatttcttc-3` and 5`-aatgtctcgatggcagatcc-3`, respectively.

Voluntary ethanol intake. Five weeks post-viral injection, ethanol consumption by AAV-GSK3B mice compared to control AAV-IRES mice was assessed using a two-bottle choice drinking paradigm (George *et al*, 2012; Meliska *et al*, 1995). Mice received increasing concentrations of ethanol for 5 days at each dose (3-15% w/v ethanol). Water was available at all times during the experiment. The positions of the alcohol and water tubes were switched every other day (L, L, R, R, etc.) to avoid a placement bias. Alcohol solutions were prepared freshly daily. Ethanol and water consumption was measured every 24 h, and body weight was recorded every 5 days. Ethanol consumption was calculated as grams of ethanol per kilogram body weight per 24 h. Percent ethanol preference for individual mice

was obtained by dividing volume of ethanol consumption by total fluid consumption for daily drinking sessions. Bottles containing ethanol or tap water were placed in an empty cage to account for evaporation loss and values were subtracted from the amount consumed for each mouse to calculate corrected preference ratios and ethanol intake. A schematic of the ethanol drinking behavior paradigm used here is shown in **Figure 5.1A**.

Blood ethanol determination. For blood ethanol pharmacokinetics, AAV-GSK3B and control littermates (n=3 per genotype) were injected with ethanol (2 g/kg, i.p.) and 100 µL of blood sample were obtained from the tail vein at 60 min and 120 min post-injection. Blood ethanol concentration was determined using the Analox AM1 Analyzer (Analox Instruments, North Yorkshire, UK).

***Taste discrimination*.** Taste preference for bitter and sweet solutions was measured using quinine and saccharin respectively using the two-bottle choice paradigm as described above. Mice were allowed to recover for 7 days following the voluntary ethanol drinking study. Half of the mice were given two bottles containing either a 0.05 mM quinine solution or tap water for 4 days to assess bitter taste preference (Wolstenholme *et al*, 2011). The remaining mice were given a choice between saccharin (0.033%) or tap water to measure non-caloric sweet taste preference. Bottles were alternated every other day to avoid side preferences. Consumption of quinine and water or saccharin and water were measured daily after which the other tastant was offered for 4 days in a counterbalanced design.

***Lithium diet treatment*.** After the taste discrimination test, mice were allowed to

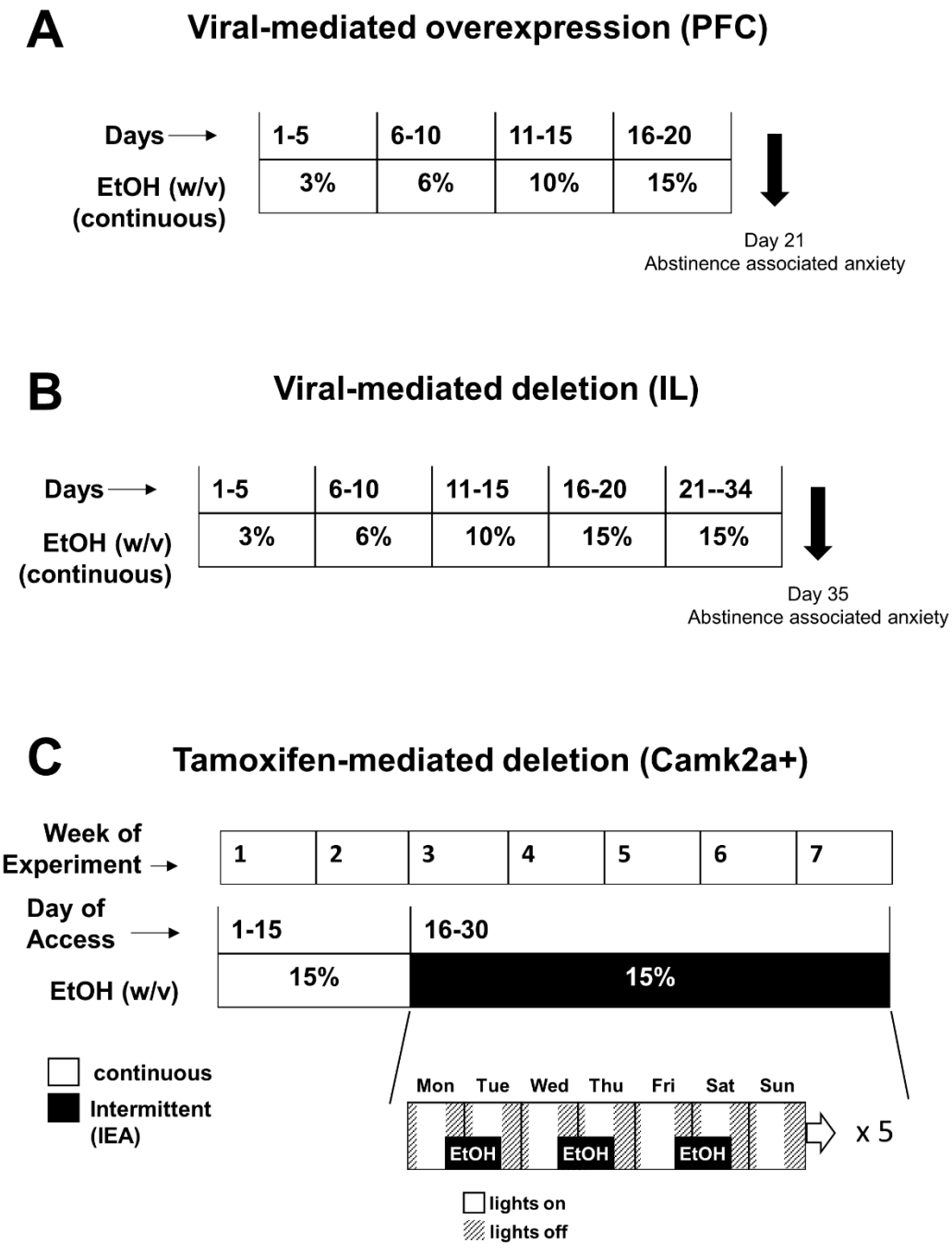

Figure 5.1 Schemata of drinking paradigms used in genetic modulation studies. A-B. Continuous ethanol access at escalating doses, initiated 3-5 weeks after viral vector injections in PFC or infralimbic cortex (IL). Abstinence associated anxiety was assayed via LD box 24 hours after last ethanol access. **C.** Continuous ethanol access at 15%w/v, followed by intermittent ethanol access.

recover for one week, after which animals were fed chow with or without 0.2% lithium chloride (LiCl, Harlan Teklad, Madison,WI) for 4 weeks. Saline (0.45% NaCl) was added to the drinking water of lithium fed mice to reduce toxicity as previously reported (Smith and Amdisen, 1983). Body weight was monitored weekly in both control and lithium fed mice. Blood lithium levels were found to be stable 3 weeks after lithium treatment, and then ethanol consumption was measured 4 weeks following lithium treatment. Upon completion of the experiment, blood samples were collected from the tail vein. The blood was collected in a microtube and was immediately centrifuged at 3,000 rpm at 4º for 10 min. Plasma was then collected and stored at -20°C for lithium level analysis. Concentrations of plasma lithium were determined by the VCU Clinical Chemistry Laboratory by atomic absorption spectrophotometry.

Loss of righting reflex (LORR). Three weeks following AAV viral injections in C57BL/6J mice, loss of righting reflex was assessed. Ethanol (3.6 g/kg, 20% v/v solution) was injected intraperitoneally, and individual mice were placed immediately in a clean Plexiglas cage. After mice lost their righting reflex, they were placed on their backs in their home cage. The duration of LORR was defined as the time from the loss of the righting reflex to the time at which it was regained. Recovery was defined as the time at which mice could right themselves 3 times in 30 seconds after being placed on their backs. The behavioral room was illuminated with a soft light, and external noise was attenuated.

***Light-Dark Box*.** Ethanol tubes were removed 20 days following commencement

of the drinking study and 24 hours later, ethanol abstinence associated anxiety was assessed using the light-dark (LD) box conflict model as described in (Putman *et al*, 2016). The LD boxes were as described in Chapter 4 with the exception that these experiments used CM1820 28V 100mA light bulbs as opposed to 180mA “stimulus” bulbs.

5.2.2 Viral-mediated deletion

Animals. Floxed *Gsk3b* ($Gsk3b^{fl/fl}$) mice were generously donated by Dr. James Woodgett (Samuel Lunenfeld Research Institute, Toronto) (Patel *et al*, 2008). Male and female $Gsk3b^{fl/fl}$ mice were maintained on a C57BL/6J background by the VCU Transgenic Core Facility, and sent to our temperature and humidity controlled vivarium at 4 weeks of age. At approximately 12 weeks of age, $Gsk3b^{fl/fl}$ mice underwent stereotaxic surgery and were subsequently singly housed. All mouse studies were conducted in accordance with the National Institute of Health Guidelines for Animal Care and Use and VCU IACUC approved protocols. All mice undergoing stereotaxic surgery were given ibuprofen (0.2 mg/mL) in their drinking water for the 24 hours pre- and 72 hours post-operation for analgesia.

Robot stereotaxic surgery. Mice were anesthetized with isoflurane (<5% in O2) and mounted onto a motorized drill-microinjection robot stereotaxic rig (Neurostar, Tubingen, Germany). Isoflurane vapor was maintained at the minimal level to achieve full anesthetic effect, assessed by toe pinch every 5-15 minutes. The surgical area was cleaned with Betadine and 70% ethanol. Bupivacaine was

injected subcutaneously to the scalp. A midline incision was made to allow bregma and lambda visualization. The drill-microinjection arm was calibrated based on bregma and lambda, as well as points 2 mm on either side of the skull to allow for roll/tilt correction. The drill and microinjector were 90 degrees perpendicular to the surface of the skull, such that holes were drilled directly above the injection target. Injection target coordinates for infralimbic cortex (IL) were AP: +1.42, ML: ±30, DV: -2.50 (compare to (Holmes *et al*, 2012)). A screenshot from the Neurostar robot control software is shown in **Figure 5.2**, which gives the predicted placement of these coordinates in an integrated mouse brain atlas.

Gsk3b$^{fl/fl}$ mice were injected with AAV2-CMV-Cre-eGFP, or as a control, the same virus but without Cre: AAV2-CMV-eGFP. The AAV2 serotype was chosen based on the relative neuronal tropism of this serotype as well as low toxicity (Howard *et al*, 2008). The CMV promoter was used based on its small size, efficient transduction and constitutive expression once within cells (Smith *et al*, 2000). Cre recombinase is the virally encoded enzyme which accomplishes the deletion via excision of the *Gsk3b* exon. Finally, eGFP allows for a fluorescent reporter label to identify and validate successful transduction.
The Cre or GFP control viruses were injected bilaterally, 0.7 µL per hemisphere. The robot was programmed to inject each 0.7 µL volume at a constant speed over a duration of 5 minutes. The virus was then given an additional 5 minutes to diffuse away from the needle before the microinjector was slowly raised and moved to the opposite hemisphere, and the process repeated. Hamilton Gastight

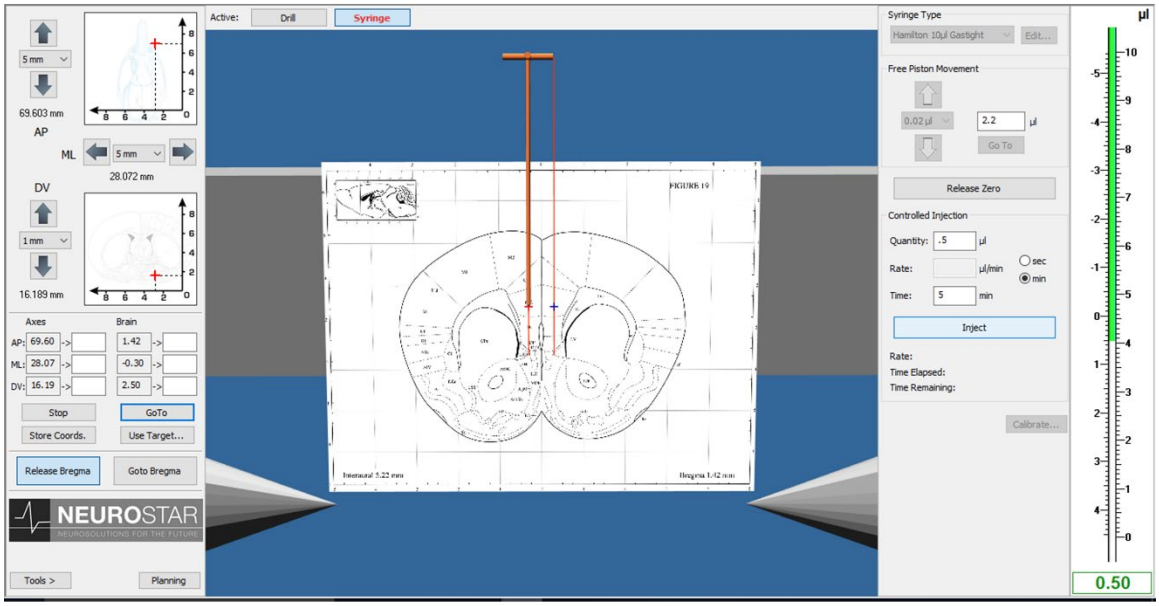

Figure 5.2 Stereotaxic target according to Neurostar robot software. Screenshot of Neurostar Stereotaxic Drill-Injection Software (StereoDrive) is shown. Injection target is top of infralimbic cortex (IL). Virus injection volume per hemisphere was 0.7 uL (not shown in figure).

10 uL syringes with 33 gauge small hub needles (Hamilton, Reno, NV) were used on the automated microinjector. Following bilateral injection, saline was applied to rehydrate the scalp and the incision resealed using surgical glue. The wound was cleaned with Betadine and ethanol. Sterile field was maintained throughout the surgery.

Immunohistochemistry. Loss of GSK3B expression in the IL was confirmed via IHC. At least 3 weeks after injection, mice were transcardially perfused with 4% paraformaldehyde and brains were stained according to the same protocol for immunofluorescent staining described in Chapter 4.2 (Materials and Methods).

Voluntary ethanol intake. As described above in 5.2.1, mice were given continuous access to escalating concentrations of ethanol (3%, 6%, 10%, 15% w/v) for 5 days at each dose. Ethanol access was begun 3-5 weeks post-viral injection. Ethanol-drinking paradigm is depicted in **Figure 5.1B**.

Taste preference. An ethanol-naïve cohort was given access to quinine (0.05 mM) for 4 days and saccharin (2 mM, 0.037% w/v) for 4 days subsequently.

Light-Dark Box. An ethanol-naive cohort of mice was assessed for basal anxiety via LD box. An ethanol drinking cohort (**Fig. 5.1B**) was tested 24 hours after last ethanol access. LD boxes were as described in Chapter 4.

Novel Object Recognition. A subset of animals from both ethanol-naïve and ethanol-drinking cohorts were tested for PFC-dependent working memory via novel object recognition (Besheer *et al*, 1999; Wolstenholme *et al*, 2017). This task consisted of 2 days of testing. On the first day, each mouse was brought into the testing room for at least 1 hour. Each mouse was placed into its own clean

and empty (without bedding) cage for 30 minutes, and then returned to its home cage. On the second day, mice were again habituated to the testing room for at least 1 hour. Each mouse was then placed into its own clean, empty test cage for 20 minutes, then returned to its home cage for at least 2 minutes. During this time, two identical objects (two small laboratory funnels or two owl-shaped pencil sharpeners) were cleaned with 10% ethanol, dried, and taped to the bottom of the test cage in opposite corners, at least 2 inches from the sides. The training phase was then begun, wherein the mouse was returned to the test cage and allowed to explore the cage containing the identical objects for 5 minutes. The time spent exploring each object (nose oriented toward object, less than 2 cm away) was recorded using a stopwatch. After the the training phase the mouse was returned to its home cage for an interval of 5 minutes. During this interval one object was replaced with a clean, novel object. After the 5 minute interval the mouse was returned for the testing phase. This consisted of a final 5-minute duration during which time the time the mouse spent exploring each object was recorded using a stopwatch.

5.2.3 Tamoxifen-inducible Cre

Animals. The floxed *Gsk3b* ($Gsk3b^{fl/fl}$) mice described in 5.2.2 were crossed with a transgenic line hemizygous for Tg(Camk2a-CreERT2) allele (Madisen *et al*, 2010). This allele encodes a Camk2a promoter driven Cre-ERT2 fusion protein. Cre-ERT2 consists of Cre recombinase fused to a triple mutant form of the human estrogen receptor which does not bind 17β-estradiol at physiological

concentrations but will bind the synthetic estrogen receptor ligand tamoxifen (Madisen *et al*, 2010). The VCU Transgenic Core Facility received the B6;129S6-Tg(Camk2a-cre/ERT2)1Aibs/J line from Jackson Laboratories (Bar Harbor, ME) and subsequently maintained a colony via back-crossing with C57BL/6J mice. C57BL/6J genotypic background was confirmed at >95% using GigaMUGA high density genotype arrays (GeneSeek, Lincoln, NE). These mice were crossed with $Gsk3b^{fl/fl}$ and subsequently inbred to generate mice homozygous for the floxed allele and hemizygous for Camk2a-cre/ERT2, which when paired with another $Gsk3b^{fl/fl}$, would generate offspring all of which were homozygous for the Gsk3b floxed allele, and half of which carried the Camk2a-cre/ERT2 gene (50% Cre+ and 50% Cre-). These offspring were sent to our climate-controlled facility at 4 weeks of age and treated with tamoxifen upon reaching adulthood (8-12 weeks of age).

Tamoxifen treatment. Upon starting the treatment regimen (Madisen *et al*, 2010), animals were moved to single housing. Tamoxifen (Sigma-Aldrich, St. Louis, MO) was dissolved in corn oil at a concentration of 20 mg/mL by bath sonication. The drug vial was wrapped in foil for to protect from light, and stored at 4 degrees C for the duration of injections. Each mouse was injected with 100 uL of the tamoxifen solution for a per weight dose of approximately 75 mg/kg, every 24 hours for 5 successive days. Validation of deletion was performed via immunohistochemistry as described above.

Voluntary ethanol intake. Ethanol access was begun 3-4 weeks post treatment. Ethanol-drinking paradigm is depicted in **Figure 5.1C**. Animals were given

continuous access to 15% w/v for 15 consecutive days, and then switched to intermittent ethanol access (15% w/v) for 5 weeks, i.e. 15 days of ethanol access.

Taste preference. A subset of animals were given access to quinine (0.05 mM) for 4 days and saccharin (2 mM, 0.037% w/v) for 2 days subsequently.

Light-Dark Box. An ethanol-naive cohort of mice was assessed for basal anxiety via LD box, 1 week after tamoxifen treatment. An ethanol drinking cohort was tested 24 hours after last ethanol access (after > 5 weeks of IEA). LD boxes were as described in Chapter 4.

5.3 Results

5.3.1 Viral-mediated Over-expression

AAV-mediated overexpression plasmid increases Gsk3b transcript and protein product. Viral vectors co-expressed humanized recombinant green fluorescent protein (hrGFP), allowing localization off AAV-GSK3B transduction. We observed hrGFP-positive labeling up to 8 weeks following AAV-GSK3B and control AAV-IRES (expressing only hrGFP) transduction (**Fig. 5.3A**). GSK3B overexpression was confirmed at the mRNA and protein level ($p<0.05$) by quantitative RT-PCR, ELISA and immunofluorescence (**Fig. 5.3B-E**). GSK3B over-expression was largely limited to NeuN-positive neurons (**Fig. 5.3E**).

GSK3B overexpression increases ethanol consumption. GSK3B over-expression in mPFC produced a significant increase in mean daily ethanol

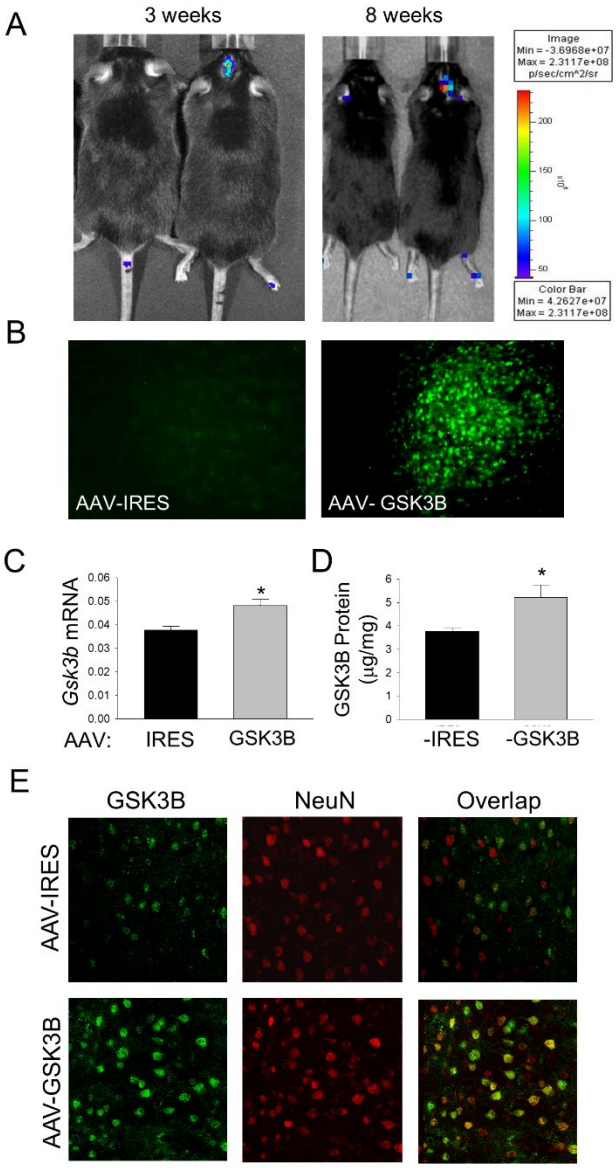

Figure 5.3 Validation of *Gsk3b* overexpression vector. AAV-GSK3B viral vector increases *Gsk3b* expression and GSK3B protein in neurons relative to AAV-IRES control. **A.** Visualization of hrGFP using an in vivo imaging system at 3 and 8 weeks, in mice injected with AAV with hrGFP tag (right) and controls. **B.** Representative immunohistochemistry of GSK3B-staining in AAV-IRES and AAV-GSK3B injected PFC. **C.** Significantly upregulated *Gsk3b* mRNA in PFC of AAV-GSK3B injected mice as measured by RT-qPCR (n=4-6, *p<0.05). **D.** Significantly higher levels of GSK3B protein in PFC of AAV-GSK3β injected mice as measured by ELISA (n=3/group, *p<0.05). **E.** Representative PFC sections from AAV-IRES or AAV-GSK3B injected mice, double-stained with GSK3B and NeuN. Overlap reveals largely neuronal localization (yellow) of GSK3B over-expression in AAV-GSK3β injected mice.

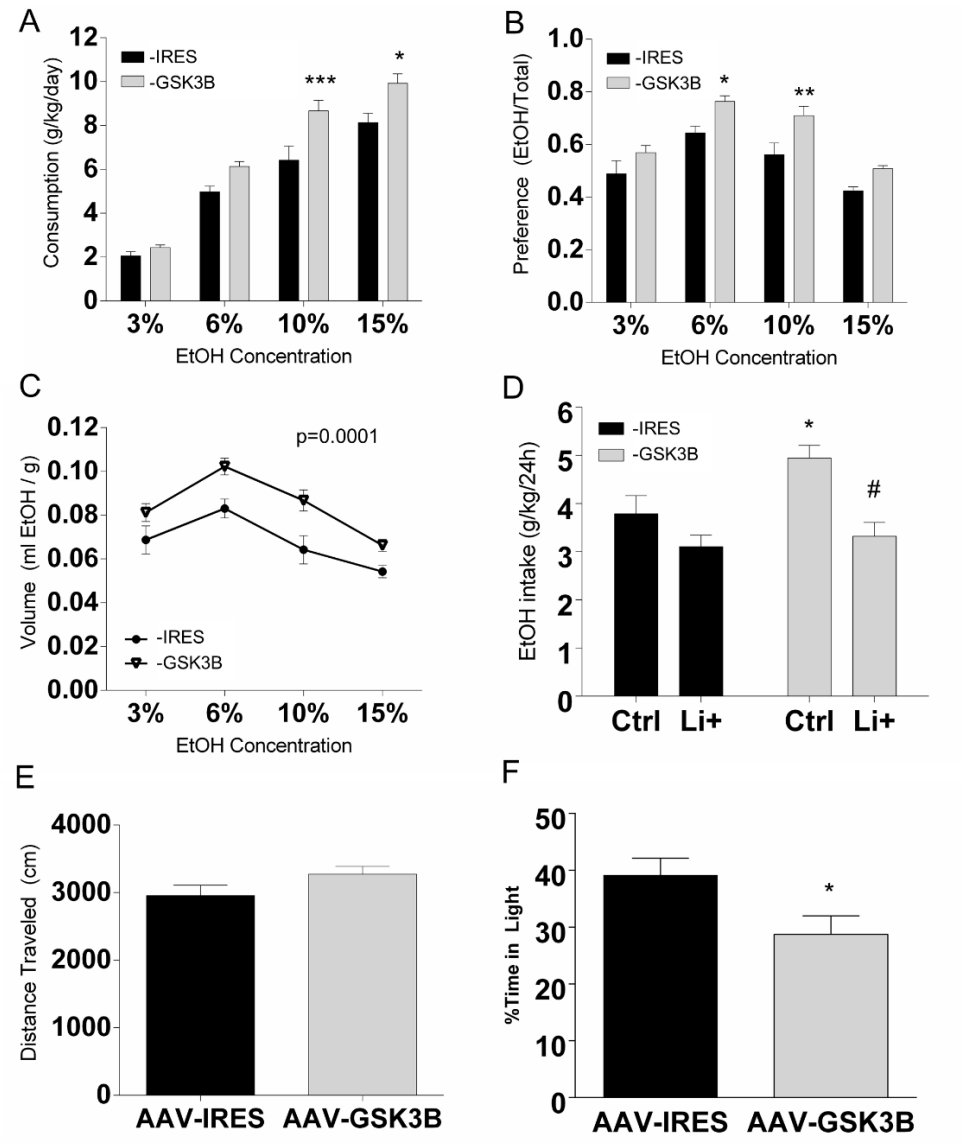

Figure 5.4 GSK3B overexpression increases ethanol consumption and preference. A. Compared to IRES mice, AAV-GSK3B mice (n=14-16) show significantly increased ethanol consumption (g/kg/day) during free access, two-bottle choice at 10% (p= 0.0005) and 15% (p=0.0147) ethanol concentrations. **B.** AAV-GSK3B mice show increased ethanol preference (EtOH/total fluid) during two-bottle choice at 6% (p=0.028) and 10% (p=0.0039) ethanol concentrations. **C.** AAV-GSK3B shifts the dose-response relationship between ethanol concentration and mL consumed significantly upward (p=0.0001) **D.** Addition of Lithium diet significantly decreased ethanol consumption in AAV-GSK3B mice (n=7-8 per group, #treatment effect of lithium in AAV-GSK3B mice, p=0.0021; *genotype effect in untreated mice, p=0.0451 vs. IRES). **E.** During a 10 minute LD box test, AAV-IRES and AAV-GSK3B (n=7-8/group) did not differ in total distance traveled. (*F*) AAV-GSK3B mice showed a significantly decreased time spent in the light (*p=0.0365), indicating increased anxiety-like behavior following withdrawal from ethanol access.

consumption (g/kg/day) using a progressive ethanol dosing regimen (**Fig. 5.4A**, $F_{1,28}$=20.68, p<0.0001 for viral genotype). AAV-GSK3B mice consumed larger (~30-40%) amounts of ethanol (g/kg/day) at 10% (p<0.001) and 15% (p<0.01) w/v ethanol concentrations compared to control AAV-IRES mice by Sidak's multiple comparisons test. There was also a significant viral genotype effect on mean ethanol preference ratio (**Fig. 5.4B**, $F_{1,28}$=19.34, p=0.0001), with AAV-GSK3B mice displaying an enhanced ethanol preference during access to 6% (p<0.05) and 10% (p<0.01) ethanol solutions. We further assessed ethanol drinking behavior as a function of ethanol concentration, wherein mean volume consumed of ethanol-containing solution was used as a proxy for reinforcers delivered. This showed an inverted U-shape dose-effect curve peaking at the 6% w/v ethanol (**Fig. 5.4C**), and with GSK3B mice consistently displaced to higher values than controls. Two-way ANOVA revealed a significant effect of viral genotype on mean volume of ethanol-containing solution per body weight ($F_{1,28}$=20.44, p=0.0001).

No significant difference in two-bottle choice voluntary consumption of saccharin (0.015% w/v) or quinine (0.05 mM) were observed between AAV-GSK3B and AAV-IRES mice (**Fig. 5.5A**, $t_{saccharin}$=0.92, p=0.36; $t_{quinine}$=0.45, p=0.66), suggesting taste preferences were not altered (Bachmanov *et al*, 1996). Additionally, blood ethanol levels were not different between AAV-GSK3B and AAV-IRES mice at 60 or 120 minutes after injection (i.p.) with 20% v/v ethanol (**Fig 5.5B**, $F_{1,4}$=1.48 , p=0.29) eliminating pharmacokinetic factors as a potential difference between the two viral genotypes.

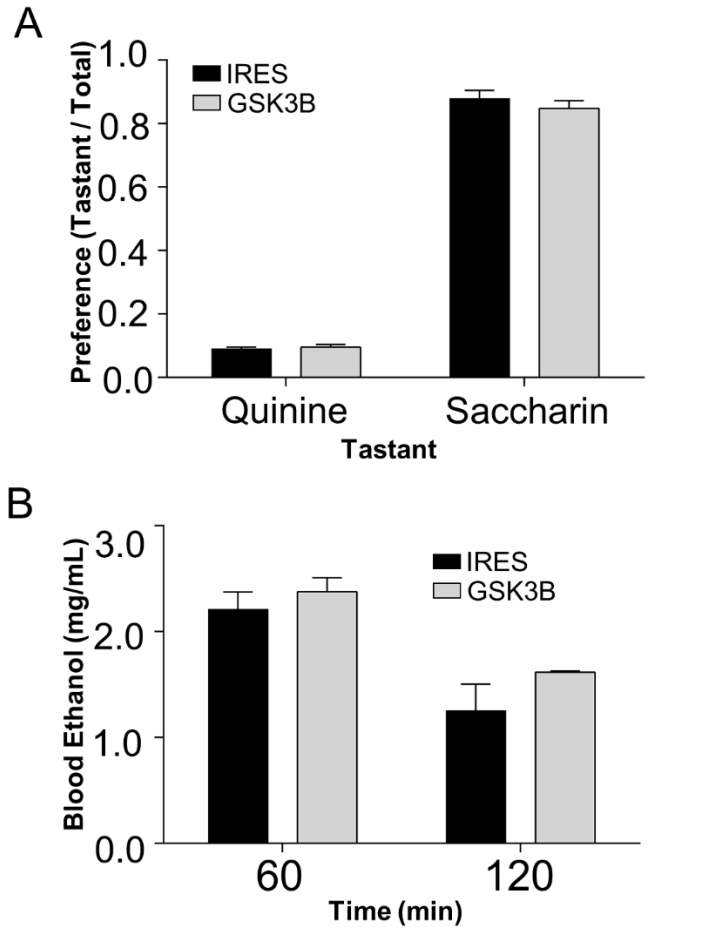

Figure 5.5 Taste preference and BEC show no differences following overexpression. AAV-GSK3B and AAV-IRES injected mice did not differ in taste preference or ethanol metabolism. **A.** Quinine and saccharin preferences, as determined by volume consumed over total fluid consumption (n=14-16/group, $p>0.05$). **B.** Blood ethanol levels at 60 or 120 minutes following an i.p. injection of ethanol (2 g/kg) (n=3/group, ANOVA $p>0.05$ for AAV-GSK3b vs. AAV-IRES at either time point).

To further confirm specificity of GSK3B overexpression on ethanol consumption, in a separate experiment we introduced lithium, a well validated GSK3B inhibitor (Chou *et al*, 2012; O'Brien and Klein, 2009), into diets for half of each experimental group for 4 weeks while receiving access to ethanol (10% w/v) and water (**Fig. 5.4D**). Lithium treatment ($F_{1,26}$=15.51, p=0.0005) and viral genotype ($F_{1,26}$=5.483, p<0.05) both significantly altered mean ethanol consumption (g/kg/day). Lithium significantly decreased ethanol consumption in AAV-GSK3B mice relative to standard chow (Tukey's post hoc, p<0.01). AAV-IRES mice fed lithium showed a non-significant decrease in ethanol consumption (95% CI: 0.4908 to -1.859 g/kg difference in mean consumption). Serum lithium levels did not differ significantly ($F_{1,2}$=0.11, p=0.771) between AAV-GSK3B (mean=0.65 mmol/L) and AAV-IRES mice (mean=0.70 mmol/L) fed lithium diets. Mice fed a standard chow had average serum lithium levels <0.3 mmol/L.

5.3.2 Viral-mediated Deletion

Viral vector mediated Cre recombinase expression completely deletes GSK3B from infralimbic cortex. The experimental vector (AAV2-CMV-Cre-eGFP) expressed Cre fused to enhanced green fluorescent protein (eGFP) to allow for visualization under fluorescent microscopy. The control vector encoded for eGFP without Cre recombinase. The injection site was confirmed while GSK3B staining demonstrated complete ablation of protein expression thereby confirming *Gsk3b* gene deletion. **Figure 5.6** shows representative GSK3B-stained sections from the infralimbic cortex region (box in top of figure), with a

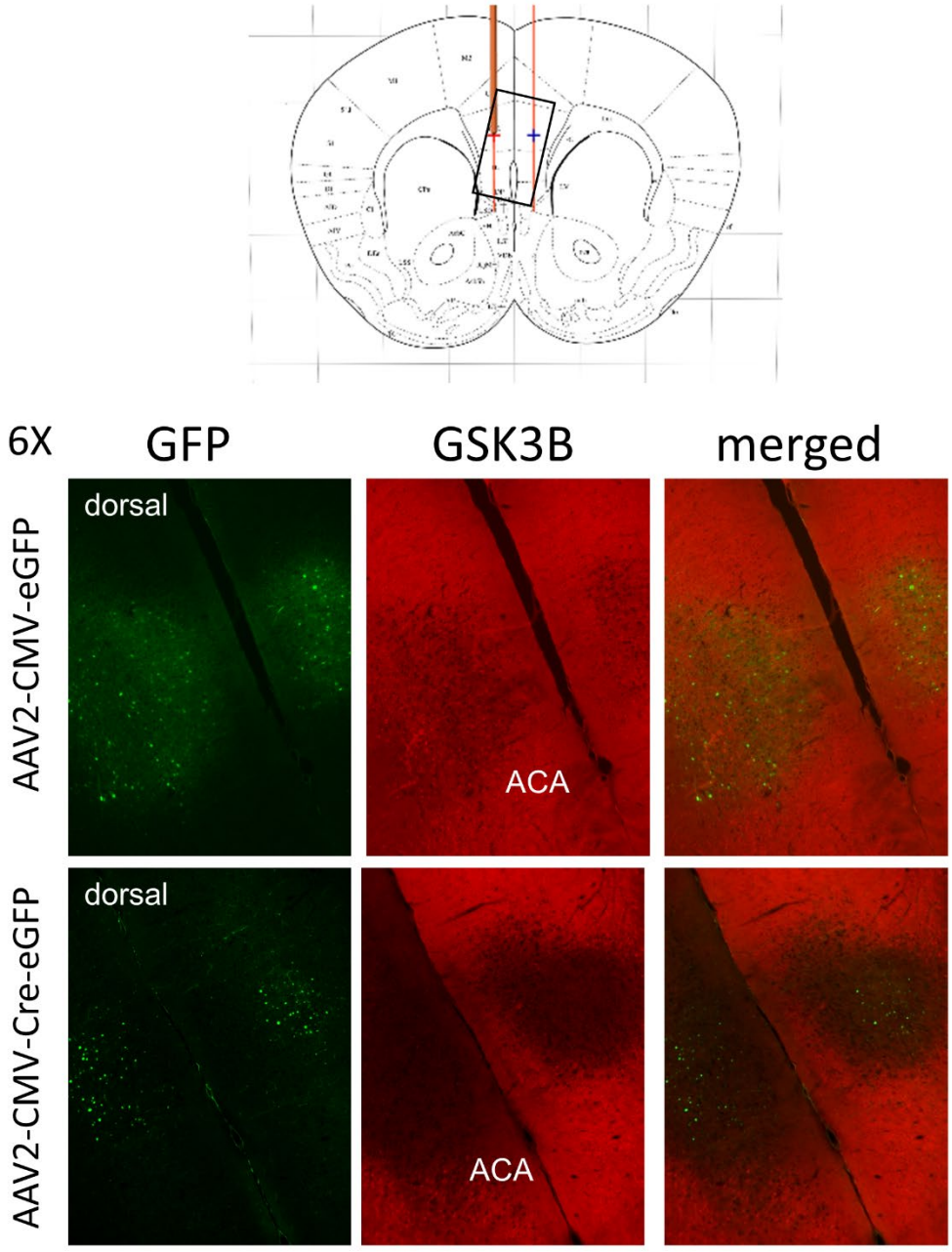

Figure 5.6 Rostral portion of Gsk3b deletion in infralimbic cortex. Rostral injection site with confirmed Gsk3b deletion. Target is shown at top of figure. Anterior Cerebral Artery (ACA) serves as a landmark. Both viruses expressed eGFP at green wavelength under fluorescent microscopy, while GSK3B was stained in the red channel. Overlap reveals *GSK3B* deletion from infralimbic cortex (IL).

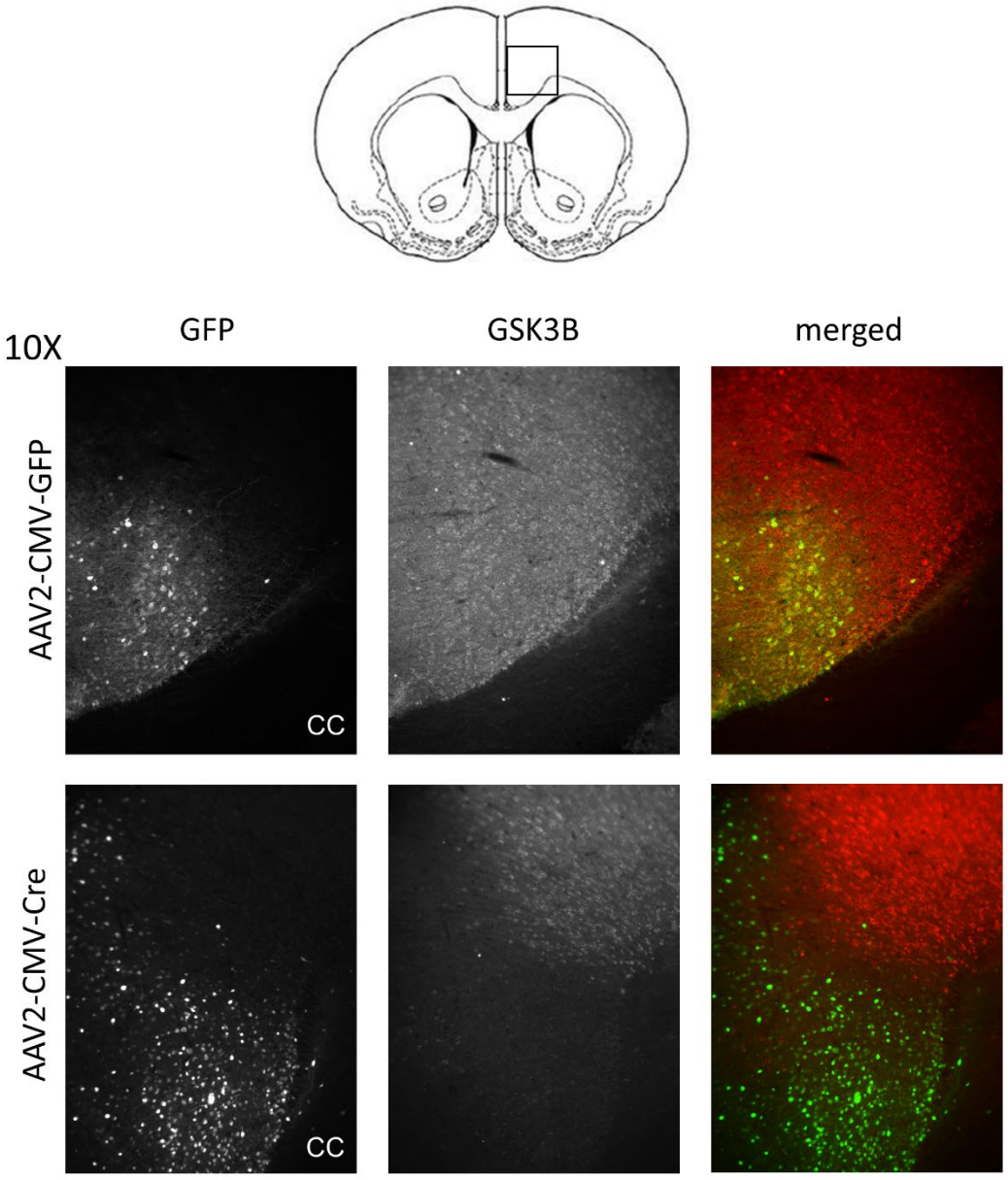

Figure 5.7 Caudal portion of injection site with confirmed *Gsk3b* deletion. GFP and GSK3B were in green and red channels, shown here in B&W. Corpus Callosum (CC) serves as landmark. Color added to merged image, again showing complete absence of GSK3B staining in region of virus.

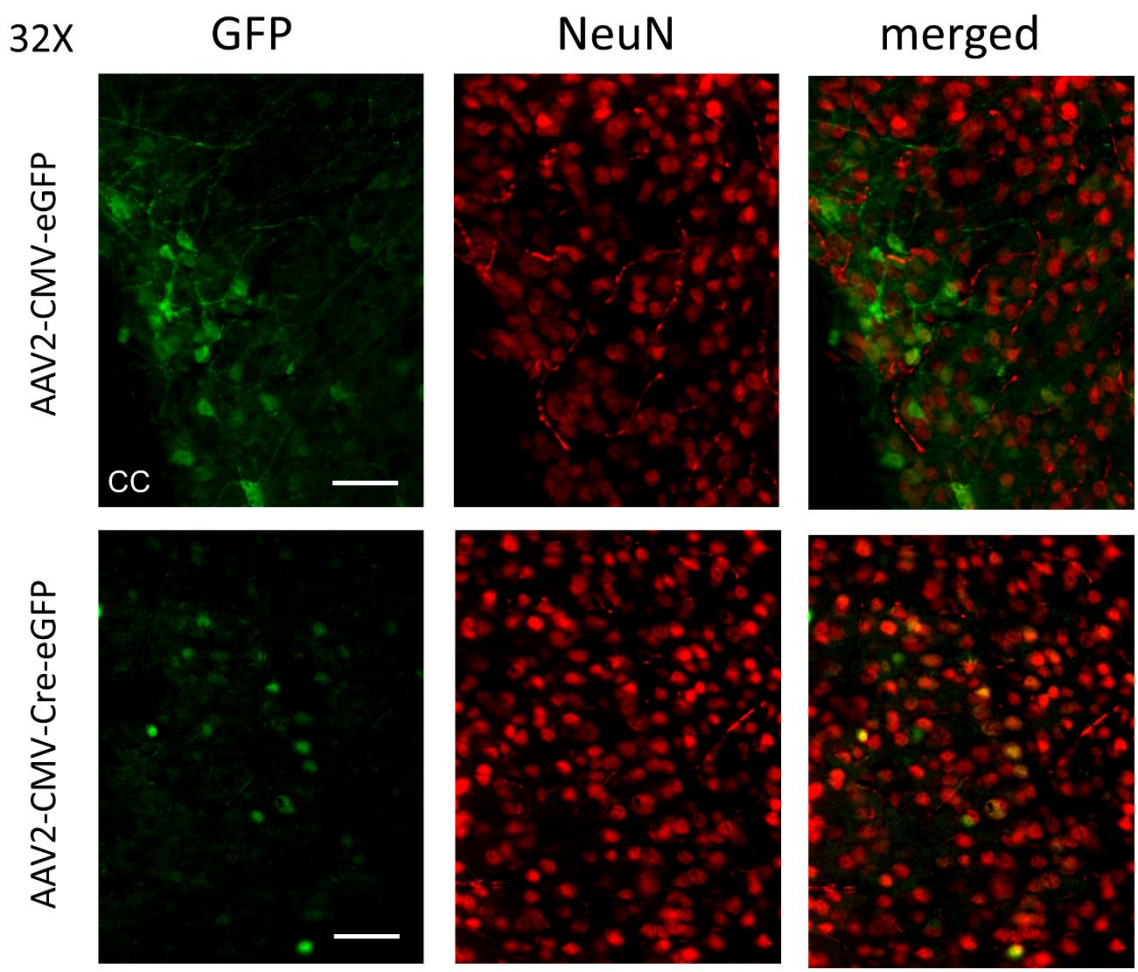

Figure 5.8 Localization of virally encoded protein in neuronal nuclei. Cre-eGFP fusion protein (bottom left) localizes in neuronal nuclei (NeuN) (overlap in bottom right), compared to cytoplasmic expression of free eGFP (top left). There is no evidence of neuronal toxicity in the injection site of either virus, based on consistent density of NeuN in injection site and surrounding region. Scale bar = 50 μM.

landmark provided by the notch of the anterior cerebral artery (ACA). Additional sectioning in the caudal direction demonstrated viral transduction *Gsk3b* deletion in the anterior cingulate cortex, just dorsal to the decussation of the corpus callosum (**Fig. 5.7**). Co-staining with the marker of neuronal nuclei (NeuN) provided visualization of the localization of Cre-eGFP fusion protein to the nuclei of neurons, compared to apparent cytoplasmic expression of the free eGFP expressed by the control virus (**Fig 5.8**). Neither virus showed signs of neuronal toxicity based on the relative density of NeuN staining through the injection site. Despite differences in cellular localization, there did appear to be a similar rate of transduction among the neuronal population (based on informal GFP-positive cell counting per high powered field). Altogether these findings confirm our injection target—with complete transduction of the IL and some additional transduction of the mPFC—and that Cre-mediated deletion of the *Gsk3bfl/fl* allele was successful.

Deletion of IL Gsk3b attenuates high-dose ethanol consumption in female mice. As above, mice were given continuous access to escalating doses of ethanol, ≥3 weeks after viral injection via stereotaxic surgery. Ethanol consumption (g/kg) was recorded daily in female and male mice for 5 days each at 3%, 6%, 10%, and 15% (w/v) ethanol. As ethanol concentration transitioned to the highest dose, we observed qualitatively that the Cre-injected mice, particularly females, showed a decrease in consumption and preference relative to GFP-injected mice. Daily consumption and preference readings in female and

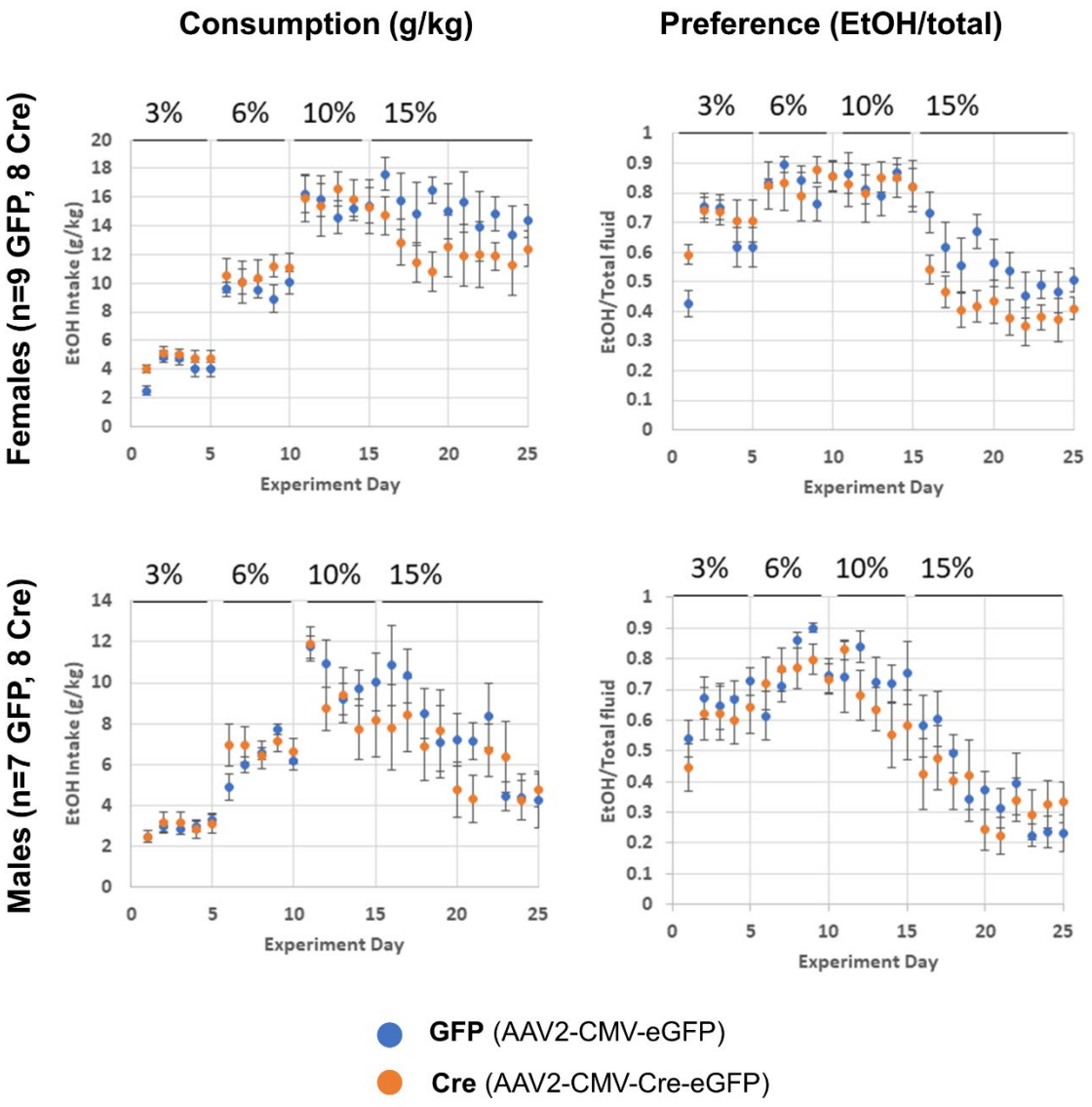

Figure 5.9 Plotted ethanol intake in GFP vs Cre-injected mice. Ethanol consumption (intake in g/kg) and ethanol preference (volume EtOH/volume total fluid) over 25 days of continuous ethanol access at escalating w/v%.

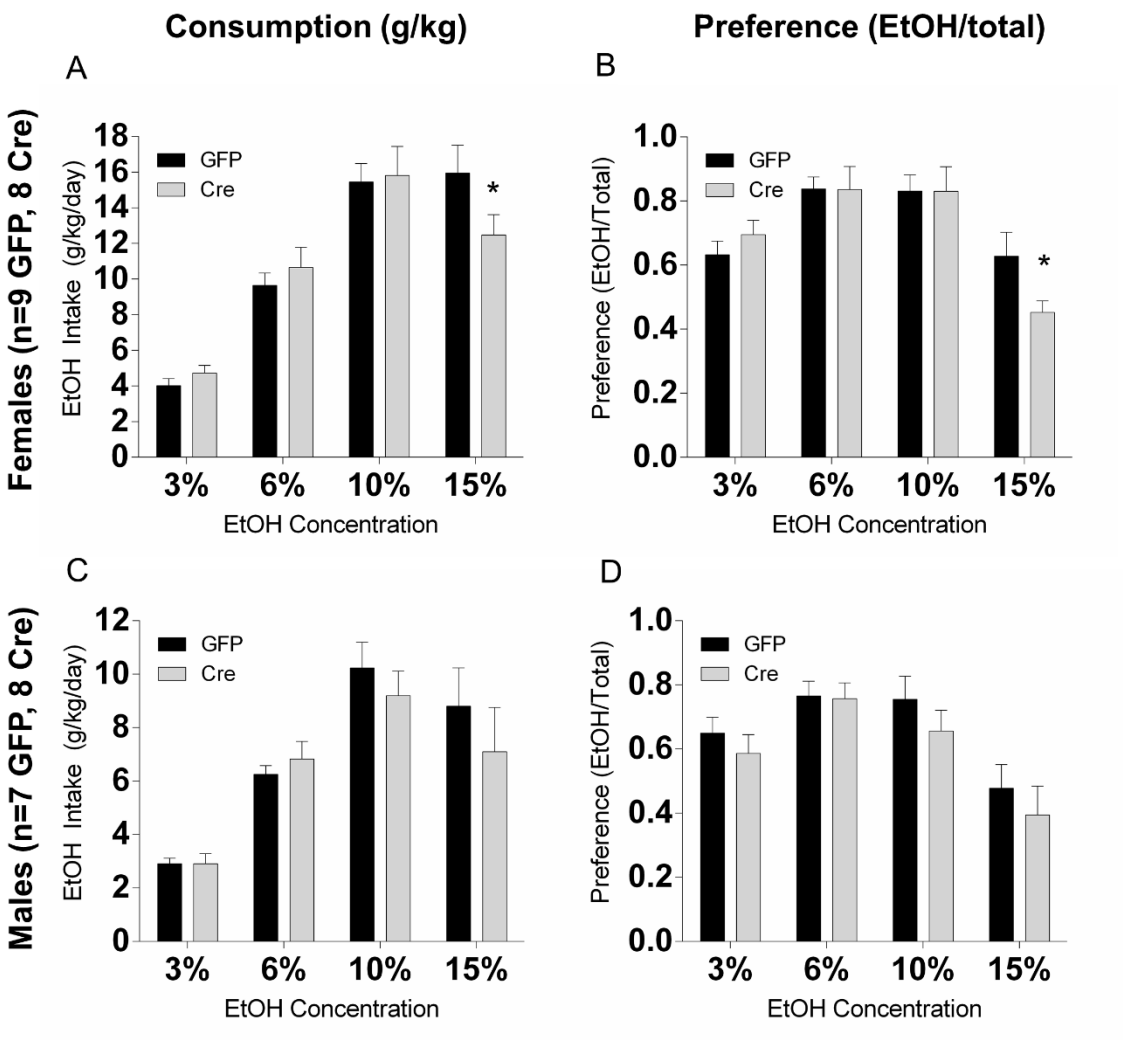

Figure 5.10 Female mice consume less high percent ethanol following Gsk3b deletion in IL. Ethanol consumption and preference in female and male mice, assessed by 2-way ANOVA finds signification interaction of genotype*concentration in female mice. Fisher's LSD finds significant effect of viral genotype at 15% ethanol in consumption (p=0.028) and preference (p=0.032).

male mice are shown in **Figure 5.9.** As for the viral-overexpression studies, 5-day means were calculated at each ethanol concentration and mean consumption and preference were analyzed via two-way ANOVA with viral genotype and ethanol concentration (within sex) (**Fig. 5.10**).

Within females, there was a significant effect of concentration ($F_{3,45}$=65.13, p<0.0001) and genotype*concentration interaction ($F_{3,45}$=2.81, p=0.050) on mean ethanol consumption (g/kg/day). The strong effect of ethanol concentration on ethanol consumption in g/kg is unsurprising given the nature of the variables—higher ethanol concentrations require lower intake volumes to achieve the same consumption by mass. However, ethanol concentration also showed a highly significant effect ($F_{3,45}$=23.05, p<0.0001) on ethanol preference, measured in (mL ethanol / (mL ethanol + water). However, in this case the higher ethanol concentration corresponded to lower preference. Again, there was a signification interaction effect of genotype*concentration ($F_{3,45}$=2.94, p=0.043). It is interesting to note that in the overexpression studies above (**Fig 5.4A-B**), genotype by itself showed a significant effect whereas for the viral deletion studies the effect is as an interaction with ethanol concentration. Because the increasing concentration, continuous access paradigm has traditionally been used to establish high ethanol drinking upon completion of the escalation rather than as multiple comparisons across each “dose” (Crabbe *et al*, 2011) we used Fisher’s LSD as a post-hoc test to assess differences at individual concentrations. At 15% ethanol, Cre-injected female mice were found to exhibit significantly lower ethanol consumption in g/kg/day (p=0.028) and lower

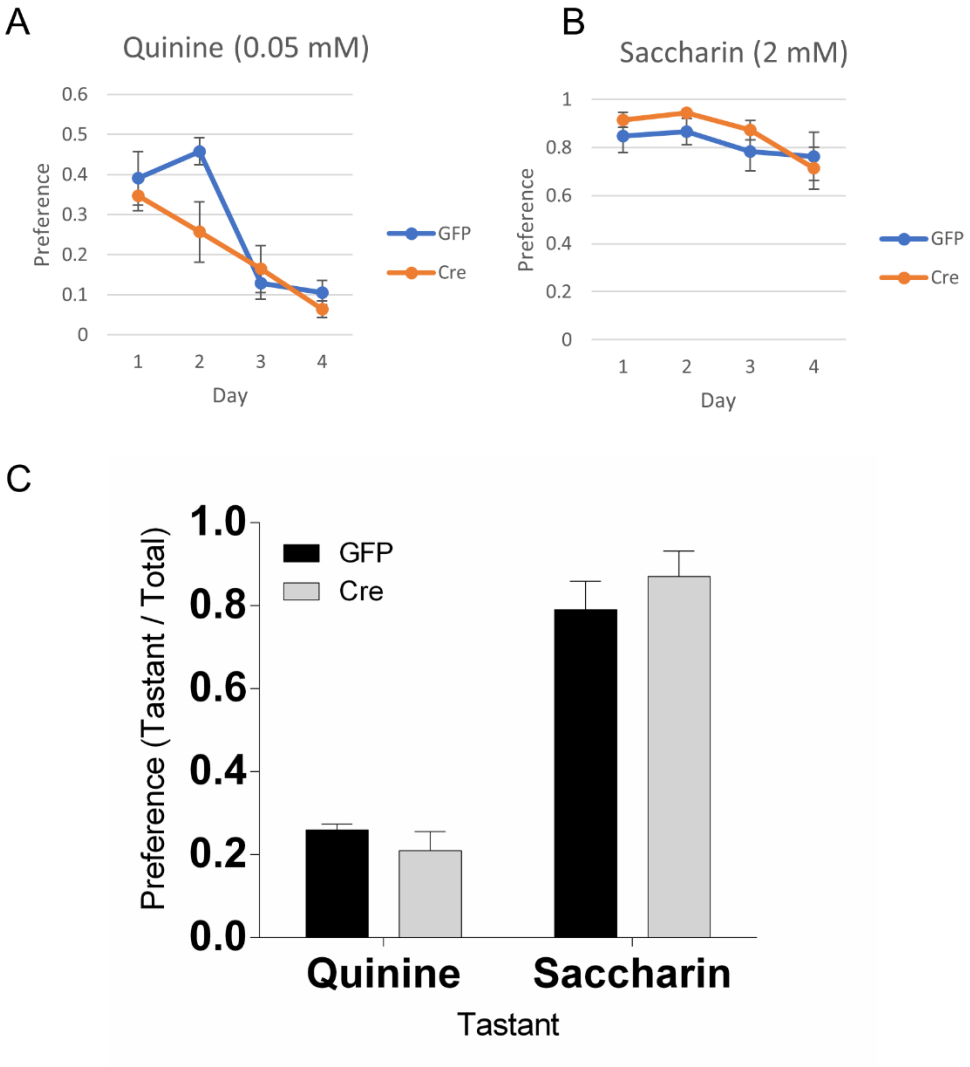

Figure 5.11 No significant taste preference differences following Gsk3b deletion in IL. Taste preferences were analyzed in a subset of ethanol naïve mice (n=8 GFP, 3 Cre). No significant differences were found for average quinine preference (p=0.18) over 4 days or saccharin preference (p=0.53) over a subsequent 4-day period.

A

LD Box Subsets		GFP	Cre
Basal	F	2	3
	M	3	4
Abstinence	F	8	8
	M	1	3

B

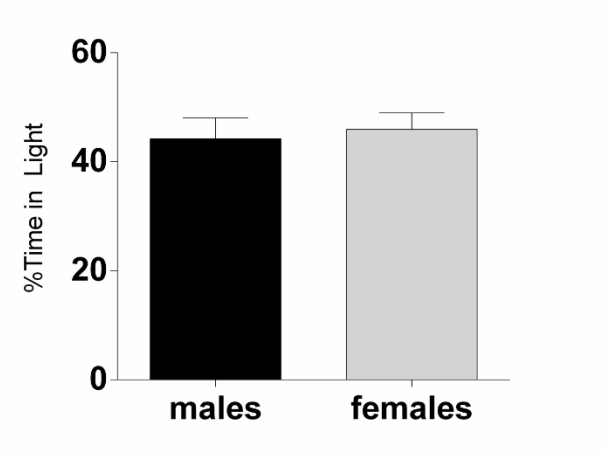

C

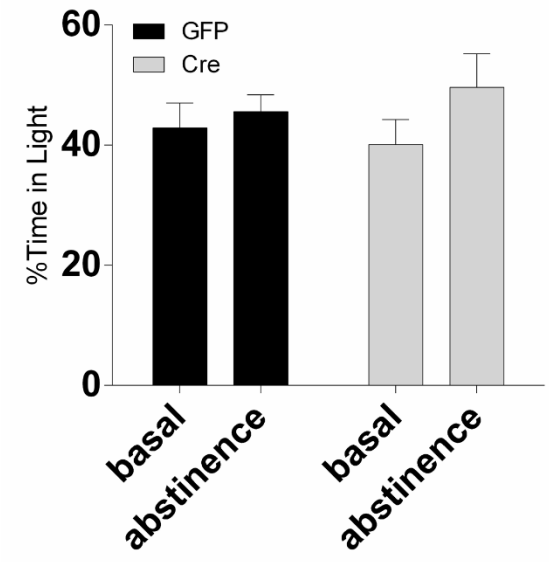

Figure 5.12 LD Box assays following Gsk3b deletion in IL.. LD Box assays were performed on an ethanol-naïve cohort of animals and an ethanol-experienced cohort after 24 hours of abstinence. Group numbers are given in A. Based on there being no observable differences across all males and females assessed (B), sexes were pooled in C. No significant differences were observed based on genotype, ethanol exposure, or interaction.

preference as a ratio over total fluid (p=0.032), than GFP-injected female mice. In male mice, ethanol concentration was the only significant effect on either ethanol consumption ($F_{3,39}$=20.12, p<0.0001) or ethanol preference ($F_{3,39}$=14.41, p<0.0001).

Deletion of IL Gsk3b does not affect taste preference or anxiety-like behavior.

To assess for potential taste differences between viral genotypes, a subset of animals were given access to quinine or saccharin (**Fig. 5.11**). No qualitative differences were observed in average preference for either tastant over a 4-day period. Across both groups, average quinine preference appeared higher in this study than in the overexpression studies above (**Fig. 5.5A**). This appears to be driven by an unusually high quinine preference during Days 1-2 of access (**Fig. 5.11A**), possibly as a novelty-type effect. Regardless, taste preference did not appear to play a role in the observed ethanol consumption differences.

As exploratory studies of the potential role of IL GSK3B in anxiety-like behavior with and without ethanol exposure, we tested subsets of virally injected animals in the LD box (**Fig. 5.12**) Studies of basal anxiety (n=5 GFP, 7 Cre) were performed in ethanol naïve animals, 3-5 weeks post viral injection. In an additional subset of animals (n=9 GFP, 11 Cre), anxiety-like behavior was tested 24 hours after the last ethanol exposure, following 34 days of continuous ethanol access. These studies were unbalanced in terms of sex ratio (**Fig 5.12A**), so

A

NOR Subsets		GFP	Cre
Basal	F	2	1
	M	6	2
Post long-term EtOH (3 Week abstinence)	F	1	2
	M	2	4

B

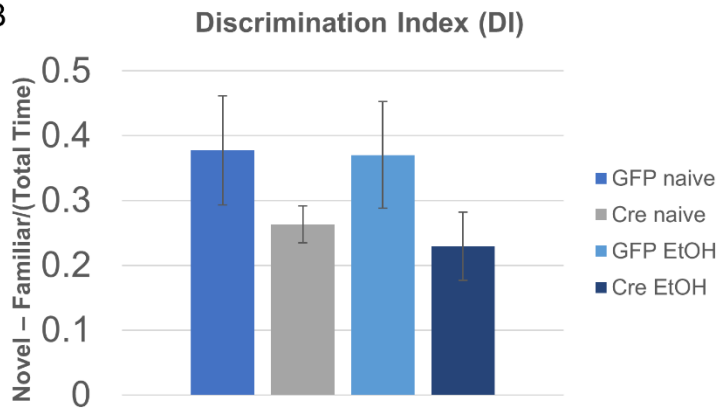

C

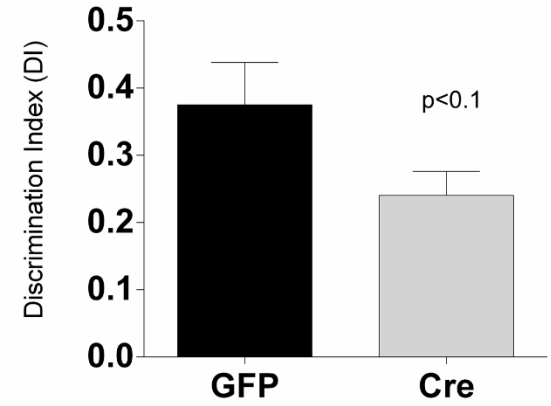

Figure 5.13 Novel object recognition task following Gsk3b deletion in IL. Novel Object Recognition tests were performed on an ethanol-naïve cohort of animals and an ethanol-experienced cohort after 24 hours of abstinence. Group numbers are given in **A**. Discrimination Index (DI) is the primary measure of the task, calculated as [(Time spent with Novel Object)-(Time spent with Familiar)]/Total Time. Viral genotype is indicated by "GFP" vs. "Cre," and ethanol exposure by "naïve" vs "EtOH." Based on observed similarity of DI values in the ethanol naïve and ethanol exposed groups (**B**), these were pooled in **C**.

males and females were compared overall, regardless of ethanol exposure (**Fig 5.12B**). As there appeared to be no evident sex effect, we compared basal and abstinence-induced anxiety without regard to sex (**Fig 5.12C**). There was no significant effect of genotype ($F_{1,28}$=0.016, p=0.90), ethanol exposure ($F_{1,28}$=1.5), or interaction ($F_{1,28}$=0.466, p=0.50). Thus, unlike in the case of the overexpression vector, there is no evidence that *Gsk3b* deletion in the IL is associated with anxiety-like behavior, before or after long-term ethanol consumption.

Deletion of IL Gsk3b shows suggestive impairment in Novel Object Recognition Task. As an additional exploratory experiment, we assessed PFC-dependent memory function using the novel object recognition task, also in ethanol naïve and ethanol experienced mice (**Fig. 5.13**) These studies were underpowered to include sex as a covariate (**Fig 5.13A**) but as above there was no difference in sexes overall (t_{18}=0.95, p=0.36) and so data was analyzed collapsed across sexes. We hypothesized there might be ethanol-induced impairments in working memory showing interaction with GSK3B deletion. However, observation of the data from the 4 groups shown in **Figure 5.13B** revealed qualitatively similar discrimination indexes between Cre-injected and GFP-injected mice regardless of ethanol exposure. Thus groups were additionally collapsed across ethanol exposure to compare the two genotypes (**Fig 5.13C**) and a suggestive effect (p<0.1) was found by t-test. This finding could indicate that GSK3B in the infralimbic cortex might be necessary for normal

working memory function, and in theory a learning-related mechanism could be related to a potential role for GSK3B in addiction. However additional investigation would be necessary to determine whether this is a meaningful effect rather than a speculative hypothesis. Overall, these studies were underpowered but are not the major focus of work and so we will not discuss them further.

5.3.3 Tamoxifen-mediated *Gsk3b* Deletion

Having observed a subtle but significant effect on ethanol drinking in female mice following Cre-mediated *Gsk3b* deletion by a viral vector in the IL, we wanted to investigate an alternative approach to Cre-mediated deletion. While viral vectors afford a high degree of regional specificity, their cellular specificity is limited due to size constraints of the promoter. Selective breeding of tamoxifen-inducible promoter-driven Cre lines with homozygous floxed animals allows for the ability of selective cell-specific deletion, with regional specificity dependent upon regional expression of the promoter. Here we compare Camk2a-Cre+ and Camk2a-Cre- mouse strains, both homozygous the Gsk3b-floxed allele, and both treated with tamoxifen. The Cre+ mice would be expected to show GSK3B deletion in Camk2a-expressing neurons (located throughout the forebrain) while the Cre- would be expected to show wild-type GSK3B expression.

Validation of tamoxifen-induced Camk2a-Cre mediated deletion.

Confirmation of GSK3B deletion was carried out after ethanol access and a subsequent wash-out (>1 week of ethanol abstinence). Effective Camk2a-Cre action had been previously validated by our group in a genetic cross with the

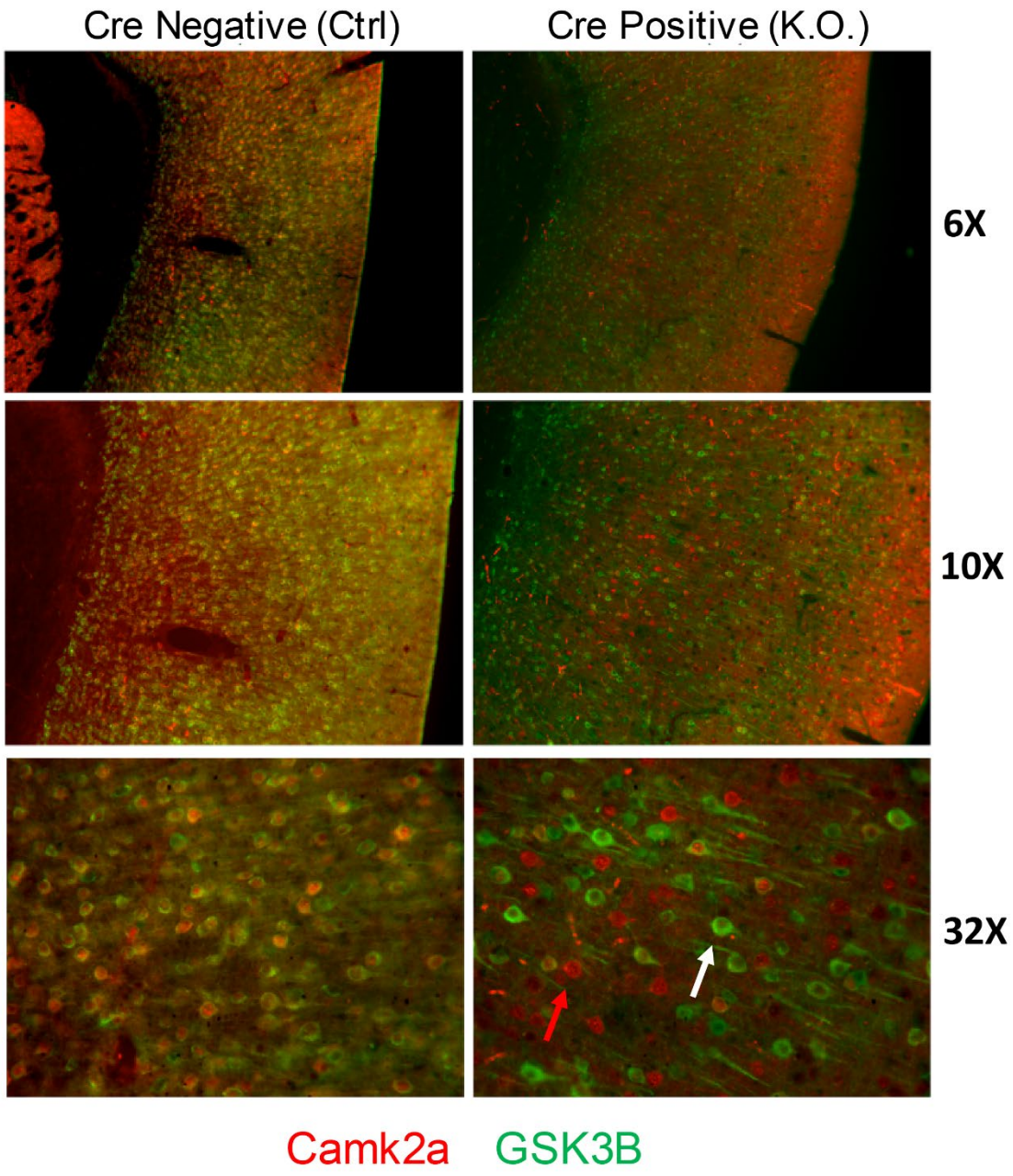

Figure 5.14 Validation of *Gsk3b* deletion in Camk2a+ neurons of Cre+ mice. GSK3B and Camk2a immunostaining in Cre^{+}/Gsk3b fl/fl vs. Cre^{-}/Gsk3b fl/fl mice. Results show highly selective loss of GSK3B staining in $Camk2a^{+}$ cells of Cre^{+} mice (red arrow). GSK3B expression remained in $Camk2a^{-}$ cells (white arrow). Sections are oriented with dorsal surface of the brain upwards.

TdTomato reporter strain (Harris et al., unpublished). Immunostaining revealed highly selective loss of GSK3B in Camk2a+ neurons of Cre+ mice (**Fig. 5.14**). Cre- animals showed extensive Camk2a-GSK3B co-localization (yellow) while Cre+ mice showed very little overlap between green staining neurons (GSK3B-expressing) and red neurons (Camk2a-expressing).

Deletion of GSK3B in Camk2a$^+$ forebrain neurons decreases ethanol consumption and preference. Given previously observed differences in GSK3B deletion specifically at higher concentration ethanol (15% w/v), we utilized this as the starting concentration animals were given in this study. Further, we were interested in a potential role for GSK3B in escalated drinking behavior, as seen under the intermittent ethanol access (IEA) paradigm (see Chapter 2.3). All mice were given 15% (w/v) ethanol under a continuous access schedule for 15 days and then switched to intermittent access 2-bottle choice for 15 days of ethanol access, i.e. 5 weeks of the IEA paradigm (see **Fig. 5.1C**).

Daily consumption values in g/kg were recorded for each 24-hour ethanol access period and are shown in **Figure 5.15**. Throughout this experiment, males and females were run concurrently and the data is shown as collapsed across sexes as well as split by sex (n=5-7 females per genotype, 8-10 males per genotype). Surprisingly female Cre- mice displayed average ethanol consumption at levels relatively similar to male Cre- mice through the course of this experiment. The potential antagonistic effect of 5-day high-dose tamoxifen

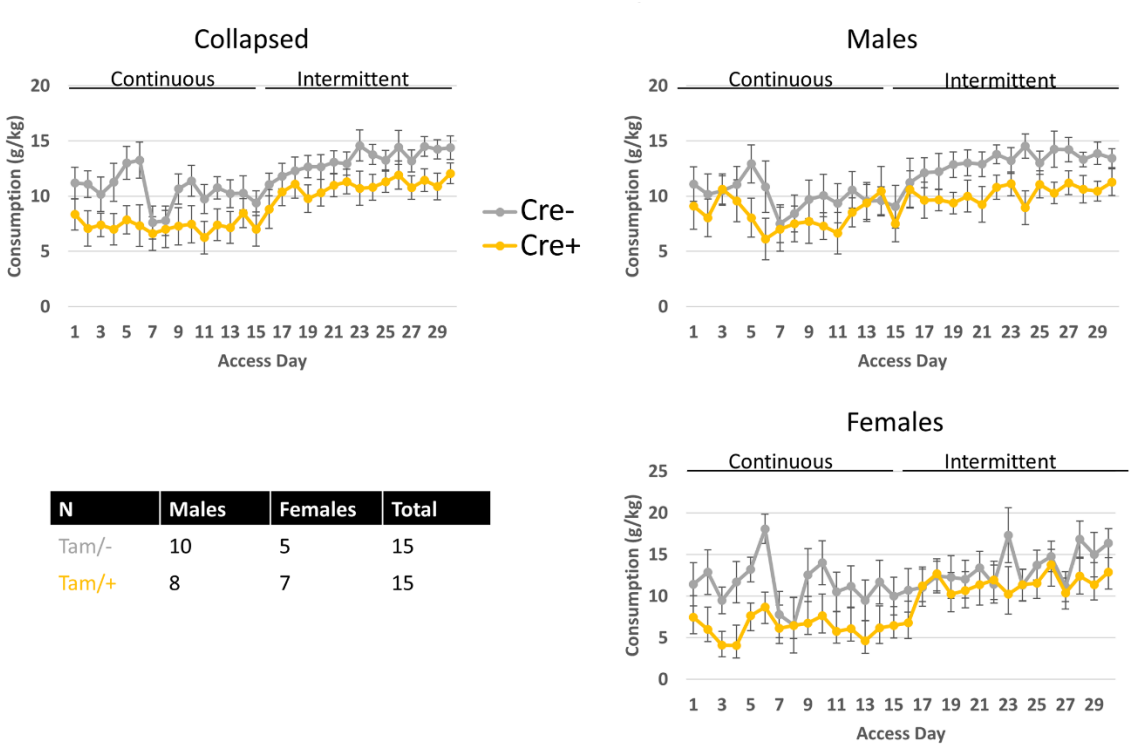

N	Males	Females	Total
Tam/-	10	5	15
Tam/+	8	7	15

Figure 5.15 Daily consumption values plotted in Camk2a-Cre+ vs. Cre- mice. Daily consumption (g/kg EtOH) was recorded over the 30 ethanol access days of the experiment. The latter 15 access days of the experiment were recorded over 5 weeks, with 3 24h recordings per week according to the IEA protocol.

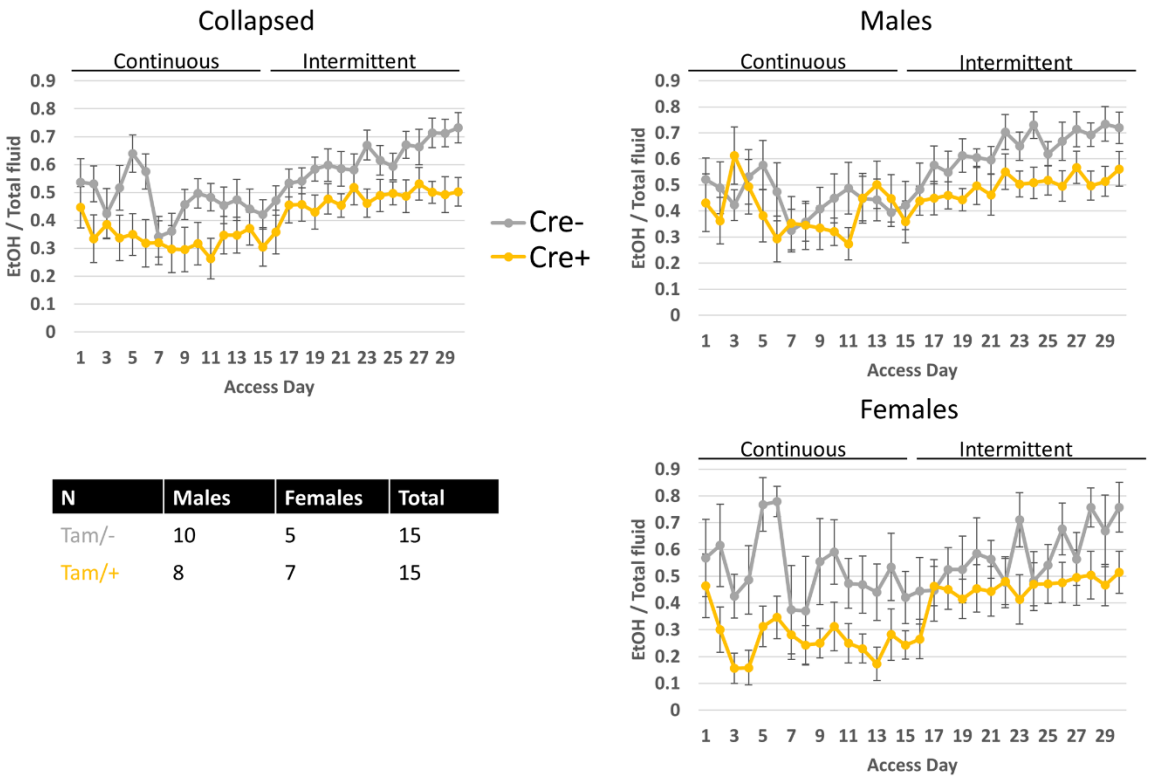

N	Males	Females	Total
Tam/-	10	5	15
Tam/+	8	7	15

Figure 5.16 Daily preference values plotted in Camk2a-Cre+ vs Cre- mice. Daily preference (mL EtOH / mL total fluid) was recorded over the 30 ethanol access days of the experiment. The latter 15 access days of the experiment were recorded over 5 weeks, with 3 24h recordings per week according to the IEA protocol. Female Cre- mice show a high degree of variability (and the lowest n) but qualitatively seem to show a delayed escalation in preference following the switch to IEA. Overall Cre+ mice appear to drink less across both paradigms while still showing an escalation during the IEA paradigm.

treatment on subsequent ethanol drinking behavior in females is beyond the scope of this work but is under investigation as a separate project.

Daily preference values showed a similar pattern and are plotted in **Figure 5.16**. There appear to be qualitative differences between the two genotypes throughout the experiment but also in the slope of escalation seen following the switch to IEA beginning on Access Day 16. The Cre- female mice also appeared to show a delayed escalation following the switch to IEA relative to the Cre+.

To analyze the data we attempted to maximize power while maintaining rigor. As an initial step we took calculated mean consumption and preference values per mouse during windows of interest in the experiment. For the continuous access period, average consumption and preference values were calculated over Access Days 2-15 (two weeks of continuous access). The first day of access is commonly dropped from ethanol-drinking studies due to novelty-type factors leading to consistently observed outlier behavior (Chester *et al*, 2006). For the intermittent access period, average consumption and preference values were calculated from the final week of ethanol access, to allow for 4 weeks of potential escalation in drinking behavior. As preliminary analyses, mean values within males and females and within paradigms were compared in a series of unpaired t-tests. These comparisons are shown in terms of consumption in **Figure 5.17A-D** and preference in **Figure 5.18A-D**. There is a trend for Cre+ animals to show lower ethanol consumption and preference across sexes and paradigms, but the strongest differences are seen in females under a continuous access paradigm ($t_{(consump,\ df=10)}$=2.43,p=0.035; $t_{(pref,}$

Table 5.1 Results of 2-way ANOVAs of sex and genotype (Camk2a Cre+ vs Cre-) on ethanol drinking measures. CONT=continuous ethanol access. IEA=intermittent ethanol access. GENO= genotype. Nparm=number of parameters.

CONT CONSUMP	Nparm	DF	Sum of Squares	F Ratio	Prob > F
GENO	1	1	75.995105	4.7786	0.0380*
SEX	1	1	26.689876	1.6783	0.2065
GENO*SEX	1	1	2.332289	0.1467	0.7049

IEA CONSUMP	Nparm	DF	Sum of Squares	F Ratio	Prob > F
GENO	1	1	75.995105	4.7786	0.0380*
SEX	1	1	26.689876	1.6783	0.2065
GENO*SEX	1	1	2.332289	0.1467	0.7049

CONT PREF	Nparm	DF	Sum of Squares	F Ratio	Prob > F
GENO	1	1	0.18525127	6.6911	0.0156*
SEX	1	1	0.00749241	0.2706	0.6073
GENO*SEX	1	1	0.08025681	2.8988	0.1006

IEA PREF	Nparm	DF	Sum of Squares	F Ratio	Prob > F
GENO	1	1	0.35163048	9.9205	0.0041*
SEX	1	1	0.00008508	0.0024	0.9613
GENO*SEX	1	1	0.00054501	0.0154	0.9023

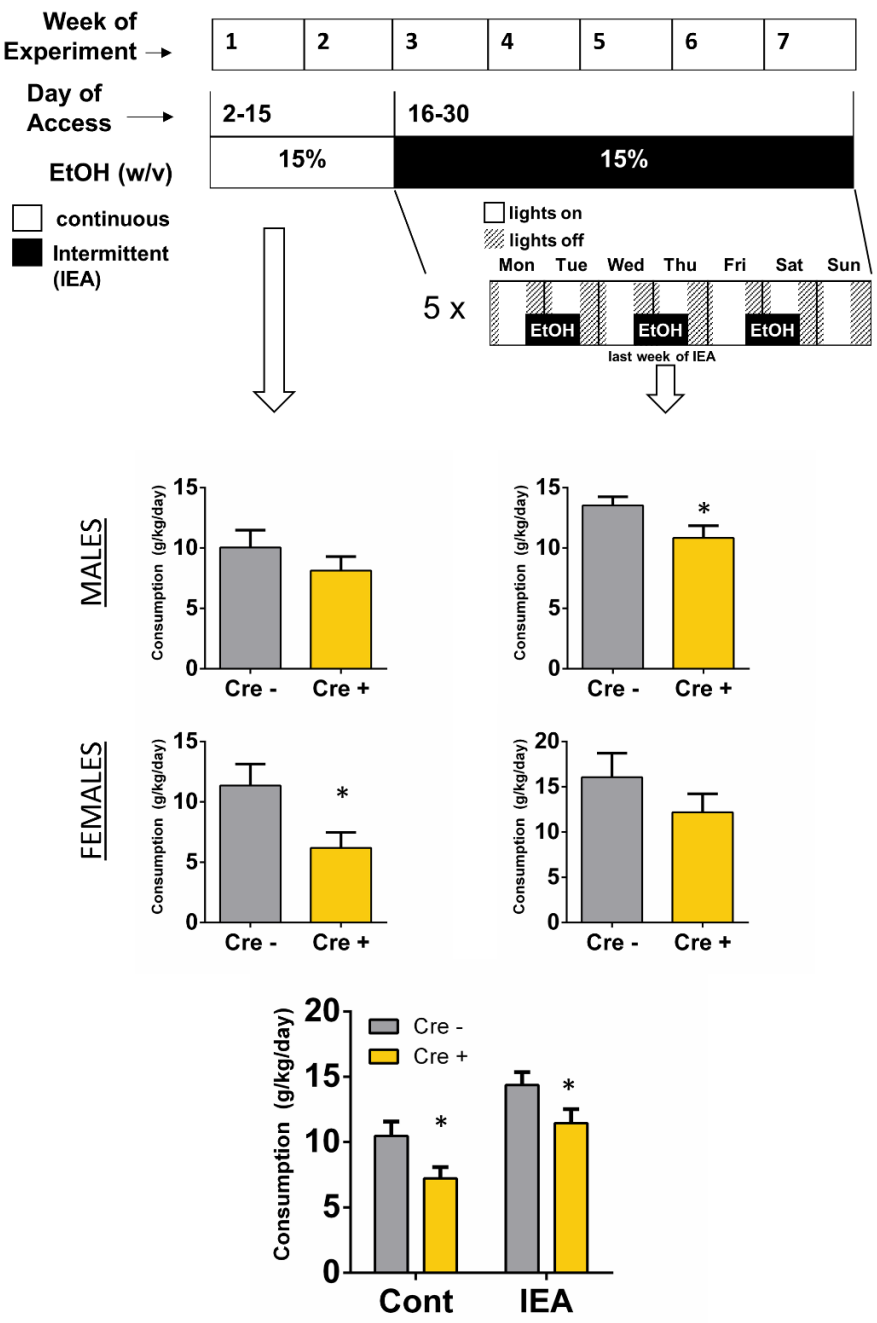

Figure 5.17 Mean ethanol consumption comparisons in Camk2a-Cre+ vs Cre- mice. Average ethanol consumption (g/kg/day) values were compared during the first two weeks of the experiment (continuous access) and during the last week of intermittent ethanol access (IEA). **A.-D.** Independent unpaired t-tests were run within males and within females, with significant differences observed between Cre+ and Cre- males during IEA and females during continuous access (Cont) (*p<0.05). Because males and females were run together and sex was found not to exert a significant effect on ethanol drinking, groups were then analyzed by RM ANOVA with sexes pooled (**E**). Cre+ animals consumed significantly less ethanol than Cre-, during both Cont and IEA (*p<0.05).

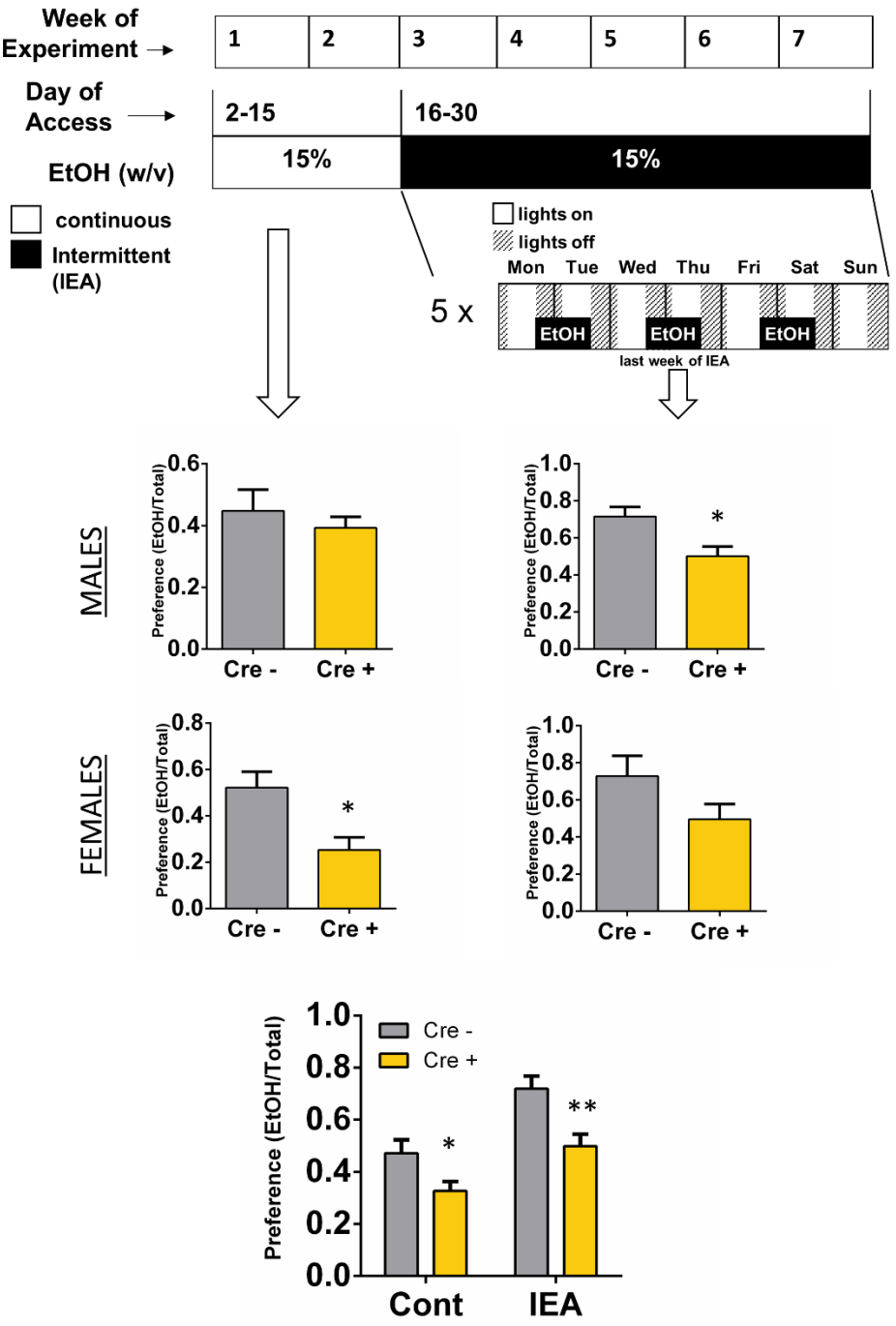

Figure 5.18 Mean ethanol preference comparisons in Camk2a-Cre+ vs Cre- mice. Average ethanol preference (volume EtOH/total fluid) values were compared during the first two weeks of the experiment (continuous access) and during the last week of intermittent ethanol access (IEA). Independent unpaired t-tests were run within males and within females, with significant differences observed between Cre+ and Cre- males during IEA and females during continuous access (cont) (*p<0.05). Groups were then analyzed via RM ANOVA with sexes pooled, and overall Cre+ animals showed significantly lower ethanol preference than Cre-, during both Cont and IEA (*p<0.05, **p<0.01).

$_{df=10)}$=3.10, p=0.011) and in males under an intermittent access paradigm ($t_{(consump,\ df=16)}$=2.26, p=0.038; $t_{(pref,\ df=16)}$=2.88, p=0.011). To analyze the data more formally, we performed 2-way ANOVAs of genotype and sex on consumption and preference values within each paradigm. Results of the 2-way ANOVAs are shown in **Table 5.1**.

As there were no significant effects of sex or sex*genotype on any of the dependent variables of interest, we pooled the sexes and dropped the factor "sex" from our analyses, thus providing additional power to perform a 2-way RM ANOVA on genotype and paradigm (IEA vs CONT). These results are displayed in terms of consumption in **Figure 5.17E** and preference in **Figure 5.18E**. Mean consumption was found to be significantly affected by genotype ($F_{1,28}$=6.48, p=0.017), paradigm ($F_{1,28}$=29.08, p<0.0001), and not significantly affected by the paradigm*genotype interaction ($F_{1,28}$=0.052, p=0.82). Similarly, mean preference showed significant effects of genotype ($F_{1,28}$=11.11, p=0.0024), paradigm ($F_{1,28}$=22.56, p<0.0001), and no significant effect of the interaction ($F_{1,28}$=1.31, p=0.26). Fisher's LSD post hoc comparisons found significantly lower ethanol consumption in Cre+ mice under continuous access (p=0.026) and IEA (p=0.046) and significantly lower ethanol preference in Cre+ mice under continuous access (p=0.027) and IEA (p=0.0011). Taken together, we conclude that GSK3B deletion in Camk2a expressing neurons decreases ethanol-drinking behavior across ethanol access paradigms. However GSK3B function in Camk2a-expressing neurons does not appear to be necessary for an escalation in drinking under IEA paradigm relative to continuous ethanol access.

Deletion of GSK3B in Camk2a^{+} forebrain neurons does not alter taste preference, ethanol metabolism, or anxiety-like behavior.

As described in above sections, subsets of animals under this deletion protocol were assessed for quinine and saccharin taste preference when provided in conjunction with a water bottle under a two-bottle choice, continuous access model (n=4/genotype) (**Fig 5.19A**). By unpaired t-tests, there was no significant difference in average quinine preference (p=0.49) but a slight suggestive difference in saccharin preference (p=0.093). In the latter case the mean values were very similar (Cre- mean±SEM: 0.928±0.006, Cre+ mean±SEM: 0.944±0.005) but the low variance in each group might indicate that additional saccharin preference tests should be run with lower concentrations than 2 mM (0.03% w/v) to assess whether a difference in sweet preference emerges. The fact that the Cre+ group showed, if anything, a suggestively higher preference would indicate that general reward-seeking type behavior is not impaired following Camk2a+ neuron GSK3B deletion.

Blood ethanol content was measured at two time points (n=4/genotype/time) following an i.p. ethanol (2 g/kg) injection (**Fig. 5.19B**). A 2-way RM ANOVA revealed a significant effect of time ($F_{1,6}$=6.175, p=0.048) but no significant effect of genotype ($F_{1,6}$=0.35, p=0.57) or time*genotype ($F_{1,6}$=0.46, p=0.53). Thus tamoxifen-induced Cre expression and subsequent GSK3B deletion shows no evidence of altering the metabolic profile of ethanol, and metabolic differences do not account for ethanol consumption differences.

Finally, a subset of animals were tested in the LD box basally (1 week

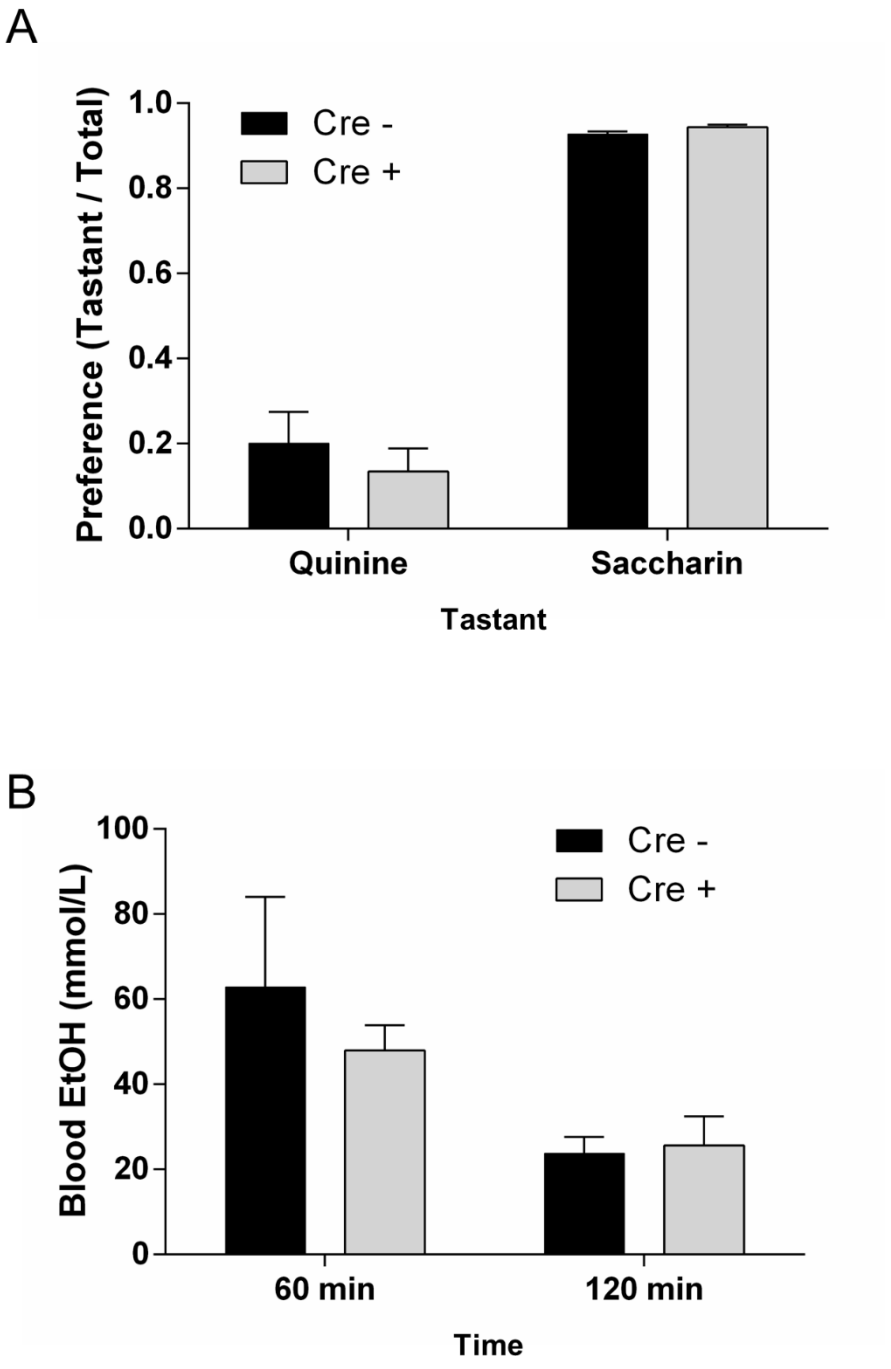

Figure 5.19 Camk2a-Cre+ and Cre- mice do not differ in taste preference or ethanol metabolism. A. Quinine and saccharin preferences, as determined by volume consumed over total fluid consumption (n=4/group, p>0.05). **B.** Blood ethanol levels at 60 or 120 minutes following an i.p. injection of ethanol (2 g/kg) (n=4/group, ANOVA p>0.05 for Cre- and Cre+ at either time point).

A

LD Box Subsets		Cre-	Cre+
Basal	F	4	4
	M	2	2
Abstinence	F	0	2
	M	3	2

B

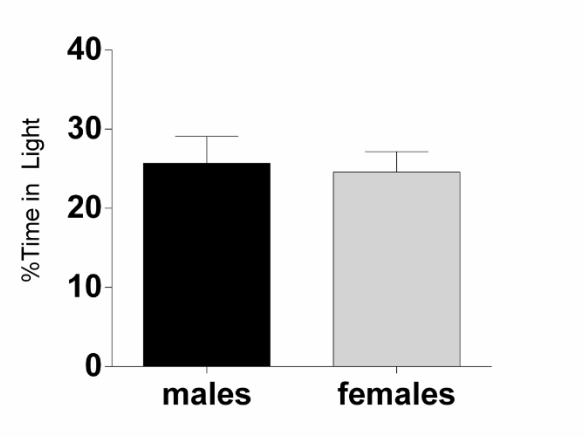

C

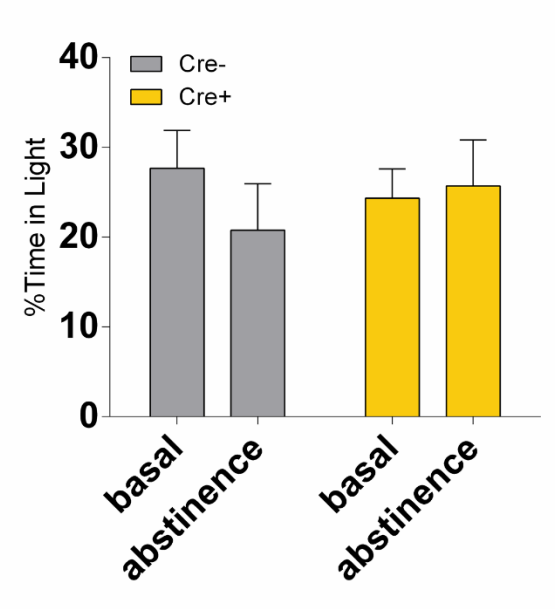

Figure 5.20 Camk2a-Cre+ and Cre- mice do not differ in locomotor behavior. Cre- and Cre+ mice do not show significant differences in locomotor behavior. LD Box assays were performed on an ethanol-naïve cohort of animals and an ethanol-experienced cohort after 24 hours of abstinence. Group numbers are given in A. Based on there being no observable differences across all males and females assessed (B), sexes were pooled in C.

after completion of tamoxifen treatment) and a separate cohort tested upon ethanol abstinence (24 hours after last ethanol access, following >5 weeks of IEA). These experiments are displayed in **Figure 5.20**. As before, sexes were unbalanced but we did not see any evident differences by sex, and subsequently pooled the animals to again find no significant differences in anxiety-like behavior ($F_{genotype(1,15)}$=0.032, p=0.86; $F_{treatment(1,15)}$=0.38, p=0.55; $F_{genotype*treatment}$=0.84, p=0.37), as measured by %time in the light. There is a notable qualitative difference in the mean %time in light in the tamoxifen-treatment experiment overall, compared to mean %time in light of the virally injected animals overall (see **Figure 5.12**).

5.4 Discussion

While the magnitude of effect varied across methods of gene modulation and the specifics of the paradigm used for assessment, there was a striking consistency in the directionality of the effect of GSK3B expression on ethanol-drinking. When expression was increased by use of an exogenous-*Gsk3b* gene expressing vector applied to mPFC of male mice, ethanol consumption and preference increase markedly at multiple ethanol concentrations (6%, 10%, 15% w/v). When expression was decreased by *Gsk3b* deletion in the IL portion of the mPFC via viral-mediated Cre expression in floxed animals, ethanol consumption and preference decrease selectively at high ethanol concentration (15% w/v), in female mice specifically. When Cre was induced in a specific forebrain neuron

population (Camk2a-positive) via tamoxifen induction, ethanol consumption and preference decreased at a high ethanol concentration (15% w/v) among male and female mice, whether ethanol was administered continuously or under an IEA schedule.

The effects of viral deletion in the IL were rather minimal when compared with the effects seen with mPFC over-expression. While it may be that there is simply a fundamental difference between increasing GSK3B and deleting it, there are several specific contributing factors that could account for the difference in effect magnitude. The overexpression vector was injected (by Annie Meng) at a volume of 1.0 µL per hemisphere, while the Cre-expressing deletion vector was injected at 0.7 µL per side, in an effort to increase specificity of the injection site. As a rough estimate, an injection results in a bolus of about 1 mm^3/uL, and so in total 0.6 mm^3 of additional cortex might be expected to have been exposed to the overexpression virus. Similarly, the target site used by Meng was selected to be the anterior cingulate cortex (ACC) portion of the mPFC, with tracking into the rostral mPFC (IL cortex) whereas the deletion vector was injected directly into the IL. Both the ACC and IL have been implicated in ethanol-seeking behavior (Gass *et al*, 2014; Gremel *et al*, 2011), but it may be that GSK3B function in the ACC exerts a stronger effect on ethanol-drinking behavior than the IL. Alternatively, it could be that GSK3B overexpression in male mice allowed for stark increases in consumption and preference, whereas GSK3B deletion, particularly in males, was simply subject to a floor effect. As pointed out in the text, male mice in the viral deletion study showed atypically low drinking for C57BL/6J mice. To this end

it may also be noted that possible subtle genetic effects can be carried in transgenic animals, given unintentional effects of LoxP site insertion or persistent loci from other lab strains despite several generations of inbred back-crossing. All this aside, it remains remarkable that both overexpression and deletion of GSK3B in mPFC produced significant effects on ethanol drinking, and in opposite (complementary) directions.

The mPFC is a component of the mesocorticolimbic reward pathway, receiving dopaminergic input from the ventral tegmental area (VTA) as well as thalamic-mediated input from other subcortical basal ganglia structures (Tzschentke, 2000). In turn, the mPFC projects efferents to the nucleus accumbens and back to the VTA (Sesack and Pickel, 1992). Given that GSK3B has been shown to be activated by dopamine signaling, particularly downstream of D2-receptor activation (Beaulieu *et al*, 2004), it could be asked if increasing prefrontal cortical GSK3B is effectively a means of amplifying the dopaminergic signal as it cycles through the mPFC along the reward pathway. That is, if certain actions of ethanol which produce increases in dopaminergic signaling through the mPFC are responsible for its induction of ethanol-seeking behavior, and increased GSK3B serves to somehow enhance these actions, ethanol-seeking behavior is in turn increased. Similarly, GSK3B deletion in the IL could effectively blunt any dopamine-dependent signal which traverses through the IL, based on the inability of D2 receptors in this region to activate GSK3B. A similar mechanism could also explain the suggested impairment in the novel object recognition task following GSK3B deletion in the IL (**Fig 5.13**), given the crucial

role of dopaminergic signaling in the IL, and mPFC generally, for working memory (Cassaday *et al*, 2014).

If this model accounts for the effects observed here, then selective means of increasing or deleting GSK3B in dopamine D2 receptor expressing neurons in the mPFC would be expected to show identical or very similar to the effects on drinking behavior as those observed here. As discussed in the introduction, mice with D2-receptor positive deletion of GSK3B show an attenuation of amphetamine-induced hyperlocomotion (Urs *et al*, 2012) but have not been tested for ethanol-related behaviors. Additionally, the mice described in Urs et al. express GSK3B deletion through all D2-positive neurons in the brain, without region specificity. Therefore these mice would only be expected to mimic the PFC-deletion mice insofar as GSK3B in other brain regions is not antagonistic to its role in the PFC.

Dopamine D2 receptors could identify an afferent pathway to the mPFC. Questions remain as to how the dopamine signal is translated intracellularly and how it is propagated to efferent projections. CAMKIIα (encoded by *Camk2a*) may provide at least a partial answer. CAMKIIα is a marker of pyramidal glutamatergic neurons, which make up the principle output of the mPFC (Warthen *et al*, 2016). CAMKIIα autophosphorylation has been found to contribute to ethanol-drinking behavior, as mice expressing CAMKIIα with a mutation in its autophosphorylation site show decreased initial ethanol preference and an absent locomotor-activating effect, compared to wild-type mice (Easton *et al*, 2013). Moreover these αCaMKIIT286A mice show no dopamine response in the nucleus

accumbens following acute or subchronic ethanol administration. It may be concluded that this protein plays a crucial part in the dopaminergic reward pathway via the functioning of glutamatergic projection neurons from the mPFC. Is it possible that active GSK3B normally serves to modulate the afferent signal of glutamatergic projections? There is only evidence of CAMKII-mediated phosphorylation of GSK3B (Song *et al*, 2010), not the reverse. We would speculate that feedback phosphorylation of GSK3B onto CAMKIIα is a possible means of regulation open to exploration. However, GSK3B could serve to modulate glutamatergic projections onto the reward circuit whether it is via CAMKIIα or some other downstream target which is also expressed in pyramidal projection neurons. It would be interesting to assess the ethanol-induced dopamine response in the NAC of mice with a Camk2a-neuron GSK3B deletion, as described by Easton et al. (2013) to determine whether GSK3B deletion exerts a similar effect to CAMKIIα autophosphorylation deficiency.

Altogether the data presented in this chapter make a compelling case that the high levels of ethanol drinking observed in C57BL/6J mice depend to some degree on intact cortical GSK3B function. Active GSK3B may contribute to the maintenance of ethanol reward-related behavior, such that its overexpression corresponds to sustained increases in consumption and preference, and its deletion corresponds to relatively low levels of ethanol self-administration. Notably we have identified a substantial role for GSK3B function specifically in Camk2a-positive, glutamatergic pyramidal neurons in mediating ethanol drinking behaviors.

Chapter 6

Potential Translational Application of GSK3B Inhibitors

6.1 Introduction

It is generally agreed that current treatments for Alcohol Use Disorder provide only modest efficacy (Batman and Miles, 2015; Franck and Jayaram-Lindstrom, 2013). While there are varied definitions of treatment efficacy, such as strict abstinence vs. avoidance of problem-drinking (Sanchez-Craig and Lei, 1986), all major AUD treatment studies have reported a treatment nonresponse rate of at least 30% (Naqvi and Morgenstern, 2015). It would seem a major portion of patients with AUD are lacking any effective therapy.

A better understanding of the neurobiology of alcohol's effects on the brain is what has allowed for the incremental progress in pharmacologic treatment options to date (Batman *et al*, 2015). Naltrexone and Acamprosate were developed into AUD treatments due to their targeting receptors in the ethanol-reward pathway—u-opioid receptors in the former case, NMDA-receptors in the latter—with the effect of blocking aspects of craving and withdrawal induced by ethanol's dysregulation of this circuitry (Franck *et al*, 2013). Based on the observations outlined in Chapters 4 and 5, we propose that GSK3B might itself

underlie aspects of ethanol's dysregulation of the mesocorticolimbic reward circuitry. Therefore specific GSK3B inhibitors represent a novel avenue of investigation for AUD treatment.

Thiadiazolidinones (TDZDs) were developed as the first non-ATP competitive GSK3B inhibitors (Martinez *et al*, 2002). Non-ATP competitive refers to the fact that TDZDs do not target the ATP-binding pocket, which is highly conserved across protein kinases (Garuti *et al*, 2010). TDZDs are instead thought to interact directly with the GSK3B enzymatic active site, possibly through covalent bonding with Cys-199 (Dominguez *et al*, 2012; Eldar-Finkelman and Martinez, 2011), and stabilization of the inhibitory phosphorylation of Ser-9 (Zhang *et al*, 2003).

One member of the TDZD family, TDZD-8, has been used extensively in the literature with findings relevant to neuropsychiatric dysfunction (Beaulieu *et al*, 2008; Storozheva *et al*, 2015; Yen *et al*, 2015). Beaulieu et al. (2008) found that TDZD-8 reversed behavioral deficits observed in *Tph2* knockin mice showing serotonin deficiency, without exerting significant effects on wild-type (WT) mice. Observed behavioral effects included reduction in immobility times in the tail suspension test and a decrease in anxiety-like behavior in the light-dark emergence test (to levels comparable with WT) (Beaulieu *et al*, 2008). While these *Tph2* mice have subsequently shown increased ethanol preference (Sachs *et al*, 2014), the effect of GSK3B inhibition has not been assessed in relation to this behavior.

Previous work by our laboratory demonstrated significant effects of TDZD-8 on ethanol-related behaviors. Angela Batman and Michael Scott Bowers tested multiple doses (1, 3, 10 mg/kg, i.p.) of TDZD-8 in operant responding experiments in Wistar rats (van der Vaart *et al*, 2018). The 3 mg/kg and 10 mg/kg doses decreased responding for ethanol as measured by active (ethanol-paired) lever presses. TDZD-8 was also found to inhibit sucrose responding as measured by sucrose-paired lever presses during the reinforcement period. However, following a 3-week abstinence period, both ethanol-trained and sucrose-trained rats were reintroduced to the operant chamber for a cue-induced reinstatement task. TDZD-8 (3 mg/kg) essentially abolished cue-induced responding in the ethanol trained animals while showing no significant effect on responding in the sucrose trained animals. Thus, in the context of cue-induced reinstatement, TDZD-8 showed ethanol-specific effects. This finding carries strong potential implications, given the relation between cue-induced reinstatement and relapse-like behavior (Vengeliene *et al*, 2006).

Intermittent ethanol access (IEA) also relies on repeated cycles of ethanol exposure and abstinence, and has been shown to increase consumption relative to continuous access (Rosenwasser *et al*, 2013). We have used the IEA model in experiments on the Phase II approved TDZD-family drug tideglusib (Lovestone *et al*, 2015). These experiments are described in the following chapter, beginning with a pilot study using the effective doses of TDZD-8 derived from the Batman studies (3, 10 mg/kg), and followed by oral tideglusib at 200 mg/kg, the gavage dose used in other pre-clinical studies of this drug (Bharathy *et al*, 2017; Sereno

et al, 2009) that have, for example, shown alterations of GSK3B-dependent tau protein phosphorylation. We set out with the hypothesis that tideglusib would decrease self-administration of ethanol, based on results described in Chapters 4-5, with corresponding alterations in synaptic function. Thus, we have also tested the effects of tideglusib (200 mg/kg) on phospho-PSD95-T19 and $GABA_A\alpha1$ expression. $GABA_A\alpha1$ expression was chosen as a proxy for measuring the effects of GSK3B on $GABA_AR$ trafficking (Tyagarajan *et al*, 2011).

Finally, as a human correlate to our studies of small molecule inhibitors in pre-clinical AUD treatment studies, we discuss here the employment of publicly available gene expression data from human alcoholic patients (McClintick *et al*, 2014) combined with the NIH Library of Integrated Network-Based Cellular Signatures (LINCS) Characteristic Direction Signature Search Engine (L1000CDS) (http://www.lincsproject.org/) and the integrated pathway enrichment tool *Enrichr* (http://amp.pharm.mssm.edu/Enrichr/) (Duan *et al*, 2014; Duan *et al*, 2016). The NIH LINCS consortium catalogs changes in gene expression across cell-lines occurring following a variety of perturbing agents, including small molecule inhibitors (Keenan *et al*, 2018). The L1000CDS allows for input gene expression data in the form of up- and down- regulated gene lists, and searches the database for perturbing agents which either mimic or reverse the input gene expression profile (Duan *et al*, 2014). We performed unbiased analyses using gene expression data from lymphoblastic cell lines (LDLs) from alcoholic vs non-alcoholic patients (McClintick *et al*, 2014) and the $L1000CDS^2$ under advisement from Dr. Matthew Reilly, who also provided the author with

generous support during the F grant application process. Dr. Reilly used McClintick et al. (2014) gene lists in queries of the initial LINCS database, and contacted us about GSK3A/B inhibitors as highly ranked candidates for “reversal” of the alcoholic gene expression signature. We subsequently queried the updated L1000CDS^2 (Duan *et al*, 2016) and found that kenpaullone, a GSK3B and cyclic-dependent kinase inhibitor, showed the highest reversal score in the database. At the time of this writing tideglusib has not been profiled in the LINCS.

6.2 Materials and Methods

Preparation of Solutions. In the pilot study using i.p. tideglusib, drug was suspended in a vehicle of 10% DMSO, 5% Tween-80 and 85% phosphate-buffered saline, to final volumes of 0.3 mg/ml and 1 mg/mL. In gavage studies, tideglusib was suspended in 26% peg-400, 15% Cremophor, and water, to 20 mg/mL. In both cases vials were placed in a sonicator heat bath (Branson) and heated to 40 degrees with sonication for 30-60 min. The formulations used for i.p. studies would show initial dissolution, but precipitated into uniform suspension after several minutes at room temperature. The formulation used for gavage was vortexed and large clumps of drug manually dispersed if necessary (using a spatula) before placement in the bath sonicator. Ethanol was prepared weekly to 20% v/v in tap water for use in IEA experiments.

Intermittent Ethanol Access (IEA). The IEA paradigm has been discussed previously (See **Figures 4.1 and 4.2**. The latter outlines the precise paradigm used in the gavage study on ethanol-drinking described here). Briefly, all animals

in ethanol-drinking studies received access to water during the entire course of the experiment. On Mondays, Wednesdays, and Fridays, at the beginning of the dark cycle, one ethanol tube was placed directly beside one water tube for a 24 hour access period. Placement sides were alternated to avoid side preference interactions. A recording of volume change on each tube was always made at the end of the 24 hour access period. During the tideglusib-gavage study, there were also 2-hour readings recorded.

Tideglusib Treatments. In the i.p. study, habituation to saline injections was begun after 4 weeks of ethanol consumption. Mice were injected with 10 mL/kg (0.01 mL/g) of saline as before each ethanol access for 5 ethanol access days, at which point ethanol-drinking volumes were confirmed as returning to near baseline. Beginning at week 6, mice (n=6-7/treatment group, all male) received either tideglusib (3, 10 mg/kg), vehicle, or saline. The saline group was included to assess for potential effects of the DMSO- and Tween-80- containing vehicle. I.p. injections were administered 30 minutes before each ethanol access period began, over 5 ethanol access days. One mouse had an adverse reaction to i.p. (vehicle), was euthanized, and all data was excluded from the experiment. Upon analyzing the data, one mouse was found to be an outlier based on average ethanol consumption over the first 4 weeks of the experiment (Grubbs test, $p<0.05$) and was removed from all analyses.

In the gavage study, habituation to gavage was begun after 3 weeks of IEA. Saccharin (0.2% w/v) was initially used to train the mice to accept the feeding tube. Gavage needles were stainless steel, 20 gauge animal feeding

needles (Cadence Science, Cranston, RI). After 3 days of saccharin gavage before each ethanol access period, vehicle was administered as pre-treatment for two ethanol access days. Tideglusib treatment began at the 6th week of IEA. Male and female mice (n=10/sex/treatment) all received tideglusib (200 mg/kg) or vehicle. Tideglusib was delivered as a 20 mg/mL solution at approximately 0.01 ml / g body weight. For example a mouse of 25.0 g (0.025 kg) would be gavaged 0.25 mL. Ethanol bottles were placed all mouse cages for the 30 min – 1 hr period after all mice were gavaged. One mouse (female, tideglusib) had an adverse reaction to gavage and was excluded from the experiment.

A separate cohort (n=7/treatment, all male) of C57BL/6J mice were treated with either tideglusib (200 mg/kg) or vehicle exactly as described above, but kept completely ethanol-naïve. Tideglusib treatments were administered on Mondays, Wednesdays, and Fridays for two weeks, to assess for the effect of repeated tideglusib treatment by itself on phospho-protein levels in PFC. These mice were harvested over a 2 hour period, beginning 2 hours after the last tideglusib gavage on the sixth treatment day (end of week 2).

Tissue Collection. Mice were sacrificed by cervical dislocation and decapitation. Brains were extracted and submerged in PBS on ice for 1 minute. Brains were then rapidly dissected into regions of interest including the medial PFC as a wedge surrounding the sagittal fissure, after having made vertical coronal cuts just rostral to the optic chiasm and just caudal to the frontal poles (Kerns *et al*, 2005a). The PFC and other regions were immediately frozen on liquid nitrogen and subsequently stored at -80° C until further studied.

Western Blotting. Tissue was homogenized on ice by suspension RIPA buffer, made up of 50 mM Tris, 150 nM NaCl, 1% NP40, 5 mM EDTA, and 0.5% sodium deoxycholate in distilled H_2O, with 1X Halt protease and phosphatase inhibitor cocktail (Thermo Fisher, Waltham, MA) added immediately before homogenization on ice with probe sonication. Total protein concentration for all samples was determined using a Pierce BCA Protein Assay Kit (Thermo), to allow for equal protein loading. Immunoblotting was performed using an Xcell Surelock Mini-Cell kit (Thermo). Tissue homogenates were denatured with NuPage LDS Sample buffer and Sample Reducing Agent (Thermo) and heated at 70° C for 10 minutes. Samples were separated via electrophoresis at 180 V for X hours on precast NuPage 4%-12% Bis-Tris 1 mm 17-well gels (Thermo) at room temperature, followed by transfer onto PVDF membrane at 12 V, at 4° C. Membranes were blocked with bovine serum albumin (5%). They were then incubated overnight at 4° C in primary antibody: 1:500 rabbit anti phospho-PSD-95-T19 (Abcam ab16496, Cambridge, MA), 1:1000 rabbit $GABA_A\alpha1$ (Synaptic Systems cat# 224 203, Goettingen, Germany), or 1:1000 rabbit p-GSK3B (Cell Signaling cat# 5558, Danvers, MA). Following incubation membranes were washed extensively in TBS-T and incubated in 1:15000 (in 1% BSA in TBS-T) Amersham ECL donkey anti-rabbit IgG, HRP-linked antibody (GE Healthcare, Chicago, IL) for 1 hour at room temperature. Membranes were again washed in TBS-T. Membranes were incubated in ECL Prime (GE Healthcare) for 5 minutes before being exposed to GeneMate Blue Ultra Autorad film (BioExpress, Kayville, UT). Multiple exposure were obtained to insure linearity of the response. Blots

were stripped using Restore Stripping Buffer (Thermo) before re-staining for total proteins using 1:1000 rabbit anti-PSD95 (Thermo cat# 51-6900), 1:2000 total GSK3B (Cell Signaling cat# 9315), and 1:10000 mouse anti-B-actin (Sigma-Aldrich cat# A5316, St. Louis, MO). Subsequent steps were repeated exactly as before except in the case of the B-actin stained membrane, which being a mouse antibody required the HRP-linked secondary antibody Amersham ECL sheep anti-mouse IgG (GE Healthcare). All films were scanned using a flatbed scanner and analyzed using densitometric analysis with ImageJ (NIH).

Ethanol Metabolism. Male C57BL/6J mice (n=25) were treated with 200 mg/kg tideglusib or vehicle and 30 minutes later injected with 2.0 g/kg ethanol, and blood was collected via submandibular cheek punch at 10, 30, 60, and 90 minute time points (n=3-4/treatment/time). Blood was collected in BD microtainer tubes containing EDTA (Fisher Scientific, Waltham, MA) to prevent clotting and stored at -20 degrees Celsius until analysis. Blood Ethanol Concentrations assessed in this Chapter were obtained by Justin Poklis and the VCU Analytics Core using headspace gas chromatography (O'Neal *et al*, 1996).

NIH LINCS Analysis of Alcoholic Patient Cellular Signatures. McClintick et al. (2014) collected and cultured lymphoblastoid cell lines (LCLs) derived from peripheral blood mononucleocytes of alcoholic patients and controls (n=21/group). Cultured cell lines were assessed for differentially regulated genes by subsequent microarray profiling (McClintick *et al*, 2014). Ninety-nine percent of differentially regulated genes were also found to be expressed in brain. The authors generated lists of up- and down-regulated genes and annotated those

which were also previously identified in expression studies in post-mortem brain samples of alcoholic patients (McClintick *et al*. 2014, Supplementary Table 2). We filtered the table for all genes with at least one annotation to create "master-lists" of externally validated genes, which were used as our input lists of up- and down-regulated genes in L1000CDS^2 (http://www.lincsproject.org/). The L1000CDS^2 is a search engine which treats the input as a gene expression signature, and then searches the LINCS database for signatures which reverse the input signature. To identify signaling pathways overrepresented in our input data, we ran the Enrichr tool (http://amp.pharm.mssm.edu/Enrichr/) on our input gene lists . PubChem (https://pubchem.ncbi.nlm.nih.gov/) was used to identify targets of output compounds.

6.3 Results

Tideglusib (i.p.) decreases ethanol consumption from baseline. Male C57BL/6J mice (n=6-7/treatment group) were given 4 weeks of IEA before habituation to saline injections was begun. Baseline consumption was calculated as the mean consumption over the 3 weeks before saline habituation (Fig 6.1A, "Baseline"). During saline habituation, ethanol consumption dropped but returned to baseline levels or above after more than a week (data not shown). Animals were then pre-treated with either saline, vehicle, or tideglusib (3 mg/kg or 10 mg/kg) before each ethanol access period for 5 ethanol access days. Mean consumption and preference values are shown in **Figure 6.1A-B**. To assess the effect of tideglusib during the treatment period as well as relative to baseline

consumption for each group, we used a two-way RM ANOVA to test the effects of “group assignment” and “treatment period.” The effect of tideglusib is therefore the measured as the interaction between group assignment and treatment period. The effect of i.p. injection by itself regardless of treatment type is assessed by “treatment period”. Groups were assigned randomly and thus there would be no expected effect of “group assignment” during baseline. Two-way RM ANOVA of ethanol consumption (**Fig. 6.1A**) revealed a significant effect of the interaction ($F_{3,21}$=7.67, p=0.0012), as well as treatment period ($F_{1,21}$=7.07, p=0.014). There was no effect of group assignment ($F_{3,21}$=0.082, p=0.97). By Sidak’s post hoc test, there was a significant effect of the 10 mg/kg tideglusib dose during treatment compared to baseline (p<0.001). Two-way RM ANOVA on mean ethanol preference (**Fig. 6.1B**) did not find a significant effect of treatment period ($F_{1,21}$=2.90, p=0.10), group assignment ($F_{3,21}$=0.41, p=0.74), or the interaction ($F_{3,21}$=2.24, p=0.11). Because of the observed variation in mean ethanol consumption during baseline (no-treatment) drinking, we calculated mean %change from baseline consumption values for each mouse and took the means of these by group (**Fig. 6.1C**). One-way ANOVA of mean %change from baseline found a highly significant effect of treatment ($F_{3,21}$=10.12, p=0.0003). Sidak’s multiple comparisons test found significant differences between the 3 mg/kg dose and vehicle (p<0.05) and the 10 mg/kg dose and vehicle (p<0.001).

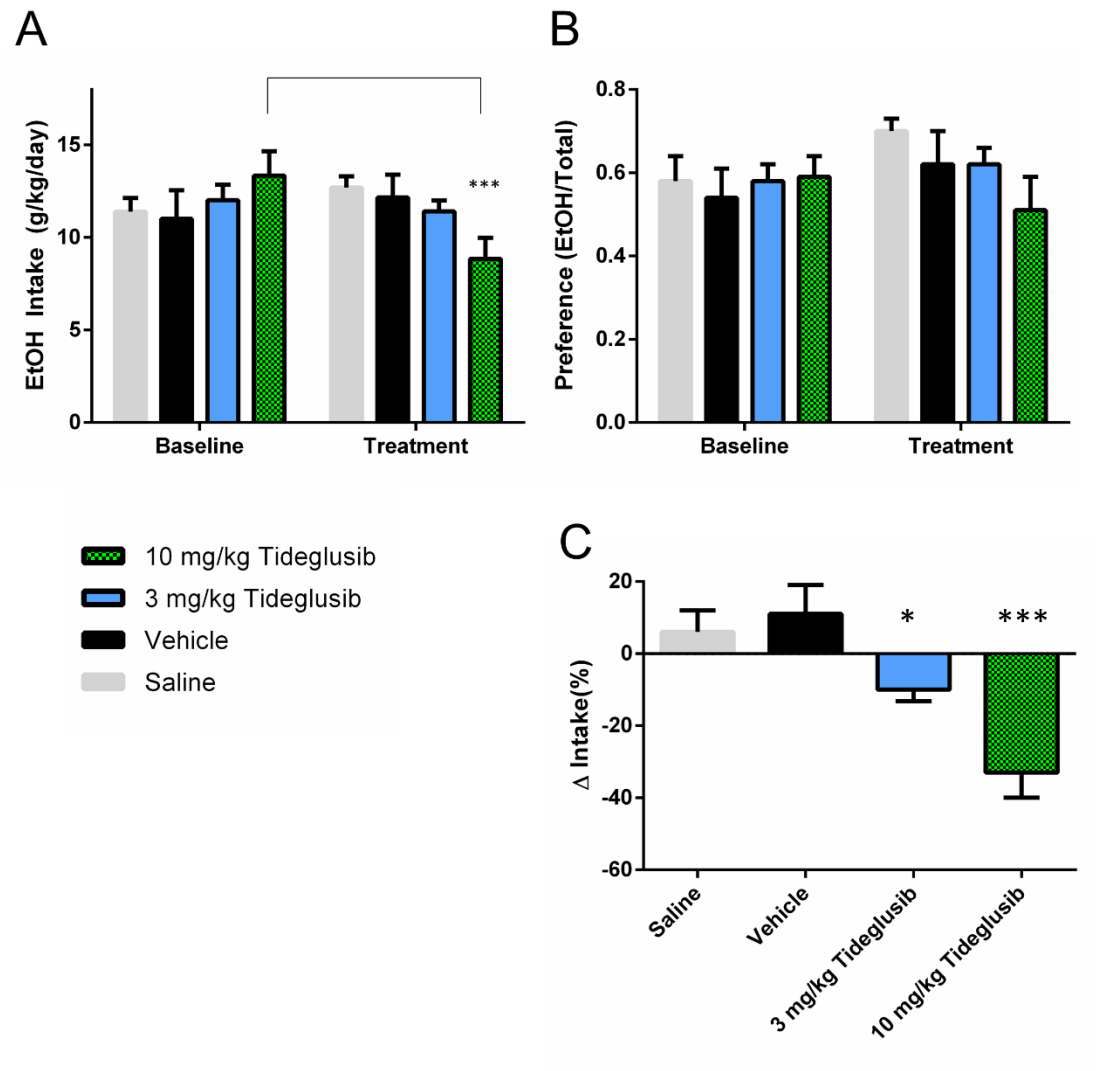

Figure 6.1 Results of i.p. tideglusib during the 6th week of IEA. (n=6-7/group). Baseline is average daily ethanol intake for the 3 weeks prior to the habituation period. Treatment is mean ethanol intake over 5 days of i.p. tideglusib pre-treatment. **A.** Two-way RM ANOVA on mean consumption finds significant effect on the interaction of "group assignment" and "treatment period" ($p<0.005$). Sidak's post hoc test finds that 10 mg/kg tideglusib significantly decreases consumption relative to baseline (***$p<0.001$). **B.** Two-way RM ANOVA on mean preference finds no significant effect of group assignment, treatment period, or the interaction. **C.** One-way ANOVA of % change from baseline finds significant effect of treatment ($p<0.001$). Sidak's post hoc tests find that the 3 mg/kg dose and 10 mg/kg dose both differ significantly from vehicle (*$p<0.05$, ***$p<0.001$).

Daily consumption and preference show altered trends during gavage treatment. Because of potential confounds from insolubility of tideglusib powder in an i.p. suspension as well as increased preclinical applicability of an oral drug delivery, we used gavage as an alternative administration approach. For this oral tideglusib experiment, mice (n=9-10/sex/treatment) were given a 3-week baseline consumption period, and subsequently gavaged with saccharin (0.2% w/v) for 3 days and vehicle (26% peg-400, 15% cremophor) for 2 days subsequently. Ethanol bottles were placed on cages immediately upon the start of the dark cycle (Mondays, Wednesdays, and Fridays). Through the course of the experiment, ethanol (20% v/v) and water intake were recorded 2 hours into the ethanol access period using a red lamp, and again at 24 hours after access (the end of the following light cycle).

Consumption and preference values at the 2-hour, “binge,” time point are plotted in **Figure 6.2**., and the 24-hour daily consumption and preference values are plotted in **Figure 6.3**. Across all measures it can be observed that at the beginning of each gavage (saccharin on day 10, vehicle on day 13) there is a trend of decreased ethanol intake for all animals. By the second day of each gavage these values generally restore to within the range previously observed. However it can be seen from the binge preference data (**Fig. 6.2C-D**) that there is an overall decrease in ethanol preference beginning with vehicle habituation through the remaining course of the experiment. Because this effect is much more pronounced in the preference data than the ethanol consumption data (**Fig 6.2A-B**), it could be inferred that increased water consumption following vehicle

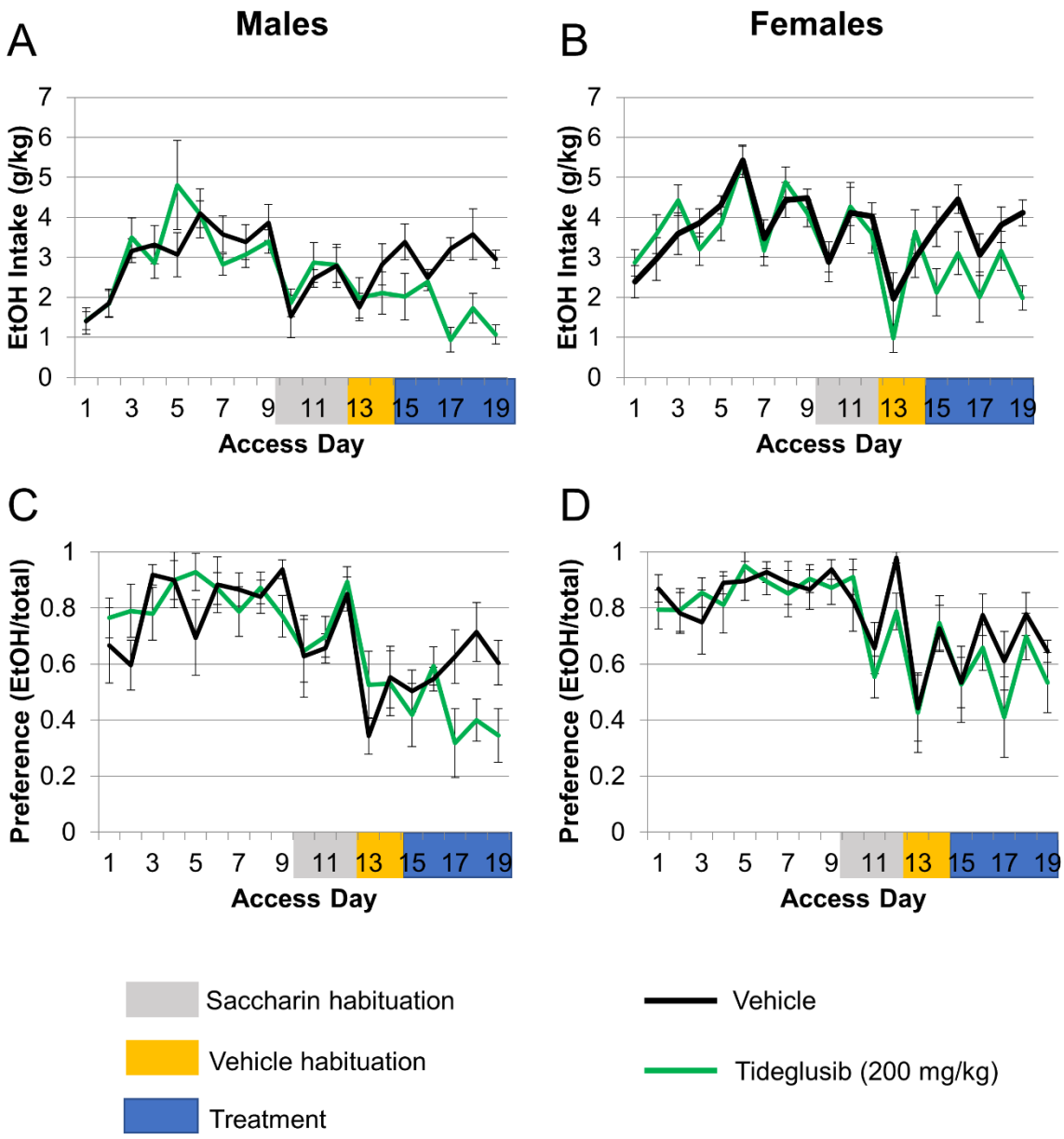

Figure 6.2 Daily consumption and preference during the 2-hour binge (gavage study). Mice (n=9-10/treatment/sex) were monitored over 19 ethanol access days. Mice assigned to the Vehicle group are in black, the Tideglusib group in green. Color coding on X-axis is also given in key. Treatment period is Access Days 15-19. **A.** Ethanol intake (g/kg) in male mice. **B.** Ethanol intake (g/kg) in female mice. **C.** Ethanol preference (mL ethanol / mL total fluid) in male mice. **D.** Ethanol preference (mL ethanol / mL total fluid) in female mice.

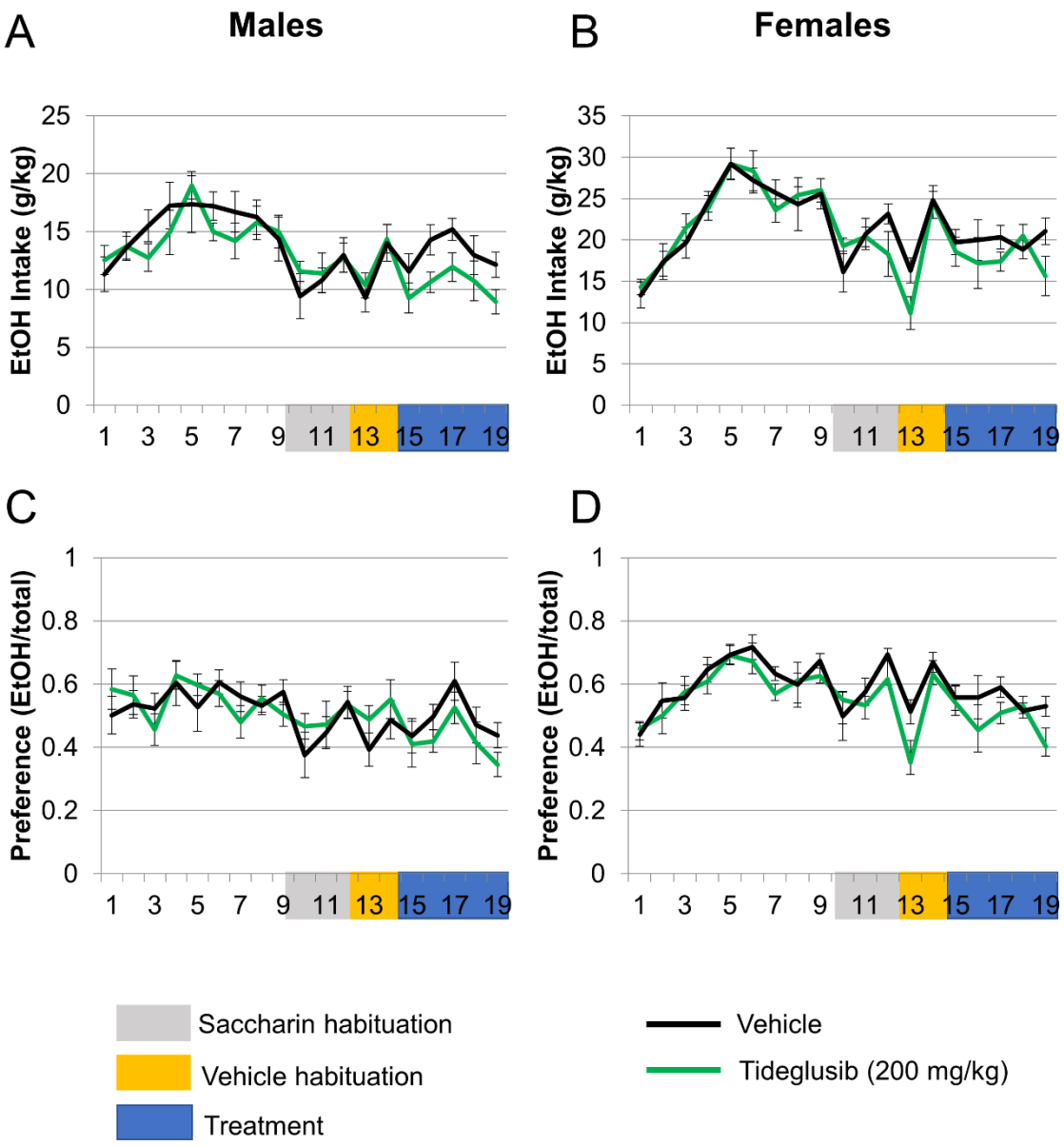

Figure 6.3 Daily consumption and preference during 24-hour access (gavage study). Mice (n=9-10/treatment/sex) were monitored over 19 ethanol access days. Mice assigned to the Vehicle group are in black, the Tideglusib gavage group in green. Color coding on X-axis is also given in key. Treatment period is Access Days 15-19. **A.** Ethanol intake (g/kg) in male mice. **B.** Ethanol intake (g/kg) in female mice. **C.** Ethanol preference (mL ethanol / mL total fluid) in male mice. **D.** Ethanol preference (mL ethanol / mL total fluid) in female mice.

pre-treatment may be driving this effect (see **Figure 6.4**, discussed in following section).

Groups had been assigned to minimize potential chance group differences based on rank order of ethanol consumption (24-hour) during baseline drinking (first 3 weeks of experiment). During the gavage habituation period, group members were selectively re-assigned in an attempt to minimize group differences both during baseline and during subsequent gavage habituation, so that groups were roughly equivalent on as many measures as possible when tideglusib vs. vehicle treatment began.

Oral tideglusib markedly decreases binge-like ethanol consumption. Analyses were performed using a two-way RM ANOVAs to determine the effects of group assignment, treatment period, and the [group assignment * treatment period] interaction. The last of these effects is the variable of interest: the effect of tideglusib (200 mg/kg by gavage) during the treatment period. A main effect of treatment period indicates the effect of oral gavage by itself relative to baseline, regardless of treatment.

All results from the 2-hour binge period are displayed in **Figure 6.4**. In male mice, 2-hour binge consumption (**Fig. 6.4A**) showed significant effects from the interaction ($F_{1,18}$=15.71, p=0.0009), treatment period ($F_{1,18}$=14.05, p=0.0015), and group assignment ($F_{1,18}$=11.03, p=0.0038). Sidak's post hoc revealed no effect of tideglusib group assignment during baseline (p=0.99) and a highly significant effect of tideglusib during the treatment period (p<0.0001). In female mice, 2-hour binge consumption (**Fig. 6.4B**) showed significant effects from the

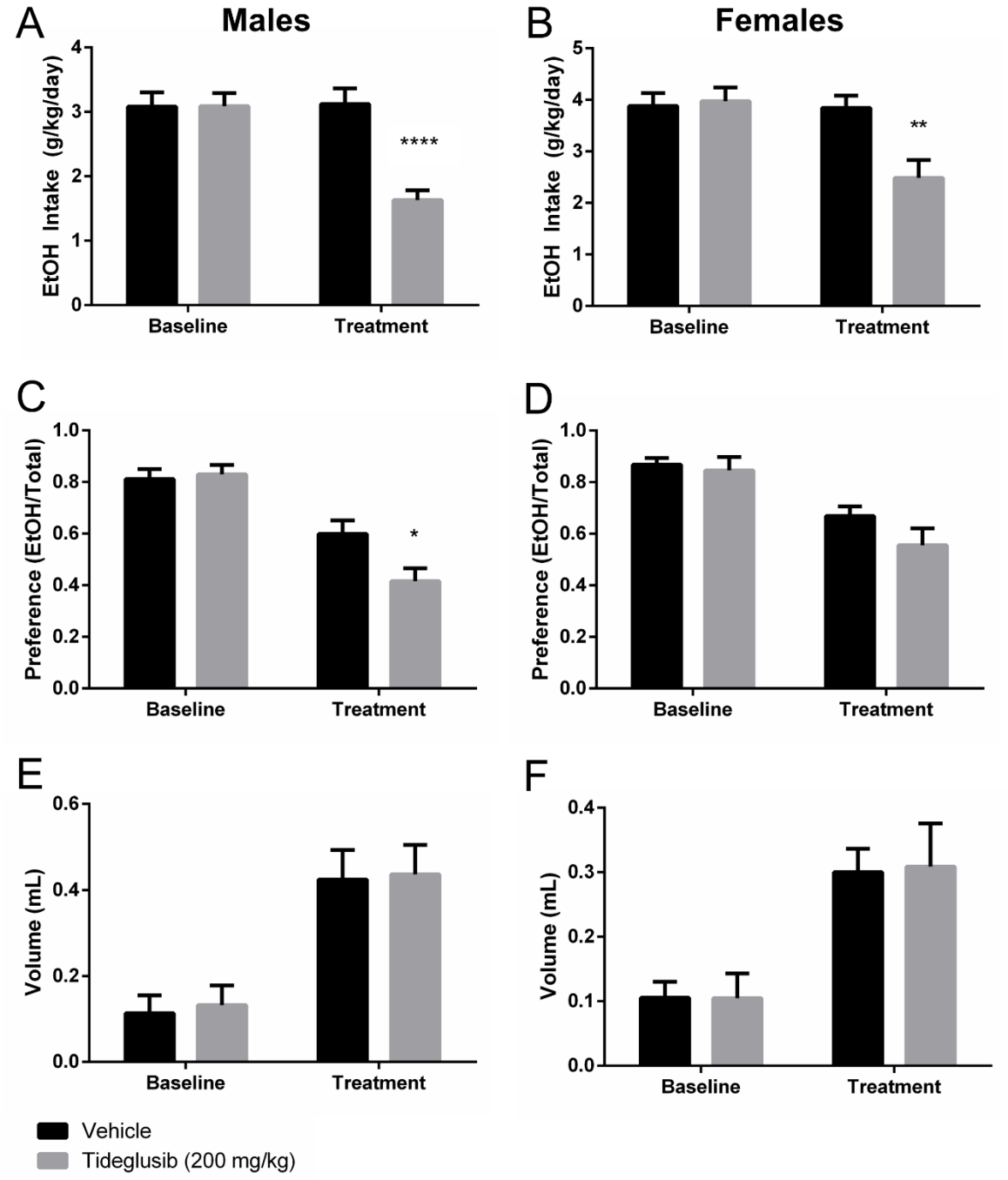

Figure 6.4 Tideglusib (200 mg/kg) decreases mean binge ethanol consumption. Mean binge (2 h) consumption and preference (n=9-10/treatment/sex) during baseline (3 weeks of IEA prior to gavage habituation) and treatment (5 days of pre-treatment with tideglusib before each access period). **A.** Tideglusib attenuates binge consumption (g/kg/day) in male mice. There was a significant effect ($p<0.01$) of "group assignment * treatment period" by 2-way RM ANOVA. Tideglusib group assignment showed no effect during baseline consumption and a significant effect during the treatment period

(****p<0.0001). **B.** Tideglusib attenuates binge consumption (g/kg/day) in female mice. There was a significant effect (p<0.01) of “group assignment * treatment period” by 2-way RM ANOVA. Tideglusib group assignment showed no effect during baseline consumption and a significant effect during the treatment period (**p<0.01). **C.** Tideglusib attenuates ethanol preference (mL ethanol / mL total fluid) during the binge period in male mice. There was a significant effect (p<0.05) of “group assignment * treatment period” by 2-way RM ANOVA. Tideglusib group assignment showed no effect during baseline consumption and a significant effect during the treatment period (*p<0.05). **D.** Tideglusib does not alter significantly alter ethanol preference during the binge period in female mice. The effect of treatment period (gavage itself) was highly significant (p<0.0001) but the interaction with tideglusib was not significant (p=0.28). **E-F.** Significant increases in water consumption during the binge period after gavage pre-treatment. Males (E) show significant effect of treatment period (p<0.0001) but no interaction with group assignment (p=0.95). Females (F) also show significant effect of treatment period (p<0.0001) but no interaction with group assignment (p=0.90).

interaction ($F_{1,17}$=9.58, p=0.0066) and treatment period ($F_{1,17}$=10.61, p=0.0046), and non-significant effect of group assignment ($F_{1,17}$=4.13, p=0.058). Sidak's post hoc revealed no effect of tideglusib group assignment during baseline (p=0.97) and a significant effect of tideglusib during the treatment period (p=0.0027).

In male mice, 2-hour binge preference (**Fig. 6.4C**) showed significant effects from the interaction ($F_{1,18}$=6.60, p=0.019), treatment period ($F_{1,18}$=63.56, p<0.0001), and no effect of group assignment ($F_{1,18}$=2.77, p=0.11). Sidak's post hoc revealed no effect of tideglusib group assignment during baseline (p=0.99) and a significant effect of tideglusib during the treatment period (p=0.012). In female mice, 2-hour binge preference (**Fig. 6.4B**) showed a highly significant effect of treatment period ($F_{1,17}$=27.64 p<0.0001), but no significant effects of group assignment ($F_{1,17}$=2.14, p=0.15), or interaction ($F_{1,34}$=11.44, p=0.337). Thus in both cases the pre-treatment with gavage, regardless of whether it contained tideglusib or vehicle, altered ethanol preference markedly compared to baseline. During baseline treatment, ethanol preference approached 1.0, indicating no water intake in the first 2 hours after ethanol access. However pre-treatment with gavage seemed to induce significant water intake during the binge period. Indeed volume of water consumed during the binge period is plotted in **Figure 6.4E-F**, and shows significant effects of treatment period in males ($F_{1,18}$=33.83, p<0.0001) and females ($F_{1,17}$=27.34, p<0.0001). Importantly, in neither group was there an effect of tideglusib on water consumption. Males showed no effect of group assignment ($F_{1,18}$=0.062, p=0.81) or the interaction of group assignment * treatment period ($F_{1,18}$=0.0042, p=0.95). Females similarly

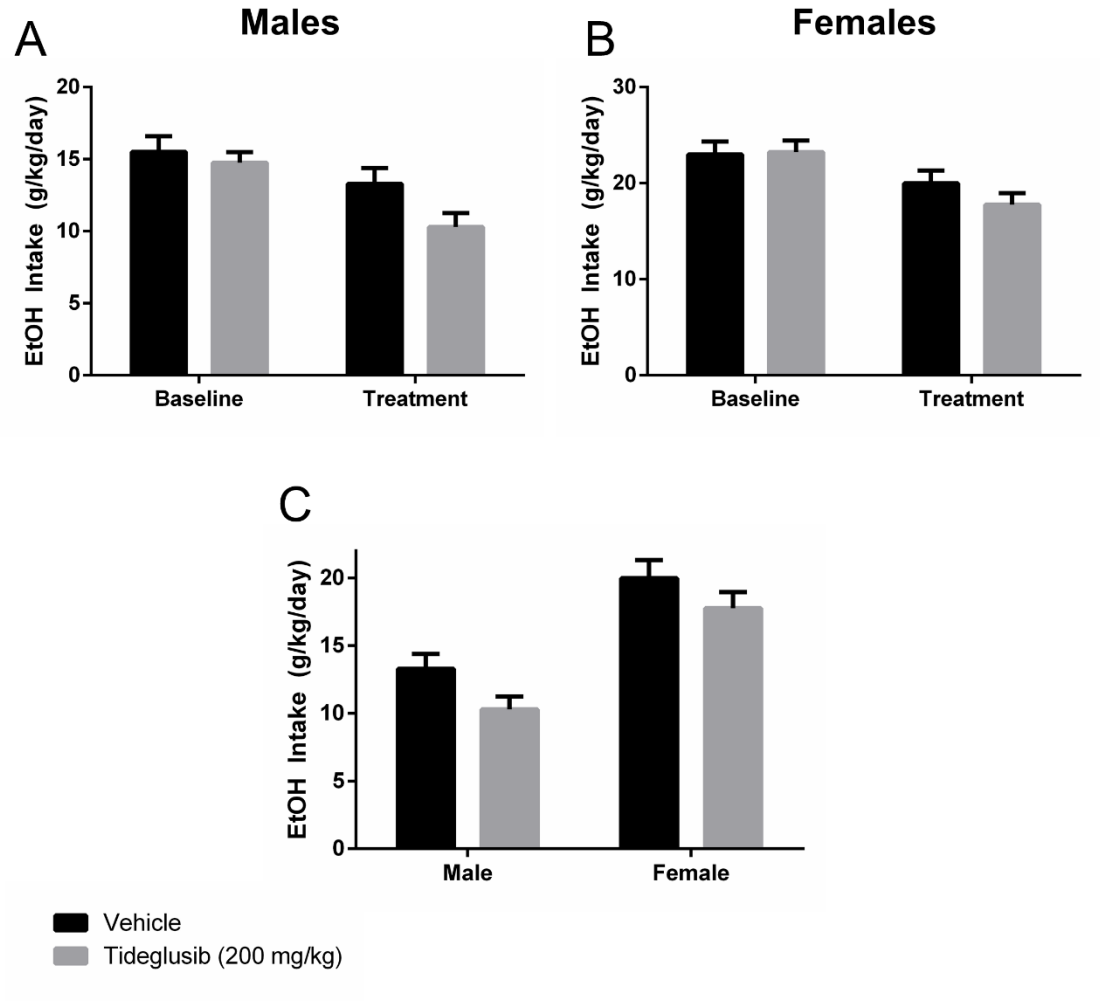

Figure 6.5 Effects of tideglusib (200 g/kg) on mean daily ethanol consumption. **A.** In male mice there was a significant effect of treatment period (gavage itself, $p<0.001$), but no significant effects of group assignment or the interaction. **B.** In female mice there was also a significant effect of treatment period ($p<0.001$) but no significant effect of group assignment or the interaction. **C.** When males and females were collapsed and assessed by 2-way ANOVA of sex and treatment (within the treatment period only), both sex ($p<0.0001$) and tideglusib treatment ($p<0.05$) were significant effects. Fishers post hoc test found a suggestive effect of tideglusib in male mice ($p<0.1$) but not within female mice.

showed no effect of group assignment ($F_{1,17}$=0.0075, p=0.93) or the interaction ($F_{1,17}$=0.016, p=0.90). Thus either the act of gavage or the vehicle used to administer the drug induced significant water intake in the 2-hour period after ethanol access, but this effect was unrelated to tideglusib.

Oral tideglusib slightly decreases 24 hour ethanol consumption. From **Figures 6.2-6.4** it can be seen that there is a less pronounced effect of tideglusib gavage on ethanol consumption measured at the end of each 24 hour access period compared to the effect in the 2 hour binge period. We first analyzed 24 hour binge consumption using the same two-way RM ANOVA design described above. Results are displayed in Figure **6.5A-B**. In male mice, there was a significant effect of treatment period ($F_{1,18}$=20.34, p=0.0003) and no significant effects of group assignment ($F_{1,18}$=2.55, p=0.13) or the interaction ($F_{1,18}$=2.28, p=0.15). In female mice there was also a significant effect of treatment period ($F_{1,17}$=22.56, p=0.0002) and no significant effects of group assignment ($F_{1,17}$=0.39, p=0.54) or the interaction ($F_{1,17}$=1.91, p=0.18). As both females and males showed a decrease in mean ethanol consumption during the treatment period, and the animals were run concurrently, we collapsed across sexes to increase our power for detecting the effect of tideglusib (**Fig. 6.5C**). We performed a two-way ANOVA to test sex and treatment within the treatment period. This analysis showed a highly significant effect of sex (F1,35=37.74, p<0.0001) and a significant effect of treatment (F1,35=5.12, p=0.030). Post hoc testing using Fisher's LSD found a suggestive effect in males (p=0.072) and no

significant effect in females (p=0.19). Overall there was an effect of treatment across all sexes (n=19-20/group) but this did not reach significance within sex.

Tideglusib (200 mg/kg) does not alter ethanol metabolism. To assess whether the gavaged dose of tideglusib described above may alter ethanol metabolism in the two hours following treatment, we took blood a separate set of ethanol-treated animals +/- tideglusib pre-treatment. Tideglusib was delivered via gavage and mice (n=12-14/treatment) were injected with ethanol (2 g/kg, i.p.) 30 minutes afterward. Blood was collected at four time points (n=3-4/treatment/time point) and assessed for ethanol content via gas chromatography. Results are plotted in **Figure 6.6**. 2-way ANOVA found a significant effect of time ($F_{3.18}$=13.02, p<0.0001) and no significant effect of treatment ($F_{1,18}$=0.027, p=0.87) or treatment*time interaction ($F_{3,18}$=0.31, p=0.82). Thus there was no evidence that tideglusib altered the pharmacokinetics of ethanol.

Tideglusib (200 mg/kg) decreases GSK3B-mediated PSD95 phosphorylation in PFC. Response of GSK3B target PSD95 to repeated tideglusib (200 mg/kg) treatment in ethanol-naïve animals (n=6-7/treatment) was assessed via Western blotting of microdissected PFC. Results are shown in **Figure 6.7**. Unpaired t-tests were used to measure all quantified densitometric ratios. In the case of p-PSD95-T19, a one-tailed t-test was used to test whether tideglusib effectively inhibited GSK3B activity at this phospho-residue. Other phospho-proteins and total proteins were assessed using two-tailed t-tests to

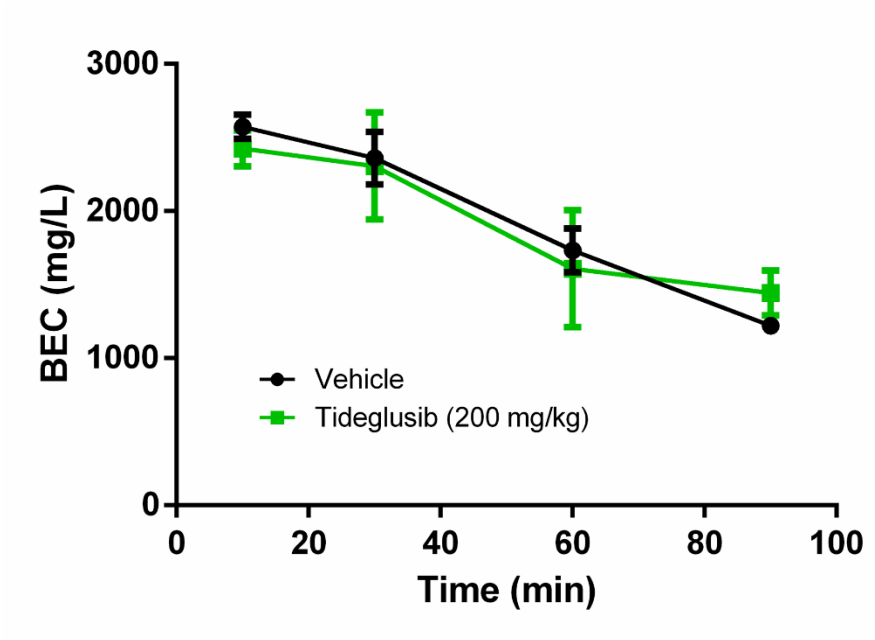

Figure 6.6 Tidegusib (200 mg/kg) does not affect ethanol metabolism. 2-way ANOVA found a significant effect of time ($p<0.0001$) and no significant effect of treatment ($p=0.87$) or treatment*time interaction ($p=0.82$).

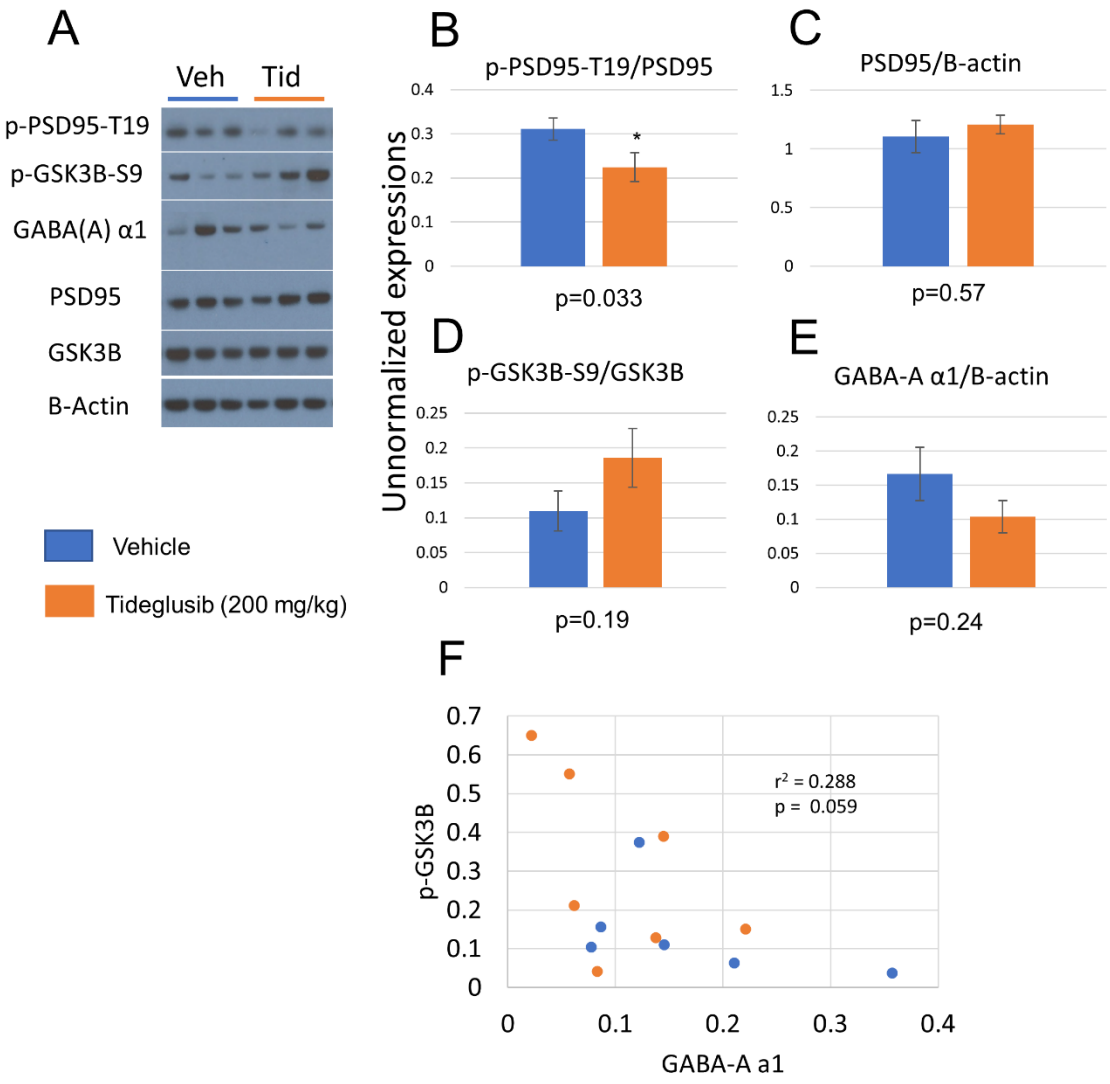

Figure 6.7 Repeated tideglusib decreases PSD95 phosphorylation. A. Representative films of Western blots of PFC following repeated Tideglusib (200 mg/kg) or vehicle treatment (n=6-7/treatment, males). **B.-E.** Relative ratios of p-PSD95-T19, total PSD95, p-GSK3B-S9, and total GABA(A) α1 based on unnormalized densitometric values. Results of t-tests are given below each graph. **F.** Linear regression of p-GSK3B-S9 expression against GABA(A) α1 shows suggestive inverse trend. Throughout figure Tideglusib treatment is in orange, vehicle in blue.

determine the potential effect and direction of the drug on their expression. Phospho-PSD95-T19 was found to be significantly decreased (p=0.033), while tideglusib did not show significant effects on p-GSK3B-S9/total (p=0.19), total PSD95 (p=0.57), or total $GABA_A\alpha1$ (p=0.24). However an interesting inverse relationship could be observed between band intensity of p-GSK3B-S9 and that of $GABA_A\alpha1$. When this relationship was plotted (**Fig. 6.7F**) I,t was found to have a suggestive inverse linear relationship by regression (p=0.059). These findings hint at the regulation of CNS excitatory/inhibitory balance by GSK3B via synaptic proteins, with tideglusib significantly altering PSD95 regulation via phospho-T19.

Interrogation of the NIH LINCS predicts reversal of alcoholic gene expression by the GSK3B inhibitor kenpaullone. Output from the L1000CDS^2 is shown in **Figure 6.8**. Gene lists obtained from McClintick et al. (2014) are shown at the left of the figure. Along the top are the highest ranked small molecule inhibitors in the LINCS database at the time of query. Ranking was according to the predicted “reverse” signature of the inhibitors, i.e. a significant effect on gene expression in the opposite direction across the multiple (human) cell lines used in the LINCS. The top two inhibitors, radicicol and kenpaullone, show the same degree of overlap (indicated by height of bars atop **Fig. 6.8**). The top-ranked small molecules and their targets are listed in **Table 6.1.**

Enriched pathways based on the up- and down- regulated gene lists were also predicted by the program Enrichr as part of the L1000CDS^2 query. The top pathway among genes increased in alcohol LCL lines was related to nerve

Table 6.1. **Top ranked small molecule inhibitors according to the L1000CDS^2 and their targets** (IC50s reported by PubChem)

Experimental Molecule	Targets
radicicol	**Hsp90** (K_d=0.0027uM)
Kenpaullone	**GSK3β** (IC50=0.023uM), **CDK-1** (IC50=0.035uM)
geldanamycin	**Hsp90-alpa** (IC50=0.02uM), **Hsp90-beta** (IC50=0.022uM)
598226	**TDP1** (IC50=4.11uM)
T8902	**TDP1** (IC50=4.11uM)
BRD-A68065211	**GSTO** (IC50=0.038uM), **SRC3** (IC50=0.503uM), **TDP1** (IC50=2.06uM)
Chemistry 2804	**VDR** (IC50=1.99 uM), **ROR gamma** (IC50=3.54uM)
17757146	**PDE4** (IC50=0.0067uM), **PDE10** (IC50=0.823uM)

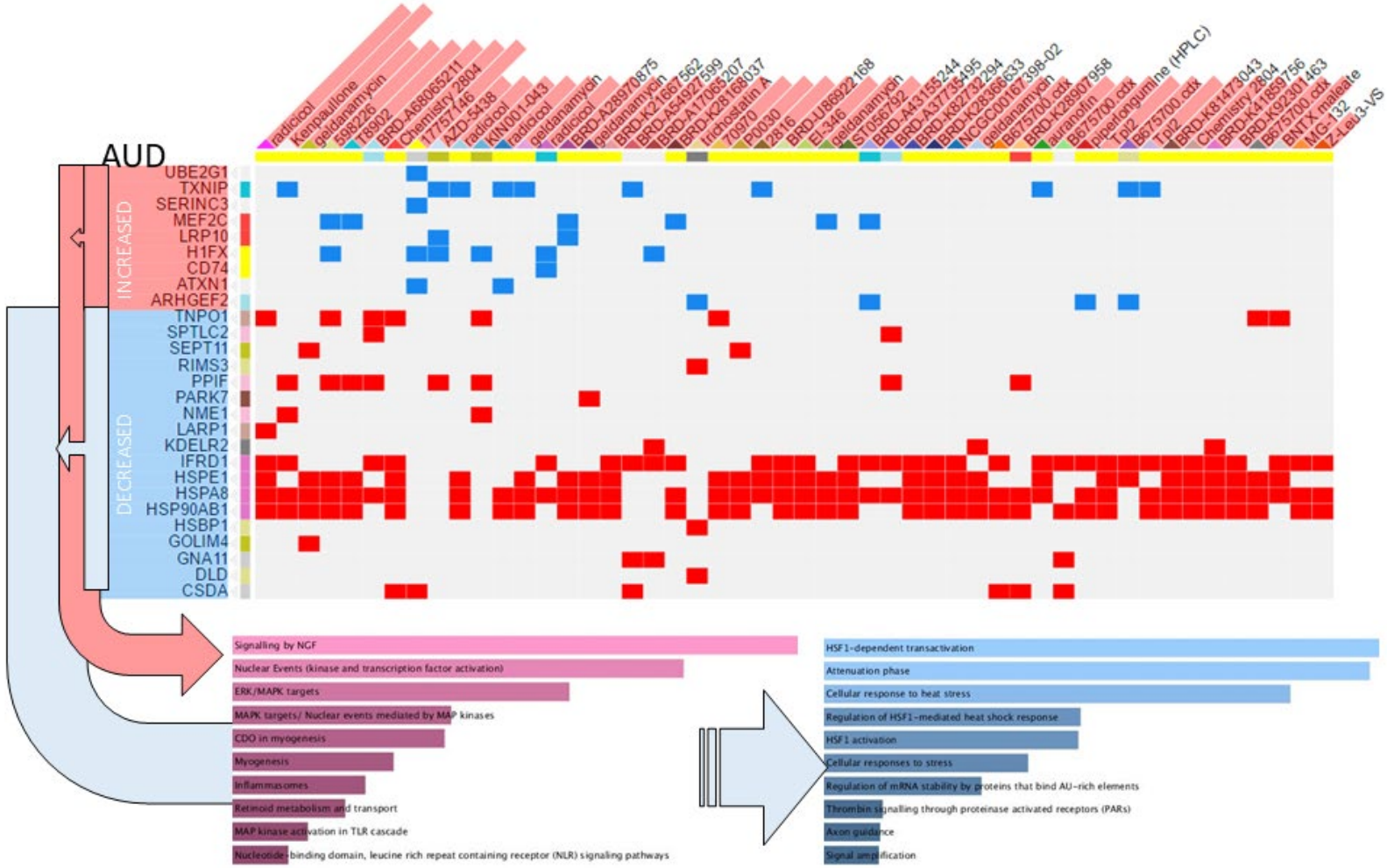

Figure 6.8 Small molecule inhibitors identified by L1000CDS, based on alcoholic LDL gene expression signature. Genes shown along the left of the figure are genes up- or down- regulated in LCLs cultured from human alcoholic patients compared to controls. Along the top of the figure are small molecule inhibitors or other perturbing agents which show a reverse effect on expression of the genes at left. At bottom of the figure are results from the enrichment program “Enrichr,” which was simultaneously performed on the up- (pink) and down- (blue) regulated gene lists. Upregulated genes in alcoholic LCL samples are enriched for nerve growth factor (NGF) signaling. Downregulated genes are enriched for involvement in heat shock and cellular stress pathways.

growth factor (NGF) signaling, while pathways enriched for the downregulated genes were largely related to heat shock and cellular stress. It may be that alcoholism is associated with an impairment in response to heat shock and stress and that overall the inhibitors ranked by this tool are predicted to restore the expression of genes related to this pathway (e.g. *HSPE1*, *HSPA8*, *HSP90AB1*).

6.4 Discussion

Here we have described the use of an FDA Phase II approved GSK3B inhibitor, tideglusib, as an intervention in a mouse model of excessive alcohol intake. When tideglusib was administered i.p., both the 3 and 10 mg/kg doses significantly attenuated daily ethanol consumption in terms of %change from baseline. When tideglusib was administered by gavage (200 mg/kg) it profoundly decreased ethanol consumption during a 2 hour binge-like ethanol drinking period, in both male and female mice. This gavaged dose was not found to alter the metabolic profile of ethanol. It was found to significantly decrease PSD95 phosphorylation in the PFC and to show a suggestive inverse relationship with total $GABA_A\alpha1$ protein levels.

6.4.1 Limitations/Alternatives

By the end gavage treatment period, 2 male and 2 female tideglusib treated, ethanol drinking mice had become evidently ill, based on poor grooming/feeding/locomotor activity. Such adverse outcomes may have been due to poor feeding due to esophageal/gastric irritation, fluid aspiration into the

lungs from gavage, or tideglusib specific effects such as liver toxicity. Overall there were 28 vehicle and 28 tideglusib-treated mice as part of this study, 20 of each of which were receiving ethanol access. We collected liver samples from all mice for the purposes of assessing potential liver toxicity of tideglusib +/- ethanol; analyses are being performed by a collaborator and results are pending. An additional caveat is that for the last 3 days of the experiment (which included 1 ethanol-drinking day) all mice were habituated to daily saline injections as outlined in **Figure 4.2**, so that by the day of harvest we could test for acute ethanol challenge in these animals (**Figures 4.16** and **4.17**) without the injection itself being a novel intervention. However, the amount of interventions occurring simultaneously at this study's end may have increased the risk of potential confounds overall. It should be noted that other preclinical studies have reported daily tideglusib (200 mg/kg) by gavage for up to 3 months with no significant effects on survival (Sereno *et al*, 2009).

In this study, significant effects of the treatment period (i.e. any gavage vs. baseline, see **Figures 6.4-6.5**) on mean ethanol intake also reflect the overall difficulties in using gavage delivery to study a behavior that relies on the esophagus. Gavage administration irrespective of treatment interfered with ethanol drinking behaviors, particularly in regards ethanol preference by inducing water drinking in the hours after gavage was administered. This is in contrast to the i.p. study, wherein control (vehicle and saline groups) actually showed relative non-significant increases in mean ethanol consumption and preference during the "treatment period." This could indicate that escalation in ethanol-

drinking behaviors was still occurring undeterred by i.p. injections; and that this delivery method shows less interference with ethanol-drinking behavior. However i.p. injection delivery has other potential problems, particularly in the case of CNS penetrant molecules which must often be non-polar and hydrophobic. Moreover oral delivery has the benefit of clinical applicability, given the vast preference for oral delivery of drugs in human patients. Therefore alternative oral routes of administration should continue to be explored in animal work (Turner *et al*, 2011), particularly in pre-clinical studies of AUD.

Regardless of the above limitations, an inhibitory effect on ethanol consumption by tideglusib was replicated across routes of administration. Tideglusib has been used in human patients with Alzheimer's disease at doses of up to 1000 mg (approximately 14 mg/kg for a 70 kg person) with no significant increase in adverse events over placebo except for a reversible increase in liver enzymes (del Ser *et al*, 2013; Lovestone *et al*, 2015). If it can be further determined that tideglusib does not pose a threat of liver toxicity in the context of alcoholism, then it might represent a novel treatment option. The fact that clinical trials for other neuropsychiatric diseases are ongoing (Anagnostou, 2018) make it an attractive option for its practical accessibility alone. However, as Mathuram et al. point out, due to GSK3B's ubiquitous expression and involvement in numerous essential pathways, inhibitors such as tideglusib carry a high risk of off-target effects (Mathuram *et al*, 2018). While it is possible that off-target effects would be mild compared to its on-target effects, as in the case of the non-specific GSK3B inhibitor lithium (Patel *et al*, 2006), it is worth continuing to explore the

GSK3B pathway as it is pertains specifically to the neurobiology of alcoholism. There could be other members in this pathway that show dysregulation specific to AUD in the CNS and that could be targeted with therapeutic agents.

6.4.2 Conclusions

Tideglusib showed striking effects on ethanol consumption across two modes of delivery. Via i.p. injection, the 3 mg/kg and 10 mg/kg doses which decreased ethanol consumption as a percent of baseline consumption (**Fig. 6.1C**), were equivalent to doses of the "tideglusib progenitor" molecule TDZD-8 which decreased operant responding for ethanol in Wistar rats (van der Vaart *et al*, 2018). A significantly higher gavage dose (200 mg/kg) decreased ethanol consumption markedly during a 2-hour binge but less robustly over the 24-hour period of IEA. Tideglusib has recently undergone pharmacokinetic profiling in male mice (Saini *et al*, 2018) at an i.p. dose of 10 mg/kg: plasma levels peaked at 0.25 h (T_{max}) and the terminal half-life ($t_{1/2}$) in vivo was determined to be 5.12 hours. Tideglusib was also found to be highly metabolized in mouse liver microsomes ($t_{1/2}$ =16 min) (Saini *et al*, 2018). Both i.p. and gavage routes of administration would be expected to undergo significant first-pass metabolism, with complete delivery to the portal vein in the case of gavage. The preferential effect of tideglusib on binge ethanol consumption may be explained by an early peak plasma concentration and quick drop-off after several hours. Thus, in a mouse model repeated or extended-release dosing might be necessary to more accurately assess actions on prolonged ethanol intake.

An alternative GSK3B inhibitor, SB216763, has been found to abrogate cocaine-induced conditioned place preference (CPP), particularly upon re-exposure to an environment previous paired with cocaine (Shi *et al*, 2014). This suggests that GSK3B activity is necessary for the memory reconsolidation and subsequent drug-seeking behavior modeled by CPP upon reintroduction to a cocaine-paired environment. Interestingly, we observed a significant inhibitory effect of TDZD-8 on cue-induced reinstatement (van der Vaart *et al*, 2018). This abrogation was observed specifically in ethanol-trained rats re-introduced to ethanol-associated cues, while sucrose-trained rats reintroduced to sucrose-associated cues did not show an effect of TDZD-8. It has not been tested whether TDZD-8 would also attenuate cue-induced reinstatement of cocaine. If this were the case it would suggest that there is something fundamentally different about re-introduction to cues associated with drugs of abuse (alcohol and cocaine) as compared to cues associated with “natural reinforcers” (i.e. sucrose).

In the studies described in this chapter, intermittent ethanol access (IEA) was used to induce an escalated level of ethanol consumption compared to constant ethanol access. This paradigm is theorized to work based on the induction of a kindling-type transition from moderate to excessive use, based on cycles of exposure and withdrawal (Hwa *et al*, 2011). It is interesting to consider that pre-treatment with tideglusib before an ethanol access period might serve to abrogate this kindling-type effect, either through diminishment of withdrawal-related symptoms or impaired reconsolidation of ethanol-related learning. A study

of tideglusib in the context of ethanol-induced CPP might help elucidate this type of effect.

As a corollary analysis we have described a data-mining expedition using genes identified by McClintick et al. (2014). Their goal of using LCLs cultured from peripheral blood mononucleocytes of alcohol-dependent and control patients was to work toward the complex but necessary task of identifying biomarkers for AUD. Given the impossibility of brain biopsies from living patients, McClintick et al. used the logic that gene expression in precursor cells is a practical read-out of DNA sequence, and could identify genes with predisposition to alterations in their expression in brain (Hu *et al*, 2006). The authors included annotations identifying which differentially regulated genes identified in LCLs had previously been reported as differentially expressed in post-mortem brain tissue of alcoholic patients. We filtered their gene lists based on these external validations as a type of quality control. The prediction that kenpaullone would reverse the expression signature identified by McClintick et al. was particularly interesting to us given our ongoing work on small molecule inhibitors of GSK3B in preclinical models of AUD. Tideglusib is not currently in the NIH LINCS small molecule database but would be a useful addition in our opinion given its clinical approval. There are a handful of in vitro studies which investigate kenpaullone in the context of neuropsychiatric disorders, e.g. its effect of GSK3B regulation of serotonin 1B receptors (Chen *et al*, 2009), but reports of its in vivo use are limited (Eldar-Finkelman *et al*, 2011). Overall we consider that our use of the NIH LINCS thus far demonstrates a rather subtle measure of internal validity, as findings

from disparate modes of investigation are in broad agreement over the applicability of GSK3B inhibitors in the context of alcoholism.

Chapter 7

Concluding Discussion and Future Directions

An enduring mystery of alcoholism is why some individuals progress from occasional to compulsive use of alcohol, to the point of destruction of their health, families, and functioning. The pathogenesis of AUD is widely believed to manifest upon neuroadaptive responses to repeated ethanol exposures, in predisposed individuals (Harris and Koob, 2017). To form an integrative picture of AUD with a view to effective treatment, both the neurobiology of repeated ethanol exposures and the predisposing factors in human alcoholic patients must be understood.

In this dissertation we began with large-scale, genome-wide expression analyses of acute vs. chronic ethanol's effects on gene expression along the mesocorticolimbic reward pathway (NAC and PFC). We found a surprising degree of overlap between acute and chronic ethanol in terms of significant gene expression perturbations. Overall, pathway enrichment analyses for ethanol-responsive genes across both exposure types and brain regions identified genes related to synaptic transmission and neuronal structure. Genes uniquely regulated after chronic ethanol in the PFC did converge on *Akt* as a predicted pathway hub (**Fig. 3.3**), an interesting finding in light of later chapters which

describe the GSK3B pathway for which AKT is a prominent upstream kinase. A major candidate gene arising from this chapter was *Dnm3*, which was identified as significantly ethanol-responsive across both treatments and brain regions. In the NAC particularly, its expression in the context of chronic ethanol was reliably altered based on presence of the D2 vs. B6 allele (see **Fig 3.8**, red vs. black bars). Because its expression in the NAC was also correlated to ethanol drinking after repeated ethanol-vapor exposure (**Fig 3.7**) *Dnm3* may represent a genetic locus which interacts with chronic ethanol allostatically to produce genotype-dependent ethanol-drinking behavior. The dynamics of the dynamin-III protein have not, to our knowledge, been studied in the context of ethanol. Dynamin proteins, of which there are 3 mammalian isoforms (I, II, III) have the conserved function of regulating membrane endocytosis, i.e. of synaptic vesicles (Ferguson and De Camilli, 2012). Effects of ethanol on dynamin-related mechanisms could conceivably be regulated via GSK3B, given its control of dynamin I mediated activity-dependent bulk endocytosis (Clayton *et al*, 2010). However there is no evidence currently for direct interaction between GSK3B and dynamin III.

Gsk3b emerged as a candidate gene for alcoholism based on our laboratory's initial studies of acute ethanol's effects on networks of genes (Wolen *et al*, 2012). *Gsk3b* was a highly interconnected node in a network of genes showing significant ethanol response across the BXD panel. Human homologs of genes this network (with the highest correlations with *Gsk3b*) were investigated in a SNP-set based analysis of human alcohol-dependent patients (Edenberg *et al*, 2005), and found to be enriched for risk-conferring SNPs (**Fig. 3.9**). The

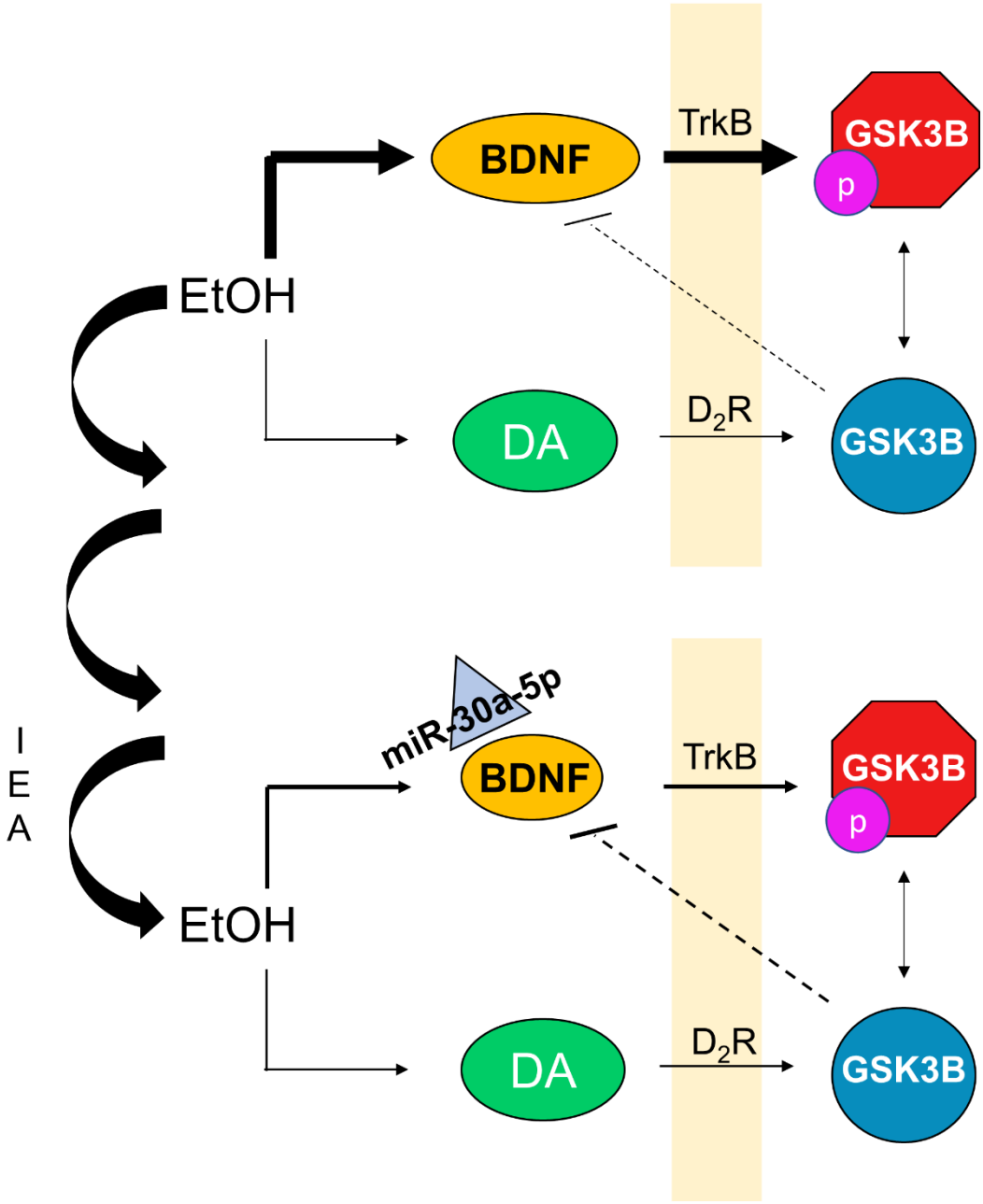

Figure 7.1 Working model of GSK3B involvement in ethanol signaling. **"**Competing pathways" downstream of ethanol converge on GSK3B phosphorylation. We observe acute ethanol-mediated phosphorylation of GSK3B-S9, but this effect diminishes after long-term IEA. BDNF expression in the mPFC is found to be protective against excessive ethanol use and also decreases following IEA (Darcq *et al*, 2015). An alternate upstream pathway is dopamine (DA) mediated, and would be expected to activate GSK3B via type 2 dopamine receptor recruitment of β-arrestin.

Gsk3b gene and its encoded protein GSK3B were the focus of subsequent studies on alcohol-related signaling and behaviors, described in Chapters 4-6.

GSK3B showed notable changes in activity and responsiveness to ethanol as assessed by phosphorylation of its inhibitory Ser-9 residue. Acute ethanol was found to markedly increase phosphorylation at this residue with apparent differences in threshold dose between males and females (**Fig. 4.3-4.4**). This finding is generally consistent with prior literature indicating GSK3B phosphorylation following acute doses of ethanol (1.8-2.0 g/kg) in PFC (Neznanova *et al*, 2009), NAC (Neasta *et al*, 2011; Sachs *et al*, 2014), and hippocampus (Sachs *et al*, 2014). However in contrast to prior work which also showed increased p-GSK3B-S9 after *chronic* ethanol in NAC (Neasta *et al*, 2011) and dorsomedial striatum (Cheng *et al*, 2016), our study of PFC after >5 weeks of IEA did not show a significant effect of ethanol on GSK3B phosphorylation (**Fig. 4.10**). We tested tissue harvested 24 hours after last access, as was done in the prior work cited. It is possible these studies of ours were underpowered (n=8/sex) as a trend toward increased p-GSK3 was observed in males and females. Regardless, while GSK3B activity did not appear to be altered basally at this time point, its *responsiveness* to ethanol was decreased, as assessed by an i.p. injection of 2.0 g/kg in IEA-exposed animals compared to ethanol-naïve controls (**Fig. 4.15—4.17**). Interestingly, decreased responsiveness of GSK3B to ethanol-induced phosphorylation has been observed in serotonin-deficient mice, which also exhibit increased ethanol consumption (Sachs *et al*, 2014). Therefore it may be that the decreased level of ethanol-induced inhibition of cortical GSK3B

is an underlying factor in the tendency of IEA-exposed mice to escalate their ethanol consumption relative to naïve mice (**Fig. 4.12—4.13**, also see (Rosenwasser *et al*, 2013)).

One potential upstream mechanism consistent with the blunting of GSK3B phosphorylation in PFC following long-term ethanol exposure would be via decreased BDNF-mediated signaling. BDNF has been found to inhibit GSK3B via Akt (Smillie *et al*, 2013). Moderate ethanol consumption has been shown to activate BDNF signaling, and this protects against the development of excessive ethanol intake (Jeanblanc *et al*, 2009; McGough *et al*, 2004). However, Darcq et al. (2015) found that intermittent ethanol access (IEA) produced a robust reduction of *Bdnf* expression in the mPFC. A microRNA targeting BDNF, mIR-30a-5p, was found to be concurrently increased. Inhibition of this miRNA using a targeted nucleic acid sequence in the mPFC restored BDNF expression and decreased drinking, while overexpression of the miRNA further escalated ethanol consumption (Darcq *et al*, 2015). This data is integrated into our findings on GSK3B in **Figure 7.1**. We propose that there are converging pathways on GSK3B following a given ethanol exposure. One of these is a BDNF-mediated pathway in the mPFC, likely through TrkB receptor activation and subsequent Pi3K-dependent Akt signaling intracellularly (Smillie *et al*, 2013), serving to inhibit GSK3B. This pathway might serve to self-regulate ethanol use under normal conditions, but is weakened following intermittent ethanol exposure, due to decreased expression of BDNF via miR-30a-5p targeting. Another pathway downstream of ethanol is dopamine release into the mPFC (Trantham-Davidson

and Chandler, 2015). Dopamine, particularly upon binding to D2 receptors (D_2R) activates GSK3B, likely through beta-arrestin recruitment of protein phosphatase 2-alpha (PP2A) (Beurel *et al*, 2015). This pathway could act antagonistically to the BDNF-dependent pathway, promoting drug-seeking behavior as is often seen with activation of corticolimbic dopamine signaling (Tzschentke, 2000). Neuroplastic changes underlying addiction-related learning may rely on a pool of active GSK3B in the context of alcohol exposure, as has been observed with cocaine (Miller *et al*, 2014). Our proposed pathway includes a feedback loop wherein activated GSK3B can itself serve to inhibit BDNF (Jope *et al*, 2006; van der Vaart *et al*, 2018), which would further promote excessive ethanol intake.

Although still speculative, the mechanism proposed in Figure 7.1 is consistent with a number of our observations of GSK3B modulation and ethanol drinking behavior. There is an interesting corollary between male-female differences in the qualitative profile of GSK3B phosphorylation and escalation in binge-like drinking. It appeared to require a higher dose of ethanol to induce GSK3B phosphorylation in female mice than males (compare **Fig. 4.3-4.4**), and female mice escalated their binge ethanol consumption almost immediately (**Fig 4.13**) while male mice escalated by the fifth week. This would be consistent with an initial “protective effect” of GSK3B inhibition. As discussed previously in Chapter 4, co-administration of a TrkB inhibitor such as ANA-12 with acute ethanol is essential in determining whether BDNF signaling is upstream of the ethanol-GSK3B phosphorylation effect (Cazorla *et al*, 2011).

In the case of GSK3B overexpression (**Fig. 5.3-5.4**), the pool of active GSK3B potentially mediating dopaminergic effects in the mPFC would have been increased. Moreover, although not discussed in this dissertation, Dr. Annie Meng found a decrease in *Bdnf* mRNA and BDNF protein in the mPFC of mice following viral vector GSK3B overexpression (van der Vaart *et al*, 2018). Together these findings suggest a strengthening of the dopaminergic pathway proposed in **Figure 7.1**. Conversely in the case of GSK3B deletion, dopaminergic signaling to the PFC (or at least the IL portion of it) could not activate GSK3B, and any effects of this pathway downstream from active GSK3B would be eliminated. However an important future step is characterizing any potential compensatory increases in GSK3A expression or activity following GSK3B deletion. Similarly in the case of tideglusib, an irreversible GSK3B inhibitor (Dominguez *et al*, 2012), dopaminergic effects mediated through GSK3B would presumably be abrogated so long as the drug is bound.

Could dopamine-dependent synaptic remodeling be mediated by GSK3B? Much of the ethanol-GSK3B downstream pathway remains to be elucidated, but there are some interesting considerations in light of GSK3B's established roles in cytoskeletal reorganization and targeting of synaptic anchor proteins (Salcedo-Tello *et al*, 2011). Overactive GSK3B promotes PSD95 mobilization by phosphorylation of its threonine-19 residue (p-PSD95-T19) (Nelson *et al*, 2013). We observed a suggestive inverse trend of p-PSD95-T19 level with increasing ethanol dose—the direction expected given GSK3B inhibition—but this was not significant (**Fig. 4.6**). There was also a significant increase in total PSD95 protein

following long-term IEA in male mice (**Fig. 4.11**). An upregulation of PSD95 could represent a compensatory increase in NMDA-receptor scaffolding following chronic exposure to ethanol. Increased PSD95 expression has been found to enhance NMDA receptor surface expression (Lin *et al*, 2006). Thus, increased PSD95 could contribute to the well-known phenomenon of NMDA receptor over-activation during periods of ethanol withdrawal. However, this finding presents something of a paradox in light of our findings on GSK3B. The inhibitor tideglusib decreases PSD95 phosphorylation at T19 (**Fig. 6.7**). According to Nelson et al. GSK3B-induced PSD95 phosphorylation is necessary for its internalization, and so a decrease in this phosphorylation would serve to stabilize PSD95 at the neuronal surface (Nelson *et al*, 2013). If this corresponded to increased surface expression of NMDA receptors, this should further exacerbate the hyper-excitable state associated with ethanol withdrawal and might serve to increase self-administration during each access period. Contrary to this logic, lithium and TDZD-8 have both previously been found to reduce NMDA currents (Chen *et al*, 2007) and tideglusib has been found to protect against NMDA-induced excitotoxicity (Armagan *et al*, 2015). In neither of these studies was the level of p-PSD95-T19 assessed for its relation to the GSK3B inhibitors' effects on NMDA expression. It is possible that GSK3B-mediated PSD95 phosphorylation regulates not only receptor internalization, but also receptor insertion, i.e. overall receptor dynamic turnover. Certainly PSD95 has been found to regulate both aspects of NMDA receptor function membrane localization (Lin *et al*, 2004). The Nelson et al. (2013) studies were performed only in cultured neurons, and so the

true in vivo effect of p-PSD95-T19 on NMDA surface expression is unknown. Useful future studies would include characterizing the p-PSD95-T19 surface expression in the PFC, with and without GSK3B modulation, and overlapping staining for NMDA receptors. Electrophysiological studies would also contribute greatly to our understanding of the effects of GSK3B on excitatory balance in neurons. In this dissertation, p-PSD95-T19 served as a useful readout for GSK3B activity at the synapse (**Fig. 6.7**) but with unclear implications downstream at the present time.

GSK3B activity shows an analogous function in regulation of inhibitory balance in neurons via its regulation of gephyrin (Tyagarajan *et al*, 2011), the scaffold protein of $GABA_A$ receptors. Given its dual effects on PSD95 and gephyrin, the regulation of excitatory-inhibitory balance via GSK3B is likely highly complex and depends upon cellular and temporal context for its combinatorial effect on neuronal signaling. Again, based on cell culture experiments, inhibition of GSK3B would be expected to increase surface $GABA_A$ receptor expression due to decreased gephyrin-dependent internalization. In the context of chronic alcohol in the dorsomedial striatum, GSK3B inhibition has been found to increase $GABA_A$ receptor expression with corresponding electrophysiological effects (Cheng *et al*, 2016). Here we found a suggestive inverse relationship between GSK3B phosphorylation and overall $GABA_A\alpha1$ subunit expression in the PFC (**Fig. 6.7**). This particular subunit has been associated with alcohol-induced tolerance and dependence (Werner *et al*, 2009), and its overall expression could be subject to regulation by gephyrin activity (Tyagarajan and Fritschy, 2014). If

overall GABAergic signaling is increased in the mPFC via GSK3B inhibition, this could represent one means of self-regulation against excessive ethanol exposure. The mPFC sends glutamatergic projections to the nucleus accumbens to maintain reward-seeking behavior via the corticolimbic circuit (Tzschentke, 2000). An upregulation of $GABA_A$ receptors in the mPFC could serve to decrease the intensity of firing of these glutamatergic projection neurons. Thus, analysis of GABA receptor expression in the PFC of mice with GSK3B overexpression or deletion could provide insight into a potential mechanism of the behaviors observed and described in Chapter 5. While lacking regional specificity of the viral studies, all glutamatergic projection neurons in the PFC would be *Camk2a+,* and so Camk2a-Cre*$Gsk3b^{fl/fl}$ mice could show a similar mechanism of PFC $GABA_A$ upregulation decreasing excessive ethanol consumption.

While regulation of PSD95 and gephyrin would each provide a means of regulating excitatory or inhibitory signaling, their dual regulation also suggests an overall regulation of dendritic spine stability. It is possible that ethanol-related learning requires not just changes in excitation/inhibition, but changes in dendritic morphology along ethanol-responsive circuits to promote behavioral adaptation. Active GSK3B allows for changes in dendritic morphology while its inhibition may serve to increase the stability of the spine (Cymerman *et al*, 2015) thereby resisting ethanol-related changes. Golgi-Cox staining and analysis of dendritic length, branching, and spine density as has been done in medium spiny neurons of the NAC (Peterson *et al*, 2015) would serve as a useful measure in the mPFC. We hypothesize that repeated ethanol exposure would alter spine density

selectively, such as increased density of mushroom-type spines in glutamatergic neurons (Kroener *et al*, 2012), but that the extent of such morphologic change might depend upon the level of GSK3B activity. Based on the requirement of GSK3B activity to induce morphological change, lower levels of GSK3B activity would be expected to show resistance to alterations in synaptic structure.

To achieve high levels of GSK3B activity, a useful transgenic line for future studies would be GSK3B-S9A mice, which have previously been proposed as a model of hyperactivity and mania (Prickaerts *et al*, 2006). The serine to alanine mutation encoded in this *Gsk3b* allele prevents its inactivation via S9 phosphorylation. This mutation serves to increase baseline GSK3B activity, which may predispose toward bipolar type symptoms but also toward increased susceptibility to excessive ethanol intake. Certainly in humans these predispositions appear to be linked (Regier *et al*, 1990). In addition to the possibility of phenotypic differences these mice might provide associated network-level changes in gene expression +/- alcohol. The GSK3B transgene is also available as a plasmid (Gozdz *et al*, 2017) which would allow regional and temporal specificity based on viral vector mediated expression.

Network-level investigations are overall an open-ended avenue for investigation in light of all that was outlined in this dissertation. We began this endeavor with the exciting observation that the *Gsk3b* gene transcript represented a molecular hub for ethanol induced changes in PFC gene expression across a genetically diverse panel of mice (Wolen *et al*, 2012). Studies on the level of protein phosphorylation provided very strong evidence

that acute ethanol greatly affects the activity of the GSK3B kinase in PFC. Inhibition at this functional level could influence genomic changes in many genes regulated by ethanol. The network of acute-ethanol related genes has shown important consequences in terms of predisposition to alcohol dependence (**Fig. 3.9**), and so further study of this network is warranted. Given the phenotypic effects observed following GSK3B deletion in *Camk2a* positive neurons, these transgenic animals could also allow for further resolution of the *Gsk3b* gene network. We would propose that following tamoxifen treatment, rather than beginning free access to ethanol, Cre+ and Cre- mice are injected with saline or ethanol and the PFC harvested as described in Wolen et al. (2012). This would allow for comparisons in gene expression at baseline (via comparison of the saline groups) and ethanol-induced expression changes (via saline-to-ethanol S-Scores). The latter of these is where changes in the previously identified Gsk3b network might be seen, but both could provide crucial insights into the relationship between GSK3B functional expression and the genomic outcome. It is through this type of analysis that human genetic panels may in turn be interrogated for specific gene expression signatures and we may begin to predict more effective treatments based on an informed prediction of a patients' neurobiology.

References

Alberts R, Schughart K (2010). QTLminer: identifying genes regulating quantitative traits. *BMC Bioinformatics* **11**: 516.

American Psychiatric Association., American Psychiatric Association. DSM-5 Task Force. (2013). *Diagnostic and statistical manual of mental disorders : DSM-5*, 5th edn. American Psychiatric Association: Washington, D.C., xliv, 947 p.pp.

Anagnostou E (2018). Tideglusib vs. Placebo in the Treatment of Adolescents With Autism Spectrum Disorders (TIDE). U.S. National Library of Medicine: ClinicalTrials.gov.

Andrade C (2017). Ketamine for Depression, 5: Potential Pharmacokinetic and Pharmacodynamic Drug Interactions. *J Clin Psychiatry* **78**(7): e858-e861.

Andreux PA, Williams EG, Koutnikova H, Houtkooper RH, Champy MF, Henry H*, et al* (2012). Systems genetics of metabolism: the use of the BXD murine reference panel for multiscalar integration of traits. *Cell* **150**(6): 1287-1299.

Armagan G, Keser A, Atalayin C, Dagci T (2015). Tideglusib protects neural stem cells against NMDA receptor overactivation. *Pharmacol Rep* **67**(5): 823-831.

Bachmanov AA, Tordoff MG, Beauchamp GK (1996). Ethanol consumption and taste preferences in C57BL/6ByJ and 129/J mice. *Alcohol Clin Exp Res* **20**(2): 201-206.

Baker EJ, Jay JJ, Bubier JA, Langston MA, Chesler EJ (2012). GeneWeaver: a web-based system for integrative functional genomics. *Nucleic Acids Res* **40**(Database issue): D1067-1076.

Barkley-Levenson AM, Crabbe JC (2014). High drinking in the dark mice: a genetic model of drinking to intoxication. *Alcohol* **48**(3): 217-223.

Batman AM, Miles MF (2015). Translating Alcohol Research: Opportunities and Challenges. *Alcohol Res* **37**(1): 7-14.

Beaudet G, Valable S, Bourgine J, Lelong-Boulouard V, Lanfumey L, Freret T*, et al* (2016). Long-Lasting Effects of Chronic Intermittent Alcohol Exposure in Adolescent Mice on Object Recognition and Hippocampal Neuronal Activity. *Alcohol Clin Exp Res* **40**(12): 2591-2603.

Beaulieu JM, Gainetdinov RR, Caron MG (2009). Akt/GSK3 signaling in the action of psychotropic drugs. *Annu Rev Pharmacol Toxicol* **49**: 327-347.

Beaulieu JM, Sotnikova TD, Yao WD, Kockeritz L, Woodgett JR, Gainetdinov RR*, et al* (2004). Lithium antagonizes dopamine-dependent behaviors mediated by an AKT/glycogen synthase kinase 3 signaling cascade. *Proc Natl Acad Sci U S A* **101**(14): 5099-5104.

Beaulieu JM, Zhang X, Rodriguiz RM, Sotnikova TD, Cools MJ, Wetsel WC*, et al* (2008). Role of GSK3 beta in behavioral abnormalities induced by serotonin deficiency. *Proc Natl Acad Sci U S A* **105**(4): 1333-1338.

Becker HC (2013). Animal models of excessive alcohol consumption in rodents. *Curr Top Behav Neurosci* **13**: 355-377.

Becker HC, Hale RL (1993). Repeated episodes of ethanol withdrawal potentiate the severity of subsequent withdrawal seizures: an animal model of alcohol withdrawal "kindling". *Alcohol Clin Exp Res* **17**(1): 94-98.

Besheer J, Jensen HC, Bevins RA (1999). Dopamine antagonism in a novel-object recognition and a novel-object place conditioning preparation with rats. *Behav Brain Res* **103**(1): 35-44.

Bespalov A, Muller R, Relo AL, Hudzik T (2016). Drug Tolerance: A Known Unknown in Translational Neuroscience. *Trends Pharmacol Sci* **37**(5): 364-378.

Bettinger JC, Leung K, Bolling MH, Goldsmith AD, Davies AG (2012). Lipid environment modulates the development of acute tolerance to ethanol in Caenorhabditis elegans. *PLoS One* **7**(5): e35192.

Beurel E, Grieco SF, Jope RS (2015). Glycogen synthase kinase-3 (GSK3): regulation, actions, and diseases. *Pharmacol Ther* **148**: 114-131.

Beurel E, Song L, Jope RS (2011). Inhibition of glycogen synthase kinase-3 is necessary for the rapid antidepressant effect of ketamine in mice. *Mol Psychiatry* **16**(11): 1068-1070.

Bhandari P, Kendler KS, Bettinger JC, Davies AG, Grotewiel M (2009). An assay for evoked locomotor behavior in Drosophila reveals a role for integrins in ethanol sensitivity and rapid ethanol tolerance. *Alcohol Clin Exp Res* **33**(10): 1794-1805.

Bharathy N, Svalina MN, Settelmeyer TP, Cleary MM, Berlow NE, Airhart SD*, et al* (2017). Preclinical testing of the glycogen synthase kinase-3beta inhibitor tideglusib for rhabdomyosarcoma. *Oncotarget* **8**(38): 62976-62983.

Bierut LJ, Agrawal A, Bucholz KK, Doheny KF, Laurie C, Pugh E*, et al* (2010). A genome-wide association study of alcohol dependence. *Proc Natl Acad Sci U S A* **107**(11): 5082-5087.

Bierut LJ, Saccone NL, Rice JP, Goate A, Foroud T, Edenberg H*, et al* (2002). Defining alcohol-related phenotypes in humans. The Collaborative Study on the Genetics of Alcoholism. *Alcohol Res Health* **26**(3): 208-213.

Blahos J, 2nd, Wenthold RJ (1996). Relationship between N-methyl-D-aspartate receptor NR1 splice variants and NR2 subunits. *J Biol Chem* **271**(26): 15669-15674.

Blanke ML, VanDongen AMJ (2009). Activation Mechanisms of the NMDA Receptor. In: Van Dongen AM (ed). *Biology of the NMDA Receptor*: Boca Raton (FL).

Bliss TV, Collingridge GL, Morris RGM (2007). Synaptic plasticity in the hippocampus. In: Andersen P, Morris RGM, Amaral DG, Bliss TV, O'Keefe J (eds). *The Hippocampus Book*. Oxford University Press: USA, pp 343-474.

Bonnet U, Scherbaum N (2015). Striking Similarities between Clinical and Biological Properties of Ketamine and Ethanol: Linking Antidepressant-After Effect and Burgeoning Addiction. *J Alcohol Drug Depend* **3**(198).

Boyce-Rustay JM, Holmes A (2006). Ethanol-related behaviors in mice lacking the NMDA receptor NR2A subunit. *Psychopharmacology (Berl)* **187**(4): 455-466.

Bradley CA, Peineau S, Taghibiglou C, Nicolas CS, Whitcomb DJ, Bortolotto ZA*, et al* (2012). A pivotal role of GSK-3 in synaptic plasticity. *Front Mol Neurosci* **5**: 13.

Bucholz KK, Cadoret R, Cloninger CR, Dinwiddie SH, Hesselbrock VM, Nurnberger JI, Jr.*, et al* (1994). A new, semi-structured psychiatric interview for use in genetic linkage studies: a report on the reliability of the SSAGA. *J Stud Alcohol* **55**(2): 149-158.

Can A, Blackwell RA, Piantadosi SC, Dao DT, O'Donnell KC, Gould TD (2011). Antidepressant-like responses to lithium in genetically diverse mouse strains. *Genes Brain Behav* **10**(4): 434-443.

Carlson SL, Kumar S, Werner DF, Comerford CE, Morrow AL (2013). Ethanol activation of protein kinase A regulates GABAA alpha1 receptor function and trafficking in cultured cerebral cortical neurons. *J Pharmacol Exp Ther* **345**(2): 317-325.

Carpenter-Hyland EP, Chandler LJ (2006). Homeostatic plasticity during alcohol exposure promotes enlargement of dendritic spines. *Eur J Neurosci* **24**(12): 3496-3506.

Carpenter-Hyland EP, Woodward JJ, Chandler LJ (2004). Chronic ethanol induces synaptic but not extrasynaptic targeting of NMDA receptors. *J Neurosci* **24**(36): 7859-7868.

Casarett LJ, Doull J (1975). *Toxicology : the basic science of poisons* Macmillan: New York, xiii, 768 p.pp.

Cassaday HJ, Nelson AJ, Pezze MA (2014). From attention to memory along the dorsal-ventral axis of the medial prefrontal cortex: some methodological considerations. *Front Syst Neurosci* **8**: 160.

Cazorla M, Premont J, Mann A, Girard N, Kellendonk C, Rognan D (2011). Identification of a low-molecular weight TrkB antagonist with anxiolytic and antidepressant activity in mice. *J Clin Invest* **121**(5): 1846-1857.

Chen L, Salinas GD, Li X (2009). Regulation of serotonin 1B receptor by glycogen synthase kinase-3. *Mol Pharmacol* **76**(6): 1150-1161.

Chen P, Gu Z, Liu W, Yan Z (2007). Glycogen synthase kinase 3 regulates N-methyl-D-aspartate receptor channel trafficking and function in cortical neurons. *Mol Pharmacol* **72**(1): 40-51.

Cheng Y, Huang CC, Ma T, Wei X, Wang X, Lu J*, et al* (2016). Distinct Synaptic Strengthening of the Striatal Direct and Indirect Pathways Drives Alcohol Consumption. *Biol Psychiatry*.

Chester JA, de Paula Barrenha G, DeMaria A, Finegan A (2006). Different effects of stress on alcohol drinking behaviour in male and female mice selectively bred for high alcohol preference. *Alcohol Alcohol* **41**(1): 44-53.

Chou CH, Chou AK, Lin CC, Chen WJ, Wei CC, Yang MC*, et al* (2012). GSK3beta regulates Bcl2L12 and Bcl2L12A anti-apoptosis signaling in glioblastoma and is inhibited by LiCl. *Cell Cycle* **11**(3): 532-542.

Chou WH, Wang D, McMahon T, Qi ZH, Song M, Zhang C*, et al* (2010). GABAA receptor trafficking is regulated by protein kinase C(epsilon) and the N-ethylmaleimide-sensitive factor. *J Neurosci* **30**(42): 13955-13965.

Clayton EL, Cousin MA (2009). The molecular physiology of activity-dependent bulk endocytosis of synaptic vesicles. *J Neurochem* **111**(4): 901-914.

Clayton EL, Sue N, Smillie KJ, O'Leary T, Bache N, Cheung G*, et al* (2010). Dynamin I phosphorylation by GSK3 controls activity-dependent bulk endocytosis of synaptic vesicles. *Nat Neurosci* **13**(7): 845-851.

Cole A, Frame S, Cohen P (2004). Further evidence that the tyrosine phosphorylation of glycogen synthase kinase-3 (GSK3) in mammalian cells is an autophosphorylation event. *Biochem J* **377**(Pt 1): 249-255.

Connolly CN, Kittler JT, Thomas P, Uren JM, Brandon NJ, Smart TG*, et al* (1999). Cell surface stability of gamma-aminobutyric acid type A receptors. Dependence on protein kinase C activity and subunit composition. *J Biol Chem* **274**(51): 36565-36572.

Costin BN, Wolen AR, Fitting S, Shelton KL, Miles MF (2013). Role of adrenal glucocorticoid signaling in prefrontal cortex gene expression and acute behavioral responses to ethanol. *Alcohol Clin Exp Res* **37**(1): 57-66.

Council NR (2011). *Guide for the Care and Use of Laboratory Animals: Eighth Edition* National Academies Press (US): Washington, D.C. , 118pp.

Crabbe JC (2014). Rodent models of genetic contributions to motivation to abuse alcohol. *Nebr Symp Motiv* **61**: 5-29.

Crabbe JC, Belknap JK, Mitchell SR, Crawshaw LI (1994). Quantitative trait loci mapping of genes that influence the sensitivity and tolerance to ethanol-induced hypothermia in BXD recombinant inbred mice. *J Pharmacol Exp Ther* **269**(1): 184-192.

Crabbe JC, Cotnam CJ, Cameron AJ, Schlumbohm JP, Rhodes JS, Metten P*, et al* (2003). Strain differences in three measures of ethanol intoxication in mice: the screen, dowel and grip strength tests. *Genes Brain Behav* **2**(4): 201-213.

Crabbe JC, Spence SE, Brown LL, Metten P (2011). Alcohol preference drinking in a mouse line selectively bred for high drinking in the dark. *Alcohol* **45**(5): 427-440.

Cymerman IA, Gozdz A, Urbanska M, Milek J, Dziembowska M, Jaworski J (2015). Structural Plasticity of Dendritic Spines Requires GSK3alpha and GSK3beta. *PLoS One* **10**(7): e0134018.

Darcq E, Warnault V, Phamluong K, Besserer GM, Liu F, Ron D (2015). MicroRNA-30a-5p in the prefrontal cortex controls the transition from moderate to excessive alcohol consumption. *Mol Psychiatry* **20**(10): 1219-1231.

Das J, Pany S, Rahman GM, Slater SJ (2009). PKC epsilon has an alcohol-binding site in its second cysteine-rich regulatory domain. *Biochem J* **421**(3): 405-413.

de Bartolomeis A, Iasevoli F (2003). The Homer family and the signal transduction system at glutamatergic postsynaptic density: potential role in behavior and pharmacotherapy. *Psychopharmacol Bull* **37**(3): 51-83.

del Ser T, Steinwachs KC, Gertz HJ, Andres MV, Gomez-Carrillo B, Medina M*, et al* (2013). Treatment of Alzheimer's disease with the GSK-3 inhibitor tideglusib: a pilot study. *Journal of Alzheimer's disease : JAD* **33**(1): 205-215.

Diana M, Pistis M, Carboni S, Gessa GL, Rossetti ZL (1993). Profound decrement of mesolimbic dopaminergic neuronal activity during ethanol withdrawal syndrome in rats: electrophysiological and biochemical evidence. *Proc Natl Acad Sci U S A* **90**(17): 7966-7969.

Diaz MR, Christian DT, Anderson NJ, McCool BA (2011). Chronic ethanol and withdrawal differentially modulate lateral/basolateral amygdala paracapsular and local GABAergic synapses. *J Pharmacol Exp Ther* **337**(1): 162-170.

Dobashi T, Tanabe S, Jin H, Nishino T, Aoe T (2010). Valproate attenuates the development of morphine antinociceptive tolerance. *Neurosci Lett* **485**(2): 125-128.

Dominguez JM, Fuertes A, Orozco L, del Monte-Millan M, Delgado E, Medina M (2012). Evidence for irreversible inhibition of glycogen synthase kinase-3beta by tideglusib. *J Biol Chem* **287**(2): 893-904.

Doss S, Schadt EE, Drake TA, Lusis AJ (2005). Cis-acting expression quantitative trait loci in mice. *Genome Res* **15**(5): 681-691.

Du J, Wei Y, Liu L, Wang Y, Khairova R, Blumenthal R*, et al* (2010). A kinesin signaling complex mediates the ability of GSK-3beta to affect mood-associated behaviors. *Proc Natl Acad Sci U S A* **107**(25): 11573-11578.

Duan Q, Flynn C, Niepel M, Hafner M, Muhlich JL, Fernandez NF*, et al* (2014). LINCS Canvas Browser: interactive web app to query, browse and interrogate LINCS L1000 gene expression signatures. *Nucleic Acids Res* **42**(Web Server issue): W449-460.

Duan Q, Reid SP, Clark NR, Wang Z, Fernandez NF, Rouillard AD*, et al* (2016). L1000CDS(2): LINCS L1000 characteristic direction signatures search engine. *NPJ Syst Biol Appl* **2**.

Easton AC, Lucchesi W, Lourdusamy A, Lenz B, Solati J, Golub Y*, et al* (2013). alphaCaMKII autophosphorylation controls the establishment of alcohol drinking behavior. *Neuropsychopharmacology* **38**(9): 1636-1647.

Edenberg HJ, Bierut LJ, Boyce P, Cao M, Cawley S, Chiles R*, et al* (2005). Description of the data from the Collaborative Study on the Genetics of Alcoholism (COGA) and single-nucleotide polymorphism genotyping for Genetic Analysis Workshop 14. *BMC Genet* **6 Suppl 1**: S2.

Eldar-Finkelman H, Martinez A (2011). GSK-3 Inhibitors: Preclinical and Clinical Focus on CNS. *Front Mol Neurosci* **4**: 32.

Ellinwood EH, Jr., Linnoila M, Easler ME, Molter DW (1983). Profile of acute tolerance to three sedative anxiolytics. *Psychopharmacology (Berl)* **79**(2-3): 137-141.

Enman NM, Unterwald EM (2012). Inhibition of GSK3 attenuates amphetamine-induced hyperactivity and sensitization in the mouse. *Behav Brain Res* **231**(1): 217-225.

Evans GJ, Cousin MA (2007). Activity-dependent control of slow synaptic vesicle endocytosis by cyclin-dependent kinase 5. *J Neurosci* **27**(2): 401-411.

Everitt BJ, Robbins TW (2005). Neural systems of reinforcement for drug addiction: from actions to habits to compulsion. *Nat Neurosci* **8**(11): 1481-1489.

Fang X, Yu SX, Lu Y, Bast RC, Jr., Woodgett JR, Mills GB (2000). Phosphorylation and inactivation of glycogen synthase kinase 3 by protein kinase A. *Proc Natl Acad Sci U S A* **97**(22): 11960-11965.

Farris SP, Mayfield RD (2014). RNA-Seq reveals novel transcriptional reorganization in human alcoholic brain. *Int Rev Neurobiol* **116**: 275-300.

Farris SP, Miles MF (2013). Fyn-dependent gene networks in acute ethanol sensitivity. *PLoS One* **8**(11): e82435.

Feil S, Valtcheva N, Feil R (2009). Inducible Cre mice. *Methods Mol Biol* **530**: 343-363.

Ferguson SM, De Camilli P (2012). Dynamin, a membrane-remodelling GTPase. *Nat Rev Mol Cell Biol* **13**(2): 75-88.

Finn DA, Crabbe JC (1997). Exploring alcohol withdrawal syndrome. *Alcohol Health Res World* **21**(2): 149-156.

Fisher RA (1922). On the Interpretation of χ2 from Contingency Tables, and the Calculation of P. *Journal of the Royal Statistical Society* **85**(1): 87-94.

Frame S, Cohen P, Biondi RM (2001). A common phosphate binding site explains the unique substrate specificity of GSK3 and its inactivation by phosphorylation. *Mol Cell* **7**(6): 1321-1327.

Franck J, Jayaram-Lindstrom N (2013). Pharmacotherapy for alcohol dependence: status of current treatments. *Curr Opin Neurobiol* **23**(4): 692-699.

French RL, Heberlein U (2009). Glycogen synthase kinase-3/Shaggy mediates ethanol-induced excitotoxic cell death of Drosophila olfactory neurons. *Proc Natl Acad Sci U S A* **106**(49): 20924-20929.

Garuti L, Roberti M, Bottegoni G (2010). Non-ATP competitive protein kinase inhibitors. *Curr Med Chem* **17**(25): 2804-2821.

Gass JT, Trantham-Davidson H, Kassab AS, Glen WB, Jr., Olive MF, Chandler LJ (2014). Enhancement of extinction learning attenuates ethanol-seeking behavior and alters plasticity in the prefrontal cortex. *J Neurosci* **34**(22): 7562-7574.

George O, Sanders C, Freiling J, Grigoryan E, Vu S, Allen CD*, et al* (2012). Recruitment of medial prefrontal cortex neurons during alcohol withdrawal predicts cognitive impairment and excessive alcohol drinking. *Proc Natl Acad Sci U S A* **109**(44): 18156-18161.

Gillman MA, Lichtigfeld FJ (1997). Alcohol withdrawal syndrome. *Lancet* **350**(9079): 737.

Glykys J, Peng Z, Chandra D, Homanics GE, Houser CR, Mody I (2007). A new naturally occurring GABA(A) receptor subunit partnership with high sensitivity to ethanol. *Nat Neurosci* **10**(1): 40-48.

Gould TD, Einat H, Bhat R, Manji HK (2004). AR-A014418, a selective GSK-3 inhibitor, produces antidepressant-like effects in the forced swim test. *Int J Neuropsychopharmacol* **7**(4): 387-390.

Gozdz A, Nikolaienko O, Urbanska M, Cymerman IA, Sitkiewicz E, Blazejczyk M*, et al* (2017). GSK3alpha and GSK3beta Phosphorylate Arc and Regulate its Degradation. *Front Mol Neurosci* **10**: 192.

Grant KA, Valverius P, Hudspith M, Tabakoff B (1990). Ethanol withdrawal seizures and the NMDA receptor complex. *Eur J Pharmacol* **176**(3): 289-296.

Gremel CM, Young EA, Cunningham CL (2011). Blockade of opioid receptors in anterior cingulate cortex disrupts ethanol-seeking behavior in mice. *Behav Brain Res* **219**(2): 358-362.

Griffin WC, 3rd, Lopez MF, Yanke AB, Middaugh LD, Becker HC (2009). Repeated cycles of chronic intermittent ethanol exposure in mice increases voluntary ethanol drinking and ethanol concentrations in the nucleus accumbens. *Psychopharmacology (Berl)* **201**(4): 569-580.

Grimes CA, Jope RS (2001). The multifaceted roles of glycogen synthase kinase 3β in cellular signaling. *Progress in Neurobiology* **65**(4): 391-426.

Gunschmann C, Chiticariu E, Garg B, Hiz MM, Mostmans Y, Wehner M*, et al* (2014). Transgenic mouse technology in skin biology: inducible gene knockout in mice. *J Invest Dermatol* **134**(7): 1-4.

Hakkarainen P, Metso L (2009). Joint use of drugs and alcohol. *Eur Addict Res* **15**(2): 113-120.

Hall FS, Sora I, Uhl GR (2001). Ethanol consumption and reward are decreased in mu-opiate receptor knockout mice. *Psychopharmacology (Berl)* **154**(1): 43-49.

Hammes-Schiffer S, Benkovic SJ (2006). Relating protein motion to catalysis. *Annu Rev Biochem* **75**: 519-541.

Harms KJ, Tovar KR, Craig AM (2005). Synapse-specific regulation of AMPA receptor subunit composition by activity. *J Neurosci* **25**(27): 6379-6388.

Harris RA, Koob GF (2017). The future is now: A 2020 view of alcoholism research. *Neuropharmacology* **122**: 1-2.

Harris RA, McQuilkin SJ, Paylor R, Abeliovich A, Tonegawa S, Wehner JM (1995). Mutant mice lacking the gamma isoform of protein kinase C show decreased behavioral actions of ethanol and altered function of gamma-aminobutyrate type A receptors. *Proc Natl Acad Sci U S A* **92**(9): 3658-3662.

Harris RA, Trudell JR, Mihic SJ (2008). Ethanol's molecular targets. *Sci Signal* **1**(28): re7.

Health USDO, Human S (2015). Opioid abuse in the United States and Department of Health and Human Services actions to address opioid-drug-related overdoses and deaths. *J Pain Palliat Care Pharmacother* **29**(2): 133-139.

Hesselbrock M, Easton C, Bucholz KK, Schuckit M, Hesselbrock V (1999). A validity study of the SSAGA--a comparison with the SCAN. *Addiction* **94**(9): 1361-1370.

Hodge CW, Mehmert KK, Kelley SP, McMahon T, Haywood A, Olive MF*, et al* (1999). Supersensitivity to allosteric GABA(A) receptor modulators and alcohol in mice lacking PKCepsilon. *Nat Neurosci* **2**(11): 997-1002.

Hoffman PL, Rabe CS, Grant KA, Valverius P, Hudspith M, Tabakoff B (1990). Ethanol and the NMDA receptor. *Alcohol* **7**(3): 229-231.

Hoglinger GU, Huppertz HJ, Wagenpfeil S, Andres MV, Belloch V, Leon T*, et al* (2014). Tideglusib reduces progression of brain atrophy in progressive supranuclear palsy in a randomized trial. *Mov Disord* **29**(4): 479-487.

Holmes A, Fitzgerald PJ, MacPherson KP, DeBrouse L, Colacicco G, Flynn SM*, et al* (2012). Chronic alcohol remodels prefrontal neurons and disrupts NMDAR-mediated fear extinction encoding. *Nat Neurosci* **15**(10): 1359-1361.

Howard DB, Powers K, Wang Y, Harvey BK (2008). Tropism and toxicity of adeno-associated viral vector serotypes 1, 2, 5, 6, 7, 8, and 9 in rat neurons and glia in vitro. *Virology* **372**(1): 24-34.

Howard RJ, Slesinger PA, Davies DL, Das J, Trudell JR, Harris RA (2011). Alcohol-binding sites in distinct brain proteins: the quest for atomic level resolution. *Alcohol Clin Exp Res* **35**(9): 1561-1573.

Hu VW, Frank BC, Heine S, Lee NH, Quackenbush J (2006). Gene expression profiling of lymphoblastoid cell lines from monozygotic twins discordant in severity of autism reveals differential regulation of neurologically relevant genes. *BMC Genomics* **7**: 118.

Hwa LS, Chu A, Levinson SA, Kayyali TM, DeBold JF, Miczek KA (2011). Persistent escalation of alcohol drinking in C57BL/6J mice with intermittent access to 20% ethanol. *Alcohol Clin Exp Res* **35**(11): 1938-1947.

Inoue K, Rusi M, Lindros KO (1981). Brain aldehyde dehydrogenase activity in rat strains with high and low ethanol preferences. *Pharmacol Biochem Behav* **14**(1): 107-111.

Irizarry RA, Hobbs B, Collin F, Beazer-Barclay YD, Antonellis KJ, Scherf U*, et al* (2003). Exploration, normalization, and summaries of high density oligonucleotide array probe level data. *Biostatistics* **4**(2): 249-264.

Jaffee WB, Griffin ML, Gallop R, Meade CS, Graff F, Bender RE*, et al* (2009). Depression precipitated by alcohol use in patients with co-occurring bipolar and substance use disorders. *J Clin Psychiatry* **70**(2): 171-176.

Janoff AS, Pringle MJ, Miller KW (1981). Correlation of general anesthetic potency with solubility in membranes. *Biochim Biophys Acta* **649**(1): 125-128.

Jeanblanc J, He DY, Carnicella S, Kharazia V, Janak PH, Ron D (2009). Endogenous BDNF in the dorsolateral striatum gates alcohol drinking. *J Neurosci* **29**(43): 13494-13502.

Jenni NL, Larkin JD, Floresco SB (2017). Prefrontal Dopamine D1 and D2 Receptors Regulate Dissociable Aspects of Decision Making via Distinct Ventral Striatal and Amygdalar Circuits. *J Neurosci* **37**(26): 6200-6213.

Johnson JW, Kotermanski SE (2006). Mechanism of action of memantine. *Curr Opin Pharmacol* **6**(1): 61-67.

Johnson T (2007). Bayesian method for gene detection and mapping, using a case and control design and DNA pooling. *Biostatistics* **8**(3): 546-565.

Jope RS, Roh MS (2006). Glycogen synthase kinase-3 (GSK3) in psychiatric diseases and therapeutic interventions. *Curr Drug Targets* **7**(11): 1421-1434.

Kaidanovich-Beilin O, Milman A, Weizman A, Pick CG, Eldar-Finkelman H (2004). Rapid antidepressive-like activity of specific glycogen synthase kinase-3 inhibitor and its effect on beta-catenin in mouse hippocampus. *Biol Psychiatry* **55**(8): 781-784.

Keenan AB, Jenkins SL, Jagodnik KM, Koplev S, He E, Torre D*, et al* (2018). The Library of Integrated Network-Based Cellular Signatures NIH Program: System-Level Cataloging of Human Cells Response to Perturbations. *Cell Syst* **6**(1): 13-24.

Kendler KS, Aggen SH, Prescott CA, Crabbe J, Neale MC (2012). Evidence for multiple genetic factors underlying the DSM-IV criteria for alcohol dependence. *Mol Psychiatry* **17**(12): 1306-1315.

Kennedy RE, Kerns RT, Kong X, Archer KJ, Miles MF (2006). SScore: an R package for detecting differential gene expression without gene expression summaries. *Bioinformatics* **22**(10): 1272-1274.

Kerns RT, Ravindranathan A, Hassan S, Cage MP, York T, Sikela JM*, et al* (2005a). Ethanol-responsive brain region expression networks: implications for behavioral responses to acute ethanol in DBA/2J versus C57BL/6J mice. *J Neurosci* **25**(9): 2255-2266.

Kerns RT, Ravindranathan A, Hassan S, Cage MP, York TP, Sikela JM*, et al* (2005b). Ethanol-Responsive Brain Region Expression Networks: Implications for Behavioral Responses to Acute Ethanol in DBA/2J versus C57BL/6J Mice. *The Journal of Neuroscience* **25**(9): 2255-2266.

Kerns RT, Zhang L, Miles MF (2003). Application of the S-score algorithm for analysis of oligonucleotide microarrays. *Methods* **31**(4): 274-281.

Kessels HW, Malinow R (2009). Synaptic AMPA receptor plasticity and behavior. *Neuron* **61**(3): 340-350.

Kessler RC, Nelson CB, McGonagle KA, Edlund MJ, Frank RG, Leaf PJ (1996). The epidemiology of co-occurring addictive and mental disorders: implications for prevention and service utilization. *Am J Orthopsychiatry* **66**(1): 17-31.

Khanna JM, Kalant H, Chau A, Shah G (1998). Rapid tolerance and crosstolerance to motor impairment effects of benzodiazepines, barbiturates, and ethanol. *Pharmacol Biochem Behav* **59**(2): 511-519.

Khanna JM, Shah G, Weiner J, Wu PH, Kalant H (1993). Effect of NMDA receptor antagonists on rapid tolerance to ethanol. *Eur J Pharmacol* **230**(1): 23-31.

Kim WY, Jang JK, Lee JW, Jang H, Kim JH (2013). Decrease of GSK3beta phosphorylation in the rat nucleus accumbens core enhances cocaine-induced hyper-locomotor activity. *J Neurochem* **125**(5): 642-648.

Kimura T, Yamashita S, Nakao S, Park JM, Murayama M, Mizoroki T*, et al* (2008). GSK-3beta is required for memory reconsolidation in adult brain. *PLoS One* **3**(10): e3540.

Klein PS, Melton DA (1996). A molecular mechanism for the effect of lithium on development. *Proc Natl Acad Sci U S A* **93**(16): 8455-8459.

Klemm WR (1998). Biological water and its role in the effects of alcohol. *Alcohol* **15**(3): 249-267.

Koob GF, Le Moal M (1997). Drug abuse: hedonic homeostatic dysregulation. *Science* **278**(5335): 52-58.

Koob GF, Roberts AJ, Schulteis G, Parsons LH, Heyser CJ, Hyytia P*, et al* (1998). Neurocircuitry targets in ethanol reward and dependence. *Alcohol Clin Exp Res* **22**(1): 3-9.

Kroener S, Mulholland PJ, New NN, Gass JT, Becker HC, Chandler LJ (2012). Chronic alcohol exposure alters behavioral and synaptic plasticity of the rodent prefrontal cortex. *PLoS One* **7**(5): e37541.

Krystal JH, Petrakis IL, Webb E, Cooney NL, Karper LP, Namanworth S*, et al* (1998). Dose-related ethanol-like effects of the NMDA antagonist, ketamine, in recently detoxified alcoholics. *Arch Gen Psychiatry* **55**(4): 354-360.

Krystal JH, Staley J, Mason G, Petrakis IL, Kaufman J, Harris RA*, et al* (2006). Gamma-aminobutyric acid type A receptors and alcoholism: intoxication, dependence, vulnerability, and treatment. *Arch Gen Psychiatry* **63**(9): 957-968.

Kumar S, Kralic JE, O'Buckley TK, Grobin AC, Morrow AL (2003). Chronic ethanol consumption enhances internalization of alpha1 subunit-containing GABAA receptors in cerebral cortex. *J Neurochem* **86**(3): 700-708.

Kumar S, Suryanarayanan A, Boyd KN, Comerford CE, Lai MA, Ren Q*, et al* (2010). Ethanol reduces GABAA alpha1 subunit receptor surface expression by a protein kinase Cgamma-dependent mechanism in cultured cerebral cortical neurons. *Mol Pharmacol* **77**(5): 793-803.

Langfelder P, Horvath S (2008). WGCNA: an R package for weighted correlation network analysis. *BMC Bioinformatics* **9**: 559.

Latapy C, Rioux V, Guitton MJ, Beaulieu JM (2012). Selective deletion of forebrain glycogen synthase kinase 3beta reveals a central role in serotonin-sensitive anxiety and social behaviour. *Philosophical transactions of the Royal Society of London Series B, Biological sciences* **367**(1601): 2460-2474.

Lee SJ, Chung YH, Joo KM, Lim HC, Jeon GS, Kim D*, et al* (2006). Age-related changes in glycogen synthase kinase 3beta (GSK3beta) immunoreactivity in the central nervous system of rats. *Neurosci Lett* **409**(2): 134-139.

Lempradl A, Pospisilik JA, Penninger JM (2015). Exploring the emerging complexity in transcriptional regulation of energy homeostasis. *Nat Rev Genet* **16**(11): 665-681.

Lewis M (2017). Addiction and the Brain: Development, Not Disease. *Neuroethics* **10**(1): 7-18.

Lin Y, Jover-Mengual T, Wong J, Bennett MV, Zukin RS (2006). PSD-95 and PKC converge in regulating NMDA receptor trafficking and gating. *Proc Natl Acad Sci U S A* **103**(52): 19902-19907.

Lin Y, Skeberdis VA, Francesconi A, Bennett MV, Zukin RS (2004). Postsynaptic density protein-95 regulates NMDA channel gating and surface expression. *J Neurosci* **24**(45): 10138-10148.

Liu B, Paton JF, Kasparov S (2008). Viral vectors based on bidirectional cell-specific mammalian promoters and transcriptional amplification strategy for use in vitro and in vivo. *BMC Biotechnol* **8**: 49.

Liu F, Laguesse S, Legastelois R, Morisot N, Ben Hamida S, Ron D (2017). mTORC1-dependent translation of collapsin response mediator protein-2 drives neuroadaptations underlying excessive alcohol-drinking behaviors. *Mol Psychiatry* **22**(1): 89-101.

Liu J, Laster MJ, Taheri S, Eger EI, 2nd, Koblin DD, Halsey MJ (1993). Is there a cutoff in anesthetic potency for the normal alkanes? *Anesth Analg* **77**(1): 12-18.

Liu KJ, Arron JR, Stankunas K, Crabtree GR, Longaker MT (2007). Chemical rescue of cleft palate and midline defects in conditional GSK-3beta mice. *Nature* **446**(7131): 79-82.

Lobo IA, Harris RA, Trudell JR (2008). Cross-linking of sites involved with alcohol action between transmembrane segments 1 and 3 of the glycine receptor following activation. *J Neurochem* **104**(6): 1649-1662.

Lobo IA, Mascia MP, Trudell JR, Harris RA (2004). Channel gating of the glycine receptor changes accessibility to residues implicated in receptor potentiation by alcohols and anesthetics. *J Biol Chem* **279**(32): 33919-33927.

Lobo IA, Trudell JR, Harris RA (2006). Accessibility to residues in transmembrane segment four of the glycine receptor. *Neuropharmacology* **50**(2): 174-181.

Logrip ML, Janak PH, Ron D (2009). Escalating ethanol intake is associated with altered corticostriatal BDNF expression. *J Neurochem* **109**(5): 1459-1468.

Lopez MF, Becker HC (2005). Effect of pattern and number of chronic ethanol exposures on subsequent voluntary ethanol intake in C57BL/6J mice. *Psychopharmacology (Berl)* **181**(4): 688-696.

Lopez MF, Griffin WC, 3rd, Melendez RI, Becker HC (2012). Repeated cycles of chronic intermittent ethanol exposure leads to the development of tolerance to aversive effects of ethanol in C57BL/6J mice. *Alcohol Clin Exp Res* **36**(7): 1180-1187.

Lovestone S, Boada M, Dubois B, Hull M, Rinne JO, Huppertz HJ*, et al* (2015). A phase II trial of tideglusib in Alzheimer's disease. *Journal of Alzheimer's disease : JAD* **45**(1): 75-88.

Lovinger DM, White G, Weight FF (1989). Ethanol inhibits NMDA-activated ion current in hippocampal neurons. *Science* **243**(4899): 1721-1724.

Lu J, Greco MA (2006). Sleep circuitry and the hypnotic mechanism of GABAA drugs. *J Clin Sleep Med* **2**(2): S19-26.

Luo J (2010). Lithium-mediated protection against ethanol neurotoxicity. *Front Neurosci* **4**: 41.

Luykx JJ, Boks MP, Terwindt AP, Bakker S, Kahn RS, Ophoff RA (2010). The involvement of GSK3beta in bipolar disorder: integrating evidence from multiple types of genetic studies. *Eur Neuropsychopharmacol* **20**(6): 357-368.

Madisen L, Zwingman TA, Sunkin SM, Oh SW, Zariwala HA, Gu H*, et al* (2010). A robust and high-throughput Cre reporting and characterization system for the whole mouse brain. *Nat Neurosci* **13**(1): 133-140.

Mai L, Jope RS, Li X (2002). BDNF-mediated signal transduction is modulated by GSK3beta and mood stabilizing agents. *J Neurochem* **82**(1): 75-83.

Malenka RC, Bear MF (2004). LTP and LTD: an embarrassment of riches. *Neuron* **44**(1): 5-21.

Martinez A, Alonso M, Castro A, Pérez C, Moreno FJ (2002). First Non-ATP Competitive Glycogen Synthase Kinase 3 β (GSK-3β)
Inhibitors: Thiadiazolidinones (TDZD) as Potential Drugs for the Treatment of Alzheimer's Disease. *Journal of Medicinal Chemistry* **45**(6): 1292-1299.

Mathuram TL, Reece LM, Cherian KM (2018). GSK-3 Inhibitors: A Double-Edged Sword? - An Update on Tideglusib. *Drug Res (Stuttg)*.

McBride WJ, Kerns RT, Rodd ZA, Strother WN, Edenberg HJ, Hashimoto JG*, et al* (2005). Alcohol effects on central nervous system gene expression in genetic animal models. *Alcohol Clin Exp Res* **29**(2): 167-175.

McClintick JN, Brooks AI, Deng L, Liang L, Wang JC, Kapoor M*, et al* (2014). Ethanol treatment of lymphoblastoid cell lines from alcoholics and non-alcoholics causes many subtle changes in gene expression. *Alcohol* **48**(6): 603-610.

McGough NN, He DY, Logrip ML, Jeanblanc J, Phamluong K, Luong K*, et al* (2004). RACK1 and brain-derived neurotrophic factor: a homeostatic pathway that regulates alcohol addiction. *J Neurosci* **24**(46): 10542-10552.

Melis M, Camarini R, Ungless MA, Bonci A (2002). Long-lasting potentiation of GABAergic synapses in dopamine neurons after a single in vivo ethanol exposure. *J Neurosci* **22**(6): 2074-2082.

Meliska CJ, Bartke A, McGlacken G, Jensen RA (1995). Ethanol, nicotine, amphetamine, and aspartame consumption and preferences in C57BL/6 and DBA/2 mice. *Pharmacol Biochem Behav* **50**(4): 619-626.

Mihic SJ, Ye Q, Wick MJ, Koltchine VV, Krasowski MD, Finn SE*, et al* (1997). Sites of alcohol and volatile anaesthetic action on GABA(A) and glycine receptors. *Nature* **389**(6649): 385-389.

Miller JS, Barr JL, Harper LJ, Poole RL, Gould TJ, Unterwald EM (2014). The GSK3 signaling pathway is activated by cocaine and is critical for cocaine conditioned reward in mice. *PLoS One* **9**(2): e88026.

Miller JS, Tallarida RJ, Unterwald EM (2009). Cocaine-induced hyperactivity and sensitization are dependent on GSK3. *Neuropharmacology* **56**(8): 1116-1123.

Mines MA, Yuskaitis CJ, King MK, Beurel E, Jope RS (2010). GSK3 influences social preference and anxiety-related behaviors during social interaction in a mouse model of fragile X syndrome and autism. *PLoS One* **5**(3): e9706.

Miyakawa T, Yagi T, Kitazawa H, Yasuda M, Kawai N, Tsuboi K*, et al* (1997). Fyn-kinase as a determinant of ethanol sensitivity: relation to NMDA-receptor function. *Science* **278**(5338): 698-701.

Mokdad AH, Marks JS, Stroup DF, Gerberding JL (2004). Actual causes of death in the United States, 2000. *JAMA* **291**(10): 1238-1245.

Moselhy HF, Georgiou G, Kahn A (2001). Frontal lobe changes in alcoholism: a review of the literature. *Alcohol Alcohol* **36**(5): 357-368.

Moss GW, Curry S, Franks NP, Lieb WR (1991). Mapping the polarity profiles of general anesthetic target sites using n-alkane-(alpha, omega)-diols. *Biochemistry* **30**(43): 10551-10557.

Moykkynen T, Korpi ER (2012). Acute effects of ethanol on glutamate receptors. *Basic Clin Pharmacol Toxicol* **111**(1): 4-13.

Nagy A (2000). Cre recombinase: the universal reagent for genome tailoring. *Genesis* **26**(2): 99-109.

Naqvi NH, Morgenstern J (2015). Cognitive Neuroscience Approaches to Understanding Behavior Change in Alcohol Use Disorder Treatments. *Alcohol Res* **37**(1): 29-38.

NCBI (2017). GSK3B. National Library of Medicine (US): Bethesda MD, p https://www.ncbi.nlm.nih.gov/homologene?cmd=Retrieve&dopt=AlignmentScores&list_uids=55629.

Neasta J, Ben Hamida S, Yowell QV, Carnicella S, Ron D (2011). AKT signaling pathway in the nucleus accumbens mediates excessive alcohol drinking behaviors. *Biol Psychiatry* **70**(6): 575-582.

Nelson CD, Kim MJ, Hsin H, Chen Y, Sheng M (2013). Phosphorylation of threonine-19 of PSD-95 by GSK-3beta is required for PSD-95 mobilization and long-term depression. *J Neurosci* **33**(29): 12122-12135.

Newton PM, Messing RO (2006). Intracellular signaling pathways that regulate behavioral responses to ethanol. *Pharmacol Ther* **109**(1-2): 227-237.

Neznanova O, Bjork K, Rimondini R, Hansson AC, Hyytia P, Heilig M*, et al* (2009). Acute ethanol challenge inhibits glycogen synthase kinase-3beta in the rat prefrontal cortex. *Int J Neuropsychopharmacol* **12**(2): 275-280.

Nickerson A, Barnes JB, Creamer M, Forbes D, McFarlane AC, O'Donnell M*, et al* (2014). The temporal relationship between posttraumatic stress disorder and problem alcohol use following traumatic injury. *J Abnorm Psychol* **123**(4): 821-834.

Nusser Z, Sieghart W, Somogyi P (1998). Segregation of different GABAA receptors to synaptic and extrasynaptic membranes of cerebellar granule cells. *J Neurosci* **18**(5): 1693-1703.

O'Brien WT, Klein PS (2009). Validating GSK3 as an in vivo target of lithium action. *Biochem Soc Trans* **37**(Pt 5): 1133-1138.

O'Dell LE, Roberts AJ, Smith RT, Koob GF (2004). Enhanced alcohol self-administration after intermittent versus continuous alcohol vapor exposure. *Alcohol Clin Exp Res* **28**(11): 1676-1682.

O'Neal CL, Wolf CE, 2nd, Levine B, Kunsman G, Poklis A (1996). Gas chromatographic procedures for determination of ethanol in postmortem blood using t-butanol and methyl ethyl ketone as internal standards. *Forensic Sci Int* **83**(1): 31-38.

Oliet SH, Malenka RC, Nicoll RA (1997). Two distinct forms of long-term depression coexist in CA1 hippocampal pyramidal cells. *Neuron* **18**(6): 969-982.

Oliveros JC (2007). VENNY. An interactive tool for comparing lists with Venn Diagrams. http://bioinfogp.cnb.csic.es/tools/venny/index.html.

Organization WH (2014). *Global status report on alcohol and health 2014* World Health Organization: Geneva.

Osterndorff-Kahanek E, Ponomarev I, Blednov YA, Harris RA (2013). Gene expression in brain and liver produced by three different regimens of alcohol consumption in mice: comparison with immune activation. *PLoS One* **8**(3): e59870.

Papadeas S, Grobin AC (2001). … Differentially Alters GABAA Receptor α1 and α4 Subunit Peptide Expression and GABAA Receptor-Mediated 36Cl− Uptake in Mesocorticolimbic Regions of Rat Brain. *Alcoholism: Clinical and …*.

Parkitna JR, Obara I, Wawrzczak-Bargiela A, Makuch W, Przewlocka B, Przewlocki R (2006). Effects of glycogen synthase kinase 3beta and cyclin-dependent kinase 5 inhibitors on morphine-induced analgesia and tolerance in rats. *J Pharmacol Exp Ther* **319**(2): 832-839.

Patel NC, DelBello MP, Bryan HS, Adler CM, Kowatch RA, Stanford K*, et al* (2006). Open-label lithium for the treatment of adolescents with bipolar depression. *J Am Acad Child Adolesc Psychiatry* **45**(3): 289-297.

Patel S, Doble BW, MacAulay K, Sinclair EM, Drucker DJ, Woodgett JR (2008). Tissue-specific role of glycogen synthase kinase 3beta in glucose homeostasis and insulin action. *Mol Cell Biol* **28**(20): 6314-6328.

Peineau S, Bradley C, Taghibiglou C, Doherty A, Bortolotto ZA, Wang YT*, et al* (2008). The role of GSK-3 in synaptic plasticity. *Br J Pharmacol* **153 Suppl 1**: S428-437.

Peineau S, Taghibiglou C, Bradley C, Wong TP, Liu L, Lu J*, et al* (2007). LTP inhibits LTD in the hippocampus via regulation of GSK3beta. *Neuron* **53**(5): 703-717.

Peterson VL, McCool BA, Hamilton DA (2015). Effects of ethanol exposure and withdrawal on dendritic morphology and spine density in the nucleus accumbens core and shell. *Brain Res* **1594**: 125-135.

Pina MM, Cunningham CL (2017). Ethanol-seeking behavior is expressed directly through an extended amygdala to midbrain neural circuit. *Neurobiol Learn Mem* **137**: 83-91.

Prickaerts J, Moechars D, Cryns K, Lenaerts I, van Craenendonck H, Goris I*, et al* (2006). Transgenic mice overexpressing glycogen synthase kinase 3beta: a putative model of hyperactivity and mania. *J Neurosci* **26**(35): 9022-9029.

Proctor WR, Poelchen W, Bowers BJ, Wehner JM, Messing RO, Dunwiddie TV (2003). Ethanol differentially enhances hippocampal GABA A receptor-mediated responses in protein kinase C gamma (PKC gamma) and PKC epsilon null mice. *J Pharmacol Exp Ther* **305**(1): 264-270.

Purcell S, Neale B, Todd-Brown K, Thomas L, Ferreira MA, Bender D*, et al* (2007). PLINK: a tool set for whole-genome association and population-based linkage analyses. *Am J Hum Genet* **81**(3): 559-575.

Putman AH, Wolen AR, Harenza JL, Yordanova RK, Webb BT, Chesler EJ*, et al* (2016). Identification of quantitative trait loci and candidate genes for an anxiolytic-like response to ethanol in BXD recombinant inbred strains. *Genes Brain Behav* **15**(4): 367-381.

Qi ZH, Song M, Wallace MJ, Wang D, Newton PM, McMahon T*, et al* (2007). Protein kinase C epsilon regulates gamma-aminobutyrate type A receptor sensitivity to ethanol and benzodiazepines through phosphorylation of gamma2 subunits. *J Biol Chem* **282**(45): 33052-33063.

Ragia G, Manolopoulos VG (2017). Personalized Medicine of Alcohol Addiction: Pharmacogenomics and Beyond. *Curr Pharm Biotechnol* **18**(3): 221-230.

Regier DA, Farmer ME, Rae DS, Locke BZ, Keith SJ, Judd LL*, et al* (1990). Comorbidity of mental disorders with alcohol and other drug abuse. Results from the Epidemiologic Catchment Area (ECA) Study. *JAMA* **264**(19): 2511-2518.

Reich T (1996). A genomic survey of alcohol dependence and related phenotypes: results from the Collaborative Study on the Genetics of Alcoholism (COGA). *Alcohol Clin Exp Res* **20**(8 Suppl): 133A-137A.

Roberto M, Madamba SG, Moore SD, Tallent MK, Siggins GR (2003). Ethanol increases GABAergic transmission at both pre- and postsynaptic sites in rat central amygdala neurons. *Proc Natl Acad Sci U S A* **100**(4): 2053-2058.

Roberts AJ, Heyser CJ, Cole M, Griffin P, Koob GF (2000). Excessive ethanol drinking following a history of dependence: animal model of allostasis. *Neuropsychopharmacology* **22**(6): 581-594.

Ron D, Wang J (2009). The NMDA Receptor and Alcohol Addiction. In: Van Dongen AM (ed). *Biology of the NMDA Receptor*: Boca Raton (FL).

Rosenwasser AM, Fixaris MC, Crabbe JC, Brooks PC, Ascheid S (2013). Escalation of intake under intermittent ethanol access in diverse mouse genotypes. *Addict Biol* **18**(3): 496-507.

Rui Y, Myers KR, Yu K, Wise A, De Blas AL, Hartzell HC*, et al* (2013). Activity-dependent regulation of dendritic growth and maintenance by glycogen synthase kinase 3beta. *Nat Commun* **4**: 2628.

Sachs BD, Salahi AA, Caron MG (2014). Congenital brain serotonin deficiency leads to reduced ethanol sensitivity and increased ethanol consumption in mice. *Neuropharmacology* **77**: 177-184.

Saddoris MP, Cacciapaglia F, Wightman RM, Carelli RM (2015). Differential Dopamine Release Dynamics in the Nucleus Accumbens Core and Shell Reveal Complementary Signals for Error Prediction and Incentive Motivation. *J Neurosci* **35**(33): 11572-11582.

Saini NK, Suresh PS, Lella M, Bhamidipati RK, Rajagopal S, Mullangi R (2018). LC-MS/MS determination of tideglusib, a novel GSK-3beta inhibitor in mice plasma and its application to a pharmacokinetic study in mice. *J Pharm Biomed Anal* **148**: 100-107.

Salcedo-Tello P, Ortiz-Matamoros A, Arias C (2011). GSK3 Function in the Brain during Development, Neuronal Plasticity, and Neurodegeneration. *Int J Alzheimers Dis* **2011**: 189728.

SAMHSA SAaMHSA- (ed) (2015). Results from the 2015 National Survey on Drug Use and Health : Summary of National Findings. *NSDUH Series.*

Sanchez-Craig M, Lei H (1986). Disadvantages to imposing the goal of abstinence on problem drinkers: an empirical study. *Br J Addict* **81**(4): 505-512.

Santhakumar V, Wallner M, Otis TS (2007). Ethanol acts directly on extrasynaptic subtypes of GABAA receptors to increase tonic inhibition. *Alcohol* **41**(3): 211-221.

Sauer B (1993). Manipulation of transgenes by site-specific recombination: use of Cre recombinase. *Methods Enzymol* **225**: 890-900.

Scannevin RH, Huganir RL (2000). Postsynaptic organization and regulation of excitatory synapses. *Nat Rev Neurosci* **1**(2): 133-141.

Schuckit MA (1994). Low level of response to alcohol as a predictor of future alcoholism. *Am J Psychiatry* **151**(2): 184-189.

Schwarz JM, Bilbo SD (2013). Adolescent morphine exposure affects long-term microglial function and later-life relapse liability in a model of addiction. *J Neurosci* **33**(3): 961-971.

Sereno L, Coma M, Rodriguez M, Sanchez-Ferrer P, Sanchez MB, Gich I*, et al* (2009). A novel GSK-3beta inhibitor reduces Alzheimer's pathology and rescues neuronal loss in vivo. *Neurobiol Dis* **35**(3): 359-367.

Sesack SR, Pickel VM (1992). Prefrontal cortical efferents in the rat synapse on unlabeled neuronal targets of catecholamine terminals in the nucleus accumbens septi and on dopamine neurons in the ventral tegmental area. *J Comp Neurol* **320**(2): 145-160.

Shi X, Miller JS, Harper LJ, Poole RL, Gould TJ, Unterwald EM (2014). Reactivation of cocaine reward memory engages the Akt/GSK3/mTOR signaling pathway and can be disrupted by GSK3 inhibition. *Psychopharmacology (Berl)* **231**(16): 3109-3118.

Shinohara Y, Konno A, Takahashi N, Matsuzaki Y, Kishi S, Hirai H (2016). Viral Vector-Based Dissection of Marmoset GFAP Promoter in Mouse and Marmoset Brains. *PLoS One* **11**(8): e0162023.

Sigel E (2002). Mapping of the benzodiazepine recognition site on GABA(A) receptors. *Curr Top Med Chem* **2**(8): 833-839.

Smillie KJ, Pawson J, Perkins EM, Jackson M, Cousin MA (2013). Control of synaptic vesicle endocytosis by an extracellular signalling molecule. *Nat Commun* **4**: 2394.

Smith DF, Amdisen A (1983). Central effects of lithium in rats: lithium levels, body weight and water intake. *Acta Pharmacol Toxicol (Copenh)* **52**(2): 81-85.

Smith KR, Muir J, Rao Y, Browarski M, Gruenig MC, Sheehan DF*, et al* (2012). Stabilization of GABA(A) receptors at endocytic zones is mediated by an AP2 binding motif within the GABA(A) receptor beta3 subunit. *J Neurosci* **32**(7): 2485-2498.

Smith ML, Lopez MF, Archer KJ, Wolen AR, Becker HC, Miles MF (2016). Time-Course Analysis of Brain Regional Expression Network Responses to Chronic Intermittent Ethanol and Withdrawal: Implications for Mechanisms Underlying Excessive Ethanol Consumption. *PLoS One* **11**(1): e0146257.

Smith RL, Traul DL, Schaack J, Clayton GH, Staley KJ, Wilcox CL (2000). Characterization of promoter function and cell-type-specific expression from viral vectors in the nervous system. *J Virol* **74**(23): 11254-11261.

Soderpalm B, Ericson M (2013). Neurocircuitry involved in the development of alcohol addiction: the dopamine system and its access points. *Curr Top Behav Neurosci* **13**: 127-161.

Song B, Lai B, Zheng Z, Zhang Y, Luo J, Wang C*, et al* (2010). Inhibitory phosphorylation of GSK-3 by CaMKII couples depolarization to neuronal survival. *J Biol Chem* **285**(52): 41122-41134.

Soutar MP, Kim WY, Williamson R, Peggie M, Hastie CJ, McLauchlan H*, et al* (2010). Evidence that glycogen synthase kinase-3 isoforms have distinct substrate preference in the brain. *J Neurochem* **115**(4): 974-983.

Starkman BG, Sakharkar AJ, Pandey SC (2012). Epigenetics-beyond the genome in alcoholism. *Alcohol Res* **34**(3): 293-305.

Storozheva ZI, Gruden MA, Proshin AT, Sewell RD (2015). Learning ability is a key outcome determinant of GSK-3 inhibition on visuospatial memory in rats. *J Psychopharmacol* **29**(7): 822-835.

Supek F, Bo?njak M, kunca N, muc T (2011). REVIGO Summarizes and Visualizes Long Lists of Gene Ontology Terms. *PLoS ONE* **6**(7): e21800.

Sutherland C (2011). What Are the bona fide GSK3 Substrates? *Int J Alzheimers Dis* **2011**: 505607.

Sutherland C, Cohen P (1994). The alpha-isoform of glycogen synthase kinase-3 from rabbit skeletal muscle is inactivated by p70 S6 kinase or MAP kinase-activated protein kinase-1 in vitro. *FEBS Lett* **338**(1): 37-42.

Sutherland C, Leighton IA, Cohen P (1993). Inactivation of glycogen synthase kinase-3 beta by phosphorylation: new kinase connections in insulin and growth-factor signalling. *Biochem J* **296 (Pt 1)**: 15-19.

Tapocik JD, Barbier E, Flanigan M, Solomon M, Pincus A, Pilling A*, et al* (2014). microRNA-206 in rat medial prefrontal cortex regulates BDNF expression and alcohol drinking. *J Neurosci* **34**(13): 4581-4588.

Tawa EA, Hall SD, Lohoff FW (2016). Overview of the Genetics of Alcohol Use Disorder. *Alcohol Alcohol* **51**(5): 507-514.

Tezuka T, Umemori H, Akiyama T, Nakanishi S, Yamamoto T (1999). PSD-95 promotes Fyn-mediated tyrosine phosphorylation of the N-methyl-D-aspartate receptor subunit NR2A. *Proc Natl Acad Sci U S A* **96**(2): 435-440.

Thanos PK, Dimitrakakis ES, Rice O, Gifford A, Volkow ND (2005). Ethanol self-administration and ethanol conditioned place preference are reduced in mice lacking cannabinoid CB1 receptors. *Behav Brain Res* **164**(2): 206-213.

Thompson W, Lande R, Kalapatapu R (2017). Alcoholism Follow-up. *Drugs & Diseases*. Medscape.

Tokuda K, Zorumski CF, Izumi Y (2007). Modulation of hippocampal long-term potentiation by slow increases in ethanol concentration. *Neuroscience* **146**(1): 340-349.

Tolosa E, Litvan I, Hoglinger GU, Burn D, Lees A, Andres MV*, et al* (2014). A phase 2 trial of the GSK-3 inhibitor tideglusib in progressive supranuclear palsy. *Mov Disord* **29**(4): 470-478.

Tomasson K, Vaglum P (1998). Psychiatric co-morbidity and aftercare among alcoholics: a prospective study of a nationwide representative sample. *Addiction* **93**(3): 423-431.

Trantham-Davidson H, Chandler LJ (2015). Alcohol-induced alterations in dopamine modulation of prefrontal activity. *Alcohol* **49**(8): 773-779.

Treistman SN, Martin GE (2009). BK Channels: mediators and models for alcohol tolerance. *Trends in neurosciences* **32**(12): 629-637.

Tsujio I, Tanaka T, Kudo T, Nishikawa T, Shinozaki K, Grundke-Iqbal I*, et al* (2000). Inactivation of glycogen synthase kinase-3 by protein kinase C delta: implications for regulation of tau phosphorylation. *FEBS Lett* **469**(1): 111-117.

Turner PV, Brabb T, Pekow C, Vasbinder MA (2011). Administration of substances to laboratory animals: routes of administration and factors to consider. *J Am Assoc Lab Anim Sci* **50**(5): 600-613.

Tyagarajan SK, Fritschy JM (2014). Gephyrin: a master regulator of neuronal function? *Nat Rev Neurosci* **15**(3): 141-156.

Tyagarajan SK, Ghosh H, Yevenes GE, Nikonenko I, Ebeling C, Schwerdel C*, et al* (2011). Regulation of GABAergic synapse formation and plasticity by GSK3beta-dependent phosphorylation of gephyrin. *Proc Natl Acad Sci U S A* **108**(1): 379-384.

Tzschentke TM (2000). The medial prefrontal cortex as a part of the brain reward system. *Amino Acids* **19**(1): 211-219.

Urrutia R, Henley JR, Cook T, McNiven MA (1997). The dynamins: redundant or distinct functions for an expanding family of related GTPases? *Proc Natl Acad Sci U S A* **94**(2): 377-384.

Urs NM, Snyder JC, Jacobsen JP, Peterson SM, Caron MG (2012). Deletion of GSK3beta in D2R-expressing neurons reveals distinct roles for beta-arrestin signaling in antipsychotic and lithium action. *Proc Natl Acad Sci U S A* **109**(50): 20732-20737.

Vaillant GE (2003). A 60-year follow-up of alcoholic men. *Addiction* **98**(8): 1043-1051.

van der Vaart A, Meng X, Bowers MS, Batman AM, Aliev F, Farris SP*, et al* (2018). Glycogen Synthase Kinase 3 Beta Regulates Ethanol Consumption and is a Risk Factor for Alcohol Dependence. *Submitted*.

van der Vaart AD, Wolstenholme JT, Smith ML, Harris GM, Lopez MF, Wolen AR*, et al* (2017). The allostatic impact of chronic ethanol on gene expression: A genetic analysis of chronic intermittent ethanol treatment in the BXD cohort. *Alcohol* **58**: 93-106.

Velazquez-Marrero C, Burgos A, Garcia JO, Palacio S, Marrero HG, Bernardo A*, et al* (2016). Alcohol Regulates BK Surface Expression via Wnt/beta-Catenin Signaling. *J Neurosci* **36**(41): 10625-10639.

Vengeliene V, Leonardi-Essmann F, Perreau-Lenz S, Gebicke-Haerter P, Drescher K, Gross G*, et al* (2006). The dopamine D3 receptor plays an essential role in alcohol-seeking and relapse. *FASEB J* **20**(13): 2223-2233.

Verhulst B, Neale MC, Kendler KS (2015). The heritability of alcohol use disorders: a meta-analysis of twin and adoption studies. *Psychol Med* **45**(5): 1061-1072.

Wallace MJ, Newton PM, Oyasu M, McMahon T, Chou WH, Connolly J*, et al* (2007). Acute functional tolerance to ethanol mediated by protein kinase Cepsilon. *Neuropsychopharmacology* **32**(1): 127-136.

Wallner M, Hanchar HJ, Olsen RW (2006). Low dose acute alcohol effects on GABA A receptor subtypes. *Pharmacol Ther* **112**(2): 513-528.

Wang J, Williams RW, Manly KF (2003). WebQTL: web-based complex trait analysis. *Neuroinformatics* **1**(4): 299-308.

Warthen DM, Lambeth PS, Ottolini M, Shi Y, Barker BS, Gaykema RP*, et al* (2016). Activation of Pyramidal Neurons in Mouse Medial Prefrontal Cortex Enhances Food-Seeking Behavior While Reducing Impulsivity in the Absence of an Effect on Food Intake. *Front Behav Neurosci* **10**: 63.

Wei W, Faria LC, Mody I (2004). Low ethanol concentrations selectively augment the tonic inhibition mediated by delta subunit-containing GABAA receptors in hippocampal neurons. *J Neurosci* **24**(38): 8379-8382.

Weight FF, Aguayo LG, White G, Lovinger DM, Peoples RW (1992). GABA- and glutamate-gated ion channels as molecular sites of alcohol and anesthetic action. *Adv Biochem Psychopharmacol* **47**: 335-347.

Weisner C, Matzger H, Kaskutas LA (2003). How important is treatment? One-year outcomes of treated and untreated alcohol-dependent individuals. *Addiction* **98**(7): 901-911.

Werner DF, Swihart AR, Ferguson C, Lariviere WR, Harrison NL, Homanics GE (2009). Alcohol-induced tolerance and physical dependence in mice with ethanol insensitive alpha1 GABA A receptors. *Alcohol Clin Exp Res* **33**(2): 289-299.

Wick MJ, Mihic SJ, Ueno S, Mascia MP, Trudell JR, Brozowski SJ*, et al* (1998). Mutations of gamma-aminobutyric acid and glycine receptors change alcohol cutoff: evidence for an alcohol receptor? *Proc Natl Acad Sci U S A* **95**(11): 6504-6509.

Wickham H (2009). *ggplot2 : elegant graphics for data analysis* Springer: New York, viii, 212 p.pp.

Williams RW (2012). "LRS". *From The WebQTL Glossary-- A GeneNetwork Resource* www.genenetwork.org/glossary.html.

Williams RW, Broman KW (2010). "LOD". *The WebQTL Glossary--A GeneNetwork Resource*: www.genenetwork.org/glossary.html.

Wolen AR, Phillips CA, Langston MA, Putman AH, Vorster PJ, Bruce NA*, et al* (2012). Genetic dissection of acute ethanol responsive gene networks in prefrontal cortex: functional and mechanistic implications. *PLoS One* **7**(4): e33575.

Wolstenholme JT, Mahmood T, Harris GM, Abbas S, Miles MF (2017). Intermittent Ethanol during Adolescence Leads to Lasting Behavioral Changes in Adulthood and Alters Gene Expression and Histone Methylation in the PFC. *Front Mol Neurosci* **10**: 307.

Wolstenholme JT, Warner JA, Capparuccini MI, Archer KJ, Shelton KL, Miles MF (2011). Genomic analysis of individual differences in ethanol drinking: evidence for non-genetic factors in C57BL/6 mice. *PLoS One* **6**(6): e21100.

Woodgett JR (1990). Molecular cloning and expression of glycogen synthase kinase-3/factor A. *EMBO J* **9**(8): 2431-2438.

Yaka R, Phamluong K, Ron D (2003a). Scaffolding of Fyn kinase to the NMDA receptor determines brain region sensitivity to ethanol. *J Neurosci* **23**(9): 3623-3632.

Yaka R, Tang KC, Camarini R, Janak PH, Ron D (2003b). Fyn kinase and NR2B-containing NMDA receptors regulate acute ethanol sensitivity but not ethanol intake or conditioned reward. *Alcohol Clin Exp Res* **27**(11): 1736-1742.

Yaka R, Thornton C, Vagts AJ, Phamluong K, Bonci A, Ron D (2002). NMDA receptor function is regulated by the inhibitory scaffolding protein, RACK1. *Proc Natl Acad Sci U S A* **99**(8): 5710-5715.

Yen YC, Gassen NC, Zellner A, Rein T, Landgraf R, Wotjak CT*, et al* (2015). Glycogen synthase kinase-3beta inhibition in the medial prefrontal cortex mediates paradoxical amphetamine action in a mouse model of ADHD. *Front Behav Neurosci* **9**: 67.

Yoshimura M, Pearson S, Kadota Y, Gonzalez CE (2006). Identification of ethanol responsive domains of adenylyl cyclase. *Alcohol Clin Exp Res* **30**(11): 1824-1832.

Yoshimura M, Tabakoff B (1995). Selective effects of ethanol on the generation of cAMP by particular members of the adenylyl cyclase family. *Alcohol Clin Exp Res* **19**(6): 1435-1440.

Zhang F, Phiel CJ, Spece L, Gurvich N, Klein PS (2003). Inhibitory phosphorylation of glycogen synthase kinase-3 (GSK-3) in response to lithium. Evidence for autoregulation of GSK-3. *J Biol Chem* **278**(35): 33067-33077.

Zhang L, Wang L, Ravindranathan A, Miles MF (2002). A new algorithm for analysis of oligonucleotide arrays: application to expression profiling in mouse brain regions. *J Mol Biol* **317**(2): 225-235.

Zhang N, Wei W, Mody I, Houser CR (2007). Altered localization of GABA(A) receptor subunits on dentate granule cell dendrites influences tonic and phasic inhibition in a mouse model of epilepsy. *J Neurosci* **27**(28): 7520-7531.

Zhao C, Du CP, Peng Y, Xu Z, Sun CC, Liu Y*, et al* (2015). The upregulation of NR2A-containing N-methyl-D-aspartate receptor function by tyrosine phosphorylation of postsynaptic density 95 via facilitating Src/proline-rich tyrosine kinase 2 activation. *Mol Neurobiol* **51**(2): 500-511.

Zong L, Zhou L, Hou Y, Zhang L, Jiang W, Zhang W*, et al* (2017). Genetic and epigenetic regulation on the transcription of GABRB2: Genotype-dependent hydroxymethylation and methylation alterations in schizophrenia. *J Psychiatr Res* **88**: 9-17.

Zuo L, Zhang F, Zhang H, Zhang XY, Wang F, Li CS*, et al* (2012). Genome-wide search for replicable risk gene regions in alcohol and nicotine co-dependence. *Am J Med Genet B Neuropsychiatr Genet* **159B**(4): 437-444.

Appendix

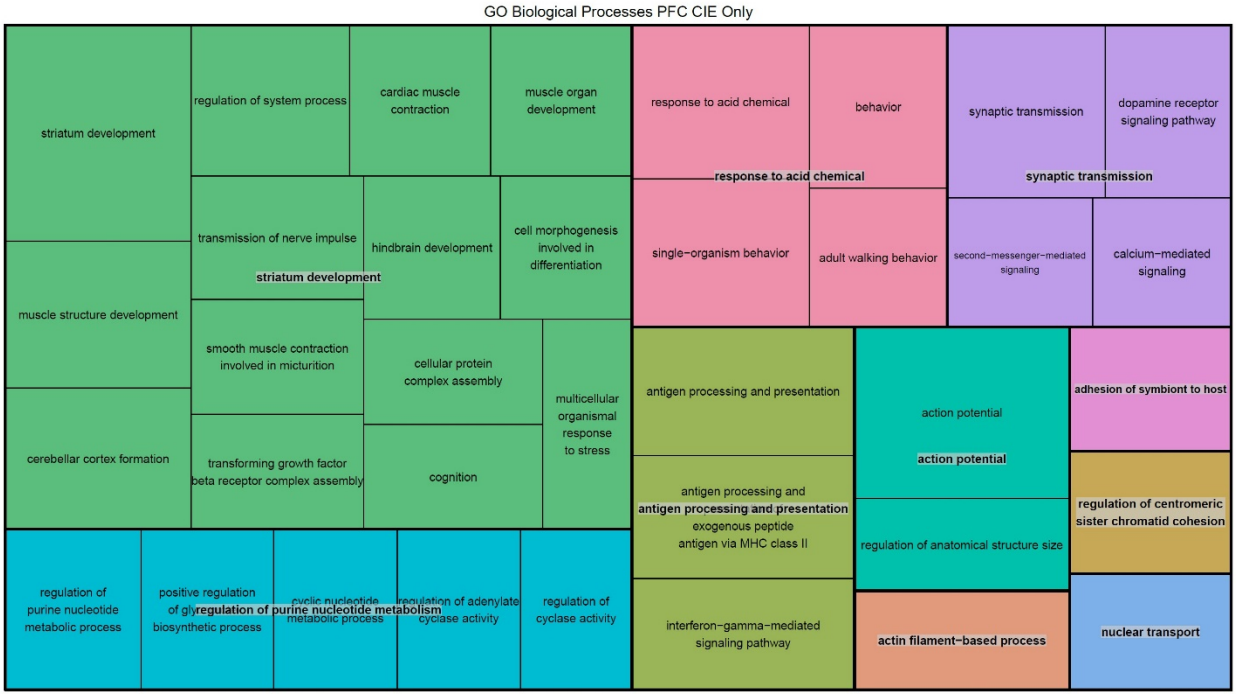

Supplemental Fig. 3.1. REVIGO treemap of Gene Ontology Biological Processes enriched in genes significantly regulated by CIE only in the PFC. GO categories clustered by semantic similarity.

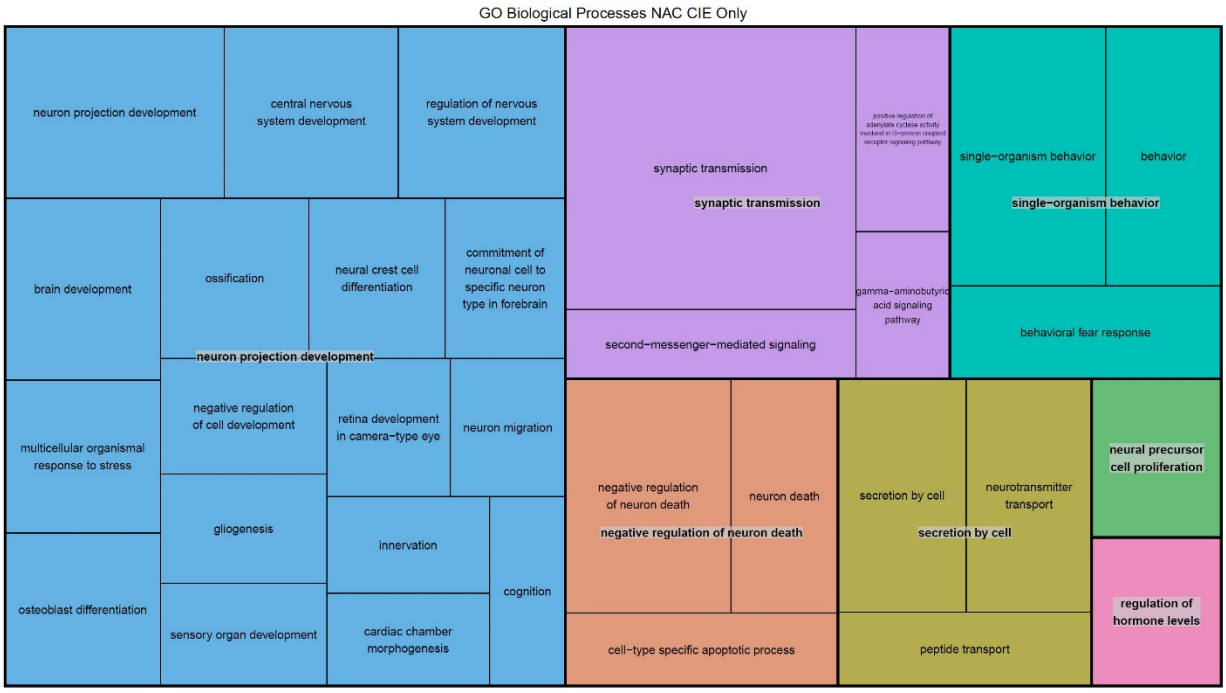

Supplemental Fig. 3.2. REVIGO treemap of Gene Ontology Biological Processes enriched in genes significantly regulated by CIE only in the NAC. GO categories clustered by semantic similarity.

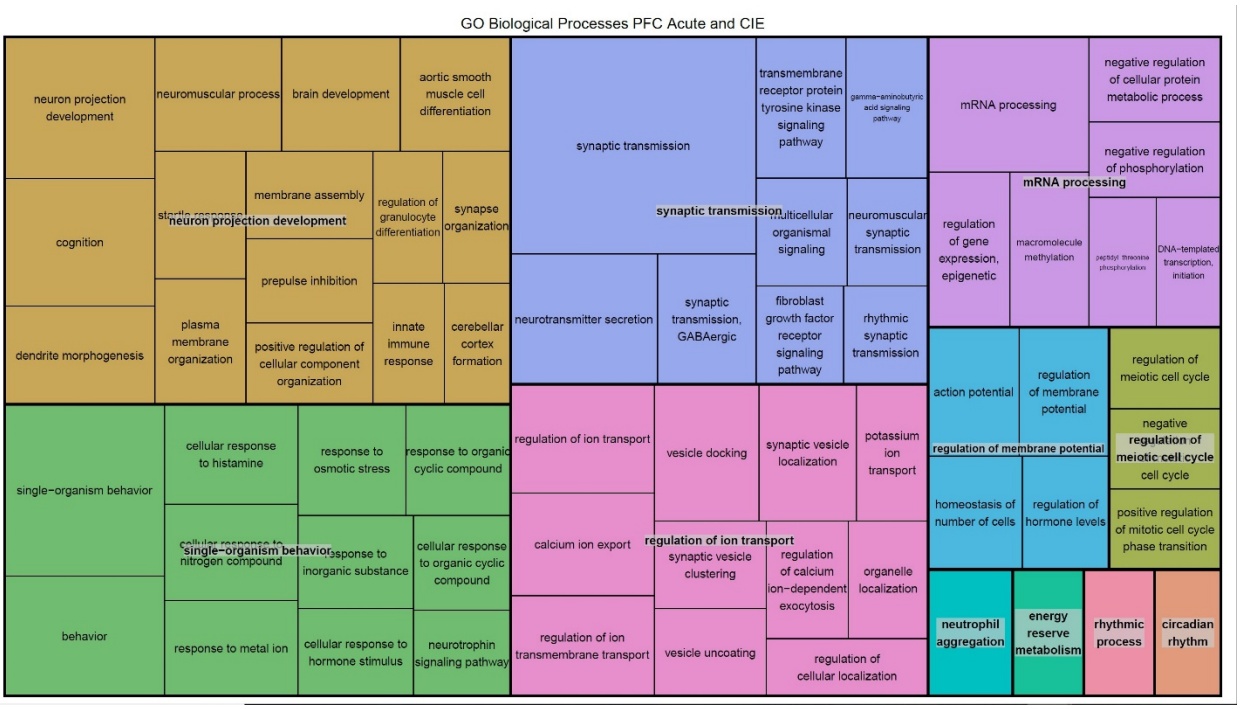

Supplemental Fig. 3.3. REVIGO treemap of Gene Ontology Biological Processes enriched in genes significantly regulated by CIE and acute EtOH in the PFC. GO categories clustered by semantic similarity.

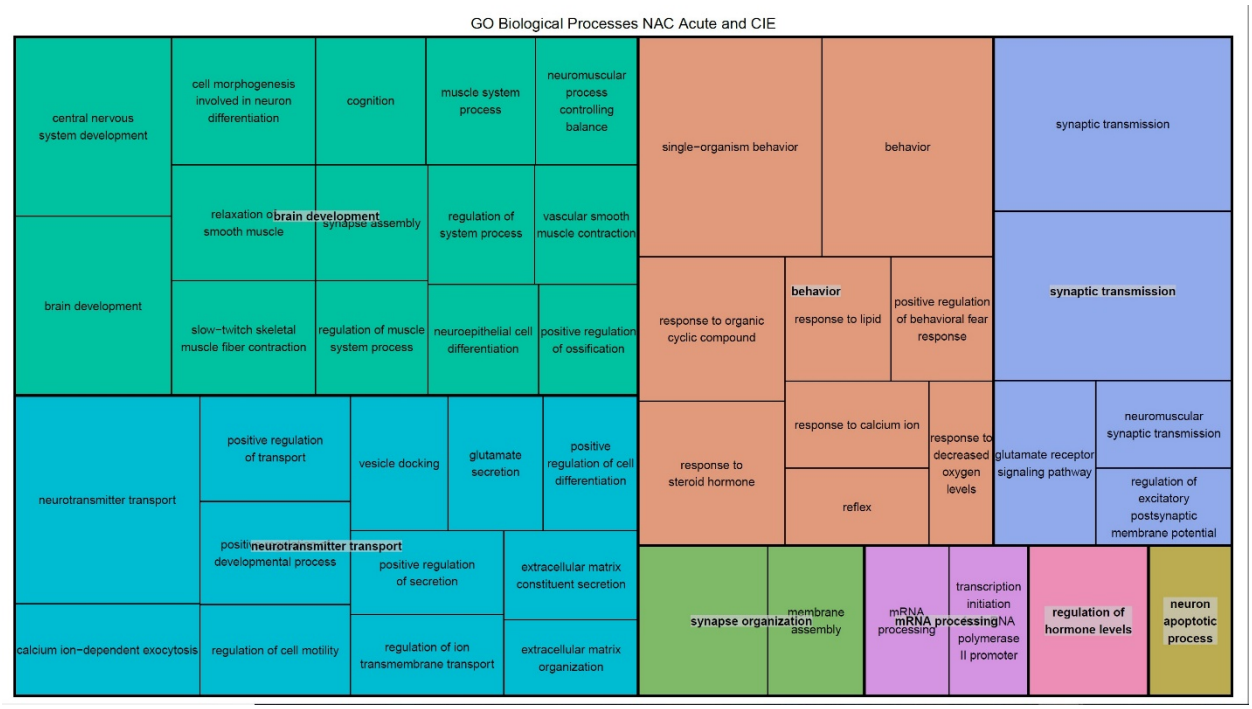

Supplemental Fig. 3.4. REVIGO treemap of Gene Ontology Biological Processes enriched in genes significantly regulated by CIE and acute EtOH in the NAC. GO categories clustered by semantic similarity.

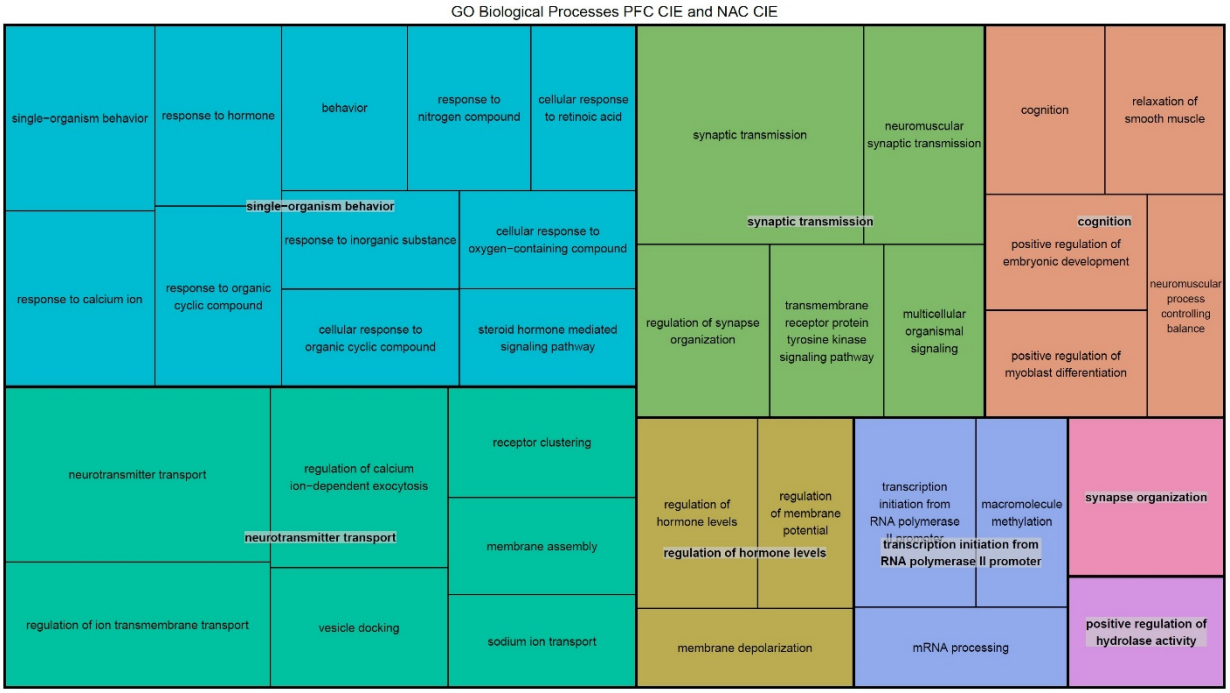

Supplemental Fig. 3.5. REVIGO treemap of Gene Ontology Biological Processes enriched in genes significantly regulated by CIE in the PFC and NAC. GO categories clustered by semantic similarity.

Vita

Andrew van der Vaart was born in Durham, NC. He graduated from St. David's School in 2005 and attended the University of Virginia (UVa) as a Jefferson Scholar from 2005-2009. He graduated with a Bachelor's in Cognitive Science with High Distinction. He then worked as a research assistant under Dr. Ming Li at the UVa Center for Addiction Research and Education from 2009-2011. He then moved to Richmond to work under Dr. Kenneth Kendler at the Virginia Institute for Psychiatric and Behavioral Genetics in 2011 and matriculated into the M.D.-Ph.D. program at Virginia Commonwealth University in 2012. He joined Dr. Michael Miles laboratory in the Summer of 2014. Under Dr. Miles' mentorship he was awarded a Ruth L. Kirschstein National Research Service Award (NRSA) from the National Institute of Alcohol Abuse and Alcoholism. He also received a Lab Grammy from the journal BioTechniques for the music video "We Found Drugs." Upon acceptance of this dissertation, he will be awarded a Doctorate of Philosophy in Pharmacology and Toxicology.